

MODELING BACTERIAL GROWTH, ATTACHMENT, EXTRACELLULAR
POLYMER PRODUCTION AND INTERACTIONS WITH TOXIC
TRANSITION METALS UNDER CONDITIONS OF VARIABLE pH

A Dissertation

Presented to the Faculty of the Graduate School

of Cornell University

in Partial Fulfillment of the Requirements for the Degree of

Doctor of Philosophy

by

George Anthony Murgel

May 2016

© George Anthony Murgel 2016

ALL RIGHTS RESERVED

MODELING BACTERIAL GROWTH, ATTACHMENT, EXTRACELLULAR
POLYMER PRODUCTION AND INTERACTIONS WITH TOXIC
TRANSITION METALS UNDER CONDITIONS OF VARIABLE pH

George Anthony Murgel, Ph.D.

Cornell University 2016

Bacteria are capable of adaptation to a variety of environmental extremes that abound in freshwater aquatic systems. One adaptation is biofilm formation and another is alteration of optimum enzyme activity. For example, enzyme activity is influenced by extremes in hydrogen ion concentration and the presence or absence of toxic trace metals. Most bacteria have a maximum activity over a narrow pH range. Computer modelling is able to quantify the interactive effects of the hydrogen ion and trace metals on cellular activity.

A cyclic-flow reactor system was constructed and tested as an experimental means of studying interactions between trace metal adsorption and bacterial attachment to inanimate surfaces under defined chemical conditions. Development of a chemically defined growth medium was required for use in the reactor system. Bacterial strains were screened for their ability to grow on the defined medium, to grow in the presence of toxic trace metals, and to attach and grow on inorganic surfaces. The bacterium *Pseudomonas cepacia* 17616 was determined to be a well suited for experimental analysis of effects of pH and trace metal interactions with bacterial biofilms.

A mechanistic, structured model was developed to simulate growth, biopolymer production and association with solid surfaces of freshwater bacteria under conditions of variable pH. A noncompetitive form of inhibition kinetics was applied to modify the maximum growth rate of suspended and attached cells to predict the effects of pH. The bacterial model was also interactively linked to a chemical equilibrium model to quantify trace metal distribution and metal effects on bacterial components as a function of pH. The output from the integrated model revealed that simulations for cell growth and polymer production were not sensitive to variation in the selected molecular dissociation constants. Model simulations were generated for reactors with a low surface to volume ratio ("Multigen") and a high surface to volume ratio (bioreactor). In simulations of batch operation of either a Multigen or bioreactor, the highest cell concentrations were predicted at neutral pH values. Model simulations of the same duration at the neutral pH values but using alkaline pH values did not retard cell growth to as great an extent as the simulations using acidic pH values. In either the alkaline or acidic pH simulations, peak concentrations of cells and polymer required much longer simulation run times to achieve than the neutral pH simulations. Polymer production increased as pH values moved above or below neutral values in both reactor types. Simulations of continuous operation to steady state in either reactor type revealed little overall variation in the final cumulative concentration of cells or polymer at acidic or alkaline levels compared to production at neutral pH. However, the simulation time to achieve steady state at acidic or alkaline pH values was much longer than at pH 7.

A decrease in the growth rates of cells and polymers was predicted under batch conditions at pH 7 or less as the total metal concentration increased from 1×10^{-9} M to

1×10^{-5} M. Under these conditions the predominant form of the metal was in the free metal ionic form which was more toxic to cellular and polymer growth. At pH 9, the free metal had little or no effect on the shape of the growth curve due to very low ion concentrations as a result of the formations of complexes and precipitation. Predictions using continuous growth conditions gave results which followed similar patterns, with the washout dilution rate decreasing with increasing total metal concentration at pH 7 or less and with no effect of the total metal on the dilution rate at pH 9. To test the transient responses to fluctuations in total metal concentrations, step increases in metal levels were simulated in the model. At alkaline pH values, there was little effect on the cells and polymer production after addition of the metal. As the pH decreased to circumneutral or acidic values, the concentrations of cells and polymers became strongly affected by the more prevalent toxic free metal ion form and washout of the cells and polymers would occur at lower dilution rates.

Models of the type described in this thesis have potential applications in assessing toxic transition metal behavior in both natural aquatic systems and engineered reactor systems with sufficient laboratory work to evaluate the necessary kinetic constants specific to the particular bacterial strains to be modeled.

BIOGRAPHICAL SKETCH

George Anthony Murgel was born in Helena, Montana on September 18, 1954. Adolescent years were spent growing up in the sheltered environment of the small smelter-town of East Helena, Montana. A stint working as a laborer the summer of 1972 at the smelter quickly solidified plans to pursue a college degree in order to prevent ever having to go back to the smelter. The first introduction to collegiate academic life was at Montana State University (MSU) in Bozeman, Montana in September 1972. At MSU he pursued a Bachelor of Science degree in Civil Engineering without initial selection of an area of specialization within Civil Engineering. During the junior year, the introductory course on Environmental Engineering taught by Howard S. Peavy presented a career path of extreme interest. The interest grew with the completion of each additional class in this field. The decision on specialization was made. A Bachelor's degree in civil engineering was granted in 1976.

He entered the graduate program at MSU in September of 1976. He worked to obtain further training and specialization in Environmental Engineering. The Master's degree was granted in August, 1978. His introduction to classroom teaching and its sense of accomplishment further shaped his plans to ultimately pursue an academic career. Toward this goal, he entered the work force in September, 1978 as a consulting engineer to obtain practical design experience in the field of Environmental Engineering. Eight years later, he entered the Ph. D. program at Cornell University to complete the requisite credentials for obtaining a faculty position in academia. He completed most of his doctoral coursework thesis requirements in August, 1991. He took a leave of absence for

three years to begin his academic career in the Civil Engineering Department at the University of North Carolina at Charlotte in Charlotte, North Carolina. He completed his dissertation requirements in January of 1995 and was cleared for the Doctor of Philosophy degree, pending submission of the final dissertation document. He continued in Environmental Engineering at UNC at Charlotte until the summer of 1996. He then took a position in a brand-new four year Civil Engineering program under development where he worked as the final documents are being submitted to receive the final award of his Doctor of Philosophy degree.

DEDICATION

To my grandmother, Mary, and my father, Anton,

who instilled in me the "Old Country" work ethic and the desire
to accomplish any goal I set for myself

and

Especially to my wife, Christine,
who gave us two sons, Joseph and Stefan,

for their patience and loving perseverance
during the long and arduous pursuit of a dream.

ACKNOWLEDGMENTS

This Dissertation is the culmination of over eight long, arduous years of learning and research. The input, advice and support of numerous people have made this Dissertation possible.

I wish first of all to extend my thanks and appreciation for the funding from the National Science Foundation of this project under grant number BCS-8617408 that made the entire process of achieving my goals possible.

I sincerely thank my major advisor Professor Leonard W. Lion for his advice and help throughout various phases of the work. I also thank co-principal investigators Professor Michael Shuler and William Ghiorse for their guidance, discussions and suggestions. I also thank Professor James Gossett for serving on my committee.

The help and friendship of colleagues in the Environmental Engineering group, friends and neighbors at Cornell, in Ithaca, and at the University of North Carolina at Charlotte has been much appreciated. The assistance and technical discussions with Monroe Weber-Shirk as well as his friendship make life in the lab just a bit easier. The friendship of Tom DiStefano and David Freedman and their help in operating the HPLC is gratefully acknowledged. Sharing the trials and tribulations of this Ph.D. program certainly created a new perspective on life.

I thank Carolyn Acheson and Bertha Rodriguez for assistance in collecting data from the cyclic-flow experiments, Maria Cochran and Mary Elizabeth Grace for performing direct cell counts on bioreactor slides, Alicia Kowalchuk for gathering data on pH dependency of a bacterial strain of *Pseudomonas*. Sharon Best in the Section of Microbiology provided

technical assistance and David Emerson in Microbiology helped with the early stages of the project during bacterial strain screening. The help of Jeff Fu in the Biochemical Engineering Group preparing the bioreactor and with medium component revision is appreciated. I gladly acknowledge the assistance of Ke Ming Hsieh (currently associated with Amoco Oil), Anthony Pelliccia and William A. Sparger (both of UNC-Charlotte) in getting the original bacterial model finally and fully operational after many long and frustrating hours of work on the VAX/VMS mainframe computer.

I would like to thank Louise in the graduate Financial Aid office in Sage Hall and Allen Gerwich at Tompkins County Trust Company for their financial advice and assistance in making it possible to remain at Cornell and continue toward my goal. The fiscal unrealities of the situation would have been unbearable without their help. The fiscal help from the American Society of Civil Engineers Research Fellowship program is also gratefully appreciated. I also wish to extend my thanks and appreciation to Dr. Ellis King, Diane Aldridge and the rest of the members of the Department of Civil Engineering at UNC-Charlotte for their help, tolerance and patience in allowing me to complete this work and still retain my faculty position. The assistance of Subramanian Kalyansundaram in compiling the complete bibliography of this manuscript is also greatly appreciated.

I reserve the majority of my appreciation for my family, especially my wife Christine, who put up with the reality of the decision to return to Graduate School to pursue my dream, after my last place of employment began to close, and was at least outwardly supportive of the decision despite our difficult five years in Ithaca.

The birth of our second son Stefan, along with our oldest son, Joseph, provided the bright spot in our lives in what otherwise seemed like a rather bleak existence. Their love and common sense prevail, making their contributions to this thesis and our family life immeasurable beyond compare.

Finally, while I owe nearly all of my current success to my wife, Christine, I am at this juncture in life today in no small part because of my father, Anton, and his mother, Mary, my grandmother. They both instilled in me a drive, determination and work ethic of which they would be proud. Unfortunately, both have passed on and neither is around to see this accomplishment or to see what more I may yet achieve. To them, my family, and especially Christine, I humbly dedicate this work.

TABLE OF CONTENTS

	<u>Page</u>
Abstract	iii
Biographical Sketch	vi
Dedication	viii
Acknowledgments.....	ix
Table Of Contents.....	xii
List of Tables	xvi
List of Figures.....	xvii
Chapter 1. General Introduction.....	1
Chapter 2. Background.....	5
Introduction	5
pH Effects on Microbial Growth.....	6
Planktonic Cell Growth Related to pH.....	11
Adherent Cell Growth Related to pH.....	22
pH _e Interactions Between Metal Ions and Cells in Solution.....	29
Modeling Bacterial Cell Growth and pH Dependency	33
Enzyme Models and pH Dependency	34
References	41
Chapter 3. Selection of a Biopolymer Producing Freshwater Bacterial Strain	51
Abstract.....	51
Introduction.....	51

Modelling Reactor Operation	53
Experimental Materials and Methods	55
Development of Minimal Mineral Salts (MMS) Medium	55
Bacterial Strains	56
Screening Metal Toxicity of Selected Bacterial Strains	59
Selection of Attachment Surface	60
Chemical and Microscopic Analyses of Cell Growth and Biofilm Formation	60
Bioreactor Design and Construction	62
Preparation of the Bioreactor for Experiments	65
Results and Discussion	67
Reactor Modelling Calculations	67
Culture-Metal Toxicity Results	73
Cyclic-Reactor Experimental Results	80
Conclusions	93
References	95
 Chapter 4. A Computer Model of The Growth of <i>Pseudomonas cepacia</i> 17616 and its Attachment to Solid Surfaces	
Abstract	100
Introduction	100
General Model Development	101
Modelling pH Dependency	103
Metal Behavior and pH Dependency	109

Derivation of Model Parameters.....	110
References	117
Chapter 5. Computer Simulations of the Growth of <i>Pseudomonas cepacia</i> 17616	
and its Attachment and Interactions With a Trace Metal	121
Abstract.....	121
Cellular Growth Without Metals	122
Cellular Growth With a Trace Metal.....	188
Discussion.....	248
References	250
Chapter 6. Summary and Recommendations for Future Research.....	251
References.....	261
Appendices	
I. Interactions of Microbial Biofilms With Toxic Trace Metals.....	262
Abstract	262
1. Modelling Microbial Cell Growth, Attachment, and Production	
of Extracellular Polymer	263
Introduction	263
Model Development.....	265
Materials.....	273
Organism.....	273
Media.....	273
Batch and Continuous Culture	274

Bioreactor Design	275
Derivation of Model Parameters.....	276
Discussion	288
2. Modelling Lead(II) Distribution in the Presence of Microbial Activity	295
Introduction	295
Materials.....	296
Model Development and Derivation of Model Parameters.....	296
Model Predictions and Comparison to Experiment	304
Conclusions.....	308
Acknowledgements.....	309
Nomenclature.....	310
References	314
II. Description of the Integrated Model With pH-Dependent Growth	
Routines	321
Reference.....	326

LIST OF TABLES

	<u>Page</u>
Table 3.1: Composition of Minimal Mineral Salts (MMS) Growth Medium	57
Table 3.2: Bacterial Strains Showing Growth on MMS Medium.....	58
Table 3.3: Bacterial Strains Selected for Toxicity Tests in Liquid Culture in the Presence of Various Concentrations of the Metal Lead.....	74
Table 3.4: Comparison of Biofilm Development on Glass Slides, as Indicated by Colloidal Iron-Cacodylate Stain After 14 Days. Growth on MMS Medium in the Cyclic-Flow Reactor.....	89
Table 3.5: Comparison of Biofilm Development on Glass Surfaces in Batch, Continuous Flow and Cyclic Flow Reactor Operation Using Pyruvate as Carbon/Energy Source in MMS Medium	91
Table 3.6: Growth Of <i>Arthrobacter 9G4D</i> On Pyruvate In MMS Medium Under Cyclic-Flow Conditions With Different Surface Materials	92
Table 4.1: Model Parameters Associated with pH-Dependent Rate Equations.....	111
Table 4.2: Initial Conditions for the pH-Dependent Bacterial Model.	112
Table 5.1: Trace Lead Speciation in MMS Medium Under Batch Solution Conditions with Variable pH Levels in The Absence of a Biophase.....	189
Table A1.1: Values of Model Parameters Associated with Rate Equations.	279
Table A1.2: Initial Conditions for the Bacterial Model.	280

LIST OF FIGURES

		<u>Page</u>
Figure 2.1	Effects of medium pH value on maximum bacterial growth rates: A, <i>Escherichia coli</i> in anaerobic casein hydrolysate medium with buffer control of pH (Pirt, 1975); B, <i>Methylococcus capsulatus</i> grown on methane with pH control by automatic addition of acid or base (Eroshin, Harwood and Pirt, 1968).....	10
Figure 2.2.	Effect of pH on activity and stability of an enzyme. Curve A: v versus pH plot. Curve B: v at pH 6.8 after preincubating the enzyme at the indicated pH values.....	12
Figure 2.3.	Effect of acid and base addition on activity and stability of an enzyme molecule. (Laidler & Bunting, 1973)	21
Figure 2.4.	Cationic—Anionic character of bacterial cells. (Daniels, 1972)	24
Figure 2.5.	Overall pH dependence of a simple one substrate reaction involving enzymes	37
Figure 3.1.	Schematic of cyclic-flow reactor system.	63
Figure 3.2.	Concentrations of substrate (1), suspended cells (2), and attached cells (3) in a Multigen with steady flow. (A) Washout of a nonadherent strain. (B) Washout of an adherent strain with the same growth parameters as in panel A except $k_A = 0.05/h$ and $k_D = 0.175/h$. (C) Selection of a more adherent strain with the same growth parameters as in panel B, except k_D reduced to $0.125/h$	68

Figure 3.3.	(A) Effect of cyclic flow (12 h on, 12 h off) on the adherent cell strain shown in Fig. 3.2B. (B) Selection of the cell strain shown in Panel 3A under cyclic-flow conditions when it is a variant (10% of initial suspended population).	71
Figure 3.4	Toxicity Effects of Various Concentrations of Lead on the Growth of <i>Arthrobacter</i> 9G4D on Pyruvate.	75
Figure 3.5.	Toxicity Effects of Various Concentrations of Lead on the Growth of <i>Pseudomonas cepacia</i> 17616 on Acetate.	76
Figure 3.6.	Toxicity Effects of Various Concentrations of Lead on the Growth of <i>Pseudomonas cepacia</i> 249-100 on Pyruvate.....	77
Figure 3.7.	Toxicity Effects of Various Concentrations of Lead on the Growth of <i>Pseudomonas cepacia</i> 17616 on Pyruvate.	78
Figure 3.8.	Toxicity Effects of Various Concentrations of Lead on the Growth of <i>Pseudomonas fluorescens</i> on Pyruvate.	79
Figure 3.9.	Biofilm surface coverage (in microequivalents of oxidizable material per slide) determined from slides in the bioreactor after 6 days (8 total days) of cyclic-flow reactor operation.	81
Figure 3.10.	Biofilm cell count from slides removed after 6 days (8 total days) of cyclic-flow operation.	84
Figure 3.11.	Fluid-phase optical density after 6 days (8 total days) of cyclic-flow reactor operation.	86

Figure 4-1	Schematic of model component interactions including interactions with hydrogen ions. The arrows associated with H^+ represent pH effects on the speciation or function of the indicated component.	104
Figure 4.2.	Derivation of molecular dissociation constants from the growth curve for <i>Escherichia coli</i> grown on casein hydrolysate.	115
Figure 5.1.	Simulation of Total Suspended Biomass (X) under batch growth conditions in a Multigen reactor under conditions of variations in the pH dependency dissociation constants K_1 and K_2	123
Figure 5.2.	Simulation of Total Attached Biomass (B) under batch growth conditions in a Multigen reactor under conditions of variations in the pH dependency dissociation constants K_1 and K_2	125
Figure 5.3.	Simulation of Suspended Cell (A) growth under batch solution conditions in a Multigen reactor under conditions of variations in the pH without trace metals.	128
Figure 5.4.	Simulation of Suspended Cell Associated Polymer (P) production under batch solution conditions in a Multigen reactor under conditions of variations in the pH without trace metals.	130
Figure 5.5.	Simulation of Surface Attached Cell (A^B) growth under batch solution conditions in a Multigen reactor under conditions of variations in the pH without trace metals.	133
Figure 5.6.	Simulation of Surface Attached Cell Associated Polymer (P^B) production under batch solution conditions in a Multigen reactor under conditions of variations in the pH without trace metals.	135

Figure 5.7.	Simulation of Free Suspended Polymer (P^*) production under batch solution conditions in a Multigen reactor under conditions of variations in the pH without trace metals.	137
Figure 5.8.	Simulation of Surface Associated Free Polymer (P^S) production under batch solution conditions in a Multigen reactor under conditions of variations in the pH without trace metals	139
Figure 5.9.	Simulation of the Limiting Substrate (C^*) usage under batch solution conditions in a Multigen reactor under conditions of variations in the pH without trace metals.	141
Figure 5.10.	Simulation of Suspended Cell (A) growth under steady state solution conditions in a Multigen reactor under conditions of variations in the pH without trace metals.	144
Figure 5.11	Simulation of Suspended Cell Associated Polymer (P) production under steady state solution conditions in a Multigen reactor under conditions of variations in the pH without trace metals.	146
Figure 5.12.	Simulation of Surface Attached Cell (A^B) growth under steady state solution conditions in a Multigen reactor under conditions of variations in the pH without trace metals.....	148
Figure 5.13.	Simulation of Surface Attached Cell Associated Polymer (P^B) production under steady state solution conditions in a Multigen reactor under conditions of variations in the pH without trace metals.....	150

Figure 5.14.	Simulation of Free Suspended Polymer (P^*) production under steady state solution conditions in a Multigen reactor under conditions of variations in the pH without trace metals.	152
Figure 5.15.	Simulation of Surface Associated Free Polymer (P^S) production under steady state solution conditions in a Multigen reactor under conditions of variations in the pH without trace metals.	154
Figure 5.16.	Simulation of the Limiting Substrate (C^*) under steady state solution conditions in a Multigen reactor under conditions of variations in the pH without trace metals.	156
Figure 5.17.	Simulation of Suspended Cell (A) growth in a Bioreactor under batch solution conditions without trace metals at variable pH and $Re = 300$	159
Figure 5.18.	Simulation of Suspended Cell Associated Polymer (P) production in a Bioreactor under batch solution conditions without trace metals at variable pH and $Re = 300$	161
Figure 5.19.	Simulation of Surface Attached Cell (A^B) growth in a Bioreactor under batch solution conditions without trace metals at variable pH and $Re = 300$	163
Figure 5.20.	Simulation of Surface Attached Cell Associated Polymer (P^B) production in a Bioreactor under batch solution conditions without trace metals at variable pH and $Re = 300$	165

Figure 5.21.	Simulation of Free Suspended Polymer (P^*) production in a Bioreactor under batch solution conditions without trace metals at variable pH and $Re = 300$.	167
Figure 5.22.	Simulation of Surface Associated Free Polymer (P^S) production in a Bioreactor under batch solution conditions without trace metals at variable pH and $Re = 300$.	169
Figure 5.23.	Simulation of the Limiting Substrate (C^*) usage in a Bio-reactor under batch solution conditions without trace metals at variable pH and $Re = 300$.	171
Figure 5.24.	Simulation of Suspended Cell (A) growth in a Bioreactor under steady state continuous flow-through solution conditions without trace metals at variable levels of pH and $Re = 300$.	174
Figure 5.25.	Simulation of Suspended Cell Associated Polymer (P) production in a Bioreactor under steady state continuous flow-through solution conditions without trace metals at variable levels of pH and $Re = 300$.	176
Figure 5.26.	Simulation of Surface Attached Cell (A^B) growth in a Bio-reactor under steady state continuous flow-through solution conditions without trace metals at variable levels of pH and $Re = 300$.	178
Figure 5.27.	Simulation of Surface Attached Cell Associated Polymer (P^B) production in a Bioreactor under steady state continuous flow-through solution conditions without trace metals at variable levels of pH and $Re = 300$.	180

Figure 5.28.	Simulation of Free Suspended Polymer (P^*) production in a Bioreactor under steady state continuous flow-through conditions without trace metals at variable levels of pH and $Re = 300$	182
Figure 5.29.	Simulation of Surface Associated Free Polymer (P^S) production in a Bioreactor under steady state continuous flow-through conditions without trace metals at variable levels of pH and $Re = 300$	184
Figure 5.30.	Simulation of the Limiting Substrate (C^*) usage in a Bioreactor under steady state continuous flow-through conditions without trace metals at variable levels of pH and $Re = 300$	186
Figure 5.31.	Simulated effects of variable concentrations of lead on the Total Suspended Biomass (X) [=suspended active cell mass (A) plus associated attached polymer (P)] production in a Multigen reactor under batch growth conditions at pH 5.	191
Figure 5.32.	Simulated effects of variable concentrations of lead on the Total Suspended Biomass (X) [=suspended active cell mass (A) plus associated attached polymer (P)] production in a Multigen reactor under batch growth conditions at pH 7.	193
Figure 5.33.	Simulated effects of variable concentrations of lead on the Total Suspended Biomass (X) [=suspended active cell mass (A) plus associated attached polymer (P)] production in a Multigen reactor under batch growth conditions at pH 9.	195

Figure 5.34.	Simulated effects of variable concentrations of lead on the Total Attached Biomass (B) [=attached active cell mass(A^B) plus attached associated cell polymer (P^B)] production in a Multigen reactor under batch growth conditions at pH 5.....	197
Figure 5.35.	Simulated effects of variable concentrations of lead on the Total Attached Biomass (B) [=attached active cell mass (A^B) plus attached associated cell polymer (P^B)] production in a Multigen reactor under batch growth conditions at pH 7.....	199
Figure 5.36.	Simulated effects of variable concentrations of lead on the Total Attached Biomass (B) [=attached active cell mass (A^B) plus attached associated cell polymer (P^B)] production in a Multigen reactor under batch growth conditions at pH 9.....	201
Figure 5.37.	Simulated effects of variable concentrations of lead on the Total Suspended Biomass (X) [=suspended active cell mass (A) plus associated attached polymer (P)] production in a Bioreactor under batch growth conditions at pH 5 and $Re = 300$	204
Figure 5.38.	Simulated effects of variable concentrations of lead on the Total Suspended Biomass (X) [=suspended active cell mass (A) plus associated attached polymer (P)] production in a Bioreactor under batch growth conditions at pH 7 and $Re = 300$	206

Figure 5.39.	Simulated effects of variable concentrations of lead on the Total Suspended Biomass (X) [=suspended active cell mass (A) plus associated attached polymer (P)] production in a Bioreactor under batch growth conditions at pH 9 and $Re = 300$	208
Figure 5.40.	Simulated effects of variable concentrations of lead on the Total Attached Biomass (B) [=attached active cell mass (A^B) plus attached associated cell polymer (P^B)] production in a Bioreactor under batch growth conditions at pH 5 and $Re = 300$	210
Figure 5.41.	Simulated effects of variable concentrations of lead on the Total Attached Biomass (B) [=attached active cell mass (A^B) plus attached associated cell polymer (P^B)] production in a Bioreactor under batch growth conditions at pH 7 and $Re = 300$	212
Figure 5.42.	Simulated effects of variable concentrations of lead on the Total Attached Biomass (B) [=attached active cell mass (A^B) plus attached associated cell polymer (P^B)] production in a Bioreactor under batch growth conditions at pH 9 and $Re = 300$	214
Figure 5.43.	Simulated effects of variable concentrations of lead on the Total Suspended Biomass (X) [=suspended active cell mass (A) plus associated attached polymer (P)] production in a steady state continuous flow-through Multigen reactor at pH 5.	216

Figure 5.44.	Simulated effects of variable concentrations of lead on the Total Suspended Biomass (X) [=suspended active cell mass (A) plus associated attached polymer (P)] production in a steady state continuous flow-through Multigen reactor at pH 7.	218
Figure 5.45.	Simulated effects of variable concentrations of lead on the Total Suspended Biomass (X) [=suspended active cell mass (A) plus associated attached polymer (P)] production in a steady state continuous flow-through Multigen reactor at pH 9.	220
Figure 5.46.	Simulated effects of variable concentrations of lead on the Total Attached Biomass (B) [=attached active cell mass (A^B) plus attached associated cell polymer (P^B)] production in a steady state continuous flow-through Multigen reactor at pH 5.	222
Figure 5.47.	Simulated effects of variable concentrations of lead on the Total Attached Biomass (B) [=attached active cell mass (A^B) plus attached associated cell polymer (P^B)] production in a steady state continuous flow-through Multigen reactor at pH 7.	224
Figure 5.48.	Simulated effects of variable concentrations of lead on the Total Attached Biomass (B) [=attached active cell mass (A^B) plus attached associated cell polymer (P^B)] production in a steady state continuous flow-through Multigen reactor at pH 5.	226

Figure 5.49. Simulated effects of variable concentrations of lead on the Total Suspended Biomass (X) [=suspended active cell mass (A) plus associated attached polymer (P)] production in a steady state continuous flow-through Bioreactor at pH 5 and $Re = 300$ 229

Figure 5.50. Simulated effects of variable concentrations of lead on the Total Suspended Biomass (X) [=suspended active cell mass (A) plus associated attached polymer (P)] production in a steady state continuous flow-through Bioreactor at pH 7 and $Re = 300$ 231

Figure 5.51. Simulated effects of variable concentrations of lead on the Total Suspended Biomass (X) [=suspended active cell mass (A) plus associated attached polymer (P)] production in a steady state continuous flow-through Bioreactor at pH 9 and $Re = 300$ 233

Figure 5.52. Simulated effects of variable concentrations of lead on the Total Attached Biomass (B) [=attached active cell mass (A^B) plus attached associated cell polymer (P^B)] production in a steady state continuous flow-through Bioreactor at pH 5 and $Re = 300$ 235

Figure 5.53. Simulated effects of variable concentrations of lead on the Total Attached Biomass (B) [=attached active cell mass (A^B) plus attached associated cell polymer (P^B)] production in a steady state continuous flow-through Bioreactor at pH 7 and $Re = 300$ 237

Figure 5.54.	Simulated effects of variable concentrations of lead on the Total Attached Biomass (B) [=attached active cell mass (A^B) plus attached associated cell polymer (P^B)] production in a steady state continuous flow-through Bioreactor at pH 9 and $Re = 300$	239
Figure 5.55.	Effects of a simulated step increase of lead at steady state from 0 to 1×10^{-7} M at a dilution rate of 0.070 hr^{-1} on the concentration of total suspended biomass (X), free suspended polymer (P^*), and the limiting substrate (C^*).	242
Figure 5.56.	Effects of a simulated step increase of lead at steady state from 0 to 1×10^{-7} M at a dilution rate of 0.155 hr^{-1} on the concentration of total suspended biomass (X), free suspended polymer (P^*), and the limiting substrate (C^*).	244
Figure 5.57.	Effects of a simulated step increase of lead at steady state from 0 to 1×10^{-7} M at a dilution rate of 0.240 hr^{-1} on the concentration of total suspended biomass (X), free suspended polymer (P^*), and the limiting substrate (C^*).	246
Figure A1.1.	Schematic of model component interactions. Each numbered interaction is described in the text.	267
Figure A1.2.	Schematic diagram of bioreactor (from Hsieh <i>et. al.</i> , 1985).	277

Figure A1.3. Equilibrium biopolymer adsorption onto glass at different dissolved biopolymer concentrations. The Y axis of the bottom graph is enlarged to show overlap of data points. The initial biopolymer concentrations used were (○) 0.0436 g/L, (●) 0.0218 g/L, (Δ) 0.0104 g/L, (+) 0.00246 g/L, (X) 0.000642 g/L, (◇) 0.00017 g/L, and (*) 0.000467 g/L.....	286
Figure A 1.4. Effect of fluid velocity, as represented by Reynolds number, or equilibrium attached cell density.	289
Figure A1.5. Linear plot for cell attachment parameters at low fluid velocity (Reynolds number is 300).....	290
Figure A 1.6. Attachment of <i>P. atlantica</i> onto clean glass slides from a culture of constant OD = 2. Cellular attachment rate can be estimated from the initial slope as shown: (o) recirculation flow = 8 L/min, Re = 350; (Δ) recirculation flow = 50 L/min, Re = 2200.	291
Figure A 1.7. Equilibrium attached cell density as a function of suspended cell concentration at Reynolds number of 300.	292
Figure A1-8. Schematic of model component interactions in the presence of metal. The arrows associated with M* represent binding with each component.	297
Figure A 1.9. Equilibrium lead adsorption onto glass and bioreactor walls. (From Hsieh, <i>et at.</i> , 1985). (○) adsorption onto glass and bioreactor walls (●) adsorption onto walls only	299

Figure A1.10. Equilibrium lead adsorption onto bacterial cells. Gamma is adsorbed lead in moles per cell. Data are corrected for lead binding to dissolved organics (see Lion & Rochlin, 1989). Original data were obtained from Rochlin, 1986..... 301

Figure A1.11. Schematic of information flow in the integrated model. 305

CHAPTER 1

GENERAL INTRODUCTION

The hydrogen ion concentration in a freshwater environment can be altered or affected by many influences including algal photosynthesis and respiration, stormwater runoff, acid rain, and acid mine drainage. The following hypothetical scenarios and the associated questions provide a basis for understanding objectives for research into pH effects: Consider the development of a river system that starts high up at the headwaters of a watershed. Water runs off the land into the stream carrying nutrients (organics and minerals) that allow the development of an indigenous population of freshwater bacterial species. These bacteria exist in the water, coating submerged structures, rocks and even suspended particulate matter. At some point, an influx of toxic trace metals originates from the remnants of a mining operation or a metal influx occurs as the stream/ river passes through a community, or a storm event sends surface runoff cascading off streets and parking lots into storm drains and out into the stream/river. We wish to know how the ecosystem of the stream or river is affected. What effects do the metals or the changed environmental pH conditions have on the growth of indigenous microbial populations? How do the microorganisms adapt to the changed environment? Can the bacterial species and bacterial products such as extracellular ligands react with metals to reduce their toxicity? These questions all have important ecological implications. Answers to some of the questions may also provide insight into ways to use the bacterial species to mitigate the effects of toxic metals. The present research was aimed at exploring a subset of the possible effects of altered environmental conditions upon the growth of freshwater

bacterial species and their subsequent interactions with trace metal species. The objectives of this research study were aimed at predictive modelling of interactions between trace metal adsorption and bacterial attachment to inanimate surfaces under conditions of variable pH using realistic growth rate constants and other parameters as needed to illustrate how metals in an aqueous environment may impact the rates of cellular growth, attachment and production of biopolymer.

The presence of many trace metals in natural and waste water systems is of keen interest, primarily because of their known toxicity and their impact upon receiving water bodies. Increasing concern over the effects from inputs of metals to natural systems from storm water runoff and a corresponding increase in Federal Regulations designed to prevent the runoff provide an additional incentive for understanding metal impacts. A predictive capability for quantifying how trace metal variations in form and concentration might affect a given water system is essential if metal fate and transport is to be understood. A predictive capability can also be applied to direct efforts to use bacterial species as a means to remove and/or recover the metals.

Although a predictive capability for an actual freshwater system is ultimately desired, the objective of the current research focused on a more fundamental study of the interactions and growth characteristics of adherent freshwater bacteria in the presence of metals. The approach adopted for this study involved an integration of experiments and mathematical modeling. Due to the complexity of natural systems, the problem was simplified to a manageable level by utilizing an experimental system consisting of a single bacterial species, a homogeneous solid surface and an aqueous phase of known chemical composition. This

simplification of the system allowed development of a mechanistically based mathematical model.

This thesis is organized into four major sections. Chapter 2 provides a discussion of the relevant literature on the effects of pH on microbial growth and association with solid surfaces. Chapter 3 presents an experimental study to select a model bacterial species for use in highly controlled experiments with stringent, chemically-defined growth conditions. The approach emphasized a rigorous screening procedure to test candidate species to find a suitable adherent organism with good growth capabilities and tolerance to a toxic trace metal.

In Chapter 4, an existing structured mathematical model that relates interactions of a bacterial species with inorganic surfaces and toxic trace metals in a sea water medium is discussed. This model is used as a basis for creation of a model for cell growth and attachment applicable to freshwater aquatic systems at variable pH. The pH-dependent interactions of toxic trace metals with microbial components and surfaces are also reviewed in this chapter.

In Chapter 5, the model results are generated under both steady-state and transient conditions and compared to responses of similar species in a seawater matrix.

The final chapter (Chapter 6) summarizes the conclusions drawn from the model simulations and suggests extensions of this research for use in process and experimental design. Some of the broader implications of this work as it relates to the world outside the laboratory setting are discussed.

Appendix chapters contain a printed version of the model discussed in Chapter 4, a detailed discussion of model modifications, and a discussion of the methods used to estimate the kinetic parameters.

CHAPTER 2

BACKGROUND

Relevant experimental and theoretical literature relating to the pH dependence of bacteria in their growth and association with surfaces is discussed in this chapter. The discussion emphasizes the biological characterization of the microbial process at scales ranging from the enzymatic level to that of whole cell cultures. The information presented provides the conceptual framework for the interpretation of the results presented in this thesis.

INTRODUCTION

Environmental extremes abound on our planet. Bacterial or cellular life can be very tenacious. Bacteria can be found nearly anywhere water is found in a liquid state. The conditions that provide for optimal growth of each organism often differ extensively (Shuler & Kargi, 1992).

Some cells can grow at temperatures as low as -20 degrees Celsius ($^{\circ}\text{C}$) while others live at temperatures approaching 110 $^{\circ}\text{C}$. Some bacteria grow only where water activity is high, while others can grow on barely moist solid surfaces or at high salt concentrations (Shuler & Kargi, 1992). Many organisms have pH optima far from neutrality; some prefer pH levels as low as 1 or 2 while others grow well at pH exceeding 9 or 10. Levels of oxygen available to the cells, the level and type of nutrients and their influence on the metabolic pathways of cells all play a role in how a particular living cell exists and functions in its environment.

The flexible nature of bacterial cells enables researchers to exploit biological diversity in controlled and useful ways. The present state of research into cellular activity

has emerged as one that incorporates principles of physics, chemistry and engineering. A useful paradigm has been to view microorganisms as expanding chemical reactors that take in chemical species (nutrients) from the environment, grow, reproduce, and release products into the surroundings (Baily & Ollis, 1986). The perspective of bacteria as chemical reactor systems leads to the development of quantitative, mathematical models as a predictive tool for bacterially-mediated reactions.

For this research, the situation of interest involves adherent freshwater bacterial cells growing in a solution containing toxic trace metals subjected to changes in hydrogen ion concentration. To model this scenario, it is useful to first consider the complex internal nature of the bacterial cell and the cellular effects of changes in hydrogen ion concentration.

pH EFFECTS ON MICROBIAL GROWTH

Cells contain large numbers of small molecules (water, inorganic ions and organic substances), but consist primarily of very large polymeric molecules (Brock & Madigan, 1988). The cell may obtain most of the small molecules from the environment, but all the large molecules are synthesized within the cell. The synthesis process requires energy that is used in various ways to assemble smaller molecules into complex, longer chains. In order to complete the synthesis process, bonds of reactant materials generally must be broken prior to recombination. There will usually be a significant activation energy involved to break bonds. The cell minimizes the energy it must expend by employing organic materials called enzymes to lower the activation energy required to break bonds (Sundstrom & Klei, 1979). Most reactions in a cell will not occur at appreciable rates

without the use of enzymatic catalysts. Enzymes are quantified in terms of their activity (ability to catalyze a process) and/or stability (residual activity).

Enzymes can accelerate or inhibit any particular reaction depending upon chemical conditions. They provide an alternate reaction mechanism (with lower activation energy) in which reactant molecules are brought in close proximity at the enzyme active site. This site is composed of ionizable functional groups (Segal, 1976). These groups can include carboxyl and/or amine groups. The functional groups of the enzyme's active site must be in a suitable form to maintain the conformation of the site in order to bind the substrates and catalyze the reaction. Substrates may also have ionizable groups such that there is only one ionic form of the substrate which may bind to the enzyme site (Segal, 1976). Unlike inorganic catalysts, however, enzymes are relatively fragile compounds that can be inactivated by any of several different conditions, including (but not limited to): moderate temperature increases, concentrations of various preservatives, the presence of metal ions, increased shear stresses from excessive mixing, and a high or low extreme in pH (Sundstrom & Klei, 1979).

If one considers natural aquatic systems, with some exceptions, shear from mixing is unlikely to influence enzyme kinetics. In engineered plants, this would be a controllable factor. Temperature effects may also prove negligible in many cases because of limited ranges of temperature found in both engineered plants and in nature (Sundstrom & Klei, 1979). Most bacterial enzymes maintain viable activity at temperatures as high as 80°C before they rapidly break down and no longer function (Sundstrom & Klei, 1979). Both natural and most engineered systems will likely operate below this extreme. Preservatives would unlikely be a problem to cells except in a laboratory setting. Pirt (1975) did find evidence in studies with Multigen cultures that some inhibitors (chloride ions; and divalent or trivalent metal

ions) would alter the amount of enzymes (alpha-amylase and fumarate hydratase) in a cell. Metals can influence enzyme activity, but such effects would be significant only under specific circumstances (*i.e.*, conditions where free metal ion activations are high). The last factor noted above, variation in pH, may have a more widely encountered significant affect upon enzyme activity and enzyme stability.

The overall analysis of pH effects on enzymes can be complicated; carboxyl and amine functional groups are both actively affected by solution pH (Sundstrom & Klei, 1979). This in turn will affect the overall velocity of the enzyme catalyzed reaction (Dean & Hinshelwood, 1966; Segal, 1976; Shuler & Kargi, 1992). A shift in solution pH can change the ionic form of the active site (Shuler & Kargi, 1992) due to protonation or deprotonation of the functional groups on the enzyme (Chitnis & Sadana, 1989) or enzyme-substrate complexation (Mahler & Cordes, 1966). Variation in pH will influence electrostatic bonds between ionic species and hydrogen bonds at the enzyme active sites (Tanford, 1968; Chitnis & Sadana, 1989).

A change in protonation can also cause conformational changes in the enzyme due to changes in the secondary (structural configuration of amino acid sequence resulting from hydrogen bonding of residues affecting sheet structure stability and resistance to stretching) and tertiary structure of the protein (3-dimensional structure resulting from folding or bending of amino acid chain) (Tanford, 1968; Baily & Ollis, 1986; Chitnis & Sadana, 1989; Shuler & Kargi, 1992). Baldwin and Eisenberg (1987) reported protein stability decreased sharply in acidic and basic ranges because of the proton participation in the unfolding process. The basis for this proposal was the difference in pK values for native and unfolded protein species. Positive functional groups near the active site would tend to repel the H⁺ ion in solution

causing the pK to decrease while negative groups would attract H⁺ ions in solution causing the pK to increase. The overall charge density of the protein would decrease as it expanded to occupy a larger volume when it unfolded.

Most enzymes have a maximum activity over a pH range between 6.5 and 8.5 (Sundstrom & Klei, 1979). Enzyme activity diminishes on either side of the narrow range (Mahler & Cordes, 1966). At very high or very low pH values, irreversible changes leading to enzyme destruction or inactivation often set in. If the pH variation is only minor, the enzyme content in the cells may change accordingly to try and maintain the same overall level of activity. For example, more urease and catalase enzymes can be formed to compensate for decreased activity of individual enzymes at an adverse pH (*i.e.*, one not at the optimum) (Segal, 1976; Pirt, 1975). Cells grown at an adverse pH and tested for these enzymes under favorable pH conditions will show a higher activity for these enzymes than cells grown and tested at a favorable pH level (Dean & Hinshelwood, 1966). Pirt (1975) reviewed batch culture studies of *Escherichia coli* grown on casein hydrolysate performed by Gale & Epps (1942) and found that the optimum pH for induction of amino acid decarboxylase was acidic (pH = 5) while in the same cell, the optimum pH for induction of a deaminase was alkaline (pH = 8); hence, they surmised metabolic changes tended to regulate the medium pH towards neutrality to accommodate the simultaneous existence of both types of enzymes. Curve A in Figure 2.1 illustrates these results. From their observations, Gale & Epps (1942) suggested that within a cell the amount of enzymes are regulated in order to maintain some nearly constant level of maximum enzyme activity about circumneutral pH to compensate for the effects of small variations in the medium pH. Similar studies by Eroshin, Harwood and Pirt (1968) with *Methylococcus capsulatus* grown on methane with pH control

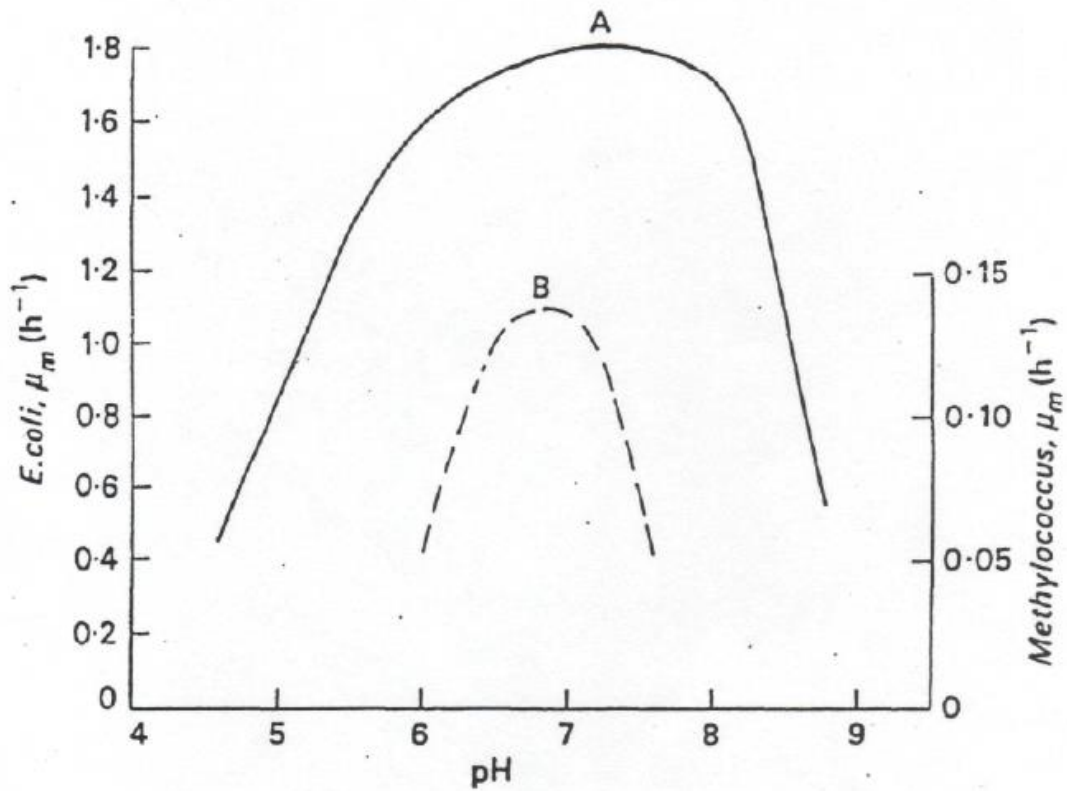


Figure 2.1 Effects of medium pH value on maximum bacterial growth rates: A, *Escherichia coli* in anaerobic casein hydrolysate medium with buffer control of pH (Pirt, 1975); B, *Methylococcus capsulatus* grown on methane with pH control by automatic addition of acid or base (Eroshin, Harwood and Pirt, 1968).

(Curve B in Figure 2.1) reinforced the tendency of cells to regulate pH toward circumneutral conditions during growth. In both cases, maximum growth rate was approximately constant over a range in pH. Segal (1976) also studied the effects of pH on the stability of cellular enzymes. *Escherichia coli* cells grown at a pH of 6.8 exhibited an optimum or maximum enzyme activity. Curve A in Figure 2.2 indicates that the results of Segal's work mirrored the results obtained by Pirt (as shown in Figure 2.1). He further compared this result to measured activity of enzymes from *E. coli* pre-incubated at pH = 5 or pH = 8. The resultant activity of the enzyme was about the same as the enzyme in cells grown at pH = 6.8, but constant in the range of pH of 5 to 8 (see curve B in Figure 2.2). Segal (1976) found that the preincubation had no measurable effect on the maximum overall activity measured at pH 6.8, only on the range over which the maximum activity would occur. The drop in activity in Curve A was attributed to improper formation of the ionic form of the enzyme and/or the substrate, and the activity drop in Curve B to partial irreversible enzyme inactivation.

Unpublished data collected by Pirt (1975) also showed that the amount of certain glycolytic enzymes in steady state Multigen studies of *Lactobacillus* varied several fold with changes in medium pH in a fashion similar to the results of Segal. A pH stability study similar to that of Curve B in Figure 2.1 is an important part of any enzyme characterization; unfortunately it is often omitted (Pirt, 1975; Segal, 1976).

PLANKTONIC CELL GROWTH RELATED TO pH.

It is possible to take the view that the only approach to the study of cellular mechanisms is in the isolation of individual enzymes with detailed study of their mode of action. However, Dean and Hinshelwood (1966) questioned whether this method could lead to the

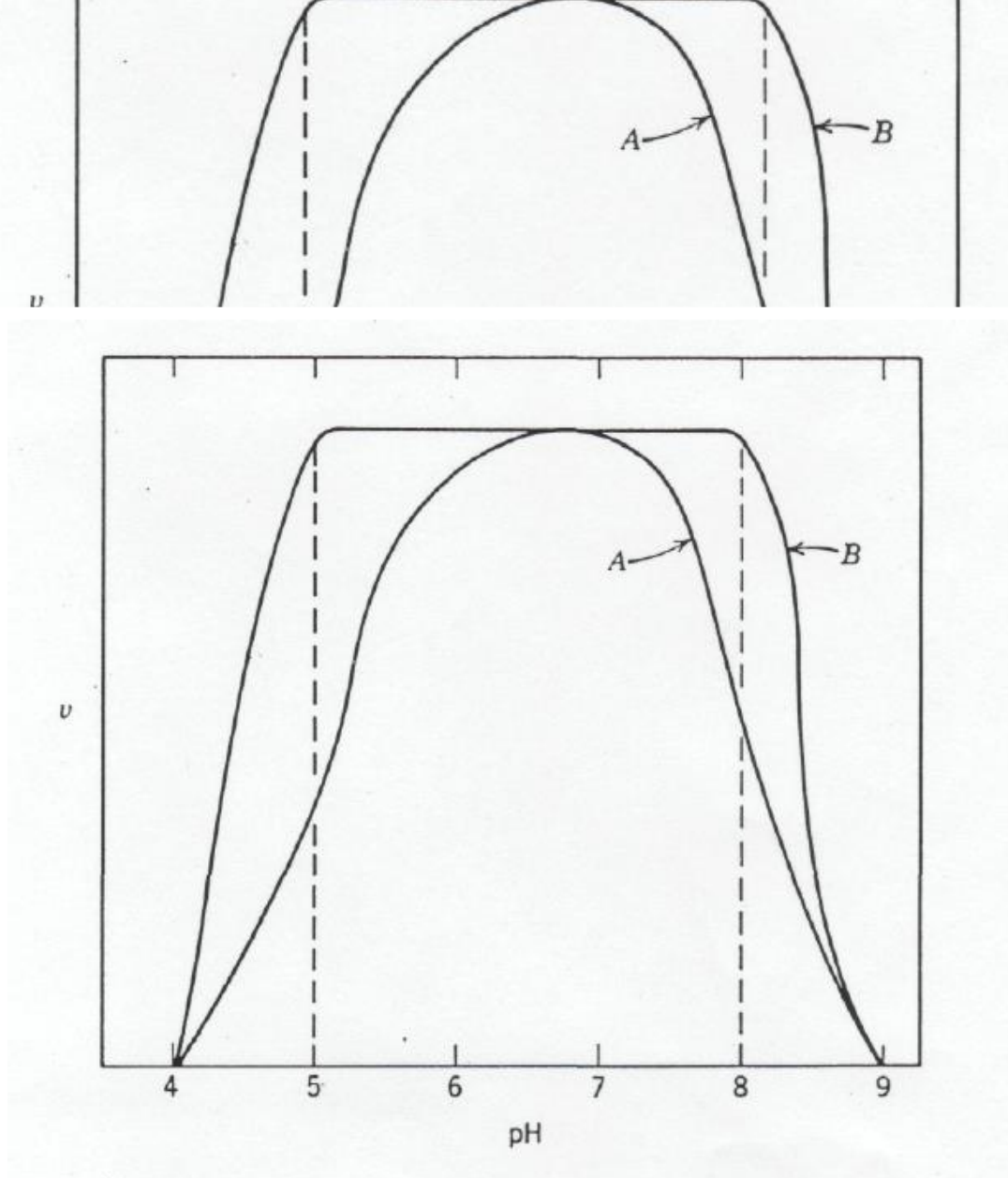


Figure 2.2. Effect of pH on activity and stability of an enzyme. Curve A: v versus pH plot. Curve B: v at pH 6.8 after preincubating the enzyme at the indicated pH values. (Segal, 1976)

solution of a central problem of how the cell is organized to display the characteristics by which it is recognized as living. The supposition is that the study of dismembered parts is valuable, but this approach in and of itself is unlikely to be sufficient. The pH control in many prior studies of cell cultures has been poor and/or the pH has not truly been constant (Pirt, 1975). Avoiding pH drift within the limits of recognized control methods has been the general norm. In the laboratory, methods such as using pH buffers (phthalate for $\text{pH} < 6$; phosphate for $6 < \text{pH} < 8$ and borate for $\text{pH} > 8$; or carbonate and/ or phosphate to simulate natural systems), balancing acid-base products, or automatic addition of an acid or base have been used to remove variable pH as an effect on cell growth or to avoid its influence on some other process under study (Sawyer, *et al.*, 1994).

The simplest bacterial cells are capable of conducting some 2,000 different complex reactions; some human cells can perform 50-100,000 reactions (Sundstrom & Klei, 1979). Many of these reactions, as noted above, require utilization of enzyme catalysts to provide active reaction centers that are regenerated at the end of a closed reaction sequence. Bacterial cells are observed to have overall growth curves that reflect the pH dependence for the activity of individual enzymes (see Figure 2.2) (Pirt, 1975).

With the understanding of how enzymes are affected by changes in pH, Dean and Hinshelwood (1966) suggested that perhaps the best way to understand pH effects on cells is to observe the cell in action. A salient feature of cell kinetics is that it is a self-regulating process. The proportions of enzymes, nucleic acids and other essential structural elements vary in response to environmental changes so as to maintain a specific biomass growth rate (Pirt, 1975).

Medium pH cannot affect the total amount of any of the essential nutrient components, although it may cause wide changes in speciation and consequently in the availability of some nutrients (Dean and Hinshelwood, 1966). This in turn can affect both the biomass composition and the nature of the cellular metabolism, although Pirt (1975) indicated the overall basis of the change is not well understood.

Medium pH has as its principal influence and effect on cell proteins, and consequently on enzyme activity. One of the most important pH effects is on the structure and permeability of the cell membrane proteins that surrounds the enzymes of a cell (Bu'lock and Kristiansen, 1987; Pirt, 1975). The protein structural changes may alter the strength and the ability, or mode, of prosthetic group binding to the surface functional groups of the cell membrane proteins (Mahler & Cordes, 1966). This will in turn affect cellular transport processes, cell-mediated reactions and hence the overall cell growth rate (Bailey & Ollis, 1986; Leelasart & Bonaly, 1988).

Internally, the cell dissociates water to generate H^+ ions needed during the reduction of O_2 to H_2O at the termination of the electron transport system in a cell. The consumption of H^+ causes a net formation of OH^- inside the membrane. The cell plasma membrane, however, is not freely permeable to hydrogen or hydroxide ions despite their small size, so a pH gradient exists across the membrane (Pirt, 1975; Brock and Madigan, 1988). The lack of diffusive transport of H^+ and OH^- ions across the membrane means an equilibrium concentration of the ions cannot be spontaneously restored. The inside of the cell becomes electrically negative and alkaline and the outside of the cell electrically positive and acidic (Brock & Madigan, 1988). These hydrogen ion gradient results in an

electrically energized state of the membrane surrounding the cell expressed as a proton motive force (in volts). This state is similar to the energized state of a battery expressed as its electromotive force (in volts) (Brock & Madigan, 1988).

The energized state of the membrane induced as a result of the electron transport processes can do useful work in the cell such as ion transport, flagellar rotation, or it can be used to drive the formation of high-energy phosphate bonds in Adenosine Triphosphate (ATP). The ATP reaction requires the use of a membrane-bound enzyme, an *ATPase* that contains the reaction subunit on the inside of the membrane and a proton-conducting tailpiece that spans the membrane (Brock & Madigan, 1988). In ATP formation, controlled reentry of protons is allowed across the energized membrane; while when ATP is required to release energy needed for cellular operations, protons are passed to the outer portion of the membrane. Van Loosdrecht, *et al.* (1990), estimated that production of 1 gram of cells would cost the cell about 0.1 mole of ATP and, if generated by the proton motive force, would require 0.3 to 0.6 moles of hydrogen ions be processed through the cell membrane. A release then of only 1% of the hydrogen ions (added to the medium) could result in a substantial pH shift in the medium that could be easily detected, but usually is not measured (Van Loosdrecht, *et al.*, 1990).

The bacterial cell function is dependent on maintaining an appropriate intracellular pH (termed pH_i) despite what may occur with regards to an external pH of the medium (termed pH_e) (O'Hara, *et al.*, 1989). Dean and Hinshelwood (1966) performed experiments using radioactive carbon tracers to illustrate the effects of lowering pH_e on cells actively metabolizing glucose. Under normal conditions of little or no change in

pH_e, the cell takes in positively charged alkali ions (*e.g.*, potassium for the strain *Aerobacter aerogenes*), balanced by simultaneous entry of negatively charged phosphate ions (Dean and Hinshelwood, 1966). The alkali ions become bound on a structure at the enzyme surface where phosphorylated intermediates arising from metabolism of the carbon source in the medium are further processed for synthesis of vital cell components (*e.g.*, nucleic acids). However, as the lowering of the pH_e proceeds, cellular substrate metabolism and phosphorylation activity is lowered due to competition from the hydrogen ions. Once internal cell readjustments have taken place, there is an increased uptake of alkali metal ions to compensate for the change in hydrogen ions. During growth or fermentation, however, a stage is reached when the increase in concentration of H⁺ (or drop in pH_e) is too great for compensatory adjustments by the cell and the enzyme reactions by which phosphate is incorporated into the cell material slow down. Alkali metal ions that otherwise would be released remain in the cell and increase in concentration, the ions serve to protect the cell against the adverse pH_e effects. They are released only when cell growth/fermentation processes are stopped.

Kakinuma (1987) reported that the overall regulation within the cell to a narrow pH_i range requires a cationic transport system, such as a Na⁺/H⁺ or K⁺/H⁺ antiport system to help regulate pH_i. The antiport system allows for the simultaneous transport of the two materials in opposite directions and is mediated by a common carrier (Neidhardt, *et al.*, 1990; Brock & Madigan, 1988; Wu, *et al.*, 1993). Antiport processes can be gradient driven or electrogenic. Some bacterial species like *Streptococcus faecalis*, which has no respiratory chain, combine proton transport via an antiport system with

proton extrusion via a proton-translocating *ATPase* to keep a near constant pH_i as pH_e fluctuates (Kakinuma 1987).

The entrance or exit or production as a metabolic by-product of a weak acid or base can also alter the proton balance inside the cell disturbing pH_i (Wu, *et al.*, 1993). While any precise relationship between pH homeostasis and acid medium tolerance is not well understood, genetic and biochemical studies point to internal pH maintenance as playing a central role (O'Hara, *et al.*, 1989).

Cases of $pH_e < pH_i$ are far more numerous than cases of $pH_e > pH_i$. Weak acids and bases from cellular metabolism can accumulate in the culture medium of long term and high cell density cell cultures causing low values of pH_e (Wu, *et al.*, 1993). Dean & Hinshelwood (1966) noted adverse pH_e had its principal influence upon cell proteins, and enzyme activities associated with the protein production would be strongly dependent upon the pH_e . One might then expect the changes in pH_e would markedly affect the cellular growth rate while having little effect on the resultant total cell population produced (compared to growth at a favorable pH_e). The change in rate would only affect the length of time to achieve the same total cell population and not the magnitude of the population (Dean & Hinshelwood, 1966).

This is not the generally observed effects, however, due in part to maintenance of a near constant pH_i . Changes in pH_e cannot alter the total supply of any of the essential nutritional components, only the rates that they are used (although pH_e variations may cause significant changes in the availability of some nutrients). The near constant pH_i means the

cellular growth rate will remain about the same as when growth would occur at a favorable pH_e .

However, an adverse pH_e may make the growth process much more sensitive to the action of toxic agents (Dean & Hinshelwood, 1966). The pH_e will also affect protonation of surface acidic or basic functional groups of the cell and therefore affect cation exchange reaction between the cell wall and the external solution. Both effects would lead to a reduction in the total cell population produced.

Dean & Hinshelwood (1966) examined the effect of pH_e on the bacteriostatic action of acridine derivatives upon the growth of *Escherichia coli*. Over the range in pH_e in which bacteriostatic action showed great changes, the drugs were found to be much less effective in acid environments than in a neutral or slightly alkaline solution even though there was little change in the degree of ionization of the drug (corresponding to a dominant cationic form). The study further determined the positively charged acridinium ion was the active molecular species. An early study by Albert, *et al.* (1945) had suggested a competition between the hydrogen ions and acridinium ions for negative centers in the proteins comprising the cell wall. A more recent study by Beveridge (1988) confirmed this effect. He reported that electropositive aminoglycoside antibiotics affected protein synthesis by perturbing the cell outer membrane allowing easier access of the drug to the protoplast affecting protein synthesis.

Dean & Hinshelwood (1966) had developed acid-base equilibrium expressions to demonstrate that the concentration of a drug to produce a fixed level of inhibition should increase in proportion to the concentration of the pH_e . Using the data from Albert, *et al.*

(1945), they found for *E. coli* a tenfold increase in drug concentration corresponded to a 1.2 pH unit increase (rather than an expected 1.0 pH increase). Data for *Aerobacter aerogenes* in a synthetic medium showed the tenfold drug increase corresponded to only a 0.7 pH unit increase. In these cases, the variation from a supposedly direct linear relationship between the acridine derivatives and the pH_e was likely influenced by the effects of buffer salts in the medium and/or the dissociation constant of the protein involved in the reaction (Dean & Hinshelwood, 1966).

The evidence in the literature indicates the pH value in a cell's cytoplasm is maintained within a very narrow range. The range can be related to the medium pH_e for optimal cell growth: (Kakinuma, 1987)

acidophiles — pH 6.5 - 7.0

neutrophiles — pH 7.5-8.0

alklophiles — pH 8.5 - 9.0

Beveridge (1981) summarized several physical studies of bacteria that illustrated the charged nature of cell walls. Addition of soluble polyvalent metals (*e.g.*, Fe^{+3}) caused the normally electronegative charged cell surface to become electropositive. At low ionic levels, the bacterial cell surface charge is dominated by the fixed ions in the wall; but at high ionic levels, the wall becomes saturated with exogenous salts with a corresponding increase in the wall permeability. Many bacterial cell walls are rich in amino (NH_3^+), phosphate (PO_4^{-3}) and carboxylate (COO^-) groups (Beveridge, 1981; Beveridge, 1988). These and other ionizable functional groups will react with soluble polyvalent cations, especially metals, in the environment. This combination of surface

functional groups and surface electrogenic charge creates electrostatic forces that bind compounds, including hydrogen ions, at cell walls (Leelasart & Bonaly, 1988; Beveridge, 1981).

The pH effect on cell behavior can be explained by postulating that only the enzyme with all functional groups in the ionized form is active and all other combinations are inactive (Laidler & Bunting, 1973; Laidler, 1987). If one supposes, for example, that the active part of the enzyme consists of a basic group such as -COO^- and an acid group such as -NH_3^+ , the active enzyme may be represented by the combination of both ionic forms attached to a backbone structure. Upon reaction with an added acid, the -COO^- group may protonate to form -COOH . The addition of a base may strip hydrogen away from the amino group to form -NH_2 . The resultant reactions that may occur are illustrated in Figure 2.3. Only the $\text{COO}^-/\text{NH}_3^+$ form is hypothesized to be active. Both the left and right combinations shown in Figure 2.3 are considered inactive. It follows that the rate of enzymatic activity will go through a maximum as the pH_e is varied and the optimum pH_e occurs when the concentration of the intermediate enzyme form is also at a maximum (Laidler & Bunting, 1973).

Some bacterial strains are more acid tolerant than others. It generally has been demonstrated they have a better ability to maintain a constant pH_i . The tighter the control of pH_i , the better the acid tolerance (O'Hara, *et al.*, 1989). In strains lacking tight control, inhibitory compounds can affect the pH_i . For example, the acid tolerant soil strain *Sarcina ventricula* survives well at pH 3.5. If acetate becomes available at pH levels below the pK_a (4.725) of acetate, more of the protonated form of acetate exists in solution and is capable of passive entry into the cell. The cell wall is reasonably permeable to acetic acid.

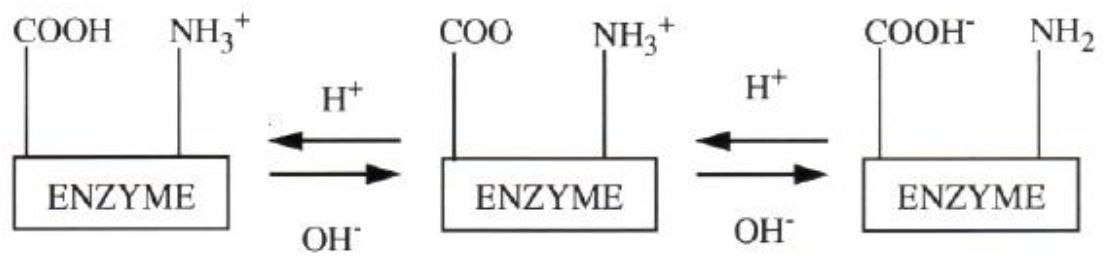


Figure 2.3. Effect of acid and base addition on activity and stability of an enzyme molecule. (Laidler & Bunting, 1973)

Inside the cell, the acid ionizes decreasing the pH_i from its optimum. The cell cannot excrete the acetate ions formed and the pH gradient across the cell wall is not maintained. The cells stop growing and further product formation ceases (Kruse, 1988). The overall pH control exerted by many cultures in nature exists as a result of the environmental conditions that they experience. Some of the control mechanisms (or other desired properties) of wild-type bacteria may be lost as the cultures adapt to laboratory conditions. The loss may in turn have a cascade effect in altering other metabolic systems within the cell. Therefore, natural sources for cultures cannot be readily employed as the primary source of organisms for the study of pH effects (Adams & Ghiorse, 1986). Studies of cell growth and pH control typically are conducted with genetically and physiologically stable laboratory-adapted strains to be able to ensure reasonable predictions may be made on the effects of pH_e on the cell.

ADHERENT CELL GROWTH RELATED TO pH

Numerous investigations have shown that microbial surface colonization is ubiquitous not only in nature but in engineering treatment facilities (*e.g.*, trickling filters and rotating biological contactors) and laboratory studies (Pirt, 1975; Costerton & Lappin-Scott, 1989; Bitton & Marshall, 1980). Attachment and the growth of adherent cells provide another means to examine microbial behavior and the influence of external environmental conditions. Bacterial cells in suspension can be thought of as colloidal particles, and are thus subject to the same physicochemical mechanisms for destabilization as any colloidal particle (Hsieh, 1988). Bacterial cells are typically covered by a glycocalyx of fibrous extracellular polymers, primarily consisting of hetero-

polysaccharides (Costerton & Lappin-Scott, 1989; Costerton & Geesey, 1978; Hsieh, 1988). The polysaccharides extend from the cell surface allowing the cells to adhere to surfaces (Marshall, et al., 1971).

Sessile, or attached, bacteria can differ markedly from planktonic, or suspended, cells in the same ecosystem, and even more markedly from cells grown in lab media as pure cultures. Some of the differences can include growth rate, cell wall structure and composition, immunogenicity, enzyme activities, and sensitivity to range of antibacterial agents and to hydrogen ion concentration (Costerton & Lappin-Scott, 1989). The general magnitude of interaction forces that determine stability in particle-particle interactions depend on the properties of each solid-solution interface (O'Melia, 1988).

Few particles, including bacterial cells, are uncharged in aquatic environments and electrostatic forces are therefore important in their interaction. Electrolytes and pH variations can strongly affect the magnitude of these electrostatic forces. Depending upon the isoelectric pH of a particular bacterial species and pH_e of the medium, the complex structure of a microbial cell surface (including amino, phosphoryl, sulfhydryl, hydroxyl, and carboxyl groups) is predominantly cationic or anionic (See Figure 2.4) (Nelson, *et al.*, 1981). In the range of pH 6 to 9 found in nature, most bacteria have an anionic surface charge.

Many clay mineral oxide surfaces in nature available for cell attachment have a negative overall surface charge (at circumneutral pH) due to varying degrees of coverage of hydroxyl groups or ions and isomorphic substitution into mineral lattice structures (Armistead, *et al.*, 1969). Silica (SiO_2) and silicate minerals comprise the bulk of the available surfaces (since they are almost 75% by mass of the earth's crust) (Petrucci, 1982; Manahan, 1991). If negatively charged bacteria are to adhere to a negatively charged solid

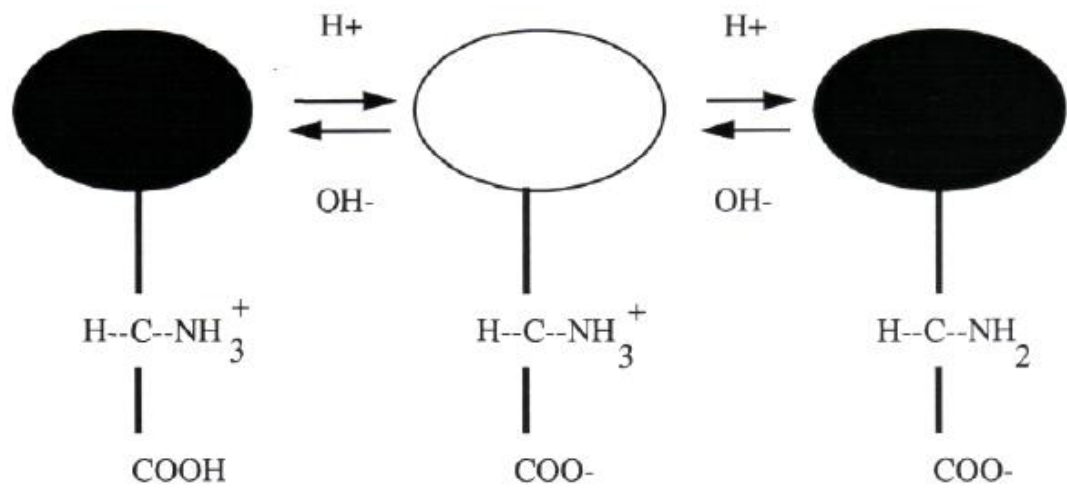


Figure 2.4. Cationic—Anionic character of bacterial cells. (Daniels, 1972)

surface, they must overcome an electrostatic repulsion barrier (Molin & Nilsson, 1983). This represents a reversible phase in the cell attachment process when the double-layer repulsion and van der Waals attraction forces are balanced (Marshall, et al., 1971; Duddridge & Wainwright, 1982). The pH alteration will influence electrical double layer thickness and the dissociation of charged groups on the solid and cell sur-faces and have a subsequent effect upon adhesion (McEldowney & Fletcher, 1988). Measurement of the surface potential, Ψ_0 , as a function of pH for the cell and attachment surfaces can provide insight into the most important parameters governing surface reactions, namely the surface density of charged sites (Bousse & Meindl, 1986).

Armistead, et al. (1969) reported on thermogravimetric studies used to determine the concentration and coordination of hydroxyl groups on the surface of silica. They indicated surface hydroxyl coverage approaching a limit of about 5 hydroxyl groups per 100 \AA^2 . Surface electronegativity dropped with decreasing pH due to the protonation of the exposed ionic surface functional groups (Molin & Nilsson, 1983). The corresponding surface reactivity with other cationic species would also be decreased as the number of protonated surface groups increases.

Recent infrared studies of the surface of goethite (a hydrated form of iron oxide, α -FeOOH, which adsorbs trace metals more strongly than most other adsorbents) by Johnson (1990) revealed surface hydroxyl groups coordinated to 1, 2, or 3 iron atoms suggesting each active site could have different levels of reactivity. The experiments showed trace metal adsorption onto the inorganic surface increased from 0% to nearly 100% coverage over a very narrow range of 1 to 2 pH units (Davis & Leckie, 1978; Johnson, 1990). The pH range (or adsorption "edge") was found to move to higher pH values as the initial

concentration of metal increased. The suggested mechanism governing these results indicated the available surface sites were generally positively charged of the form SOH_2^+ , where SO designates the oxide surface and H_2 the exchangeable protons, at low pH levels (< 4.0). With pH levels increasing toward alkaline values, the available surface sites were neutralized to SOH and finally to SO^- (at $\text{pH} > 8.5$). Positively charged species were then more readily adsorbed on the neutral and negatively charged sites. The shift in solution pH allowed a change in the apparent reactivity of surface sites and the subsequent degree of adsorption of the trace metal. This mirrors results found by Davis & Leckie (1978) using amorphous iron oxide as the inorganic surface.

The oxide surfaces available for interactions with bacterial cells have similar configurations and behavioral patterns under conditions of increasing solution pH as the bacterial cells themselves (see Figure 2.4). Thus, it is not surprising a surface attached biofilm could influence subsequent attachment and growth of cells on a surface since both the polymer and cell surface charge and the oxide surface charge are pH dependent (O'Melia, 1988; Johnson, 1990; Davis & Leckie, 1978). In many cases, the apparent influence of a solid surface on the bacterial cell attachment and biofilm activity is an indirect feature since the medium composition and its pH influences the functional group activity on the solid surface rather than being influenced by the bacterial cell itself (Van Loosdrecht, *et al*, 1990).

Daniels (1972) noted that, depending upon the relative isoelectric points of the bacterial cells and the type of solid surface, the pH for optimum cellular attachment will vary considerably, but is strongest in the slightly acidic range (pH 3 to 6). The presence of multivalent cations can neutralize or reverse the anionic site charge of bacteria suspended in an acidic medium and increase adsorption of the cells onto the surface. Studies with lead in

concentrations below the threshold level found to be inhibitory or toxic to cells ($\sim 10^{-6}$ M) found the cells largely immobilized the metal on the cell membrane with none entering the cytoplasm (Wong, *et al.*, 1978). This is further evidence of electrostatic surface interactions which can be altered or affected by pH variations. In fact some researchers feel that hydrogen ion concentration is the most important factor influencing metal adsorption on both inorganic and organic surfaces (Nelson, *et al.*, 1981).

In a series of experiments, Nelson, *et al.* (1981) observed the addition of inorganic metal salts of copper, cadmium and zinc to have much greater affinity for adsorption to bacterial cells (over 90% at pH 10) at high pH values. At low pH values, metal adsorption was significantly reduced (less than 15% at pH 4). The pH effects on adsorption were explained in terms of competitive adsorption by the hydrogen ion to the surface functional groups on the bacteria which are known to change protonation level with pH (Nelson, *et al.*, 1981; Gould & Genetelli, 1978). The effect of pH on adsorption of metals by bacteria contrasts with the prior description of adsorption "edges" for metals and inorganic surfaces. The adsorption "edge" for attachment of metals to bacterial cells found by Nelson, *et al.* (1981) had a range of 3-6 pH units and may represent a greater range over which protonation of the functional groups on the surface of the bacterial cell can occur.

Bacterial cells appear to be the first colonizers of clean surfaces in aquatic environments (Marshall, *et al.*, 1971; Hsieh, 1988). Molin and Nilsson (1983) performed attachment studies using *Pseudomonas putida* ATCC 11172 to gauge the effect of variable pH on biofilm development. They prepared carbon limited Multigen cultures of these cells grown in the presence of glass rods immersed in the fermentation broth kept at a dilution rate of 0.7 hr^{-1} with one set of glass rods immersed in the culture for 30 seconds and another set

immersed for a 24 hour exposure. The effects of pH were studied by repeating the experiments at pH values of 5.5, 6.0, and 6.7. Biofilm attachment to the glass rods (recorded in cfu's or colony-forming units) at the short exposure time was on the order of $1 - 5 \times 10^5$ cfu/cm². At the long exposure time, colony counts of cells ranged from 8×10^6 to 1.6×10^8 cfu/cm² with the suspended culture relatively constant at from 1.1 to 2×10^7 cfu/mL (Molin & Nilsson, 1983). The conclusion was the rate of biofilm buildup as well as final biofilm density on the surface was affected by pH while the growth in suspended cultures was not substantially affected by the different pH values. McEldowney and Fletcher (1988), working with gliding and non-gliding bacteria found a permanent adhesion optimally occurred in the pH range of 5.5 to 7.0 and adhesion was dramatically reduced for the gliding bacteria as the pH increased. This result was expected since it has been shown that pH variation modifies the viscosity of the bacterial cells external biopolymer and thus affects the adhesion ability of the cells (McEldowney and Fletcher, 1988).

Surface attachment by bacterial cells is thought to provide them with an advantage over planktonic cells through the influence of the surface on adsorbing materials (like substrates or other nutrients) rather than the direct influence of the surface on the cells. In fact, the microenvironment near a surface may be greatly enhanced in substrate and other nutrients due to adsorption reactions (Hsieh, 1988). System pH influences the attraction of nutrients and colloidal inorganic and/or organic material besides cells. But as in many situations, continued cellular growth and attachment can ultimately represent too much of a good thing. As the depth of cells in the biofilm builds up, the ability of the bottom cells to continue to grow and remain attached to the surface becomes limited. Diffusional resistance develops in the biofilm to the inward flux of substrate, nutrients and

bicarbonate ions (to buffer solution pH variations as a result of growth). A diffusional resistance also develops in the biofilm to outward diffusion of CO₂ from the growing cells. The pH in the biofilm will decrease at a faster rate than in the bulk solution if the buffering capacity is low because of the increased acidity production at the higher cell density. The pH in a deep biofilm is reported to level off at a value of 5.7 because hydrogen ion toxicity inhibits cell metabolism (Szwering, *et al.* 1986).

pH_e INTERACTIONS BETWEEN METAL IONS AND CELLS IN SOLUTION

Distribution and transport of metals in the environment is affected by direct inputs of solid waste materials, releases from natural and man-made sources and by aqueous solutions (Forstner, 1986). In an aqueous solution, the introduction of a metal species results in the metal ions surrounded by coordinating water molecules. The coordination reactions in which metal cations participate in aqueous solutions are replacement reactions with the coordinated water molecules exchanged for other ligands. Reactions of the metal cation with water to form metal hydroxide complexes are common (Sawyer, *et al.*, 1994).

The concentrations of metal cations in aqueous solution are affected by the equilibrium interactions with other constituents found in solution. Reactions of the cation to form hydroxide complexes will reduce the concentration of the aquo-ion. Metals may also react with anions to form precipitates. The pH of water not only affects solubility of metal hydroxides, but also affects other equilibria in water, which in turn can affect metal solubility (Sawyer, *et al.*, 1994). In many natural systems, the chemical behavior of metals is affected, or mediated, by the presence of inorganic as well as organic particle surfaces

(Forstner, 1986; Honeyman & Santschi, 1988). Inorganic surfaces like clays and organic solid surfaces, including bacterial cells and associated biopolymers, usually have a net negative, or anionic, character over a wide range of pH (Flemming, *et al.*, 1990). Inorganic surfaces will retain cations at hydroxyl, carboxyl or phosphoryl surface sites, and cations will be attracted to hydroxyl, carboxyl or phosphoryl groups on the bacterial surfaces.

The walls and associated structure of gram-negative and gram-positive bacteria consist of an anionic matrix of biopolymers such as peptidoglycan, teichoic acid, teichuronic acid, phospholipid and lipopolysaccharide as well as various polypeptides and polysaccharides (Beveridge, 1981; Mayers and Beveridge, 1989; Laidler, 1987). The chemical structure of these compounds contains sites that can attract and interact with the metallic aquo-ions. It is reasonable to assume the cell envelope, while strongly knitted together by chemical bonds, still maintains these reactive groups in the ionized form for interaction with extraneous solutes. Forstner (1985) reported the binding sites in soluble polymers contained in a mixed culture biological treatment unit were the hydroxyl units of the hexose/pentose rings of neutral polysaccharides. He further found the binding sites for metals were carboxyl groups on the polymers directly attached to the cell wall. It is these wall components and polymers that enable bacteria to adsorb and bind significant amounts of metals from their surroundings by a perceived electrostatic phenomenon mediated by the interactions between the soluble metal cation and the fixed anionic sites at the hydrophilic surfaces of the membrane (Ferris & Beveridge, 1986; Ferris, *et al.*, 1989).

The solubility, mobility and bioavailability of particle-bound metals can be increased by alteration of the pH of the water environment and corresponding effects on redox conditions in solution (Forstner, 1986). The extent to which a metallic cation interacts with

the surface determines the concentration of metal that will be in solution (Mullen, *et al.*, 1989). At pH values less than 4 (Hemming, *et al.*, 1990), the soluble free ion form of metals is typically dominant (Sawyer, *et al.*, 1994). It is the free metal ion form that causes the greatest toxicity to a cell (Chang, *et al.*, 1986). The properties of the surface, including net charge and functional groups, are also affected by pH. Ferris, *et al.* (1989) determined there was a reduction of cellular surface charge density with decreasing pH levels because of the protonation of negatively charged carboxyl, amino, and phosphoryl groups in the walls (COO^- , NH_3^+ , and PO_4^{3-} respectively) for binding metal cations.

The solution pH controls the extent to which protons dissociate from the reactive acidic groups. Flemming, *et al.* (1990) found that copper and silver ions were more mobile at pH 3 than at pH 9, presumably because bound metal ions were being replaced by a competing proton. Fletcher and Beckett (1987) also observed the controlled uptake of copper by bacterial cells in the pH range of 5 to 8 was dominated by a reversible exchange of copper for protons on the cells surface. Conversely, metallic ion adsorption and the strength of the electrostatic interaction is usually enhanced under neutral pH conditions by a proportional increase in the number of ionized acidic groups (Ferris, *et al.*, 1989). Increasing pH increases the stability of the metallic complex formed at the cell surface and implies less metal (in the free ion form toxic to the cell) is available for biological uptake (Gould & Genetelli, 1978).

Experiments with single metals confirm that cell walls are capable of concentrating a wide variety of metals from solution (Mayers & Beveridge, 1989). Bacterial cells will have however a more selective accumulation of heavy metals when exposed to more than a single metal at a time. Interionic competition and the spacing of anionic binding sites will

cause some metals to be adsorbed to a greater extent than others (Ferris & Beveridge, 1986). Nakajima & Sakaguchi (1986) found adsorption of cobalt by bacterial cells, from a solution where cobalt was the only metal ion, to be high at an average of 136 $\mu\text{moles/g}$ of cells. Adsorption of cobalt from a solution of 9 metals averaged only 2 $\mu\text{moles/g}$ of cells. Mullen, *et al.* (1989) found binding by bacterial cells of each of the metals copper, cadmium, silver and lanthanum was reduced when the others were present indicating some competition for metal binding sites on the cell surface. Mayers & Beveridge (1989) found that metal adsorption from harbor waters on Lake Ontario containing a mixture of metals was limited in that copper and zinc would not be adsorbed, while aluminum and chromium uptake was enhanced in the presence of iron.

Chang, *et al.* (1986) postulated that the removal of soluble and finely divided metal particulates from a biological system by the bacteria and biological flocs was a two-step process consisting of a rapid initial uptake step followed by a slow, long-term uptake phase. Experiments conducted by Mayers and Beveridge (1989) with *Bacillus subtilis* confirmed the two step metal sorption process. In the first step, the metals were found to associate with the reactive sites in the wall matrix (primarily carboxyl groups in peptidoglycan). The second step involved some of the sites serving to nucleate the precipitation of the mineral within the wall fabric (Mayers & Beveridge, 1989; Mullen, *et al.*, 1989; Chmielowski & Kłapcińska, 1986). Ferris, *et al.* (1989) noted precipitation of the complexed metals at the cell surface could be influenced by metal hydrolysis reactions, a change in metal oxidation state or through reactions with counter ions in solution. The precipitation reaction converts metal ions to a form less toxic to bacterial cells since they are not able to be transported to the interior of the cell (Chmielowski & Kłapcińska, 1986).

Macaskie, *et al.* (1987) observed cadmium binding to *Citrobacter* species. They found after passive adsorption of the cadmium to cell-surface components, enzymes in the cell mediated a cleavage of organic phosphates to create HPO_4^{-2} ions which were available for precipitation reactions with cadmium at discrete loci on the cell wall. Mullen, *et al.* (1989) equilibrated 1 mM solutions of silver and lanthanum with four separate bacterial strains and used electron microscopy to ascertain the location of the metal. The results indicated a precipitation reaction at the surface due to the presence of large deposits of each metal in each case on the cell surface.

MODELING BACTERIAL CELL GROWTH AND pH DEPENDENCY

The literature contains numerous references to models useful in predicting cell growth, product formation and biofilm development on a surface in response to environmental stimuli. Hsieh (1988) reviewed available literature regarding models for predicting heterogeneous biofilm growth. The general conclusion was existing models were primarily unstructured with a tendency to be correlative rather than predictive. Additionally, none of the models Hsieh (1988) examined explicitly considered pH as a variable in its description of the experimental system.

Typically a model that seeks to reflect the basic nature of living organisms must also recognize the dynamic nature of such organisms. The model must be capable of dividing the cell into as many subcomponents as needed in order to reflect the basic biochemistry of the cell and its sub-processes. A structured model allows the division of the cell into two or more components (Shuler, 1985; Bu'Lock & Kristiansen, 1987). Structured models can be verified if the components are measurable chemical classes of material such as DNA, RNA, protein,

etc. (Shuler, 1985). Since bacterial cells and biofilms in natural aquatic systems and most engineered treatment systems are exposed to fluctuations in feed flow rates, organic concentrations, toxic metal concentrations and hydrogen ion concentrations that can alter the internal composition and biosynthetic capabilities of the cells, the use of a chemically structured model is essential if dynamic system responses are to be predicted (Shuler, 1985; Hsieh, 1988; Bu'Lock & Kristiansen, 1987).

A structured computer model for biofilm growth and biopolymer production in the presence of a toxic trace metal resulted from experimental observations by Hsieh (1988). The model had no adjustable parameters and, after revision by the author of this thesis, was able to successfully predict many features of both steady-state and transient operating conditions for cellular growth and for metal distribution in a model aquatic system (refer to Appendix I for a complete discussion of the model development and parameter selection). Although the model was tested using a defined seawater laboratory reactor system, the success of the model predictions compared to experimental results suggested the overall soundness of this approach for adaptation to a freshwater aquatic system.

A major model modification required in a freshwater environment is to account for the effect of variable medium pH on the growth of the cells, their surface attachment and, ultimately, their interaction with toxic metal species. Hsieh's (1988) model (see Appendix I) provided the basic framework for further model building. To consider the form of pH affects, it is useful to consider models for pH effects on enzyme activity.

ENZYLE MODELS AND pH DEPENDENCY

Models for pH dependence of enzymatic activity have generally been based upon characterization of enzyme as having an ionizable form that interacts via a simple

one-substrate reaction (Mahler & Cordes, 1966; Shuler & Kargi, 1990; Han and Levenspiel, 1988; Dean & Hinshelwood, 1966; Segal, 1976; Tipton & Dixon, 1983; Laidler & Bunting, 1973). The amino acids in the enzymatic proteins possess basic, neutral or acidic groups (Baily & Ollis, 1986). An intact enzyme may thus contain both positively and negatively charged groups at any given pH value.

In general, the effects of variations of the hydrogen ion concentration on the activity of enzymes and whole cells (if viewed as a collection of enzymes) have close similarities to the effects of activators and inhibitors. The kinetic methods and theory used for enzyme activation and inhibition can therefore be applied to pH effects (Tipton and Dixon, 1983). Most enzymes contain many ionizing groups. The characteristic "bell shaped" activity curve for a single enzyme shown in Figure 2.1 for the variation of initial reaction velocity as a function of pH mirrors similar curves developed for whole cells as shown in Figure 2.2 (Laidler & Bunting, 1973; Laidler, 1987). The early interpretation for pH effects on enzyme activity was that an enzyme contained two ionizable groups that were essential for activity (Tipton and Dixon, 1983; Bailey and Ollis, 1986; Laidler, 1987). The ionization of other groups at pH values farther from the pH optimum will be undetectable because they would affect only the equilibrium between inactive enzyme forms. This simple model implied that the pH dependence of an enzyme, and by extension whole cell activity, can be considered as governed by the dissociation of a diprotic acid. Subsequent model analysis therefore involves equations describing the ionization of such compounds.

In the entirety of the model cases previously referenced, the following underlying assumptions were made (Mahler & Cordes, 1966):

1. there was only one state of ionization of the substrate (S) and of the ionizable enzyme that was capable of reaction,
2. the enzyme (E) behaved as a diprotic acid in which completely deprotonated E^{-2} and diprotic EH_2 forms are completely inactive with regard to substrate binding, and,
3. that similar considerations applied with regard to the catalytic function of the active enzyme-substrate complex (EHS).

Uptake and release of the protons would be expected to be rapid. Figure 2.5 illustrates these assumptions. Application of the steady-state treatment to the mechanism results in the rate equation:

$$v = \frac{k_{+2}[E_0][S]}{K_m \left(1 + \frac{K_{e2}}{[H^+]} + \frac{[H^+]}{K_{e1}} \right) + [S] \left(1 + \frac{K_{es2}}{[H^+]} + \frac{[H^+]}{K_{es1}} \right)} \quad (2.1)$$

The simplification of this steady-state solution for the mechanism has the familiar Monod form:

$$v = \frac{V'[S]}{K' + [S]} \quad (2.2)$$

where V' and K' , the observed parameters, are now functions of pH ($[H^+] \equiv$ hydrogen ion activity):

$$V' = \frac{V}{1 + \frac{[H^+]}{K_{es1}} + \frac{K_{es2}}{[H^+]}} \quad (2.3)$$

where V is the pH-independent maximal velocity $= k_{+2}[E_0]$; and $[E_0] = [E^{-2}] + [EH^-] + [EH_2] + [ES^{-2}] + [EHS^-] + [EH_2S]$, the total amount of available enzyme, and;

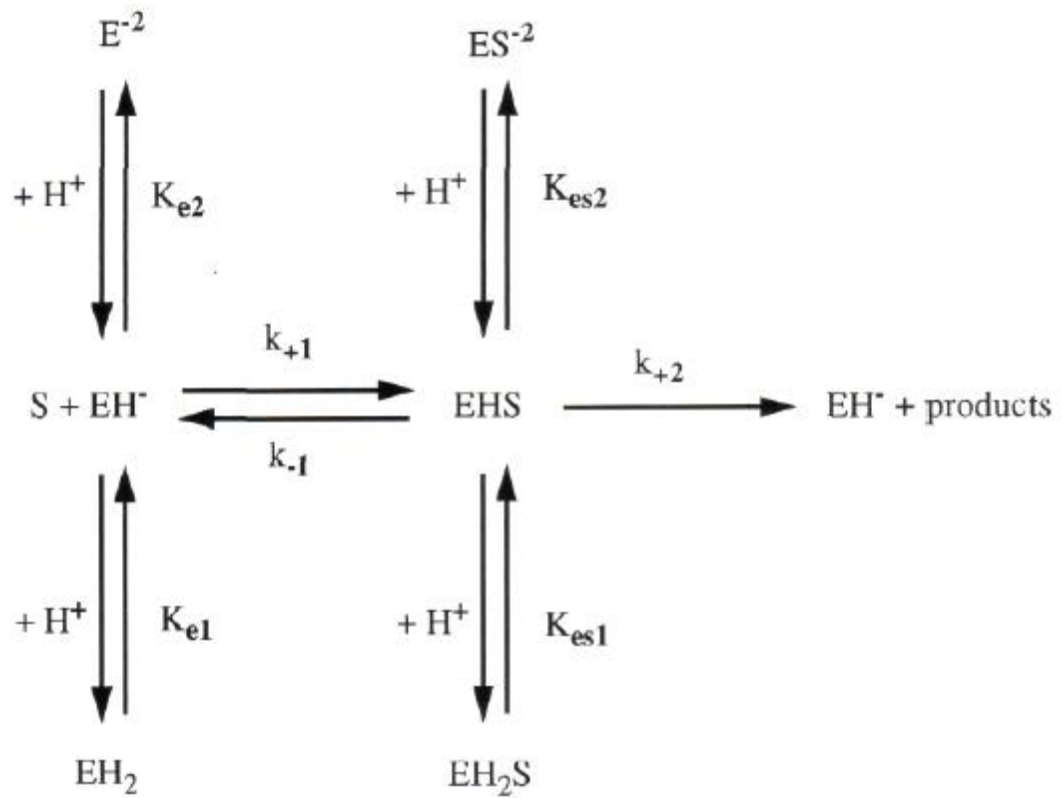


Figure 2.5. Overall pH dependence of a simple one substrate reaction involving enzymes (Mahler & Cordes, 1966; Tipton & Dixon, 1983).

$$K' = K_m \frac{1 + \frac{[H^+]}{K_{e1}} + \frac{K_{e2}}{[H^+]}}{1 + \frac{[H^+]}{K_{es1}} + \frac{K_{es2}}{[H^+]}} \quad (2.4)$$

where K_m is the pH-independent Michaelis constant = $(k_{-1} + k_{+2})/k_{+1}$. Combining equations 2.2 and 2.3 gives a relationship between V and K_m which is valid at low substrate concentrations when $S \ll K_m$:

$$\frac{V'}{K'} = \frac{V}{K_m} \left(\frac{1}{1 + \frac{[H^+]}{K_{e1}} + \frac{K_{e2}}{[H^+]}} \right) \quad (2.5)$$

The parameters V' and K' are pH-corrected. They will be the limits to which V and K_m tend at pH values between relevant ionization constants pK_1 and pK_2 values if the pK values of the ionizable groups are far enough apart (Chitna & Sadana, 1989).

Comparing the conventional Monod equation with equation 2.1 (including the substituted pH-dependent forms in equations 2.2 and 2.3) indicates that the hydrogen ion concentration will affect both the apparent K_m and V values; thus hydrogen ions can be considered to be noncompetitive inhibitors of the enzyme activity (Tipton & Dixon, 1983). If K_1 and K_2 for both $[E]$ and $[ES]$ differ enough, there will be pH values where terms containing one of the K values can be neglected and terms containing the other are appreciable.

The most convenient method for the treatment of pH effects is evaluating the above equations utilizing two ranges of substrate concentration, high ($[S] \gg K_m$) and low ($[S] \ll K_m$), and three ranges of pH: acidic, neutral and basic (Laidler, 1987; Tipton & Dixon, 1983; Chitnis & Sadana, 1989). At low substrate concentrations in a sufficiently acid solution (pH

< 4), the term $[H^+]/K_{e1}$ in equation 2.1 predominates in the denominator and a concomitant simplification in the working equation results in:

$$v = \frac{k_{+2} [E_0]^{[S]} K_{e1}}{K_m [H^+]} \quad (2.6)$$

$$\text{or } \log_{10} v = \text{constant} - \log_{10}[H^+] = \text{constant} + \text{pH}.$$

The plot of $\log_{10} v$ versus pH therefore is expected to have a slope of +1 at low pH values ($\text{pH} < 4$). Assumptions for circumneutral and basic pH values ($\text{pH} > 10$) result in the plot of $\log_{10} v$ versus pH having slopes of 0 and -1 respectively. This analysis will also allow calculation of pK_1 and pK_2 as occurring at the intersection points of the 3 straight line curves which result in the plot of $\log_{10} v$ versus pH.

Few enzyme systems, however, conform to the simple mechanism described above (Tipton & Dixon, 1983). Some examples of complications include the presence of more than one enzyme substrate intermediate, more than one form of enzyme-substrate intermediate, more than one form of enzyme binding to the substrate, a change in the rate-determining step with pH and more than one form of enzyme-substrate complex yielding products. Each case can presumably be solved in a manner analogous to the simplified model discussed above to yield information on the pH-dependent values of V and K_m .

The application of the simplified model to describe interactions with whole cells and hydrogen ions is reasonable, assuming a cell represents a group of enzymes, each of which is capable of following the above model and assuming the presence of active surface binding sites that are ionizable functional groups (Brock and Madigan, 1988; Stanier, *et al.*, 1986). Based on the prior discussions of the make-up of a cell's surface,

the model can be adapted to describe the pH dependency of cellular interactions with the aquatic environment.

REFERENCES

Adams, L.F. and W.C. Ghiorse. 1986. Physiology and Ultrastructure of *Leptothrix discophora* SS-1. Arch. Microbiol. 145: 126-135.

Albert, A., Rubbo, S.D., Goldacre, R.J., Davey, M.E., and Stone, J.D. 1945. The Influence of Chemical Constitution on Antibacterial Activity. II. A General Survey of the Acridine Series. Br. J. Exp. Path. 26: 160-192.

Armistead, C.G., Tyler, A.J., Hambleton, F.H., Mitchell, S.A. and Hockey, J.A. 1969. The Surface Hydroxylation of Silica. J. Phys. Chem. 73: 3947-3953.

Baily, I.E., and Ollis, D.F. 1986. Biochemical Engineering Fundamentals. Second Ed. McGraw-Hill Book Company, New York.

Baldwin, R.L., and Eisenberg, D. 1987. Chapter 11. Protein Stability. In: Protein Engineering. Ed. by D.L. Oxender & C.F. Fox. Alan R. Liss, Inc. New York.

Beveridge, T.J. 1981. Ultrastructure, Chemistry and Function of the Bacterial Wall. Int. Rev. Cytol. 72: 229-317.

Beveridge, T.J. 1988. The Bacterial Surface: General Considerations Towards Design and Function. Can. J. Microbiol. 34: 363-372.

Bitton, G. and Marshall, K.C (editors). 1980. Adsorption of Microorganisms to Surfaces. John Wiley & Sons, NY.

Bousse, L. and Meindl, J.D. 1986. Surface Potential-pH Characteristics in the Theory of the Oxide-Electrolyte Interface. Chapter 5. In: Geochemical Processes at Mineral Surfaces. American Chemical Society.

Brock, T.D., and Madigan, M.T. 1988. Biology of Microorganisms. Fifth Ed. Prentice-Hall, Inc. Englewood Cliffs, NJ.

Bu'Lock, J. and Kristiansen, B. 1987. Basic Biotechnology. Academic Press, Inc. Harcourt, Brace, Jovanovich, Publishers. Orlando, Florida.

Chang, S-Y., Huang, J-C, and Liu, Y-C. 1986. Effects of Cd(II) and Cu(II) on a Biofilm System. J. Environ. Eng., ASCE. 112: 94-104.

Chitnis, A. and Sadana, A. 1989. pH-Dependent Enzyme Deactivation Models. Biotech. Bioengr. 34:804-818.

Chmielowski, J. and Kłapcińska, B. 1986. Bioaccumulation of Germanium by *Pseudomonas putida* in the Presence of Two Selected Substrates. App. Environ. Micro-biol. 51: 1099-1103.

Costerton, J.W., Geesey, G.G. and Cheng, K.-J. 1978. How Bacteria Stick. *Sci. Amer.* 238:86-95.

Costerton, J.W. and Lappin-Scott, H.M. 1989. Behavior of Bacteria in Biofilms. *ASM News.* 55: 650-654.

Crist, R.H., Oberholser, K., Schwartz, D., Marzoff, J. and Ryder, D. 1Q88. Interactions of Metals and Protons with Algae. *Env. Sci. and Technol.* 22:755-760.

Daniels, S.L. 1972. Chapter 19. The Adsorption of Microorganisms onto Solid Surfaces: A Review. In Volume 13, *Developments in Industrial Microbiology.* 1979.

Davis, J.A., and Leckie, J.O. 1978. Effect of Adsorbed Complexing Ligands on Trace Metal Uptake by Hydrous Oxides. *Env. Sci. and Technol.* 12: 1309-1315.

Dean, A.C.R., and Hinshelwood, S.C. 1966. *Growth, Function and Regulation in Bacterial Cells.* Oxford at the Clarendon Press, Great Britain.

Duddridge, I.E. and Wainwright, M. 1982. Enzyme Activity and Kinetics in Substrate-Amended River Sediments. *Water Res.* 16: 329-334.

Eroshin, V. K., Harwood, J. H. and Pirt, S. J. 1968. Influence of Amino Acids, Carboxylic Acids and Sugars on the Growth of *Methylococcus capsulatus* on Methane. J. Appl. Bact. 31:560-567.

Ferris, F.G., and Beveridge, T.J. 1986. Physicochemical Roles of Soluble Metal Cations in the Outer Membrane of *Escherichia Coli* K-12. Can. J. Microbiol. 32: 594-601.

Ferris, K.G., Schuytze, S., Witten, T.C., Fyfe, W.S., and Beveridge, T.J. 1989. Metal Interactions with Microbial Biofilms in Acidic and Neutral pH Environments. Appl. Environ. Microbiol. 55: 1249-1257.

Flemming, C.A., Ferris, F.G., Beveridge, T.J., and Bailey, G.W. 1990. Remobilization of Toxic Heavy Metals Adsorbed to Bacterial Wall-Clay Composites. Appl. Environ. Microbiol. 56:3191-3203.

Fletcher, P. and Beckett, P.H.T. 1987. The Chemistry of Heavy Metals in Digested Sewage Sludge-II. Heavy Metal Complexation with Soluble Organic Matter. Water Res. 10: 1163-1172.

Forster, C.F. 1985. Factors Involved in the Settlement of Activated Sludge-II. The Binding of Polyvalent Metals. Water Res. 19: 1265-1271.

Forstner, U. 1986. Changes in Metal Mobilities in Aquatic and Terrestrial Cycles. In: Proceedings of the International Symposium on Metal Speciation, Separation and Recovery. Chicago, IL.

Gale, E. F., and Epps, H.M.R.. 1942. The Effect of the pH of the Medium during Growth on the Enzymic Activities of Bacteria (*Escherichia coli* and *Micrococcus lysodeikticus*) and the Biological Significance of the Changes Produced. *Biochem. J.* 36(7-9): 600-618.

Gould, M.S., and Genetelli, E.J. 1978. Heavy Metal Complexation Behavior in Anaerobically Digested Sludges. *Water Res.* 12: 505-512.

Han, K. and Levenspiel, O. 1988. Extended Monod Kinetics for Substrate, Product, and Cell Inhibition. *Biotech. Bioeng.* 32: 430-437.

Honeyman, B.D. and Santschi, P.H. 1988. Metals in Aquatic Systems. *Environ. Sci. Technol.* 22: 862-871.

Hsieh, K.M. 1988. The Growth and Attachment of a Biopolymer Producing *Pseudomonas* Species and the Characterization of its Interactions with a Toxic Trace Metal. Ph.D. Thesis. Cornell University, Ithaca, NY.

Johnson, B.B. 1990. Effect of pH, Temperature, and Concentration on the Adsorption of Cadmium on Goethite. *Environ. Sci. Technol.* 24: 112-118.

Kakinuma, Y. 1987. Lowering Cytoplasmic pH is Essential for Growth of *Streptococcus faecalis* at High pH. J. Bacteriol. 169: 4403-4405.

Kessels, B.G.F., Theuvenet, A.P.R., Peters, P.H.J., Dobbelmann, J., and Borst-Pauwels, G.W.F.H. 1987. Changes in ^{45}Ca and ^{109}Cd Uptake, Membrane Potential and Cell pH in *Saccharomyces cerevisiae* Provoked by Cd^{+2} . J. Gen. Microbiol. 133: 843-848.

Kruse, R.E., I. 1988. Control of Pyruvate Dissimilating Pathways in *Sarcina ventriculi*. Ph.D. Thesis. Cornell University, Ithaca, NY.

Laidler, K.J. 1987. Chemical Kinetics. Third Ed. Harper & Row, Publishers. New York.

Laidler, K.J., and Bunting, P.S. 1973. The Chemical Kinetics of Enzyme Action. Second Ed. Chapter 5. Clarendon Press. Oxford, Great Britain.

Leelasart, B. and Bonaly, R. 1988. Effect of Control of pH on the Excretion of Acid Phosphatase by *Rhodotorula glutinis*. Appl. Microbial Biotechnol. 29: 579-585.

Mahler, H.R. and Cordes, E.H. 1966. Biological Chemistry. Harper and Row Publishers, New York, NY.

Macaskie, L.E., Dean, A.C.R., Cheetham, A.K., Jakeman, R.J.B. and Skarnulis, A.J. 1987. Cadmium Accumulation by a *Citrobacter sp.*: The Chemical Nature of the Accumulated Metal Precipitate and its Location on the Bacterial Cells. *J. Gen. Microbiol.* 133: 539-544.

Manahan, S.E. 1991. *Environmental Chemistry*. Lewis Publishers, Inc., Chelsea, MI. pp. 359-380.

Marshall, K.C., Stout, R., and Mitchell, R. 1971. Mechanism of the Initial Events in the Sorption of Marine Bacteria to Surfaces. *J. Gen. Microbiol.* 68: 337-348.

Masscheleyn, P.H., Delaune, R.D., and Patrick, W.H., Jr. 1991. Effect of Redox Potential and pH on Arsenic Speciation and Solubility in a Contaminated Soil. *Environ. Sci. Technol.* 25: 1414-1419.

Mayers, I.T. and Beveridge, T.J. 1989. The Sorption of Metals to *Bacillus subtilis* Walls from Dilute Solutions and Simulated Hamilton Harbor (Lake Ontario) Water. *Can. J. Microbiol.* 35: 764-770.

McEldowney, S. and Fletcher, M. 1988. Effect of pH, Temperature, and Growth Conditions on the Adhesion of a Gliding Bacterium and Three Non-gliding Bacteria to Polystyrene. *Microbial Ecol.* 16: 183-195.

Molin, G. and Nilsson, I. 1983. Effect of Different Environmental Parameters on the Biofilm Build-up of *Pseudomonas putida* ATCC 11172 in Chemostat. Eur. J. Appl. Microbiol. Biotechnol. 18: 114-119.

Mullen, M.D., Wolf, D.C., Ferris, F.G., Beveridge, T.J., Flemming, C.A. and Bailey, G.W. 1989. Bacterial Sorption of Heavy Metals. Appl. Environ. Microbiol. 55: 3143-3149.

Nakajima, A. and Sakaguchi, T. 1986. Selective Accumulation of Heavy Metals by Microorganisms. Appl. Microbiol. Biotechnol. 24: 59-64.

Neidhardt, EC., Ingraham, J.L., and Schaechter, M. 1990. Physiology of the Bacterial Cell. Sinauer Associates, Inc. Publisher. Sunderland, MA.

Nelson, P.O., Chung, A.K., and Hudson, M.C. 1981. Factors Affecting the Fate of Heavy Metals in the Activated Sludge Process. J. Water Pollution Control Fed. 53: 1323-1333.

O'Hara, G.W., Goss, T.J., Dilworth, M.J., and Glenn, A.R. 1989. Maintenance of Intracellular pH and Acid Tolerance in *Rhizobium meliloti*. Appl. Environ. Microbiol. 55: 1870-1876.

O'Melia, C.R. 1988. Macromolecules at the Solid-Water Interface: Conformations and Consequences. Paper presented at: AEEP Conference on Fundamental Research Directions in Environmental Engineering. Arlington, Virginia.

Petrucci, R.H. 1982. General Chemistry: Principles and Modern Applications. Third Ed. MacMillan Publishing Co., Inc. NY.

Pirt, S. J. 1975. Principles of Microbe and Cell Cultivation. Chapters 14, 15, 17, 23-25. John Wiley & Sons, NY.

Sawyer, C.N., McCarty, PL., and Parkin, G.F. 1994. Chemistry for Environmental Engineering. Fourth Ed. McGraw-Hill, Inc. New York, NY.

Segal, I.H. 1976. Biochemical Calculations: How to Solve Mathematical Problems in General Biochemistry. Second Ed. John Wiley & Sons, NY.

Shuler, M.L. 1985. Dynamic Modelling of Fermentation Systems. Chapter 6. In: Bioreactor Design, Operation and Control, pp. 119-131.

Shuler, M.L. and Kargi, F. 1992. Bioprocess Engineering: Basic Concepts. Prentice-Hall, Englewood Cliffs, NJ.

Stanier, R.Y., Ingraham, J.L., Wheelis, M.L., and Painter, PR. 1986. The Microbial World. Fifth Ed. Prentice-Hall, Englewood Cliffs, New Jersey. Chapter 8.

Stumm, w. and Morgan, JJ. 1981. Aquatic Chemistry: An Introduction Emphasizing Chemical Equilibria in Natural Waters. John Wiley & Sons. New York, NY.

Sundstrom, D. W., and Klei, H.E. 1979. Wastewater Treatment. Prentice Hall, Inc. Englewood Cliffs, NJ.

Szwerinski, H., Arvin, E., and Harremoës, P. 1986. pH-Decrease in Nitrifying Biofilms. *Water Res.* 20: 971-976.

Tanford, C. 1968. Protein Denaturation. In: *Advances in Protein Chemistry*, Volume 23. Ed. by: C.B. Anfinsen, Jr., M.L. Anson, J.T. Edsall and KM. Richards. Academic Press. New York, NY.

Tipton, K.F. and Dixon, H.B.F. 1983. Chapter 5. Effects of pH on Enzymes. In: *Contemporary Enzyme Kinetics & Mechanism*. Ed. by D.L. Purich. Academic Press. New York, van Loosdrecht, M.C.M., Lyklema, I., Norde, W. and Zehnder, A.J.B. 1986. Influence of Interfaces on Microbial Activity. *Microbial Rev.* 54: 75-87.

Wong, P.T. Silverberg, B.A., Chau, Y.K., and Hodson, P.V. 1978. Lead and the Aquatic Biota. Chapter 17. In: *The Biogeochemistry of Lead in the Environment. Part B. Biological Effects*. Ed. by J.O. Nriagu. Elsevier/North-Holland Biomedical Press. NY.

Wu, P., Ray, N.G., and Shuler, M.L. 1993. A Computer Model for Intracellular pH Regulation in Chinese Hamster Ovary Cells. *Biotechnol. Prog.* 9: 374-384.

CHAPTER 3
SELECTION OF A BIOPOLYMER PRODUCING
FRESHWATER BACTERIAL STRAIN¹

ABSTRACT

This chapter provides a discussion of relevant theory and experiments related to the selection of an adherent, freshwater associated, biopolymer producing, bacterial species for experimental use. The discussion emphasizes the apparatus and procedures employed to develop a chemically defined growth medium, to screen bacterial strains for their ability to grow and adhere in the defined medium, and to investigate the metal tolerance characteristics of the strains.

INTRODUCTION

Batch or chemostat culture techniques are commonly employed for testing adhesion of bacterial strains under desired experimental and/or environmental constraints (Baier, 1980; Daniels, 1980). Batch systems lack an advective fluid flow and therefore are unable to apply a selective pressure for variants within a culture that have strong adhesion characteristics. Chemostat systems may have flow rates that are too high to

1. Portions of the following published journal paper are reproduced in this chapter to describe the methodology and apparatus used in strain selection with permission of the coauthors: Lion, L.W., Acheson, C., Shuler, M.L., Emerson, D., and Ghiorse, W.C. "Experimental Apparatus for Selection of Adherent Microorganisms Under Stringent Growth Conditions". *Applied and Environmental Microbiology*. Vol. 57, no.7, pp 1987-1996. July, 1991.

permit retention of slow growing cells in the reactor unless the cells adhere strongly to surfaces. When an additional constraint is imposed, such as reduced nutrient concentrations or the presence of a toxic substance, the selection of suitable strains for study becomes more difficult.

Bacteria have been found to grow preferentially on available surfaces in nearly all habitats studies to date (Costerton & Lappin-Scott, 1989). The use of a cyclic flow reactor system allowed selection of adherent populations from cultures of bacterial strains that, because of growth limitations or unfavorable attachment characteristics, failed to form a biofilm during more commonly employed batch and chemostat testing procedures. The use of cyclic flow increased the probability of obtaining bacterial populations that attach to surfaces under restrictive growth conditions since it combined the best aspects of both batch culture and chemostat systems. During the flow stage of operation, cells not capable of adhesion to a surface would be washed out of the system. In the absence of flow, both suspended cell populations may increase while nutrients are depleted.

A long term research goal at Cornell University has been to study and model interactions between trace metal adsorption and bacterial attachment to inanimate surfaces under conditions of variable pH. Daniels (1979), in his summary review of the adsorption of bacterial cells, noted there was an observed dependence on the cellular adsorption process upon both the pH and the concentration of electrolytes in the suspension. The anticipated experimental work for this research also required development of a defined medium with a chemical composition that permitted calculation of trace metal speciation. This medium is referred to as "chemically defined", and necessitated use of components with defined metal binding constants. Thus, organic growth factors (vitamins, amino acids, etc.) were excluded.

Low phosphate concentrations were required to prevent metal precipitate formation. In addition, it was necessary to avoid iron (or other metal) supplements because dissolved iron would compete for available ligands in solution, and iron oxide precipitates would adsorb trace metals. A consequence of these restrictions was that many strains of bacteria tested initially did not grow in the chemically defined medium. Furthermore, candidate strains that were capable of growth frequently did not attach to surfaces under batch or continuous-flow growth conditions. The impetus for development of the reactor apparatus described below was the need to test axenic cultures of film-forming bacteria under the chemically defined experimental conditions.

MODELLING REACTOR OPERATION

In theory, operation of a flow-through reactor system by oscillating the flow could improve bacterial colonization of a surface by allowing sufficient time for growth and attachment to occur. During the time when flow is on, washout of bacteria that either are not capable of attachment or are not firmly attached to the surface would occur. When the flow is off, attached bacteria could either detach and grow in the fluid phase of the reactor or continue to spread on the surface. Some of the suspended cells might return and attach to other sites on the surface. It is reasoned that cycling of the flow would apply a selective pressure for variants within a bacterial culture that adhere strongly to a surface under conditions when their growth rate is stringently constrained (such as by toxic substances or limited nutrient availability). Surface colonization and growth would be enhanced, and the magnitude of the washout dilution rate required to remove the cells from the reactor would be greatly increased (Howel, *et al*, 1972).

A simple model was developed to study the influence of various cyclic flow regimes on growth and attachment of adherent bacteria in a theoretical chemostat system. The following equations were used to describe substrate (S) utilization and growth of suspended and attached cells (X_S , and X_A respectively).

$$\frac{dS}{dt} = \frac{Q}{V}(S_0 - S) - \frac{kX_S S}{K_S + S} - \frac{kX_A S}{K_S + S} \quad (3.1)$$

$$\frac{dX_S}{dt} = -\frac{QX_S}{V} + \frac{YkX_S S}{K_S + S} - k_A X_S + k_D X_A - k_d X_S \quad (3.2)$$

$$\frac{dX_A}{dt} = \frac{YkX_S S}{K_S + S} + k_A X_S - k_D X_A - k_d X_A \quad (3.3)$$

where:

Q = volumetric flow rate (length³/time) [potentially varying with time]

V = reactor volume (length³)

S_0 = substrate feed concentration (mass/length³)

k = maximum substrate utilization rate (time⁻¹)

K_S = half velocity or saturation constant for substrate utilization (mass/length³)

Y = yield coefficient (mass of cells/mass substrate)

k_A = attachment rate constant (time⁻¹)

k_D = detachment rate constant (time⁻¹)

and k_d = bacterial death rate (time⁻¹).

For simplicity in the example calculations, growth of attached and suspended cells uses Monod expressions with the same kinetic coefficients. The use of the same kinetic coefficients is supported by work of van Loosdrecht, *et al.* (1990) who found no conclusive evidence that adhesion directly influenced bacterial metabolism. Their

investigations demonstrated that adherent cell growth on an inorganic surface was not significantly different than would occur in planktonic growth. The observed differences were attributed to an indirect mechanism where the surfaces influenced the environment around the cell rather than the cell itself. Similarly, for the purpose of illustrating the general effect of variable flow cycles, a simple first order term for surface attachment and detachment was assumed. Calculations were performed assuming initial (time = 0 hrs.) substrate and attached cell concentrations were zero, and that the initial suspended cell concentration was 0.28 mg dry weight cell mass/mL. These conditions approximated those ultimately used in the experimental reactor system (described below). The hydraulic retention time and substrate feed concentration used in the calculations were comparable to those used in the actual experiments (6 hours and 1.0 mg/mL, respectively). For purposes of illustrating the model operation, the kinetic coefficients for cells were set to approximately equal those obtained in prior experiments for growth of *Pseudomonas atlantica* in a chemically defined seawater medium ($Y = 0.5$, $K_s = 0.00035$ mg/mL, $k = 0.25$ /hour) (Hsieh, *et al.*, 1985; Hsieh, *et al.*, 1988).

EXPERIMENTAL MATERIALS AND METHODS

Development of Minimal Mineral Salts (MMS) Medium. A chemically defined medium was needed to allow for planned studies of the influence of the bacterial films on trace metal adsorption. The chemical speciation program MINEQL (Westall, *et al.*, 1976) was employed to calculate interactions of proposed chemical components of the medium based upon known stability constants (Bjerrum, 1957; Bjerrum, 1958; Hogfeldt, 1982; Perrin, 1979; Sillen & Martell, 1964; Sillen & Martell, 1971). A balanced mineral

salts mixture was altered by iterative calculations with variable component concentrations using MINEQL to select the final medium composition (Adams & Ghiorse, 1986). The MMS medium composition (Table 3.1) did not produce precipitates that would influence lead (Pb) or cadmium (Cd) adsorption and it allowed Pb or Cd to exist predominantly (90%) in the free ion form at circumneutral pH. The MMS medium was low in phosphate because of the potential for formation of insoluble phosphate salts. A variable amount of NaNO₃ was added to maintain constant ionic strength (0.05 M) with different organic carbon/energy sources.

Bacterial Strains. Twenty four aerobic or facultative, heterotrophic, bacterial strains from various sources were initially selected for study. Their inclusion was based upon their reported ability to produce extracellular polymers, and/or produce a surface attached biofilm to bind trace metals, and their ability to grow in a freshwater defined medium. Cultures were maintained on a peptone/yeast extract/glucose (PYG) medium consisting of (per liter of solution): 0.25 g peptone, 0.25 g yeast extract, 0.25 g glucose, 0.6 g MgSO₄·7H₂O, 0.7 g CaCl₂, and 15 g agar, in 10 mM HEPES (N-hydroxyethylpiperazine-N'-2-ethane sulfonic acid) buffer with pH adjusted to 7.0. The strains were screened in Nunc tissue culture plates (3.6 mL well volume) for their growth ability on the MMS medium supplemented with various carbon/energy sources. Fourteen of the selected strains (2 Gram-positive, 12 Gram-negative) had visible growth with acetate, pyruvate or succinate as a carbon/energy source (see Table 3.2). These strains were then tested for surface attachment and biofilm formation in the cyclic-flow reactor.

Table 3.1: Composition of Minimal Mineral Salts (MMS) Growth Medium

COMPONENT	COMPOSITION	
	mg/L	Moles/L
CaCl ₂ -2H ₂ O	30.0	2.04 x 10 ⁻⁴
MgSO ₄ -7H ₂ O	34.5	1.40x 10 ⁻⁴
(NH ₄) ₂ SO ₄	120.0	9.08 x 10 ⁻⁴
KNO ₃	14.8	1.46x 10 ⁻⁴
NaHCO ₃	0.840	1.00 x 10 ⁻⁵
KH ₂ PO ₄	0.136	1.00 x 10 ⁻⁶
Carbon/energy ^a	1000.0	Variable ^b
NaNO ₃	Variable ^c	Variable ^c

a Acetate, Pyruvate, or Succinate

b Acetate-1.22 x 10⁻² M; Pyruvate-9.09 x 10⁻³ M; or Succinate-6.17x 10⁻³ M

c To maintain constant ionic strength of 0.05 M

Table 3.2: Bacterial Strains Showing Growth on MMS Medium*

Culture	Gram Reaction	Source
<i>Arthrobacter globiformis</i>	+	ATCC ¹ 8010
<i>Arthrobacter</i> sp. 9G4D ²	+	R. Beloin, Cornell Univ.
<i>Acinetobacter calcoaceticus</i>	-	ATCC 31012
Isolate, Frazer River, CA	-	G. Geesey, Montana State Univ.
<i>Leptothrix discophora</i> SP-6	-	D. Emerson, Cornell Univ.
<i>Leptothrix discophora</i> SS-1	-	W. Ghiorse, Cornell Univ.
<i>Pseudomonas cepacia</i> 17616	-	T. Lessie, Univ. of Mass.
<i>P. cepacia</i> 249-100	-	T. Lessie, Univ. of Mass.
<i>P. fluorescens</i>	-	ATCC 13524
<i>P. pickittii</i>	-	B. Pyle, Montana State Univ.
<i>P. sacchrophilia</i>	-	ATCC 15946
<i>Zoogloea</i> sp U106	-	R. Unz, Penn St. U.
<i>Zoogloea</i> sp WG04	-	R. Unz, Penn St. U.
<i>Zoogloea</i> sp WNJ8	-	R. Unz, Penn St. U.

1 ATCC--American Type Culture Collection, Rockville, MD

2 Isolated from groundwater aquifer sediment

* Containing either acetate, pyruvate or succinate as carbon/energy source

Screening Metal Toxicity of Selected Bacterial Strains. One of the criteria for selecting a freshwater bacterial strain was the effect of the experimental trace metals on the growth of the strains. An initial screening test involved evaluation of growth on agar plates in the vicinity of small disks soaked in known concentrations of Pb and Cd. The selected concentrations of 10^{-5} , 10^{-6} , 10^{-7} , and 10^{-8} M provided a range of metal concentrations likely to be found in engineered reactors (treatment systems) and in natural aquatic environments (Nriagu, 1978; Nriagu, 1980). The disks were placed on disposable petri dishes containing the MMS medium in an agar gel. A zone of inhibition around the disk was taken to indicate metal toxicity to cell growth.

A refinement in the test procedure was devised to better quantify the metal-cell toxicity for a relatively few short-listed strains. The tests were carried out in liquid culture instead of on petri dishes. A 140 mL volume of sterilized MMS medium, pH adjusted to 7.0 and with 1 g/L pyruvate as carbon/energy source was dispensed into each of 10-250 mL sterilized side arm flasks (Nephelo Culture Flasks, Bellco Glass, Inc., Vineland, NJ). Ten mL of inoculum was added to eight of the flasks. Two remained as control blanks without cells, one of which was a negative control without metals as well as cells. Then 100 μ L of the appropriate concentration of the premixed, pre-sterilized metal solution was added to each flask including the control.

After thorough mixing of the solution, a 50 μ L sample was withdrawn to check the flask pH using pH paper. An initial reading of percent transmittance at 600 nm was taken on a Spectronic 21 (Bausch & Lomb, Inc., Rochester, NY). Further readings were taken at intervals of twice a day, more frequently if growth was rapid. The samples were held at 25 °C constant temperature on an orbital shaker table (New Brunswick Scientific, Edison,

NJ) at 150 rpm between readings. The frequency of the tests increased with passing time as the cells went into log-phase growth. Measurements continued until apparent stationary phase growth was reached, usually a period of from 3 to 7 days.

Selection of Attachment Surface. The choice of a material for an attachment surface was limited by the requirements that the material: (1) have a low binding affinity for trace metals, (2) be manufactured without use of trace metals, (3) be resistant to autoclave temperature and (4) be resistant to repeated exposure to nitric acid for cleaning (Juran, 1975-1986). Five materials fitting these criteria were selected: glass microscope slides (a material that simulates natural silicon oxides such as sand); polypropylene (used in rotating biological contactors) and high density polyethylene (used in trickling filters) (both from Almac Plastics, Rochester, NY); Teflon and glass slides silanated with dichloro-dimethyl-silane (Eastman Kodak Co., Rochester, NY) (both employed as hydrophobic surfaces with low metal binding properties). The Teflon, polypropylene, and high density polyethylene used in the reactor were cut from larger sheets to the same dimensions as standard microscope slides.

Chemical and Microscopic Analyses of Cell Growth and Biofilm Formation. A majority of bacterial strains in natural and engineered reactor systems utilize production of fibrous polysaccharide exopolymers as a means of mediating attachment to surfaces (Costerton, et al., 1976). The biofilm assays employed in this research included both direct counts of attached cells as well as techniques which quantitatively and qualitatively measured polymer production. Surfaces immersed in the cultures were examined for bacterial cell attachment and biopolymer formation by two methods. Slides from sterile, uninoculated control reactors were carried through all analyses as blanks. Glass slides

were rinsed under a gentle stream of deionized water from a water bottle, and allowed to air dry. A pair of slides from each reactor was subjected to the standard chemical oxygen demand (COD) procedure (American Public Health Association, 1976). Results were reported as microequivalents (μeq) of oxidizable material per total slide surface area. Assuming that all oxidizable material in the COD assay was carbon with an average oxidation number of zero, then 1 μeq corresponds to 3 μeq carbon. By further assuming a typical cell weight (1×10^{-12} g) and an average cell carbon content (50% by weight), the difference in total carbon from the COD assay and conversion of each slide cell count data would be representative of exopolymer coverage.

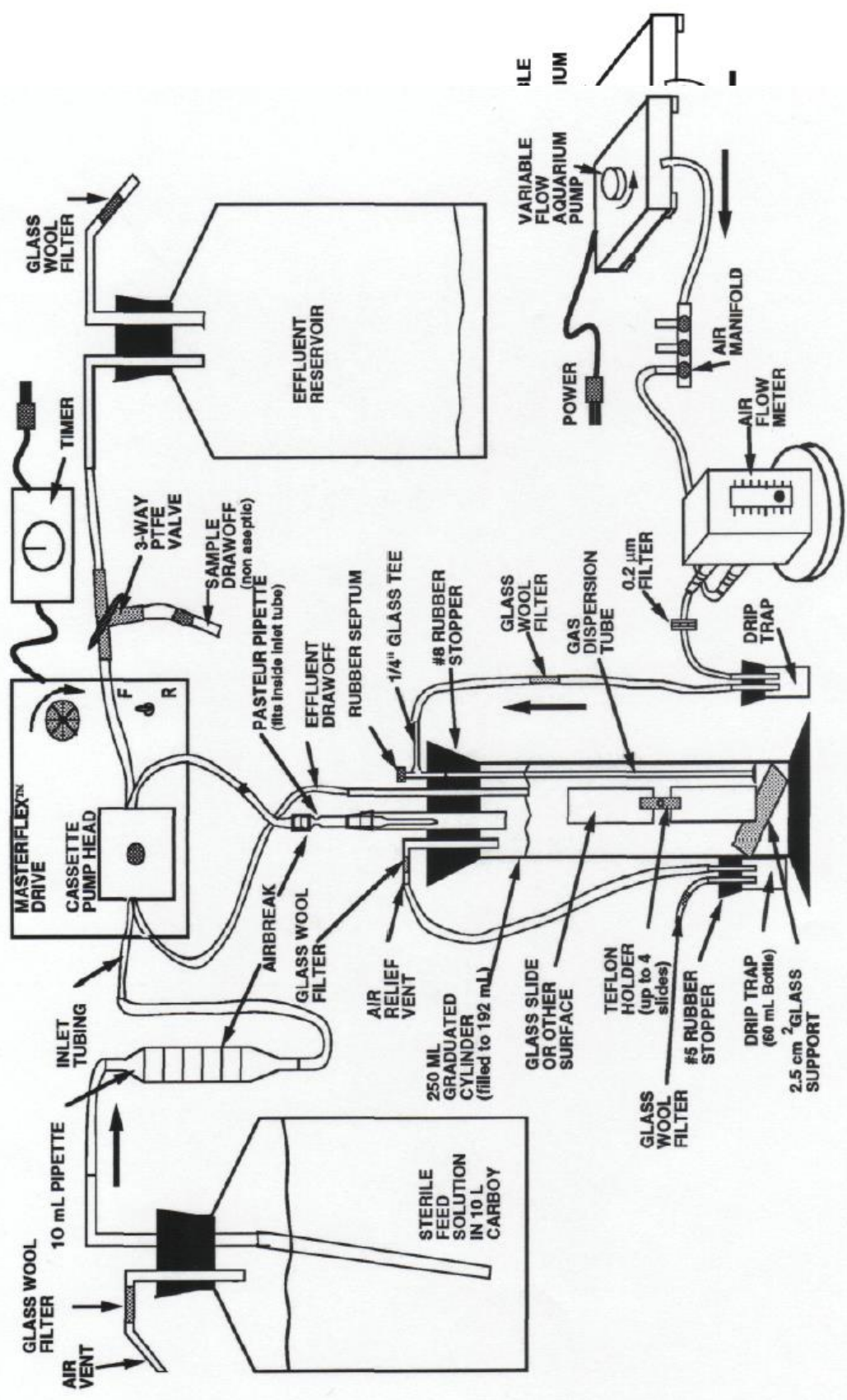
A second pair of slides was stained with colloidal iron-cacodylate stain (Seno, *et al.*, 1983; Seno, *et al.*, 1985) and examined microscopically to evaluate biopolymer production and to obtain direct counts of cells on the surface. For staining, the slides were flooded with iron-cacodylate at pH 7.0 for 10 minutes, washed with distilled water, acidified with 2 to 3 drops of 0.1 N HCL, counter-stained with 2 to 3 drops of 10% potassium ferrocyanide (Prussian Blue Reagent), allowed to stand for 3 to 5 minutes, rinsed a final time with distilled water and blotted dry. For the materials that were optically clear (glass and silanated glass), the slides were examined and cells counted employing a Zeiss Universal light microscope equipped with phase contrast optics and a calibrated square eyepiece reticle to determine the number of cells per unit surface area (cm^2). For the opaque materials (Teflon, polypropylene and high density polyethylene), 0.1% aqueous acridine orange was employed to stain the cells previously stained with the colloidal iron stain before performing direct counts of cells on the surface using epifluorescence microscopy. The colloidal iron stain was not sufficient to allow resolution of the cells by

epifluorescence without the acridine orange stain. A cover slip was placed on the stained area and sealed with Vaspar (a standard mixture by weight of 50% paraffin and 50% petroleum jelly) to prevent drying. Cell counts were of 20 fields per sector and 2 sectors per slide.

Growth of cells in suspension was monitored by optical density at 600 nm (Spectronic 20, Bausch & Lomb Inc, Rochester, NY; Model 3600 Spectrophotometer, Beckman Instruments, Inc., Irvine CA). Suspended cells were also observed with the light microscope under phase-contrast optics to monitor consistency in cell morphology and for cell clumping (an indication of exopolymer production). Spread plates containing PYG agar medium were also utilized to check for maintenance of pure cultures.

Bioreactor Design and Construction. A schematic diagram of the reactor system is shown in Figure 3.1. The bioreactor vessel consisted of a Stoppered 250 mL graduated cylinder filled to 192 mL capacity. The reactor was initially washed with a 10% reagent grade nitric acid solution and rinsed with deionized water. This was followed by a wash in a 10% redistilled nitric acid solution and a rinse with deionized water prior to each use. The reactor was connected to four separate lines: a 1 cm I.D. "T" connecting tube with a 1 cm O.D. rubber septum and a butyl rubber hose as air inlet; a 15 cm length of 6 mm. I.D. glass tubing as effluent draw-off; a 15 cm L-shaped 6 mm I.D. glass tube as air relief vent, and a 12 mm I.D. glass tube containing a Pasteur pipette as inlet feed. A 2.5 cm square piece of glass was placed on the bottom of the vessel at approximately a 45 degree angle to keep a set of 4 slides from resting on the bottom. The slides were stacked vertically in pairs. A clip fabricated from Teflon was used to hold up to 4 slides in place during an experiment.

Figure 3.1. Schematic of cyclic-flow reactor system.



A 60 mL glass bottle with rubber stopper was used as a drip trap on both the air exhaust line and the air inlet line. Glass wool plugs were placed in both lines to prevent contamination by airborne bacteria. Aeration was achieved by bubbling with a constant temperature air stream provided by an aquarium pump. Air was passed through a flow meter throttled to $1.97 \text{ cm}^3/\text{s}$ at 25° C and 1 atm. (1.013 bar), then through a 0.2 mm disposable syringe filter, a drip trap and finally a glass wool filter prior to entering the reactor through a gas dispersion tube (25-50 mm pore diameter).

A Masterflex (Cole-Parmer Instrument Co., Chicago, IL) 1-100 rpm drive powered a multi-channel pump head to simultaneously inject feed solution from a 10 L carboy through 0.8 mm I.D. silicone tubing and to withdraw reactor effluent through 1.6 mm I.D. silicone tubing for collection in the waste carboy. A 10 mL disposable glass pipette was inserted in the feed line ahead of the pump to act as an air break to prevent back contamination by microorganisms from the reactor into the sterile feed solution carboy. A Pasteur pipette at the feed inlet to the bioreactor acted as a second air break to prevent back contamination by headspace aerosols. A 3-way polytetrafluoroethylene (PTFE) valve inserted in the effluent line between the pump and the collection bottle allowed for draw-off of non-aseptic samples for optical density and pH measurements.

Preparation of the Bioreactor for Experiments. The bioreactor apparatus was assembled as two separate components: (1) the inlet tubing attached to the 10 L feed solution carboy of MMS medium without carbon source; and (2) the assembled bioreactor containing slides and tubing with drip traps, and attached effluent carboy. The two components were sterilized together in an autoclave at 121° C for 90 minutes. All joints, exposed tubing connectors and ends were wrapped in aluminum foil to protect sterility.

After sterilization, the two components were transported to a laminar-flow hood to mate the feed solution carboy line aseptically to the bioreactor inlet tube. A sterile 0.2 mm disposable syringe filter was inserted aseptically in the air inlet line and then attached by silicone tubing to the airflow meter and air pump. Finally, 100 mL of a 0.2 mm filter sterilized 10 g/L carbon source was added aseptically to the 10 L of MMS medium in the feed carboy.

Sterile medium (mineral components plus carbon source) was pumped into the bioreactor until all slides were immersed and the effluent draw-off began removing excess medium (192 mL volume mark to immerse all slides). A sterile syringe was used to inject 10 mL of inoculum through the septum into the bioreactor while the air pump was operating. The air flow pushed the injected cells through the gas dispersion tube into the medium. For each experiment, two duplicate reactors were inoculated with a test strain while a third reactor was not inoculated, to serve as a sterile control.

After inoculation, the entire apparatus was transferred to a 25°C constant temperature room and allowed to operate as an aerated batch reactor for 48 hours to allow the test bacteria to acclimate to the reactor environment and to initiate growth (as determined by the appearance of any measurable optical density). At 48 hours, the pumps were activated and subsequently were cycled on and off at 12 hour intervals using a timer switch. The 12 hour cyclic on-off flow regime was continued for the duration of the experiment. During the flow phase, the feed pump controlled the dilution rate (i.e. fluid residence time) at a hydraulic residence time of approximately 6 hours (*e.g.*, flow = 32 mL/hr; dilution rate = 0.167/hr). The airflow provided mixing of the reactor contents during operation. Experiments using a dye tracer verified that the reactor behaved as a completely mixed system. Samples taken from

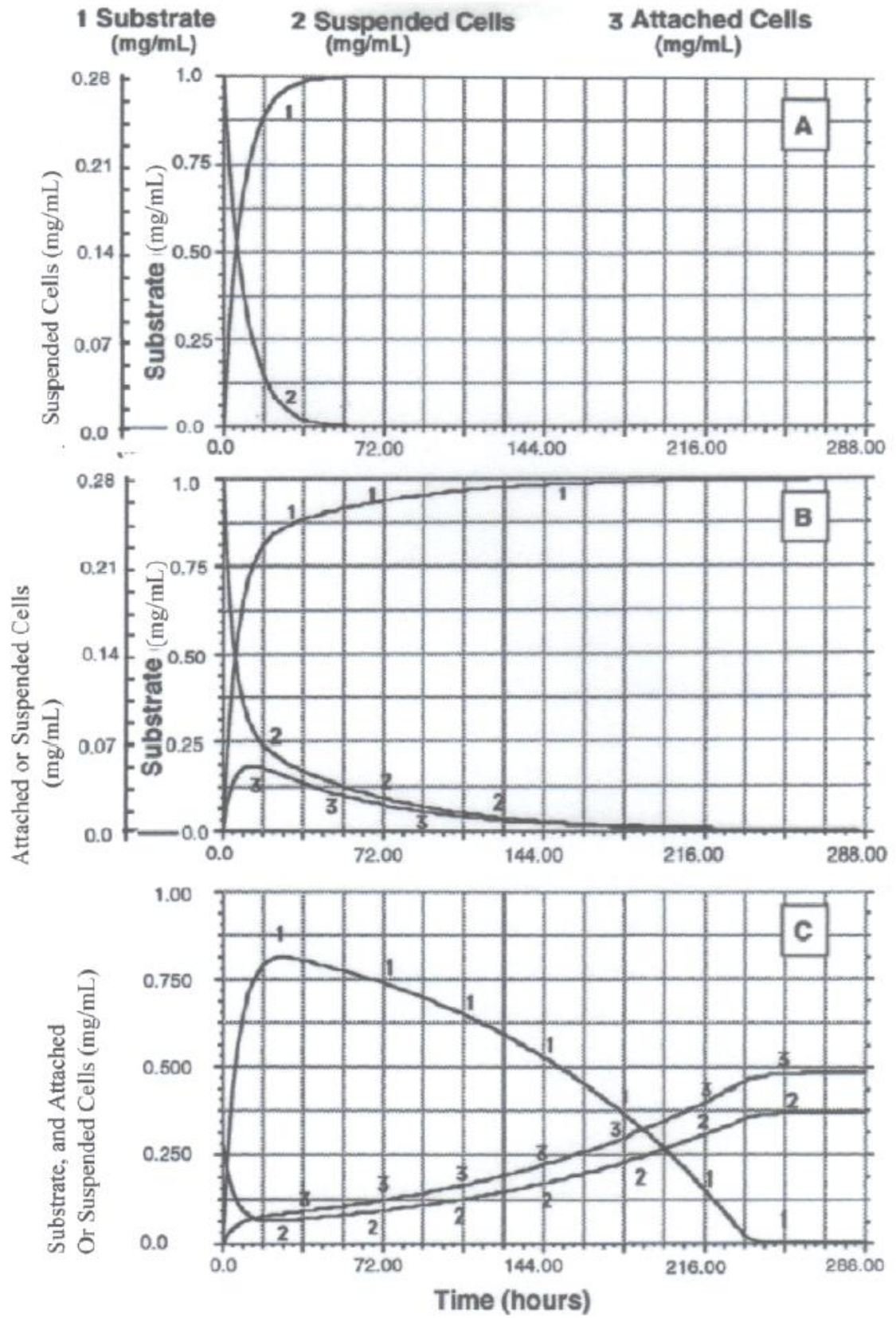
the effluent sampling tube shortly after the pumps were activated each day to determine the liquid phase optical density and pH. After 6 days of cyclic operation (8 days total), one of the two inoculated reactors (for each strain) was sacrificed and the attachment surfaces withdrawn for the chemical and microscopic analyses of bacterial attachment and biofilm growth. After 12 days of cyclic operation (14 days total), the second inoculated reactor (for each strain) was sacrificed and the attachment surfaces withdrawn for the chemical and microscopic analyses of bacterial attachment and biofilm growth performed in the same manner as the first.

RESULTS AND DISCUSSION

Reactor Modelling Calculations. Example results illustrating the operation of simple model reactors are shown in Figures 3.2 and 3.3. The 12-day simulation period matched the maximum length of our operation of the experimental reactor system under conditions of cyclic flow (see Materials and Methods). Figure 3.2 corresponds to normal chemostat operation with constant flow, Q . Comparison of Figures 3.2A and 3.2B, illustrates the hypothetical washout of nonadherent (Fig. 3.2A) and adherent (Fig. 3.2B) ($k_D = 0.175/\text{hour}$, $k_A = 0.05/\text{hour}$) cell strains with otherwise identical growth characteristics. As expected in the model, attachment acts to retard reactor system washout. Simulations with a 30% reduction in the detachment rate constant (from $k_D = 0.175/\text{hour}$ to $0.125/\text{hour}$, with $k_A = 0.05/\text{hour}$) confirm the well-established fact that a conventional chemostat can select for organisms with strong adhesive properties (Fig. 3.2C).

The simulation in Figure 3.2B depicts the bacterial strain being washed out of the reactor in spite of the fact that it was able to attach to a surface. Figure 3.3A illustrates

- Figure 3.2. Concentrations of substrate (1), suspended cells (2), and attached cells (3) in a Multigen with steady flow.
- (A) Washout of a nonadherent strain.
 - (B) Washout of an adherent strain with the same growth parameters as in panel A except $k_A = 0.05/\text{h}$ and $k_D = 0.175/\text{h}$.
 - (C) Selection of a more adherent strain with the same growth parameters as in panel B, except k_D reduced to $0.125/\text{h}$.
- (Note the vertical scale for cell concentration is magnified in panels A and B).

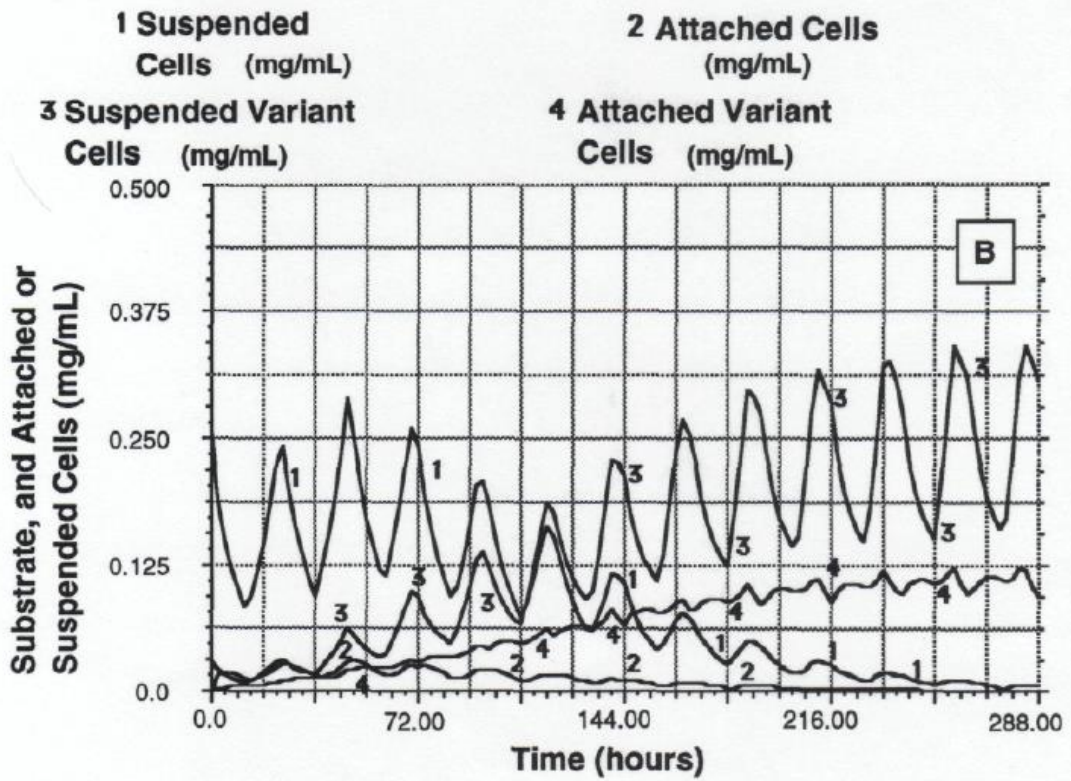
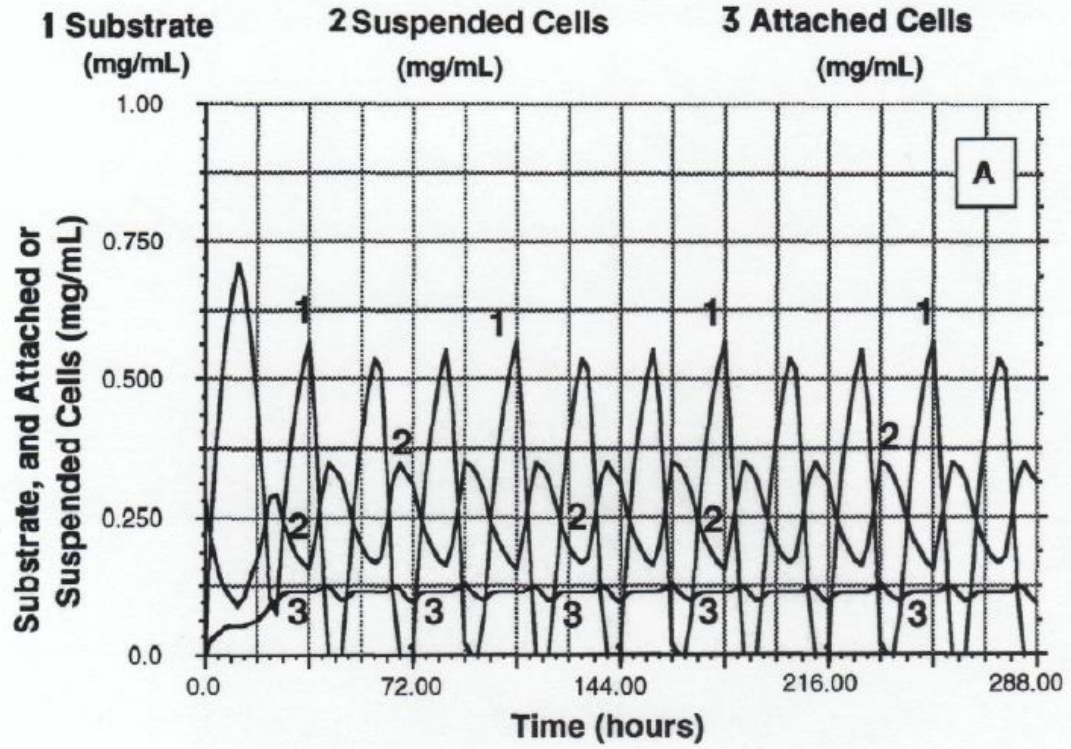


the results for the same strain if the flow into the reactor follows on/off cycles. The model predicts retention of the strain under these conditions. A 12 hour period of flow oscillation is employed to simulate the period which was ultimately chosen for the experiments. However, the cycle period could serve as an experimental variable which might be optimized, for example, to insure maintenance of a desired minimum substrate concentration. As shown in Figure 3.3A, during the "off" cycle the higher cell density in solution forces the system to higher levels of cell attachment while nutrients are depleted. During the "on" cycle nutrients are replenished, and the suspended population declines through washout. A stable oscillation is established in the reactor population. In figure 3.3B the same strain is modelled as an attached variant which comprises 10% of the initial population. The remainder of the population is assumed to have identical kinetic constants for cell growth and death but has a higher detachment rate of 0.5 /hr (vs. the variant detachment rate of 0.175/hr). The model results show that the reactor will operate to select the variant with superior adherent properties and (given the assumed kinetic constants) the variant will constitute the preponderance of the reactor population after 12 days.

The above model calculations confirmed the intuitive expectation that flow cycles can provide favorable attachment conditions for adherent bacteria that would be washed out under normal continuous flow chemostat operation due to limitations of growth rate or attachment properties. In the experiments described below, such limitations were imposed by the need for a chemically defined medium that lacked many of the nutrient components normally provided to support rapid bacterial growth. The results obtained from the experiments confirmed that cyclic-flow operation would yield growth and attachment that the continuous and batch culture procedures were not capable of achieving.

- Figure 3.3. (A) Effect of cyclic flow (12 h on, 12 h off) on the adherent cell strain shown in Fig. 3.2B.
- (B) Selection of the cell strain shown in Panel 3A under cyclic-flow conditions when it is a variant (10% of initial suspended population).

(Note for 1 and 2, detachment rate constant $K_D = 0.5/h$; for 3 and 4, $K_D = 0.175/h$).



Culture-Metal Toxicity Results. Two different methods were evaluated to ascertain which bacterial strains and at what concentration Pb or Cd toxicity influenced growth of the bacterial strains. All 24 initial candidate strains were tested with the metal soaked disks at all four concentrations of Pb and Cd on disposable petri dishes. However, none of the plates showed any inhibition zones of growth. This outcome was possibly caused by metal ion adsorption to dish surfaces, complexation with the agar medium or because of some undefined shielding effect of cell growth on the surface.

The tests in liquid culture were restricted to the strains that showed the best degree of surface coverage during growth in liquid culture of the MMS medium (See Table 3.3). Of these five strains, two of them (*Zoogloea* sp. WGO4 on pyruvate and *Arthrobacter* 9G4D on succinate) were severely growth inhibited by the presence of metals and were eliminated from further consideration. Figure 3.4 illustrates one set of results from the tests. These data indicated that *Arthrobacter* 9G4D grown on pyruvate was generally not affected by metal concentrations of Pb up to 10^{-5} M, the highest concentration used. The results for *P. cepacia* 17616 grown on acetate showed the widest range of impacts on growth in the presence of Pb (see Figure 3.5). Growth inhibition at 10^{-5} M Pb was severe with about 75% reduction in optical density of the culture. Growth inhibition at 10^{-6} M Pb was less severe (a 30% reduction in optical density) and still lower at 10^{-7} M Pb (less than 20% reduction in optical density).

Experimental results also showed that *P. cepacia* 17616, *P. fluorescens*, *P. cepacia* 249-100, all grown on pyruvate, were severely inhibited by the 10^{-5} M concentration of Pb (see Figures 3.6, 3.7, and 3.8 respectively). A concentration of 10^{-6} M and 10^{-7} M of Pb had very limited growth inhibition upon both *P. cepacia* strains. The growth of *P. fluorescens* strain

Table 3.3: Bacterial Strains Selected for Toxicity Tests in Liquid Culture in the Presence of Various Concentrations of the Metal Lead.

Bacterial Strain	Gram Stain	Carbon Source
<i>Arthrobacter</i> 9G4D	+	Succinate, Pyruvate
<i>Pseudomonas cepacia</i> 17616	-	Acetate, Pyruvate
<i>Pseudomonas cepacia</i> 249-100	-	Pyruvate
<i>Pseudomonas fluorescens</i>	-	Pyruvate
<i>Zoogloea</i> sp. WGO4	-	Pyruvate

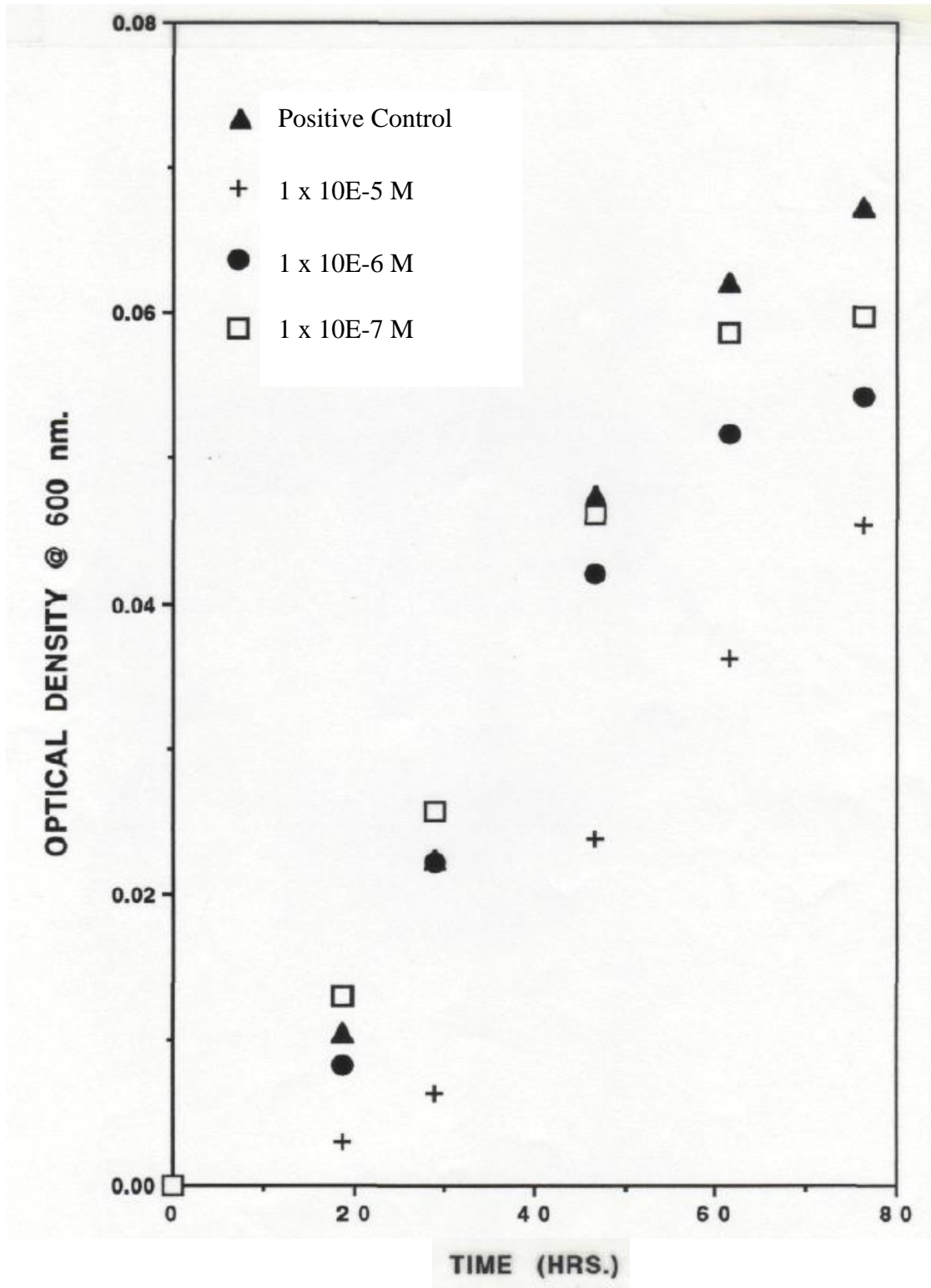


Figure 3.4 Toxicity Effects of Various Concentrations of Lead on the Growth of *Arthrobacter* 9G4D on Pyruvate.

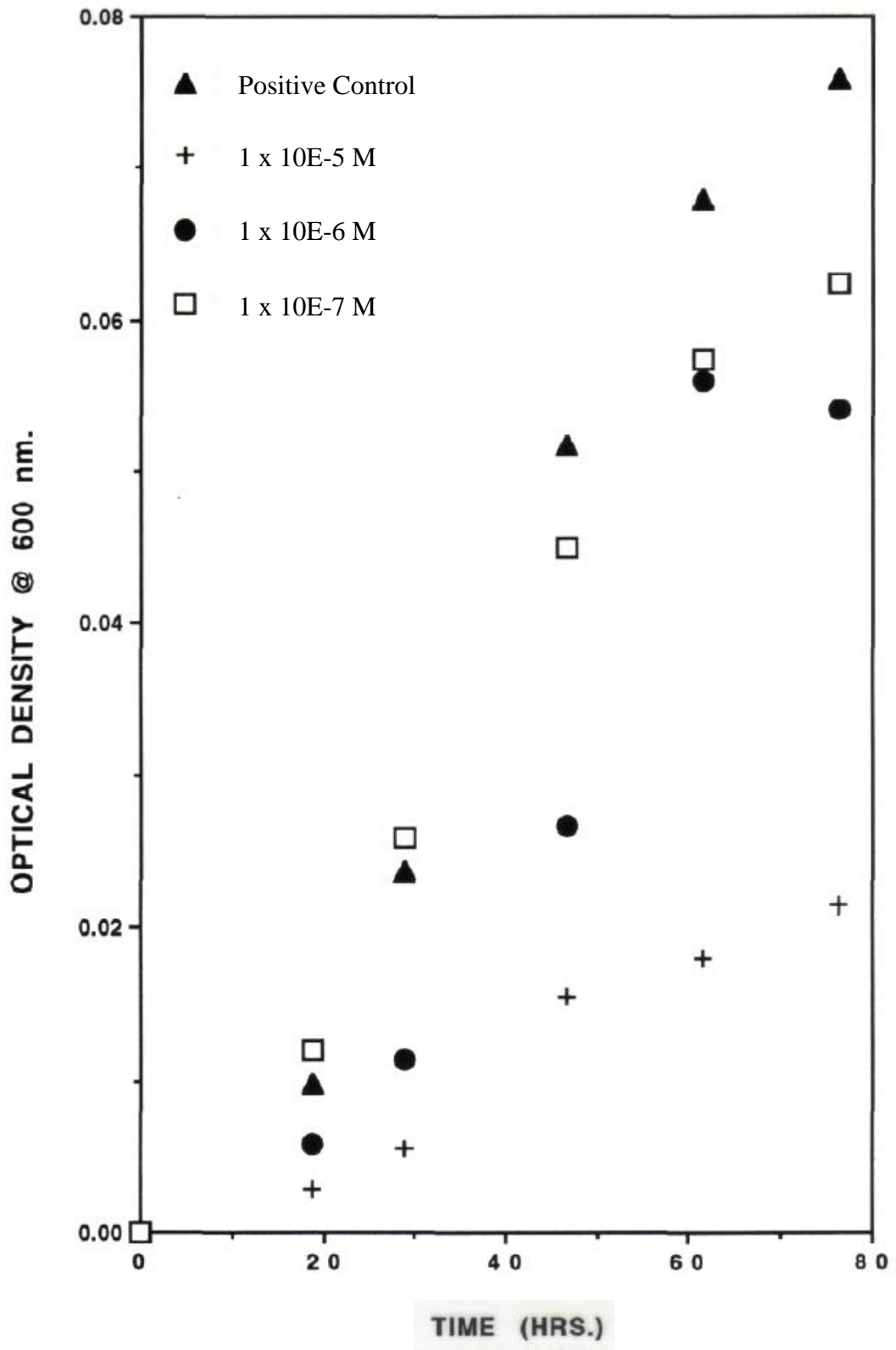


Figure 3.5. Toxicity Effects of Various Concentrations of Lead on the Growth of *Pseudomonas cepacia* 17616 on Acetate.

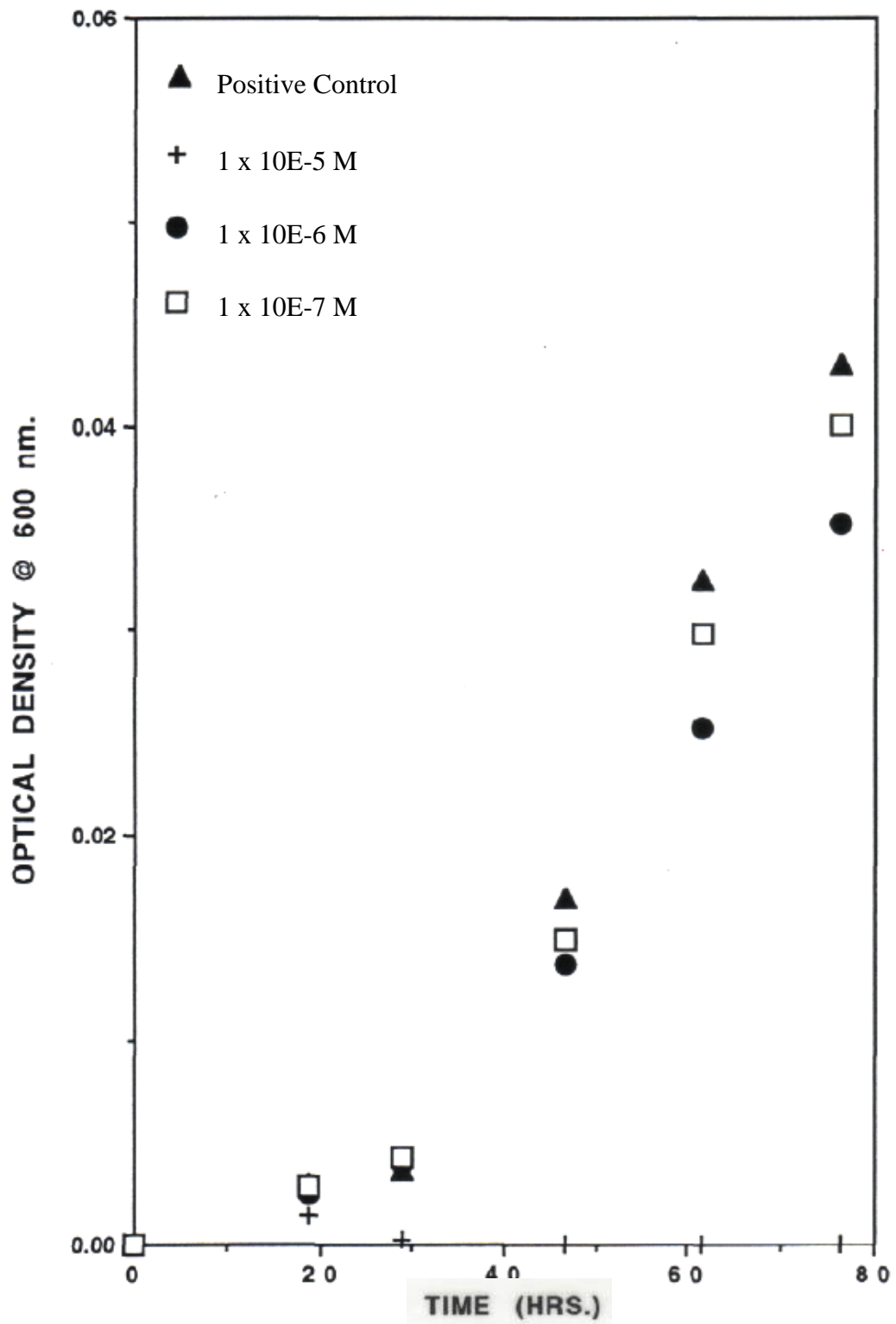


Figure 3.6. Toxicity Effects of Various Concentrations of Lead on the Growth of *Pseudomonas cepacia* 249-100 on Pyruvate.

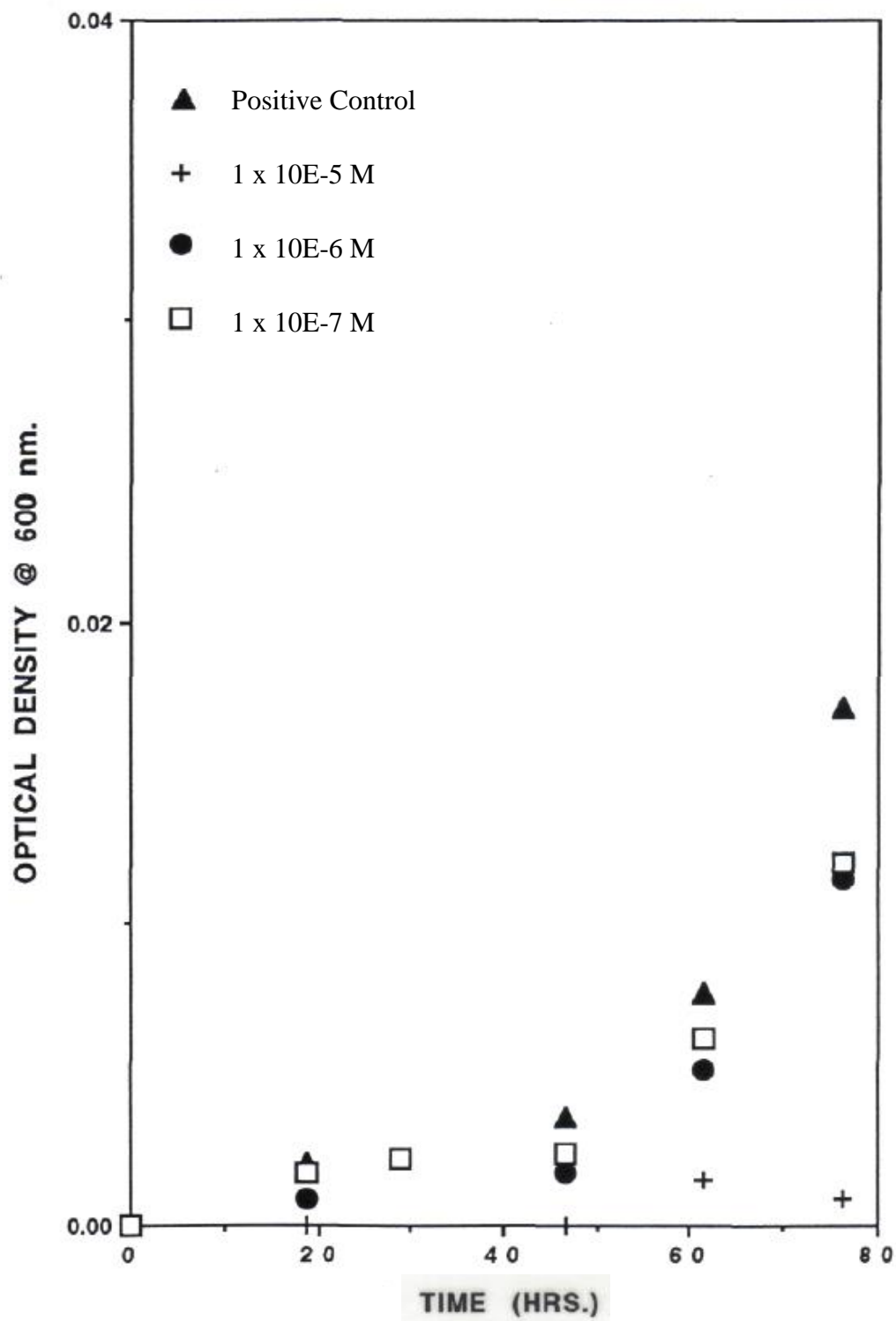


Figure 3.7. Toxicity Effects of Various Concentrations of Lead on the Growth of *Pseudomonas cepacia* 17616 on Pyruvate.

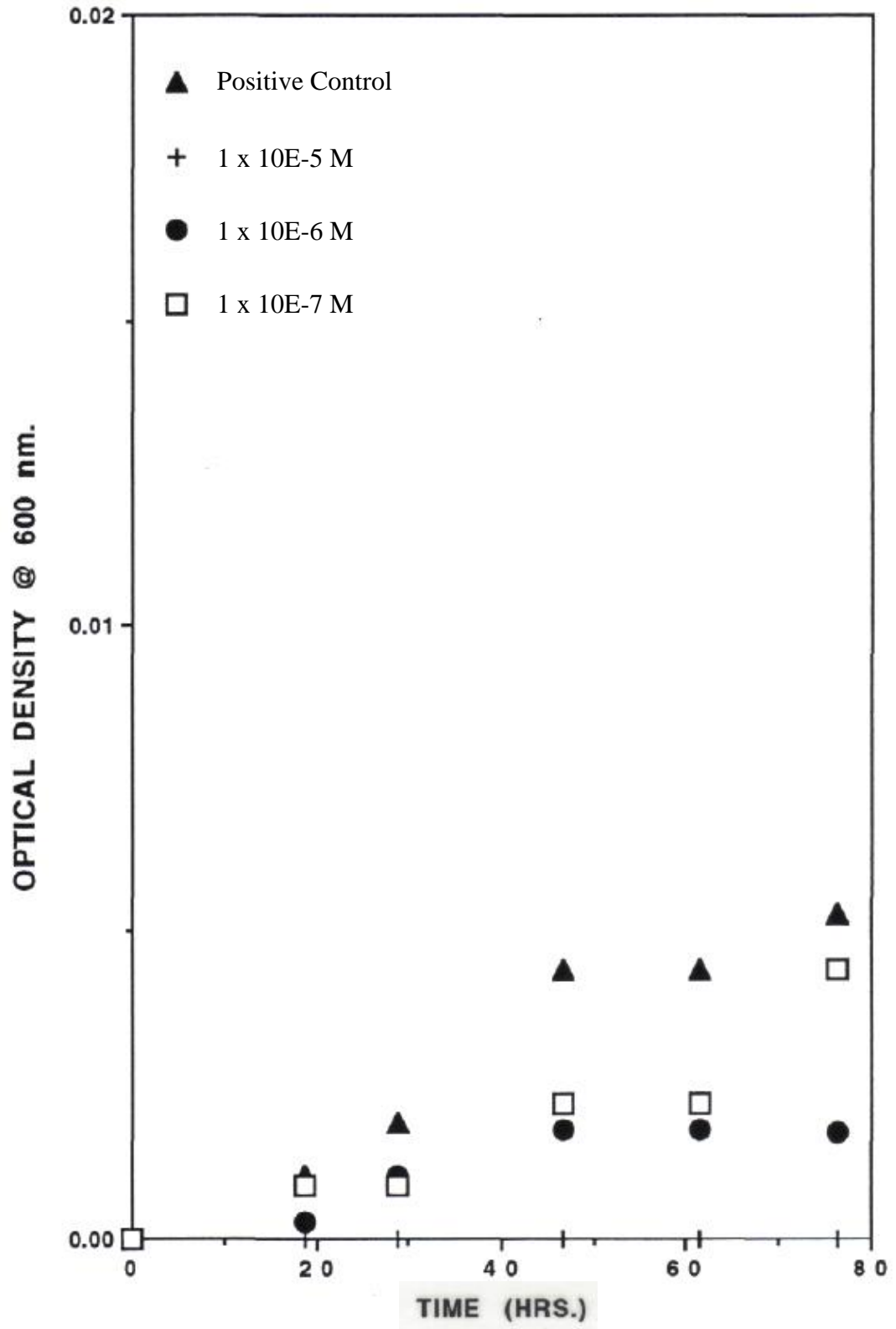


Figure 3.8. Toxicity Effects of Various Concentrations of Lead on the Growth of *Pseudomonas fluorescens* on Pyruvate.

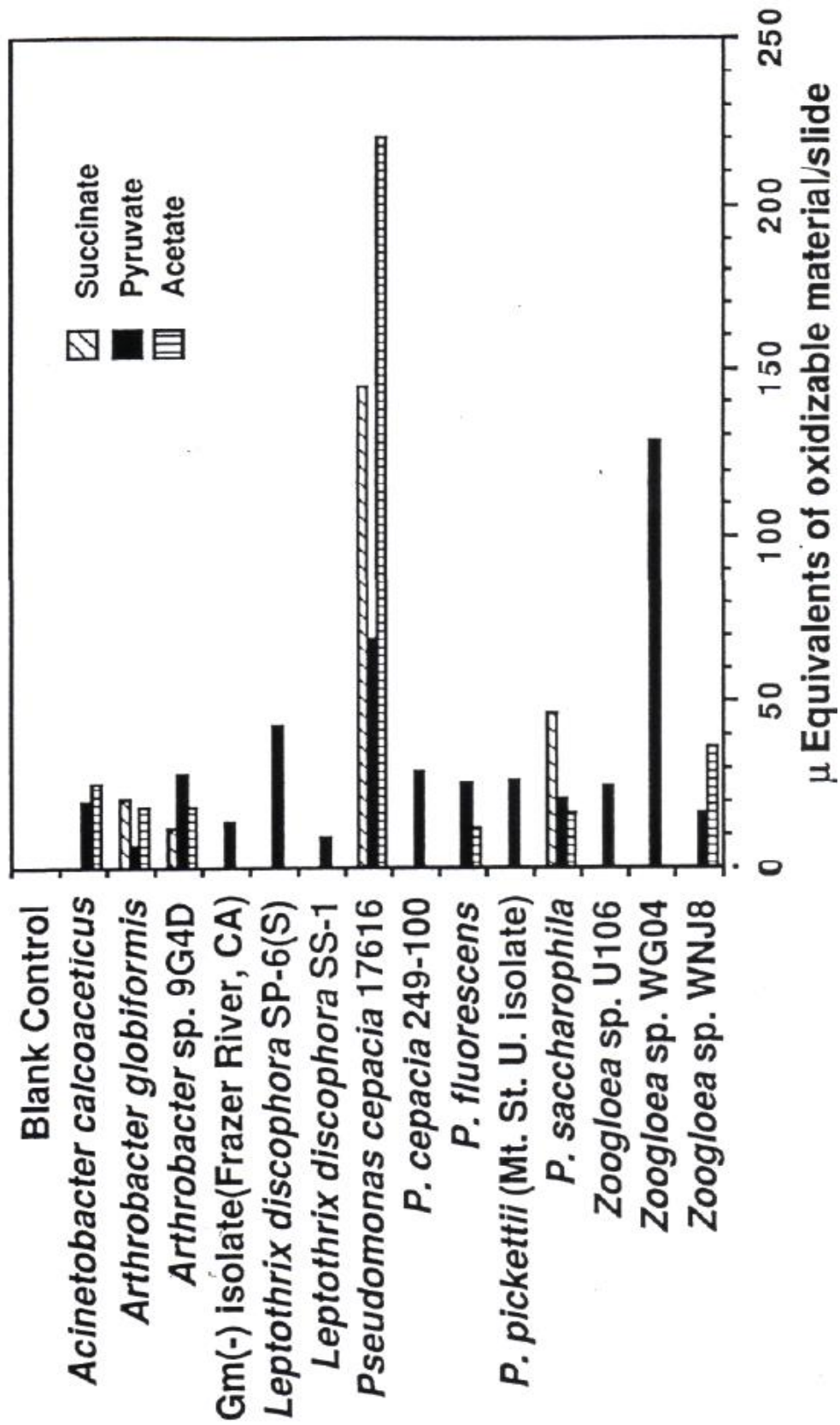
(Figure 3.8) was impacted to a greater degree at the 10^{-6} M than the 10^{-7} M Pb concentration. The growth of *P. cepacia* 17616 on acetate showed the highest optical density in the positive control, with growth of *Arthrobacter* 9G4D on pyruvate being nearly the same. The other three strains had total growth less than 50% of this level of growth as measured by optical density.

Cyclic-Reactor Experimental Results. The reactor system was used to evaluate biofilm development by each of the 14 strains previously selected (from the initial group of 24 test strains) on glass slides over an 8 to 14 day time period in the MMS medium (Table 3.2). All 14 strains grew in MMS-pyruvate medium. Six grew on acetate and four on succinate. In most cases, COD results, which provide a measure of attached cells plus polymer, were confirmed by direct microscopic cell counts.

Figure 3.9 shows the results of COD tests on slides from the reactors. The results shown are for the reactor slides destructively processed after 6 days of cyclic operation (8 days total run time). The results from the 8 day reactors for a majority of the bacterial strains yielded partial monolayer cell coverage greater than 1.5×10^4 cells/cm² (Figure 3.10) making accurate cell counts difficult even at a magnification of 2000 power. Surface coverage by biofilm on slides after 14 days of reactor operation for a majority of the bacterial strains was higher than was found at 8 days. Cell coverage for strains at day 14 had to be estimated as a percentage of the total slide surface area (40.74 cm²). Some representative 14 day results include: *P. cepacia* 17616 on MMS-acetate - 94%, *P. cepacia* 249-100 on MMS-pyruvate - 89%, *P. fluorescens* on MMS-pyruvate - 81%, *Zoogloea* sp. WGO4 on MMS-pyruvate - 90%, *Acinetobacter calcoaceticus* on MMS-pyruvate -52% and on MMS-acetate - 36%,

Figure 3.9. Biofilm surface coverage (in microequivalents of oxidizable material per slide) determined from slides in the bioreactor after 6 days (8 total days) of cyclic-flow reactor operation.

(Note: the *Leptothrix* cultures contained a *Caulobacter* sp contaminant. Coverage for *Leptothrix* strains was reduced by a 2:1 ratio of cell counts of *Caulobacter* spp. and *Leptothrix* spp. on the slides.)



Frazer River, CA. isolate on MMS-pyruvate - 10% and both *P. sacchrophilia* and *P. pickittii* on MMS-pyruvate - 11%.

Based on the COD analysis in Figure 3.9, *P. cepacia* 17616 produced the highest biofilm surface coverage with acetate and succinate as the carbon/energy source (220 and 145 microequivalents/slide, respectively). Only the *Zoogloea* sp. WGO4 strain on MMS-pyruvate exhibited a surface coverage comparable to that of *P. cepacia* 17616 on MMS-acetate (Figure 3.4). Direct cell counts also showed high surface coverage (cells per slide) for *P. cepacia* 17616 as well as *Zoogloea* sp. WGO4 with MMS-pyruvate, *Zoogloea* sp. WNJ8 with MMS-acetate, *P. sacchrophilia* with MMS-pyruvate, the Frazer River isolate with MMS-pyruvate, and *Acinetobacter calcoaceticus* with MMS-pyruvate and acetate (Figure 3.10). Most of the gram-negative strains showed significantly better biofilm development on all carbon/energy sources as judged by both COD analysis and direct microscopic cell counts than the two gram-positive *Arthrobacter* Strains (Figure 3.9 and 3.10). However, many of the gram-negative strains displayed less growth in the fluid phase than the *Arthrobacter* sp. as indicated by optical density measurements (Figure 3.11). For example, *Arthrobacter* sp. 9G4D grew in the fluid phase on the MMS-pyruvate medium to an OD nearly twice that of *Zoogloea* sp. WNJ8 and *P. fluorescens* on MMS-pyruvate, *P. cepacia* 17616 on MMS-acetate, and *Acinetobacter calcoaceticus* on MMS-succinate. The strain *Zoogloea* sp. WGO4 produced large clumps or aggregates that tended to settle out of suspension and may have reduced optical density measurements. Only the gram-negative strain *P. pickittii* on MMS-pyruvate showed comparable fluid phase growth to that of the *Arthrobacter* spp. The low OD and high surface coverage achieved by strains such as *P. cepacia* 17616 and *Zoogloea* sp. WG04

Figure 3.10. Biofilm cell count from slides removed after 6 days (8 total days) of cyclic-flow operation.

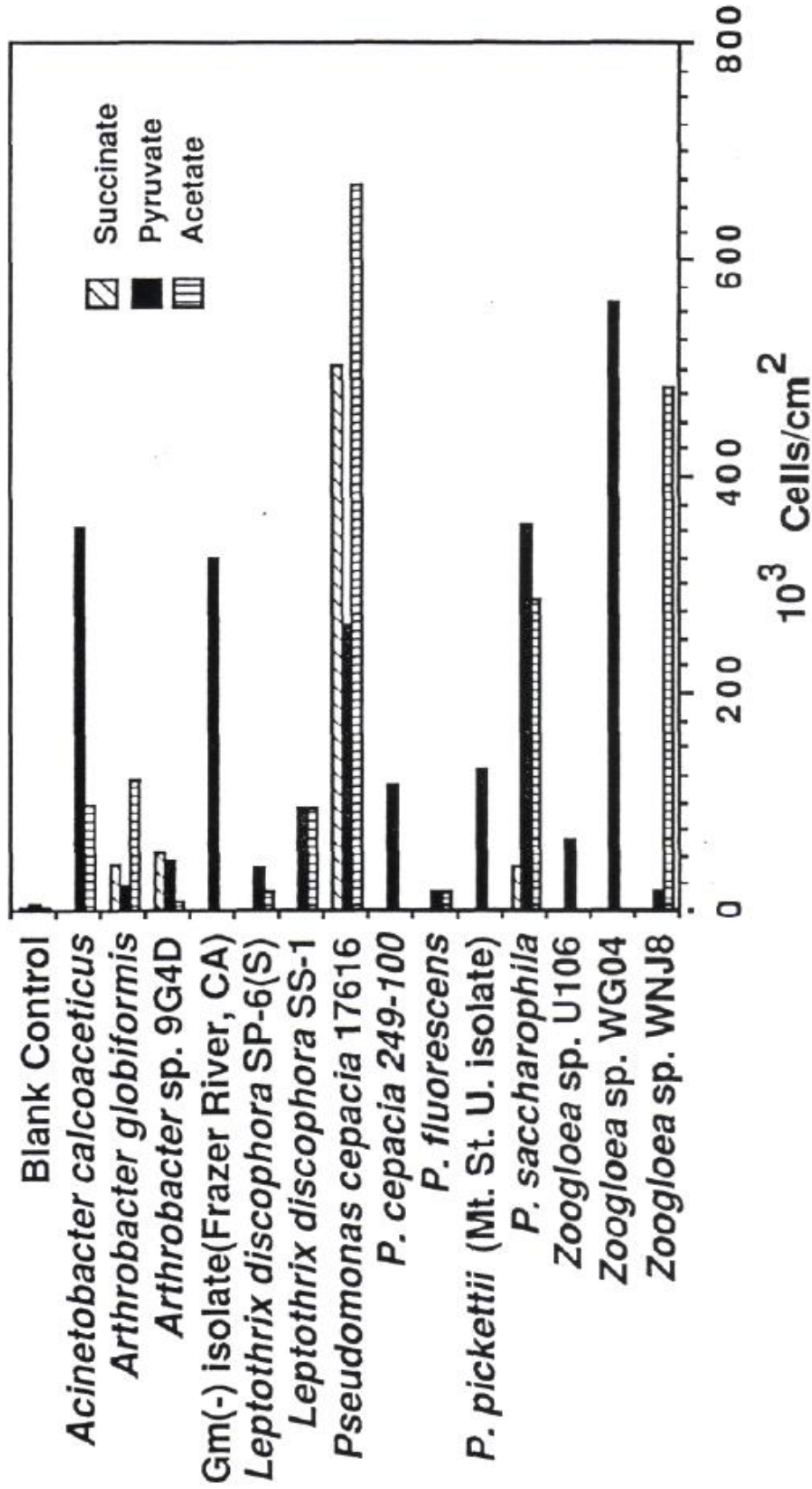
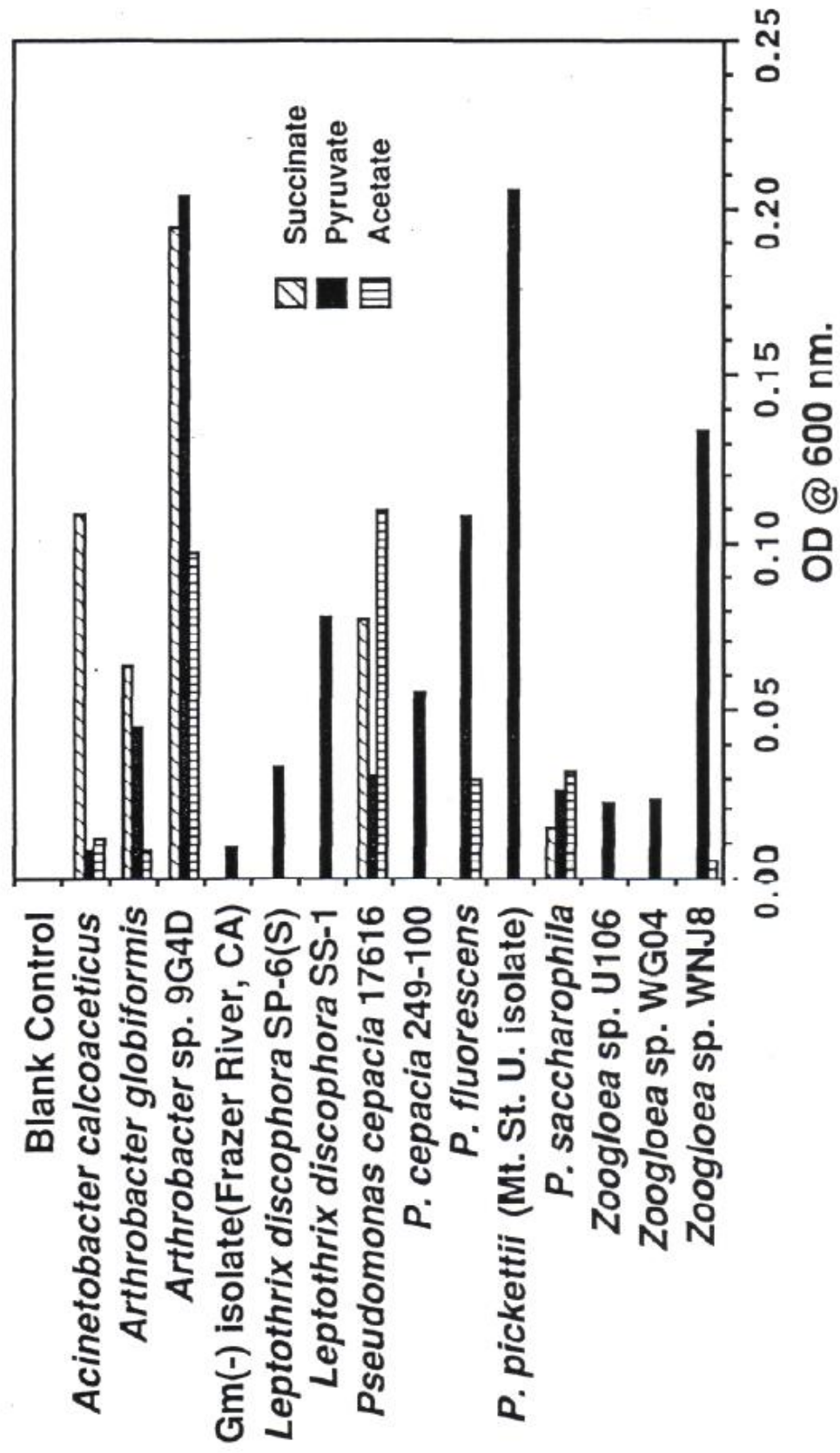


Figure 3.11. Fluid-phase optical density after 6 days (8 total days) of cyclic-flow reactor operation.



supports the concept that attachment to a surface allows bacteria to maintain their populations in environmental conditions that, otherwise, would not support their growth. Some strains (*e.g.*, *P. cepacia* 249-100) exhibited both moderate growth in the fluid phase and biofilm development, indicating their adaptability under the stringent environmental conditions imposed by the minimal MMS medium.

Cell coverage of the slides in the reactor was generally limited to a partial mono-layer. However, there were instances (*e.g.* *Pseudomonas fluorescens*, MMS-pyruvate) where distinct microcolonies were found on the slide surfaces taken from the 14 day reactors. The cell colonies were several layers thick with patchy monolayer coverage between colonies. Microcolonies were not evident on slides from the 8 day reactors.

Biofilm formation and polymer production were qualitatively evaluated by microscopic observation of color development after staining with the colloidal iron-cacodylate stain. Results are summarized in Table 3.4. Biofilms of *P. fluorescens* (on MMS-pyruvate), *P. cepacia* 17616 (on MMS-acetate) and *Acinetobacter calcoaceticus* (on MMS-pyruvate or acetate) displayed the most intense reaction with the stain. The results of the latter two strains correlated well with the data in Figures 3.9 and 3.10 for biofilm and cell coverage. For most of the other strains, however, the staining data in Table 3.4 (obtained after 14 days of reactor operation) does not directly correlate with the biofilm and cell coverage data in Figures 3.9 and 3.10 (obtained after 8 days of reactor operation). The differences in staining results may reflect differences in the types or amounts of acidic functional groups that the exopolymer contains as it ages. Since the Fe(II) used in the staining process binds to anionic functional groups on the polymer and cell surface, low relative visibility of the stain may imply a higher percentage of non-ionic and/or cationic groups. The intense reaction may

Table 3.4: Comparison of Biofilm Development on Glass Slides, as Indicated by Colloidal Iron-Cacodylate Stain After 14 Days Growth on MMS Medium in the Cyclic-Flow Reactor

Bacterial Culture	Carbon/Energy Source		
	Pyruvate	Succinate	Acetate
<i>Arthrobacter globiformis</i>	1+ ^a	1+	B
<i>Arthrobacter</i> sp. 9G4D	2+	+	3+
<i>Acinetobacter calcoaceticus</i>	5+	-	5+
Isolate, Frazer River, CA	2+	-	-
<i>Leptothrix discophora</i> SP-6	3+	-	-
<i>Leptothrix discophora</i> SS-1	1+	-	-
<i>Pseudomonas cepacia</i> 17616	1+	2+	5+
<i>P. cepacia</i> 249-100	4+	-	-
<i>P. fluorescens</i>	5+	-	-
<i>P. pickittii</i>	3+	-	-
<i>P. sacchrophilia</i>	2+	2+	1+
<i>Zoogloea</i> sp U106	1+	-	-
<i>Zoogloea</i> sp WG04	2+	-	-
<i>Zoogloea</i> sp WNJ8	3+	-	1+

a Symbols: 1+ to 5+ relative rating of biofilm staining (1 + = barely visible; 5+ = very intense blue color); - not tested

b No results: reactor became contaminated before completion of the experiment.

correspond to a larger density of anionic groups for which the stain has the greatest specificity.

Table 3.5 provides a comparison of results from batch culture, cyclic and continuous flow experiments utilizing the cyclic flow reactor apparatus. The continuous, batch and cyclic-flow values are the results of analyses performed on glass slides 8 days after starting the experiment (6 days after starting flow cycles). The strains *P. cepacia* 249-100 and *Zoogloea* sp. U106 were selected for this experiment. Both strains, while not the best candidates in terms of growth and attachment, showed consistent, moderate growth in the fluid phase (Figure 3.11) and adequate attachment as a biofilm (Figures 3.9 and 3.10). The resulting data show cyclic-flow growth of both strains generally exhibited a higher degree of biofilm coverage than attained with the batch and continuous-flow reactor operation. The fluid phase optical density was also significantly lower than the batch reactor but generally higher than the continuous-flow reactor.

The experimental apparatus was also used in a preliminary experiment to study attachment of *Arthrobacter* sp. 9G4D to several alternative surfaces. Table 3.6 shows that normal glass slides supported the densest surface coverage. The normal glass slide-containing reactors also produced the highest mean liquid phase optical density indicating more growth occurred in the reactor. After 12 days of cyclic-flow reactor operation, silanated glass and high-density polyethylene surfaces supported a less dense biofilm than at 6 days indicating detachment from the hydrophobic surface had occurred during the experiment. The opposite effect was observed with normal glass slides which may have more affinity for the gram-positive *Arthrobacter* sp. 9G4D cell surface.

Table 3.5: Comparison of Biofilm Development on Glass Surfaces in Batch, Continuous Flow and Cyclic Flow Reactor Operation Using Pyruvate as Carbon/Energy Source in MMS Medium^a

Bacterial Culture	Surface Coverage ((μ -Equivalents of Oxidizable Material/slide) ^b)		
	Batch	Continuous	Cyclic-Flow
Control	3.7	2.7	0.0
<i>P. cepacia</i> 249-100	19.7	25.3	81.8
<i>Zoogloea</i> sp. U106	2.5	7.0	8.1
	Direct Cell Count (X 10 ³ cells/cm ²)		
Control	17.8	17.9	17.6
<i>P. cepacia</i> 249-100	2,100	738	24,100
<i>Zoogloea</i> sp. U106	35.2	38.1	69.6
	Fluid Phase O.D. (Abs @ 600 nm.)		
Control	0.003	0.000	0.000
<i>P. cepacia</i> 249-100	0.22	0.032	0.13
<i>Zoogloea</i> sp. U106	0.174	0.002	0.002

a All experiments were performed for a 72 hour duration

b Glass slide area is 40.742 cm²

Table 3.6: Growth Of *Arthrobacter* 9G4D On Pyruvate In MMS Medium Under Cyclic-Flow Conditions With Different Surface Materials

Substratum	Surface Cell Count (X 10 ³ cells/cm ²) ^a		Bulk fluid Optical Density ^b (@ 600 nm)
	Day6 ^c	Day 12 ^c	
Silanated glass	4.2	0.44	0.06
Polypropylene (PP)	0.66	0.69	0.08
PTFE (Teflon) ^d	0.37	0.81	0.06
High-Density Polyethylene(HDPE) ^e	15.0	3.7	0.07
Normal Glass	1.9	4.9	0.36

a Mean values from 2 slides per reactor, 2 sectors per slide, 20 fields per sector.

b All values are the mean of 14 daily measurements.

c Time of reactor operation under cyclic flow conditions (8 and 14 days total).

d The Teflon surface was uneven and a cover slip could not be used. Counts were performed directly in oil without a cover slip with a neofluoar lens.

e The HDPE surface was uneven and malleable making focusing difficult. There were loose cells suspended in the solution under the cover slip that were not counted due to problems with drift and focus.

CONCLUSIONS

Employing the reactor and cyclic-flow regime described, bacterial strain attachment was studied under operating conditions which conventional batch culture or continuous flow bioreactor methods could not accomplish. Comparison of the data collected from batch and continuous flow experiments demonstrate the utility of cyclic flow patterns for selection of slow growing adherent strains. The data indicated that many strains which did not grow well in the MMS medium (*e.g.*, *P. sacchrophilia*, *Leptothrix* spp.) exhibit sufficient surface attachment to prevent the strain from being washed out of the cyclic-flow reactor system. This result was consistent with calculations obtained using a simple model of the reactor system illustrating the utility of the technique.

The cyclic-flow apparatus was found to be advantageous for studying 14 fresh water candidate organisms to select a strain for use in further studies of metal binding bacterial biofilms under conditions restrictive to bacterial growth. The reactor system and cyclic flow operation should also be useful for selection of adherent cells under a wide variety of conditions other than those employed. A major advantage of this system is its adaptability to different experimental conditions. The reactor system is suitable for studies of a variety of factors that may influence bacterial attachment to inanimate surfaces. This could include influences of the type of attachment surface (Baier, 1980; Fletcher & Loeb, 1979) or microbial exopolysaccharides (Sutherland, 1983), thermodynamic, electrostatic, and kinetic considerations (Daniels, 1980; Kjellenberg, 1989; Roper & Marshall, 1978; Rutter, 1980; Rutter & Vincent, 1984), and predation (Fletcher & Marshall, 1982; Hoppe, 1984), or competition between two or more bacterial strains on biofilm formation and maintenance. The reactor system could also be used to evaluate the effects of fluid shear on bacterial

attachment by altering gas flow rates or hydraulic residence times, the effects of nutrient limitations (other than carbon) on attachment, the influence of toxic substances such as metal ions, and the influence of solution pH.

REFERENCES

Adams, L.F. and W.C. Ghiorse. 1986. Physiology and Ultrastructure of *Leptothrix discophora* SS-1. Arch. Microbiol. 145: 126-135.

American Public Health Association. 1976. Standard Methods for Examination of Water and Wastewater. 14th Ed. Washington, DC. 550-554.

Baier, R.E., 1980. Substrata Influences on Adhesion of Microorganisms and Their Resultant New Surface Properties, p. 59-104. In: G. Bitton, and K.C. Marshall (ed.), Adsorption of Microorganisms to Surfaces. John Wiley & Sons, New York, NY.

Bjerrum, J. (compiler). 1957. Organic Ligands. In: Stability Constants of Metal-Ion Complexes, IUPAC Special Publication No. 6. The Chemical Society, London, England.

Bjerrum, J. (compiler). 1958. Inorganic Ligands. In: Stability Constants of Metal-Ion Complexes, IUPAC Special Publication No. 7. The Chemical Society, London, England.

Costerton, J.W., G.G. Geesey and K.J. Cheng. 1978. How Bacteria Stick; Sci. Amer. 238: 86-95.

Costerton, J.W. and Lappin-Scott, H.M. 1989. Behavior of Bacteria in Biofilms. ASM News. 55: 650-654.

Daniels, S.L. 1972. Chapter 19. The Adsorption of Microorganisms onto Solid Surfaces: A Review. In Volume 13, Developments in Industrial Microbiology. 1979.

Daniels, S.L., 1980, Mechanisms Involved in Sorption of Microorganisms to Solid Surfaces, p. 7-58. In: G. Bitton, and K.C. Marshall (ed.), Adsorption of Microorganisms to Surfaces. John Wiley & Sons, New York, NY.

Fletcher, M. and G.I. Loeb. 1979. The Influence of Substratum Characteristics on the Attachment of a Marine Pseudomonad to Solid Surfaces. *Appl. Environ. Microbiol.* 37: 67-72.

Fletcher, M. and K.C. Marshall. 1982. Are Solid Surfaces of Ecological Significant to Aquatic Bacteria? *Adv. Microb. Ecol.* 6: 199-236.

Hogfeldt, E. (compiler). 1982. Part A: Inorganic Ligands. In: *Stability Constants of Metal-Ion Complexes*, IUPAC Chemical Data Series No. 21. Pergamon Press, Elmsford, NY.

Hoppe, H.G. 1984. Attachment of Bacteria: Advantage or Disadvantage for Survival in the Aquatic Environment, p. 283-302. In: K.C. Marshall (ed.), *Microbial Adhesion and Aggregation*. Springer-Verlag, Berlin.

Howell, J.A., C.T. Chi, and U. Paulowsky. 1972. Effect of Wall Growth on the Scale-up Problems and Dynamic Operating Characteristics of the Biological Reactor. *Biotech. Bioeng.* 14: 253-265.

Hsieh, K.M., L.W. Lion, and M.L. Shuler. 1985. Bioreactor for the Study of Defined Interactions of Toxic Metals and Biofilms. *Appl. & Environ. Microbiol.* 50: 1155-1161.

Hsieh, K.M., L.W. Lion, M.L. Shuler, and W.C. Ghiorse. 1988. Trace Metal Interactions with Microbial Biofilms in Natural and Engineered Systems. *CRC Crit. Rev. in Environ. Cont.* 17: 273-306.

Juran, R.(ed.). 1975-1986. *Modern Plastics Encyclopedia*. McGraw-Hill, Inc., New York, NY.

Kjellenberg, S. 1984. Adhesion to Inanimate Surfaces, p. 51-70. In: K.C. Marshall (ed.), *Microbial Adhesion and Aggregation*. Springer-Verlag, Berlin.

Nriagu, J.O. (editor). 1978. *The Biogeochemistry of Lead in the Environment: Pan A. Ecological Cycles*. Elsevier/North Holland Biomedical Press. Amsterdam, The Netherlands.

Nriagu, J.O. (editor). 1980. *Cadmium in the Environment: Part 1. Ecological Cycling*. John Wiley & Sons, New York, NY.

Perrin, D.D. (compiler). 1979. Part B: Organic Ligands. In: Stability Constants of Metal-Ion Complexes, IUPAC Chemical Data Series No. 22. Pergamon Press, Elmsford, NY.

Roper, M.M. and K.C. Marshall. 1978. Effects of a Clay Mineral on Microbial Predation and Parasitism of *Escherichia coli*. *Microb. Ecol.* 4:279-289.

Rutter, P.R. 1980. The Physical Chemistry of the Adhesion of Bacteria and Other Cells, p. 103-135. In: A.S.G. Curtis, and J.D. Pitts (ed.), *Cell Adhesion and Motility*. Cambridge University Press, NY.

Rutter, P.R., and B. Vincent. 1984. Physicochemical Interactions of the Substratum, Microorganisms, and the Fluid Phase, p. 21-38. In: K.C. Marshall (ed.), *Microbial Adhesion and Aggregation*. Springer-Verlag, Berlin.

Seno, S., M. Abata, T. Ono, and T. Tsujii. 1985. Fine Granular Cationic Iron Colloid. *Histochem.* 1.82:307-312.

Seno, S., T. Tsujii, T. Ono, and S. Ukita. 1983. Cationic Cacodylate Iron Colloid for the Detection of Anionic Sites on Cell Surface and the Histochemical Stain of Acid Mucopolysaccharides. *Histochem. J.* 78: 27-31.

Sillen, L.G. and A.E. Martell (compilers). 1964. Stability Constants of Metal-Ion Complexes. Special Publication No. 17. The Chemical Society, London, England.

Sillen, L.G. and A.E. Martell (compilers). 1971. Stability Constants of Metal-Ion Complexes, Special Publication No. 25, Supplement No. 1 to Special Publication No. 17. The Chemical Society, London, England.

Sutherland, I.W. 1983. Microbial Exopolysaccharides-Their Role in Microbial Adhesion in Aqueous Systems. *Crit. Rev. Microbiol.* 10: 173-201.

van Loosdrecht, M.C.M., Lyklema, J., Norde, W. and Zehnder, A.J.B. 1990. Influence of Interfaces on Microbial Activity. *Microbial Rev.* 54:75-87.

Westall, J.C., J.L. Zachary, and F.M.M. Morel. July 1976. MINEQL-A Computer Program for the Calculation of Chemical Equilibrium Composition of Aqueous Systems, Technical Note No. 18, Water Quality Laboratory. Department of Civil Engineering, Massachusetts Institute of Technology, Cambridge, MA.

CHAPTER 4

A COMPUTER MODEL OF THE GROWTH OF *PSEUDOMONAS CEPACIA* 17616 AND ITS ATTACHMENT TO SOLID SURFACES

ABSTRACT

In this chapter, a structured model is described that simulates growth and biopolymer production of a *Pseudomonas* species and its association with solid surfaces and toxic trace metals under conditions of variable pH. The model is constructed as an extension of a model developed by Hsieh (1988). The form of the initial model is discussed in Appendix I. Based on a simple structure, the model can predict growth, attachment processes and extracellular polymer production for operation in batch, continuous, and transient (step-wise metal increase) modes under conditions of variable pH in the solution environment.

INTRODUCTION

Microbial attachment to solid surfaces occurs frequently in natural aquatic systems and engineered reactor systems whenever bacterial cells are present. Conditions of solution pH can play a role on the degree of attachment which may occur as a result of the cell being transported close to the surface by either bulk fluid transport or simple cellular motion, or both. Bacterial cells are also of importance due to their ability to adsorb trace metals. The ability to describe how a trace metal interacts with a solid surface is complicated both by the presence of sessile and/or planktonic bacterial cells and by the possibility of variable pH conditions.

Hsieh (1988) discussed several mathematical models for describing biofilm development. Using laboratory system measurements of the kinetic processes of the marine bacterium, *Pseudomonas atlantica*, he developed a mechanistic mathematical model that was able to predict growth and attachment processes for operation in batch, continuous and step-wise metal increase modes. A more detailed discussion of the basics of this model as the starting point for a similar mechanistic model for a freshwater system with the addition of variable pH can be found in Appendix I.

GENERAL MODEL DEVELOPMENT

The cell is a complex, self-regulating, chemical reactor that responds to environmental stimuli, like changed nutrient levels and pH, by altering internal composition and biosynthetic capabilities (Shuler, 1985). These changes do not occur instantaneously; rather they follow a characteristic lag period whereby the metabolic pathways are adjusted. If one is thus to model cellular actions, one must recognize and account for the dynamic nature of the organism(s).

A model is usually built to fulfill at least one of the following objectives:

1. To discriminate mechanisms for cellular metabolic control,
2. For bioreactor design and optimization,
3. For overall process control.

Specific requirements for each model type will generally depend upon the objective the model builder is seeking to accomplish. The latter two cases are generally used to develop a more basic understanding of the bioreactor performance. In either case productivity is emphasized because the number of parameters to be considered generally must be tied directly to the product. These models are valid over a limited operating

range and subject to a lesser degree of experimental validation than the models for the first case (Shuler, 1985).

Models for mechanism discrimination must be much more generalized, subject to very low levels of empiricism, and require a large number of parameters to reflect basic cell biochemistry. This requires the use of a predictive, rather than correlative type of model. A reasonable strategy in model building is that input parameters must be accessible through independent experiment so model calculations are performed in the absence of adjustable parameters to improve goodness of fit (Shuler, 1985). The model building process is generally carried out in an interactive manner with experiments guiding model development and model calculations suggesting additional experiments. Under these conditions any disagreement between model calculations and experimental observations indicates a need for modification in the interactions or degree of structure considered by the model. Agreement between the model and experiments is taken as evidence that the model contains a sufficient level of detail to describe the experimental system over the range of conditions of interest.

A required structure in the model explicitly recognizes the fact that processes such as dynamic growth of bacterial populations and cellular productions of extracellular polymer are transitory. Dynamic responses of each system component vary and result in unbalanced growth during transient conditions. Only models with chemical structure have an inherent capability to predict this type of process behavior (Hsieh, 1988).

The proper form of a chemically structured model requires the reaction kinetics be formulated in terms of intrinsic concentrations, the amount of the component per unit cell volume or unit cell mass. (See Shuler, 1985 for a discussion of model structure and the

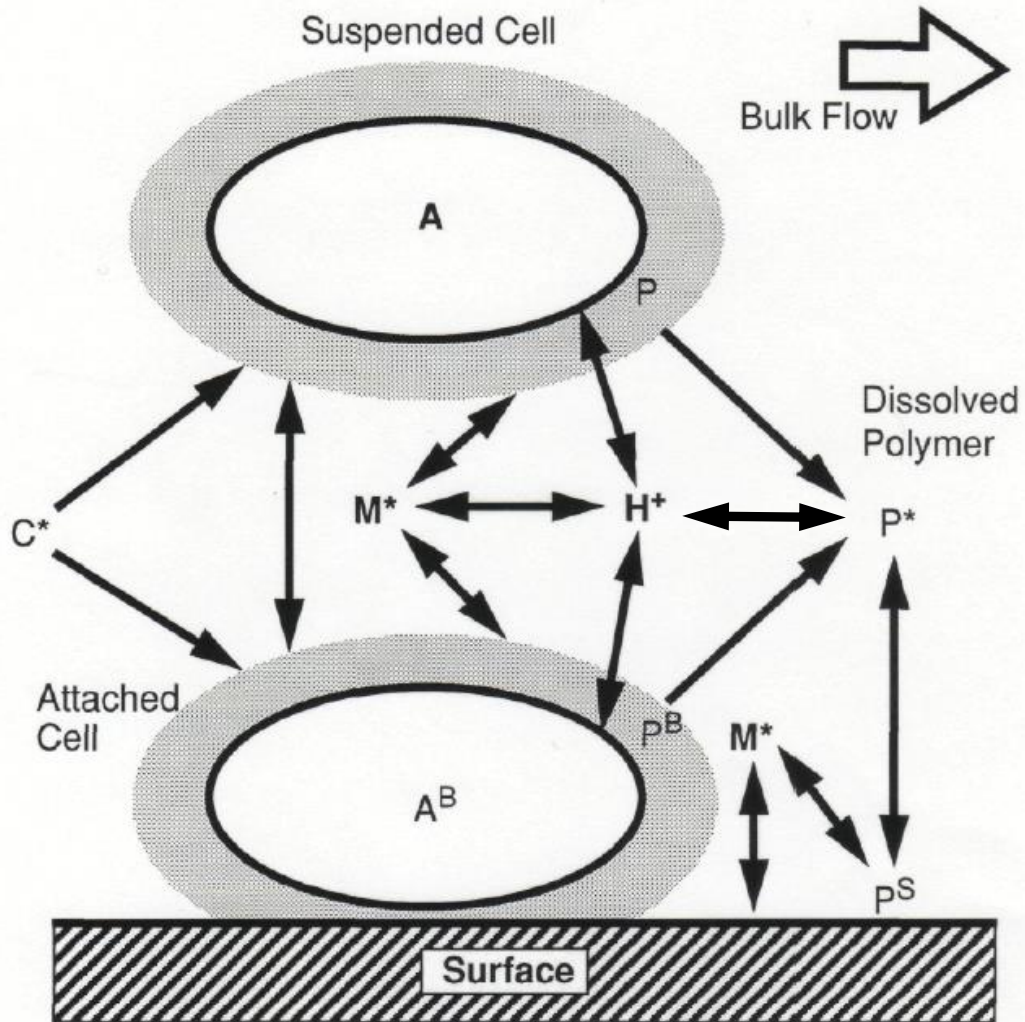
importance of structure in making predictions of transient responses). It is also important that the model have as few adjustable parameters as possible and that most of the input parameters are experimentally verifiable.

The model developed by Hsieh (1988) with extensive revisions (see Appendix I) (Hsieh, *et al.*, 1994a; Hsieh, *et al.*, 1994b) combined all of the above requirements to predict bacterial growth, biopolymer production, interactions of bacterial components with solid surfaces and of a trace metal with the bacteria, biopolymers, and solid surfaces. Chapter 2 previously discussed the interactions of hydrogen ions with bacterial growth. In this chapter the pH dependency is modeled by combining the structured biofilm model form (described in detail in Appendix I) with equations of the desired form for describing the effects of pH.

MODELLING pH DEPENDENCY

The information on enzymatic and, consequently, cellular growth described in Chapter 2 can be easily incorporated into the structured biofilm model. The desired form is based upon the cellular surface having ionizable chemical groups [likely a carboxyl, amino and/or phosphoryl group; after Beveridge (1988); Laidler (1987)] that interact with substrates. The basic model processes and interactions including consideration of the effects of hydrogen ion concentration are shown in Figure 4.1. The schematic interactions follow the nomenclature outlined in Appendix I from work by Hsieh (1988).

The development of the pH-dependent bacterial attachment model requires two additional assumptions (in addition to the ones described in Chapter 2). First, the surface chemical structures of active planktonic and sessile cells are equally able to interact with



Schematic of Model Component Interactions in the Presence of Hydrogen ion

- A = Active biomass, suspended
- P = Biopolymer
- A^B = Active biomass, attached
- P^B = Biopolymers associated with
- A^BP* = Dissolved Biopolymer
- P = Surface-sorbed biopolymer
- C* = Bulk limiting nutrient concentration
- H⁺ = Hydrogen ion concentration
- M* = Free trace metal ion concentration

Figure 4-1 Schematic of model component interactions including interactions with hydrogen ions. The arrows associated with H⁺ represent pH effects on the speciation or function of the indicated component.

hydrogen ions in solution. That is, the cell's location in the reactor system does not alter cell surface chemistry.

The second assumption involves the nature and form of the four equilibrium constants (see Figure 2.5). In the most general case, all four constants could exist within the framework of the original assumptions listed in Chapter 2 (Mahler & Cordes, 1966). It remains to determine which combinations of the indicated reactions are likely to occur in bacterial cells. In Eq. (2.1), K_{e1} and K_{es1} refer to groups on the free enzyme and enzyme-substrate complex that must be dissociated for the enzyme to be active, while K_{e2} and K_{es2} refer to groups on the enzyme and enzyme-substrate complex that must be associated for the enzyme to be active (Zeffren & Hall, 1973). Inspection of Eq. (2.1) and the mechanism detailed in Figure 2.5 shows that three possible interactions can occur. Consideration of the interactions will enable selection of the one that best describes the action of the hydrogen ion in the cell. Tipton & Dixon (1983) detailed these interactions as follows:

- 1) If hydrogen ions inhibit the reaction rate by acting as substrate analogs and compete with substrate for the active site on the free enzyme ($K_{es1} \rightarrow \infty$, $K_{es2} \rightarrow 0$), the effect of H^+ on substrate utilization will be termed competitive. A double reciprocal plot of $1/v$ against $1/S$ confirms the competitive nature of the inhibition if the slope K_m/V is affected, but not the maximal velocity V .
- 2) If hydrogen ions inhibit the reaction rate by having an affinity only for the enzyme-substrate complex ($K_{e1} \rightarrow \infty$, $K_{e2} \rightarrow 0$) and none for the free enzyme, the effects of pH on substrate utilization will appear

uncompetitive. The uncompetitive nature of the inhibition is confirmed if V and K_m are changed in the same proportion and the slopes in a double reciprocal plot of $1/v$ against $1/S$ are unchanged.

- 3) If hydrogen ions do not act as substrate analogs, they will bind on sites other than the active site to reduce enzyme affinity for substrate. The binding of the hydrogen ions does not affect the H^+ ionization constants ($K_{e1} = K_{es1}$ and $K_{e2} = K_{es2}$), and the effects of pH on substrate utilization will appear to be noncompetitive. A double reciprocal plot of $1/v$ against $1/S$ confirms the noncompetitive nature of the inhibition if the maximal velocity V and slope K_m/V is affected, but K_m is unaffected.

In each of the above three cases, the nomenclature was previously described in Chapter 2. It has generally been assumed that K_{e1} and K_{es1} (and also K_{e2} and K_{es2}) refer to the ionizations of a prototropic group whose dissociation constant value shifts due to complex formation, though generally only a few tenths of a pH unit or less (Zeffren & Hall, 1973). If the shift is negligibly small, then Case 3 referenced by Tipton & Dixon (1983) represents the most likely interaction that can occur, however, it is not the only option. Each bacterial cell strain would need to be checked to confirm the validity of this assumption (Dixon & Webb, 1964; Wong, 1975; Fersht, 1977; Lee, 1992; Palmer, 1981, Zeffren & Hall, 1973). Pure noncompetitive kinetics is characterized by the EHS complex breaking down to products to the exclusion of ES^{-2} and EH_2S forms, which have been completely inactivated. While few clear-cut instances of a pure noncompetitive kinetic pattern for single-substrate enzyme-catalyzed reactions are known, hydrogen ions may be regarded as providing one of the simplest examples (Zeffren & Hall, 1973).

The above discussion makes it apparent that a noncompetitive model form may be a useful simplified form to apply to whole cells as described in Chapter 2 (Shuler & Kargi, 1992; Bu'Lock & Kristiansen, 1987; Baily & Ollis, 1986). Modeling pH-dependency by the mechanism illustrated in Figure 2.5 allows use of the specific forms in Eqs. (2.2), (2.3), and (2.4). The most general case to be modeled thus allows for $K_{el} \neq K_{es1}$ (and also $K_{e2} \neq K_{es2}$). The above described modifications would apply only to the active cell mass of planktonic and attached bacterial cells. Bakke, *et al.* (1984) previously demonstrated that the same kinetic and stoichiometric coefficients can be used to describe processes in planktonic cells and those in biofilms. Equations (A1.1), (A1.3), (A1.8), and (A1.10) thus become:

$$r_A = \left[\mu'_A \left(\frac{C^*}{K'_{AC^*} + C^*} \right) - k_{dA} \left(\frac{K_{dAC^*}}{K'_{dAC^*} + C^*} \right) \right] A \quad (4.1)$$

$$r_{A^B} = \left[\mu'_{A^B} \left(\frac{C^*}{K'_{A^B C^*} + C^*} \right) - k_{dA^B} \left(\frac{K_{dA^B C^*}}{K'_{dA^B C^*} + C^*} \right) \right] A^B \quad (4.2)$$

$$r_{A,syn} = \mu'_A \left(\frac{C^*}{K'_{AC^*} + C^*} \right) A \quad (4.3)$$

and

$$r_{A^B,syn} = \mu'_{A^B} \left(\frac{C^*}{K'_{A^B C^*} + C^*} \right) A^B \quad (4.4)$$

$$\text{where: } \mu'_A = \mu_A \left(1 + \frac{[H^+]}{K_{es1}} + \frac{K_{es2}}{[H^+]} \right)^{-1} \quad (4.5)$$

and

$$\mu'_{A^B} = \mu_{A^B} \left(1 + \frac{[H^+]}{K_{es1}} + \frac{K_{es2}}{[H^+]} \right)^{-1} \quad (4.6)$$

and where:

$$K'_{AC^*} = K_{AC^*} \left(\frac{1 + \frac{[H^+]}{K_{e1}} + \frac{K_{e2}}{[H^+]}}{1 + \frac{[H^+]}{K_{es1}} + \frac{K_{es2}}{[H^+]}} \right) \quad (4.7)$$

$$K'_{A^B C^*} = K_{A^B C^*} \left(\frac{1 + \frac{[H^+]}{K_{e1}} + \frac{K_{e2}}{[H^+]}}{1 + \frac{[H^+]}{K_{es1}} + \frac{K_{es2}}{[H^+]}} \right) \quad (4.8)$$

The second simplifying assumption involving the nature and form of the four equilibrium constants will be application of pure noncompetitive kinetics described by Zeffren & Hall (1973). The assumption in the above equations will use $K_{e1} = K_{es1} = K_1$ and $K_{e2} = K_{es2} = K_2$ which reduces Eq. (2.4) to the form:

$$K' = K_m \frac{1 + \frac{[H^+]}{K_{e1}} + \frac{K_{e2}}{[H^+]}}{1 + \frac{[H^+]}{K_{es1}} + \frac{K_{es2}}{[H^+]}} = K_m \frac{1 + \frac{[H^+]}{K_{e1}} + \frac{K_{e2}}{[H^+]}}{1 + \frac{[H^+]}{K_{e1}} + \frac{K_{e2}}{[H^+]}} = K_m \quad (4.9)$$

The simplification in the model will reduce Eqns. 4.7 and 4.8, respectively, to the forms:

$$K'_{AC^*} = K_{AC^*} \quad \text{and} \quad (4.10)$$

$$K'_{A^B C^*} = K_{A^B C^*} \quad (4.11)$$

METAL BEHAVIOR AND pH DEPENDENCY

The presence of metal ions in solution was described in Chapter 2 to also be affected by alterations in the pH of a system. The alteration in turn can have an effect upon the partitioning of the metals onto solid surfaces and microbial components (Beveridge, 1986; Corpe 1975). The microbial components in turn can accelerate or inhibit metal partitioning, complicating the chemistry of metal-solid surface interactions and producing metal-cellular surface adsorbing components.

The experimental work by Hsieh (1988) on interactions of cellular components with the toxic trace metal lead was used to calculate lead distribution in a model aquatic system. The resultant model equations formulated an inhibition term based on a product inhibition form $K_m^*/(K_m^* + M^*)$ where K_m^* is the saturation, or half-velocity, coefficient for production of a cellular component in the presence of a metal and where M^* is the free metal ion concentration. Chapter 2 discussed metal toxicity effects on cellular growth as a function of free ion activity. Cell growth can then also be altered by the effect of pH on the metal speciation, which changes M^* in the metal inhibition term.

In all solution environments, bare metal ions participate in coordination reactions with water molecules. These aquo-metal complexes in turn undergo replacement reactions in which coordinated water molecules are exchanged for other ligands (Stumm & Morgan, 1981). The reaction of particular interest for this thesis is the formation of polyhydroxy species $[M(OH)_n]$ which are sensitive to fluctuations in system pH. The establishment of hydrolysis equilibria is usually very fast when the hydrolysis species are simple. The tendency of the metal-ion solutions to hydrolyze increases with dilution and decreasing $[H^+]$ (Stumm & Morgan, 1981). Hydrolyzed metal species also appear to

adsorb more readily at all particle-water interfaces (including organic matter like bacterial cells) than non-hydrolyzed species (Ferris, *et al.*; Stumm & Morgan, 1981). Therefore, in the model, changes in pH will influence metal ion toxicity through both changes in the free metal ion activity (*i.e.*, formation of metal hydroxyl complexes) and through pH effects on metal ion adsorption. When the metal is present in the solution, the model will explicitly calculate the free-metal ion concentration at every time step, using the computer program MINEQL for the calculation of chemical equilibrium composition of the aqueous system. Specific subroutines, as discussed in Appendix II, are utilized to include association and complexation reactions with the goal of determining the new free metal ion concentration. The main program model will then use the new value of the free metal ion concentration in the iteration of the bacterial model to determine how the metal binds to the various components of the cell, polymer and surfaces.

DERIVATION OF MODEL PARAMETERS

The model parameters utilized for model evaluation under freshwater conditions have been primarily derived from the literature, as noted in the following discussion, and experimental work by Hsieh (1988) (See Appendix I). The model parameters are summarized in Table 4.1. The initial conditions employed in testing the model predictions are given in table 4.2. The procedures for determination of most of the constants in Table 4.1 are detailed in Appendix I. Values corresponding to parameters for attached cells were assumed to be the same as the parameters for the planktonic cells (Bakke, *et al.*, 1984; Hsieh, *et al.*, 1990). However, the model equations permit this assumption to be relaxed if data are obtained to show that unique kinetic constants are needed for sessile cells.

Table 4.1: Model Parameters Associated with pH-Dependent Rate Equations

Active Cell Mass	suspended:	A	surface attached:	A ^B
Biopolymer	suspended:	P*	surface adsorbed:	P ^S
	associated with suspended cells:	P*	associated w/ attached cells:	P ^B
Carbon Source		C*		
<u>Saturation Constants</u>			<u>Decomposition Rates</u>	
	$K_{AC^*} = 4.7 \times 10^{-4}$ g/l		$k_{dA} = 0.031$ hr ⁻¹	
	$K_{PC^*} = 4.4 \times 10^{-3}$ g/l		$k_{dAB} = 0.031$ hr ⁻¹	
	$K_{ABC^*} = 4.7 \times 10^{-4}$ g/l		<u>Maximum Rates of Synthesis</u>	
	$K_{PBC^*} = 4.4 \times 10^{-3}$ g/l		$\mu_A = 0.25$ hr ⁻¹	
	$f_{AP} = 0.95$ gP/gA		$\mu_{AB} = 0.25$ hr ⁻¹	
	$f_{ABP} = 0.95$ gP ^B /gA ^B		$\mu_P = 0.24$ hr ⁻¹	
	$K_{P^*P} = 0.1$ gP/gA		$\mu_{PB} = 0.24$ hr ⁻¹	
	$K_{P^*PB} = 0.1$ gPB/gAB		$\mu_{P^*} = 0.04$ hr ⁻¹	
	$K_{dAC^*} = 0.01$ g/L		$\mu_{P^*B} = 0.04$ hr ⁻¹	
	$K_{dABC^*} = 0.01$ g/L		<u>Stoichiometric Coefficients</u>	
<u>Molecular Dissociation Constants</u>			$\alpha_A = 3.6$	
	$K_{e1} = 1.0 \times 10^{-6}$ M		$\alpha_P = 1.7$	
	$K_{es1} = 1.0 \times 10^{-6}$ M		$\alpha_{AB} = 3.6$	
	$K_{e2} = 7.9 \times 10^{-9}$ M		$\alpha_{PB} = 1.7$	
	$K_{es2} = 7.9 \times 10^{-9}$ M			
Biopolymer Partition coefficient	k_P	=	0.04 L/m ²	
Biopolymer degradation rate constant	k_{dP^*}	=	0.16 hr ⁻¹	
Biomass attachment rate constant	k^A	=	4.7 L/g-hr	
Biomass detachment rate constant	k^D	=	0.0035 hr ⁻¹	
Maximum attached biomass conc.	B^{\max}	=	8.5×10^{-3} g/m ²	
Total Surface area	a	=	0.321 m ² (bioreactor), 0.061 m ² (Multigen)	
Total Volume	V	=	1.42 L (bioreactor), 1.5 L (Multigen)	
Reynolds number	Re	=	varies, depending upon recirculation rate (Re = 300 used for bioreactor simulations; Re=2,000 for Multigen simulations).	

Table 4.2: Initial Conditions for the pH-Dependent Bacterial Model.

$A_0 = 0.03 \text{ g/L}$
$P_0 = 0.01 \text{ g/L}$
$A_0^B = 6.0 \times 10^{-4} \text{ g/m}^2$
$P_0^B = 3.0 \times 10^{-4} \text{ g/m}^2$
$P_0^* = 1.0 \times 10^{-6} \text{ g/L}$
$P_0^S = 1.0 \times 10^{-9} \text{ g/m}^2$
$C_0^* = 2.0 \text{ g/L}$

The parameters used in Table 4.1 are the same as listed in Appendix Table A1.1. It was reasoned that the selected freshwater strain *Pseudomonas cepacia* 17616, being in the same genus as the strain *Pseudomonas atlantica*, could exhibit relatively similar characteristics under similar growth conditions. The growth and attachment experiments reported in Chapter 3 for *P. cepacia* 17616 showed biofilm development on surfaces was an incomplete monolayer which is qualitatively similar to the observed growth of *P. atlantica* in defined seawater medium (Hsieh, 1988).

The remaining model parameters to be estimated are the molecular dissociation constants: K_{e1} (assumed equal to K_{es1}) and K_{e2} (assumed equal to K_{es2}). Several methods have been detailed for finding these constants for enzyme reactions (Zeffren & Hall, 1973; Palmer, 1981; Tipton & Dixon, 1983; Laidler & Bunting, 1973; Engel, 1977; Gutfreund, 1972). The most convenient and widely used method was first detailed by Malcolm Dixon in 1953 (Tipton & Dixon, 1983; Dixon & Webb, 1964) which involves plotting the logarithm of kinetic constants against the pH. The resulting plot of $\log v$ versus pH might look like Figure 2.1. In this Figure, for low pH values and considering the logarithm of Eq. (2.3), the resulting form is Eq. (4.10):

$$\log(v') = \log(v) - \log\left(1 + \frac{[H^+]}{K_{es1}} + \frac{K_{es2}}{[H^+]}\right) \quad (4.12)$$

This reduces to the simplified equation when $[H^+] \gg K_{es1}$ and $[H^+] \gg K_{es2}$:

$$\log(v') = \log(v) - \log\left(\frac{[H^+]}{K_{es1}}\right) = \log(v) + (pH - pK_{es1}) \quad (4.13)$$

Thus the slope of the graph will be +1. As the pH is raised there will be a range where $K_{es1} \gg [H^+] \gg K_{es2}$ which reduces Eq. (4.10) to:

$$\log(v') = \log(v) \quad (4.14)$$

which will have a slope of zero on the graph. As the system pH is raised toward alkaline levels (high pH), the dependence is governed by $K_{es2}/[H^+]$ and Eq. (4.10) reduces to:

$$\log(v') = \log(v) - \log\left(\frac{K_{es2}}{[H^+]}\right) \log(v) + (pK_{es2} - pH) \quad (4.15)$$

which will give a slope of -1 on the graph. The overall graph then of $\log(v)$ versus pH (see Figure 2.1) can be represented by 3 linear sections joined by curved segments (Tipton & Dixon, 1983; Laidler & Bunting, 1973; Stumm & Morgan, 1981). Figure 4.2 illustrates this behavior for *Escherichia coli* grown on casein hydrolysate (Pirt, 1975). Figure 4.2 takes the general curve from Figure 2.1 and superimposes the linear segments from the procedure just described. The values derived from Figure 4.2 are $pK_{es1} = 6.0$ ($K_{es1} = K_{e1} = 1 \times 10^{-6}$ M/L) and $pK_{es2} = 8.1$ ($K_{es2} = K_{e2} = 7.9 \times 10^{-9}$ M/L).

Similar behavior was demonstrated by Alberty and coworkers for the enzyme fumarate hydratase in the catalyzed reversible reaction of fumarate to malate (Wigler & Alberty, 1960; Brant, *et al.*, 1963). The intersection points on the plot of the pH dependence of V/K_m gave average pK values for ionization of the free enzyme rather than the enzyme-substrate complex. The plot gave molecular dissociation constants with pK values of 5.8 and 7.9, respectively. These values were judged to be those of the fumarate enzyme-substrate complexes. Many other researchers have also investigated pK ranges of ionizable groups in cellular proteins (Engel, 1977; Tipton & Dixon, 1983; Bell & Bell, 1981; Gutfreund, 1972; Zeffren & Hall, 1973; Dixon & Webb, 1964; Palmer, 1981; Fersht, 1977; Wong, 1975). Their findings illustrate a wide range of values dependent upon both the type of ionizable side group under consideration and its interaction with the surrounding environment in the protein molecule (Palmer, 1981). Many of the researchers also indicate that because of the

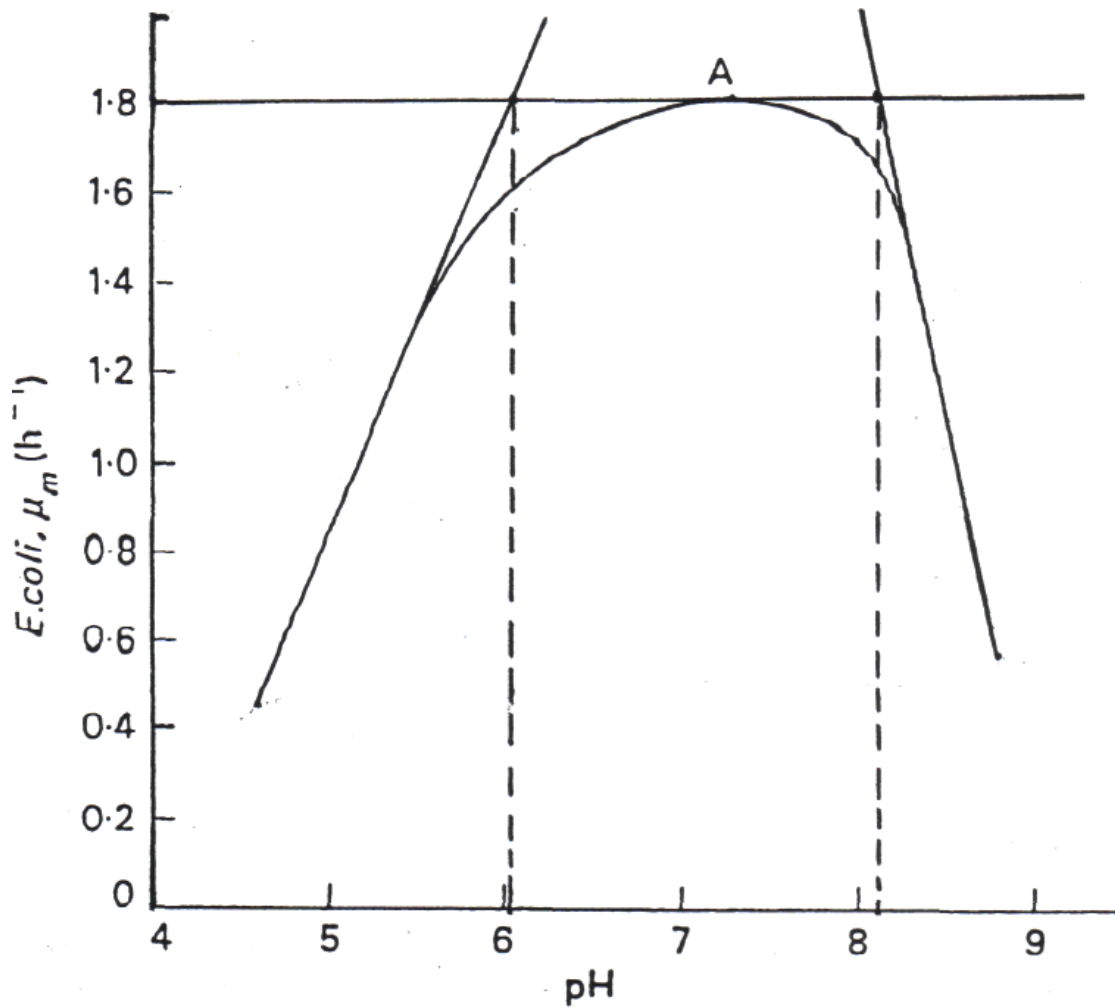


Figure 4.2. Derivation of molecular dissociation constants from the growth curve for *Escherichia coli* grown on casein hydrolysate.

diversity of acidic and basic groups in a protein and associated with the enzymes, their derived ionization constants for specific groups will be somewhat interdependent (Zeffren & Hall, 1973). Dixon & Webb (1964) echoed a prevalent sentiment that further reliable work is needed to better define the pK values of enzyme- substrate complexes and to compare these results to those of free enzymes.

While one may generalize pK values for use with a cell, detailed individual analyzes are necessary for each bacterial strain to ascertain the dominant ionizable groups and the resultant equilibrium constant. In the absence of this specific data for *Pseudomonas cepacia* 17616, the values derived in Figure 4.2 (which are similar to values derived by Brant, *et al.* (1963), have been utilized as the constants to permit illustrative modeling of pH-dependence.

REFERENCES

Baily, I.E., and Ollis, D.F. 1986. Biochemical Engineering Fundamentals. Second Ed. McGraw-Hill Book Company, New York.

Bakke, R., Trulear, M.G., Robinson, J.A. and Characklis, W.G. 1984. Activity of *Pseudomonas aeruginosa* in Biofilms: Steady State. Biotechnol. Bioeng. 26: 1418-1428.

Bell, J.E. and Bell, E.T. 1981. Proteins and Enzymes. Prentice-Hall, Inc. Englewood Cliffs, New Jersey.

Beveridge, T.J. 1988. The Bacterial Surface: General Considerations Towards Design and Function. Can. J. Microbiol. 34: 363-372.

Brant, D.A., Barnett, L.B. and Alberty, R.A. 1963. The Temperature Dependence of the Steady State Kinetic Parameters of the Fumarase Reaction. J.Am. Chem. Society. 85: 2204-2209.

Bu'Lock, J. and Kristiansen, B. 1987. Basic Biotechnology. Academic Press, Inc. Harcourt, Brace, Jovanovich, Publishers. Orlando, Florida.

Engel, PC. 1977. Enzyme Kinetics: The Steady State Approach. Chapman and Hall, a Division of John Wiley & Sons, London, England.

Dixon, M. and Webb, E.G. 1964. Enzymes. Second Edition. Academic Press Inc. New York, NY

Fersht, A. 1977. Enzyme Structure and Mechanism. Chapters 3 & 5. W.H. Freeman & Co., Ltd. San Francisco, CA.

Gutfreund, H. 1972. Enzymes: Physical Principles. Wiley-Interscience, John Wiley & Sons, Ltd. Bristol, England.

Hsieh, K.M. 1988. The Growth and Attachment of a Biopolymer Producing *Pseudomonas* Species and the Characterization of its Interactions with a Toxic trace Metal. Ph.D. thesis. Cornell University, Ithaca, NY.

Hsieh, K.M., Murgel, G.A., Lion, L.W. and Shuler, M.L. 1994a. Interactions Of Microbial Biofilms With Toxic Trace Metals: 1. Observation And Modelling Of Cell Growth, Attachment, And Production Of Extracellular Polymer. Biotechnol. and Bioeng. 44: 219-231.

Hsieh, K.M., Murgel, G.A., Lion, L.W. and Shuler, M.L. 1994b. Interactions Of Microbial Biofilms With Toxic Trace Metals: 2. Prediction and Verification of an Integrated Computer Model of Lead (II) Distribution in the Presence of Microbial Activity. Biotechnol. and Bioeng. 44: 232-239.

- Laidler, K.J. 1987. Chemical Kinetics. Third Ed. Harper & Row, Publishers. New York.
- Laidler, K.J., and Bunting, P.S. 1973. The Chemical Kinetics of Enzyme Action. Second Ed. Chapter 5. Clarendon Press. Oxford, Great Britain.
- Lee, J.M. 1992. Biochemical Engineering. Chapter 2. Prentice-Hall. Englewood Cliffs, New Jersey.
- Mahler, H.R. and Cordes, E.H. 1966. Biological Chemistry. Harper and Row Publishers, New York, NY.
- Palmer, T. 1981. Understanding Enzymes. Ellis Harwood Limited, a Division of John Wiley & Sons. West Sussex, England.
- Pirt, S. J. 1975. Principles of Microbe and Cell Cultivation. Chapters 14, 15, 17, 23-25. John Wiley & Sons, NY.
- Shuler, M.L. 1985. Dynamic Modelling of Fermentation Systems. Chapter 6 in Bioreactor Design, Operation and Control, pp. 119-131.
- Shuler, M.L. and Kargi, F. 1992. Bioprocess Engineering: Basic Concepts. Prentice-Hall, Englewood Cliffs, NJ.

Stumm, W. and Morgan, James J. 1981. Aquatic Chemistry: An Introduction Emphasizing Chemical Equilibria in Natural Waters. Second Ed. John Wiley & Sons, New York.

Tipton, K.F. and Dixon, H.B.F. 1983. Chapter 5. Effects of pH on Enzymes. In: Contemporary Enzyme Kinetics & Mechanism. Ed. by D.L. Purich. Academic Press. New York.

Wigler, P.W. and Alberty, R.A. 1960. The pH Dependence of the Competitive Inhibition of Fumarase. J. Am. Chem. Society. 82: 5482-5488.

Wong, J. T.-F. 1975 Kinetics of enzyme Mechanisms. Chapter 10. Academic Press Inc. New York, NY.

Zeffren, E. and Hall, P.L. 1973. The Study of Enzyme Mechanisms. Chapter 4. John Wiley & Sons, Inc. New York, NY.

CHAPTER 5

COMPUTER SIMULATIONS OF THE GROWTH OF *PSEUDOMONAS CEPACIA* 17616 AND ITS ATTACHMENT AND INTERACTIONS WITH A TRACE METAL

ABSTRACT

To test the viability of the proposed pH dependency mechanisms for the bacterial model, computer simulations were performed under various operating conditions. Input parameters used in the simulations were obtained primarily from the work of Hsieh (1988) and from the literature. A sensitivity analysis was performed on the molecular dissociation constants (pK values) for the pH-dependency of μ' . The model simulated bacterial growth and attachment to glass surfaces in a bioreactor with a high surface to volume ratio (Hsieh, 1985; Hsieh, 1988) and a glass-jar fermenter (Multigen) with a low surface to volume ratio under both batch and continuous operation and variable pH levels. Additional simulations were performed in conjunction with a chemical speciation model capable of quantifying a trace metal in the reactor system. The interactions of the free ion form of a trace metal, lead, with cellular components of the gram-negative film forming bacterium *Pseudomonas cepacia* 17616 in a freshwater environment at variable pH were simulated. Dynamic toxic responses of the biophase to transient lead concentration increases were also simulated. The simulations resulted in a demonstration of the model utility to describe bacterium, free ion trace metal and surface interactions under conditions of variable pH. The reasonable predictions achieved by the model in all simulations lays the groundwork for application of the model to more complex systems and other types of bacterial strains.

CELLULAR GROWTH WITHOUT METALS

The proposed mechanism for pH dependency detailed in Chapter 4 assumed the molecular dissociation constants for the enzyme and enzyme-substrate complex could be assumed equal. Values for the constants were derived from data of Pirt (1975). Model simulations using batch operation of the Multigen at a pH of 7 in the absence of a toxic metal were performed to ascertain the effect upon the outcome by variations in one or both of the constants. The MMS medium developed in Chapter 3 was utilized for fresh water organisms with an ionic strength fixed at 0.05 M.

Figure 5.1 shows the results of shifts in K_1 and/or K_2 , compared to the originally computed values of $K_1 = 1 \times 10^{-6}$ and $K_2 = 7.9 \times 10^{-9}$ M, on the concentration of suspended biomass (X) [comprised of active cell mass (A) plus suspended cell associated polymer (P)] for conditions of batch growth. Figure 5.2 shows the results of shifts in K_1 and/or K_2 on the concentration of attached biomass (B) [comprised of attached cell mass (A^B) plus attached cell associated polymer (P^B)] for conditions of batch growth. Only shifts in K_1 to a value of 1×10^{-7} M had any noticeable effects on the outcomes. In all cases, the maximum concentrations of biomass were within +4% of the simulation using the selected values. The effect of lowering K_1 was to shift the occurrence of the maximum biomass concentration to a time near 21 hours instead of around 12 hours.

Given the relatively low sensitivity of the results to changes in K_1 and K_2 , the continued use of the selected values of K_1 and K_2 appeared reasonable. Predictive application of the model, however, would require that experimental values be obtained for the molecular dissociation constants for the particular strain or strains being modeled.

Figure 5.1. Simulation of Total Suspended Biomass (X) under batch growth conditions in a Multigen reactor under conditions of variations in the pH dependency dissociation constants K_1 and K_2 .

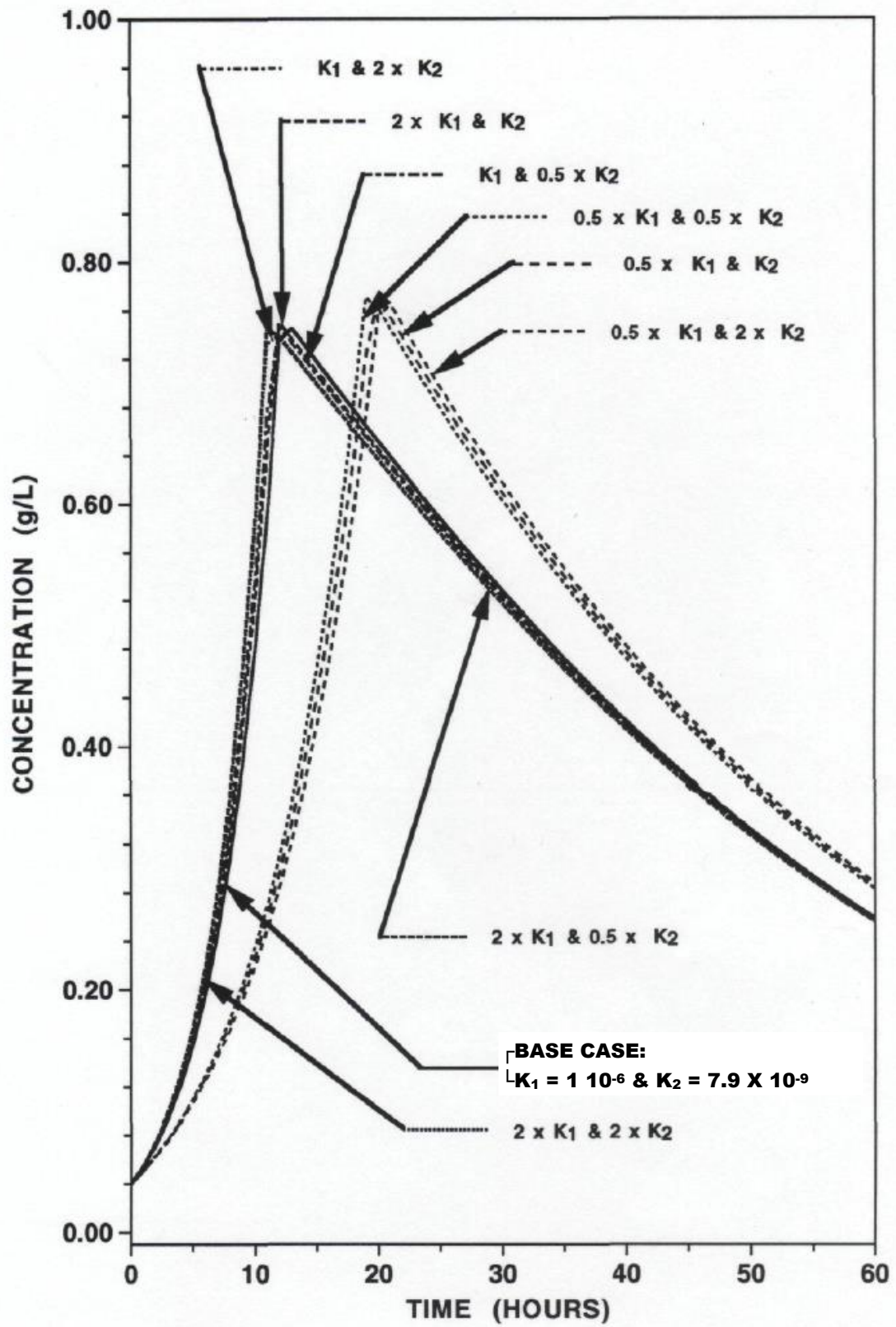
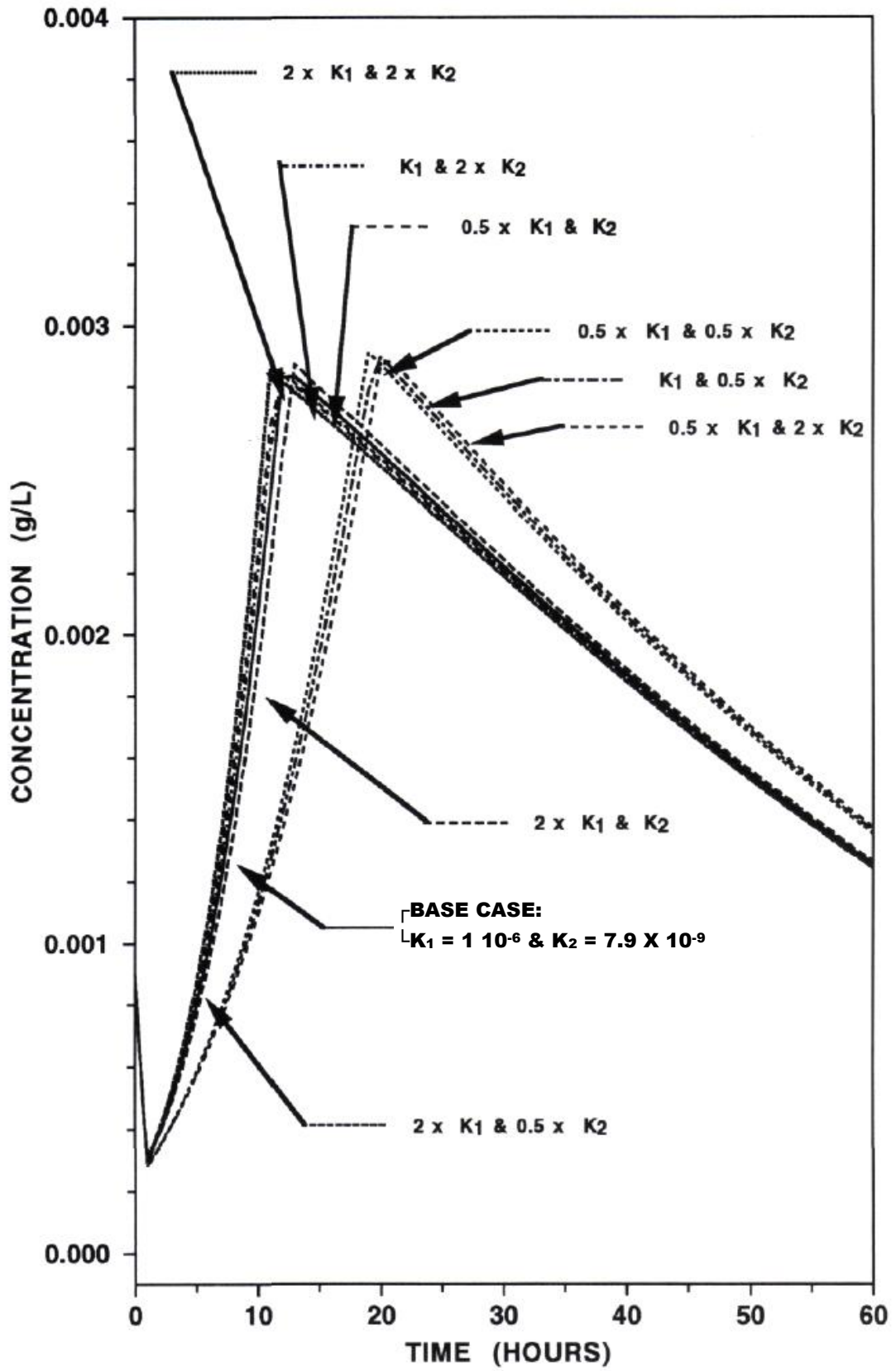


Figure 5.2. Simulation of Total Attached Biomass (**B**) under batch growth conditions in a Multigen reactor under conditions of variations in the pH dependency dissociation constants K_1 and K_2 .



To test the effects of variations in the solution pH upon the resultant cellular growth without a metal present, model predictions of suspended and surface attached cellular components were performed over a range of solution pH. Figures 5.3 to 5.9 show these simulations. Calculations assumed a Multigen environment with a total volume of 1.50 L, mixing achieving a $Re = 2,000$ and a wetted perimeter surface area of 0.061 m^2 . The simulation for pH 7 in all the figures represents the case most frequently described in the literature (Pirt, 1975; Segal, 1976). The assumption that most parameters used in the model for *P. cepacia* 17616 are the same as for *P. atlantica* [as used by Hsieh (1988)] enables some comparison of the pH dependent results to those of Hsieh. The results of Hsieh (1988) were assumed to be applicable to circumneutral pH values. In all cases, the simulations using the pH dependent model outlined in Chapter 4 (included as Appendix II) at a pH value of 7 compared very favorably to the results of Hsieh (1988).

Figure 5.3 shows the simulated results for a variation in solution system pH from 3 to 11 on the concentration of suspended cells (A). The maximum production occurs at about 12 hours with a pH value of 7. Results using pH values of 6 and 8 indicate peak concentrations reduced only 15 to 20% and shifted to a later time of 15 to 18 hours. As the pH is varied in either direction further away from circumneutral, the peak cell concentration diminishes and occurs at a longer time in batch growth (in excess of 50 hours for pH 3, 4, 5, 10, and 11). These results appear to mimic the bacterial growth curve versus pH plot of Pirt (1975) shown previously in Figure 2.1. Figure 5.4 shows the simulation results for the suspended cell associated polymer. The minimum "defined" peak occurs at pH 7. Relative to pH 7, the concentration of polymer increases

Figure 5.3. Simulation of Suspended Cell (A) growth under batch solution conditions in a Multigen reactor under conditions of variations in the pH without trace metals.

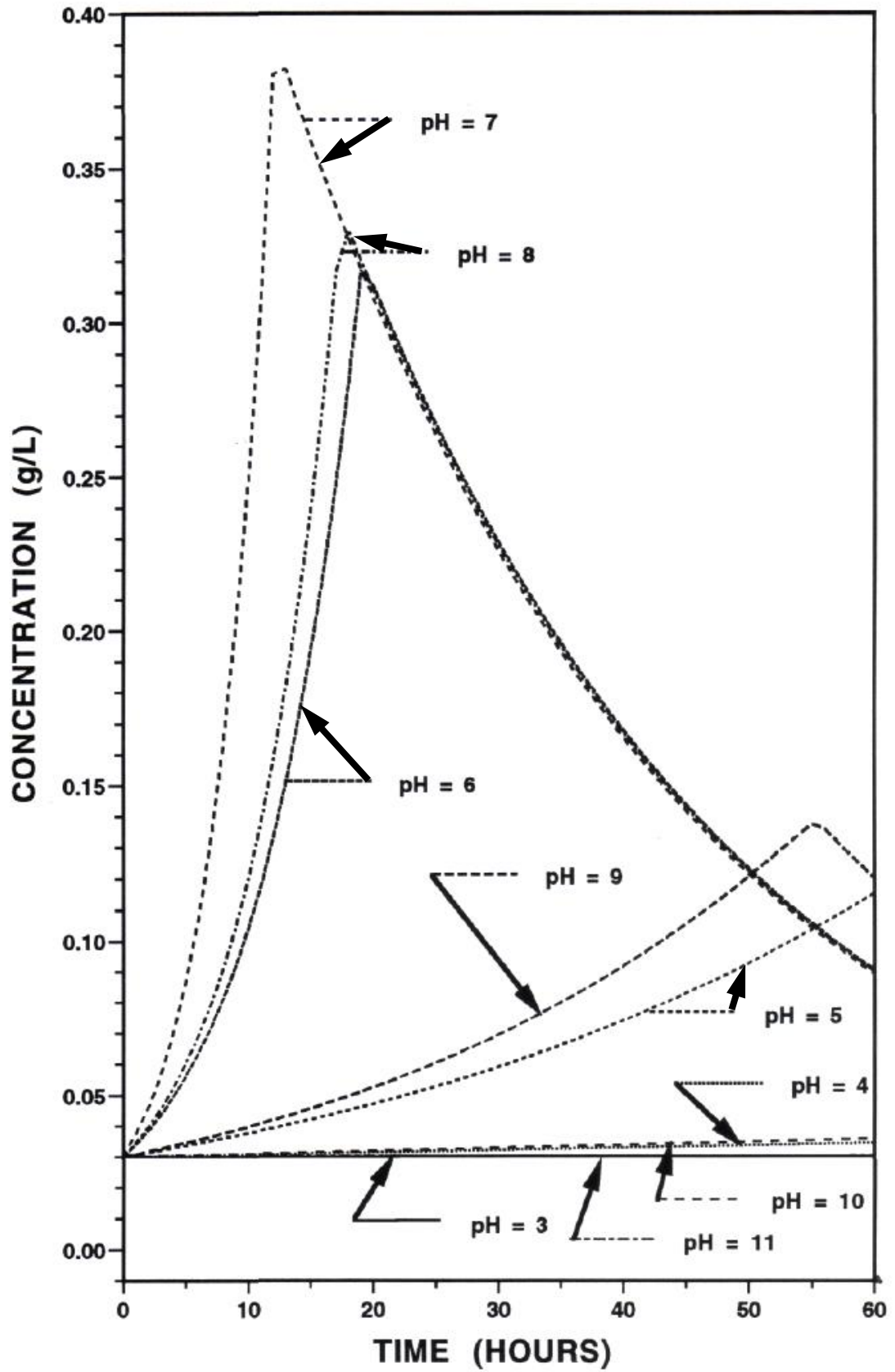
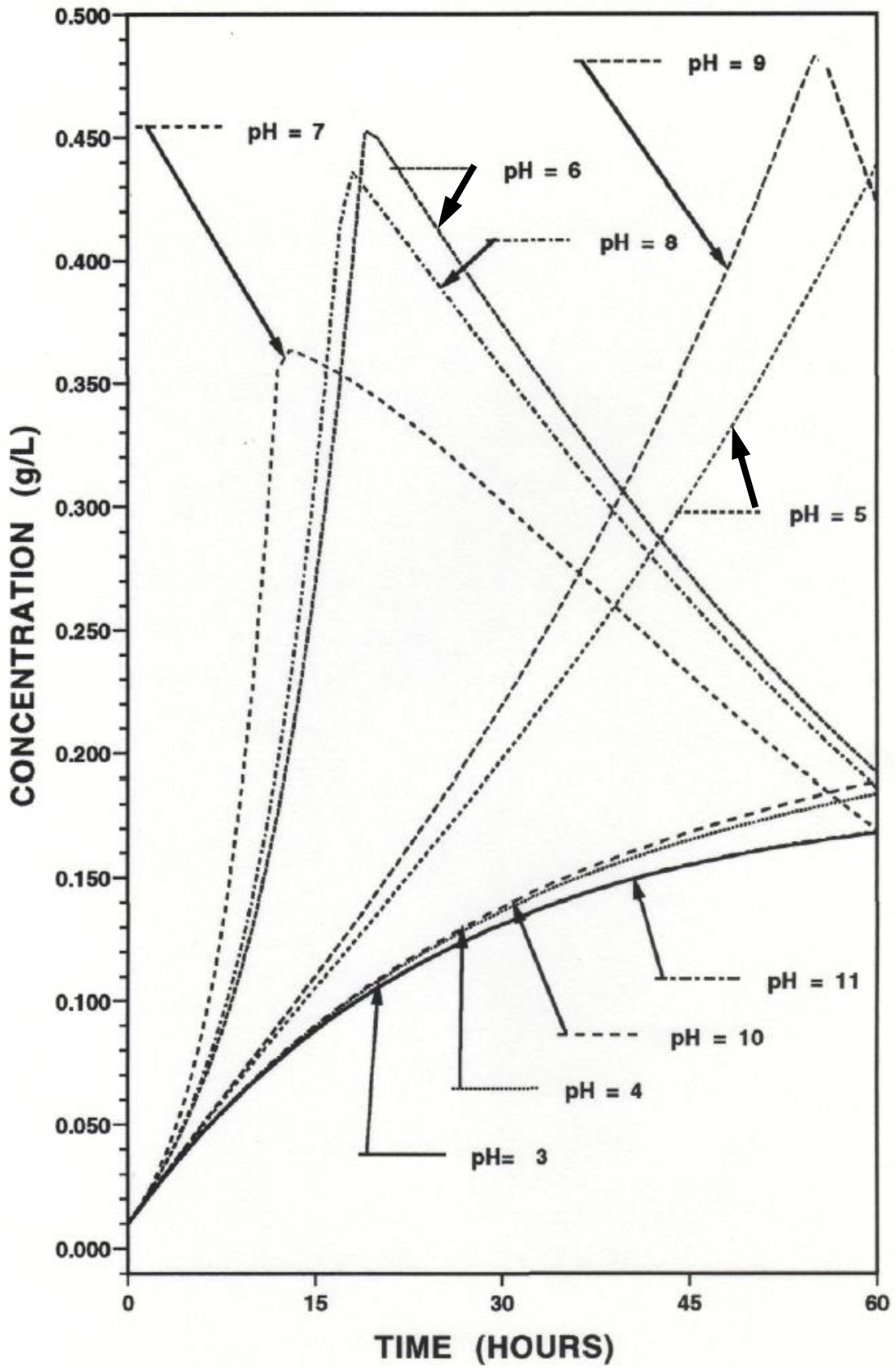


Figure 5.4. Simulation of Suspended Cell Associated Polymer (P) production under batch solution conditions in a Multigen reactor under conditions of variations in the pH without trace metals.



by some 30% at pH values of 6 and 8 and by over 50% at pH values of 5 and 9. This result is a consequence of the model assumption that polymer production competes with cell growth for available substrate. At more extreme pH values of 3 or 4 and 10 or 11, the polymer concentration approaches a plateau at about 50% of the concentration achieved at pH 7. Simultaneous review of the production of suspended cells in Figure 5.3 at the same pH values shows marked decreases in the concentrations likely due to the inability of the cells to obtain the necessary substrate to grow and reproduce as noted in Chapter 2 by Pirt (1975) and others. The pH inhibition of cell growth at the extreme pH values used in the model test demonstrated an increased polymer concentration to cell concentration ratio of nearly 3:1 compared to the nearly 1:1 ratio at the pH value of 7.

Both the attached cell (A^B) and attached cell associated polymer (P^B) simulations in Figures 5.5 and 5.6, respectively, mimic the same patterns shown in Figures 5.2 and 5.3. Figure 5.7 shows the simulated production of dissolved polymer (P^*). Figure 5.8 shows the results for surface associated polymer (P^S). Since polymer sorption is assumed to obey a reversible linear isotherm, the results for P^S are similar to those for P^* in Figure 5.7. Figure 5.9 shows the concentration of the limiting nutrient (C^*) in solution. The nutrient is consumed at 12 hours for the pH 7 case. The length of time needed to completely utilize the initial 2 g/L concentration increases markedly as the pH is adjusted on either side of the circumneutral value. This result is consistent with the calculated decrease in bacterial growth rates away from pH 7. The resultant increase in production of all polymer components (P , P^B , P^* , and P^S) in response to adverse, or non-optimum, pH values is in reasonable agreement with the previously described functional relationship between P and the quantity of A and C available.

Figure 5.5. Simulation of Surface Attached Cell (A^B) growth under batch solution conditions in a Multigen reactor under conditions of variations in the pH without trace metals.

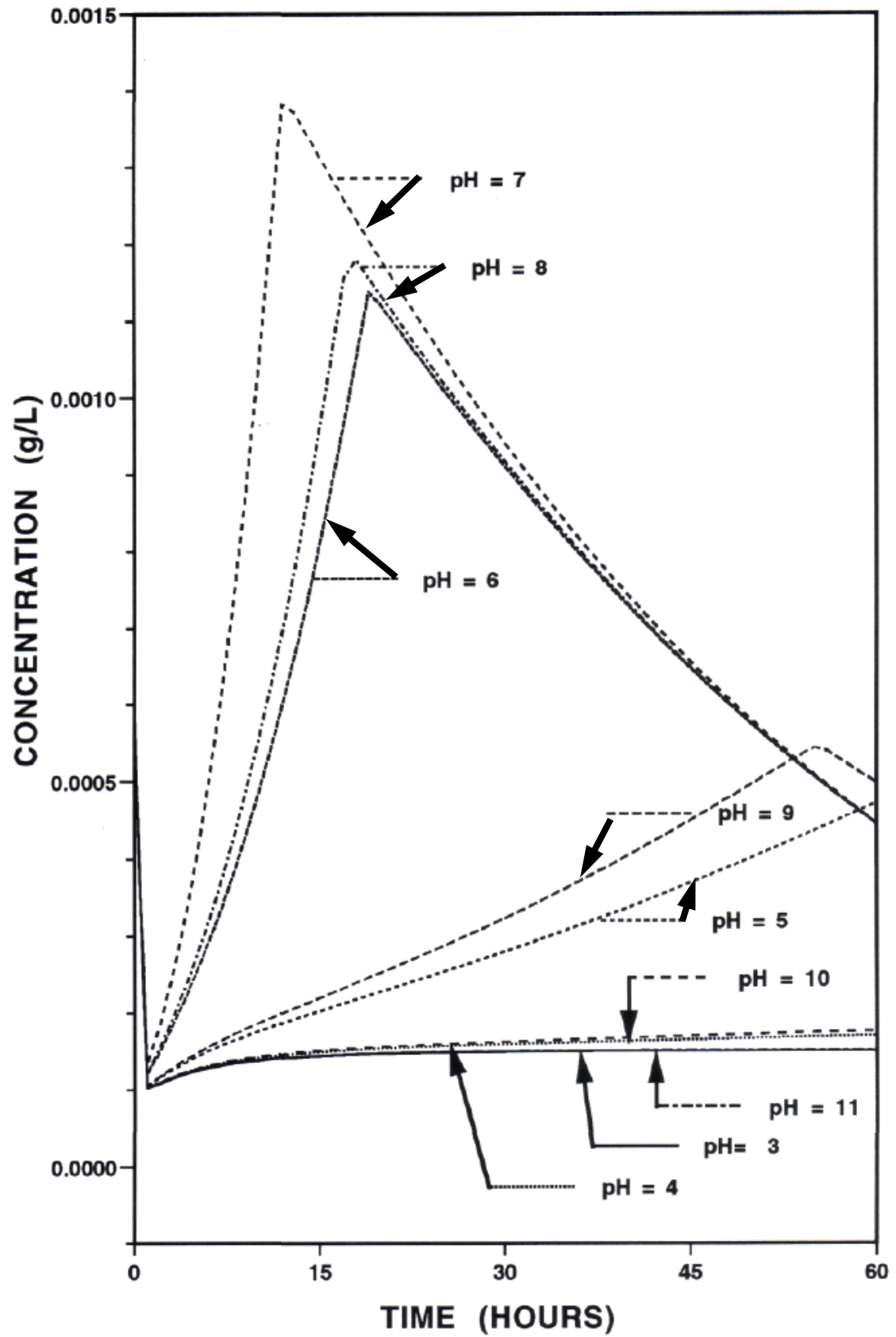


Figure 5.6. Simulation of Surface Attached Cell Associated Polymer (P^B) production under batch solution conditions in a Multigen reactor under conditions of variations in the pH without trace metals.

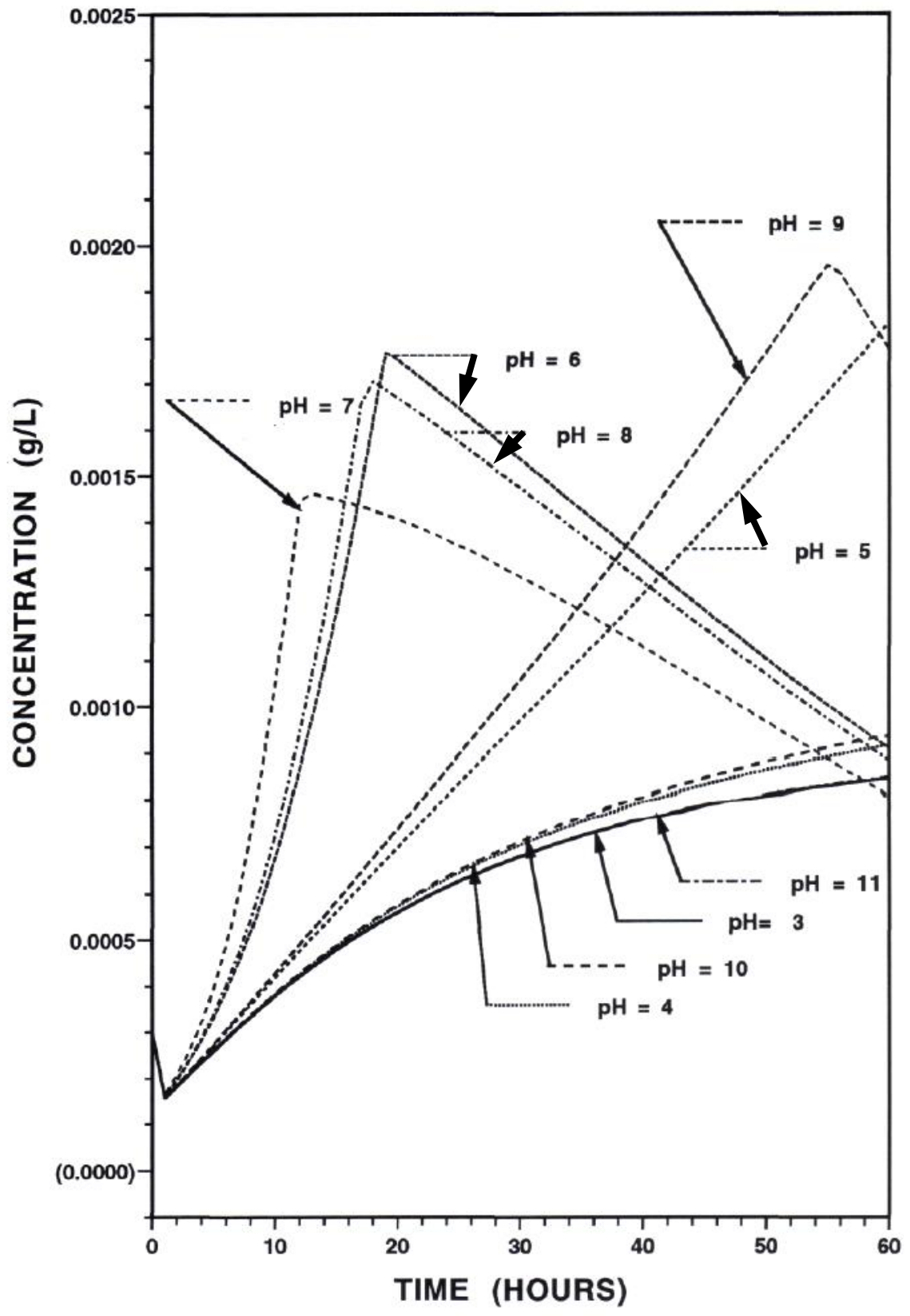


Figure 5.7. Simulation of Free Suspended Polymer (P*) production under batch solution conditions in a Multigen reactor under conditions of variations in the pH without trace metals.

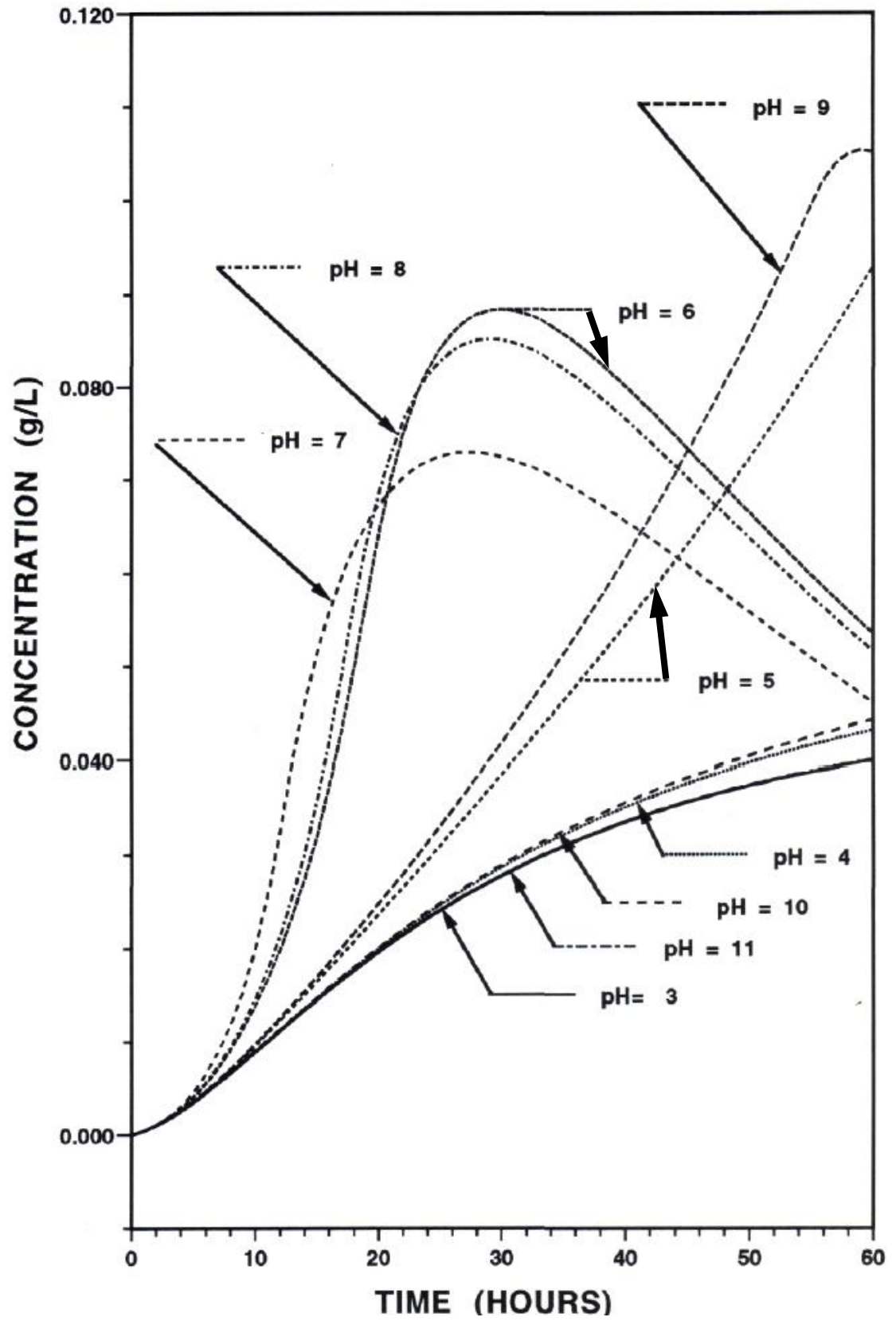


Figure 5.8. Simulation of Surface Associated Free Polymer (P^S) production under batch solution conditions in a Multigen reactor under conditions of variations in the pH without trace metals

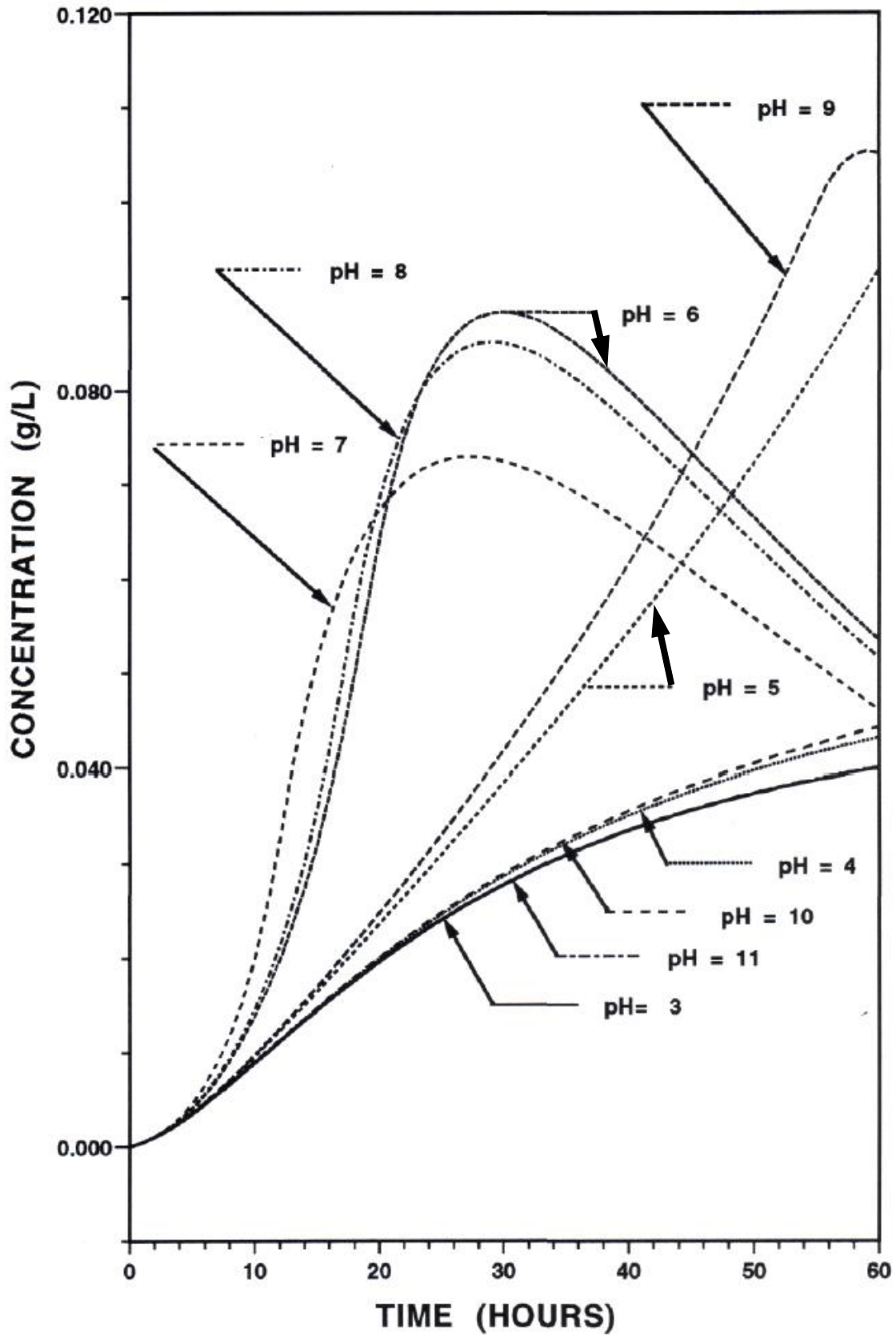
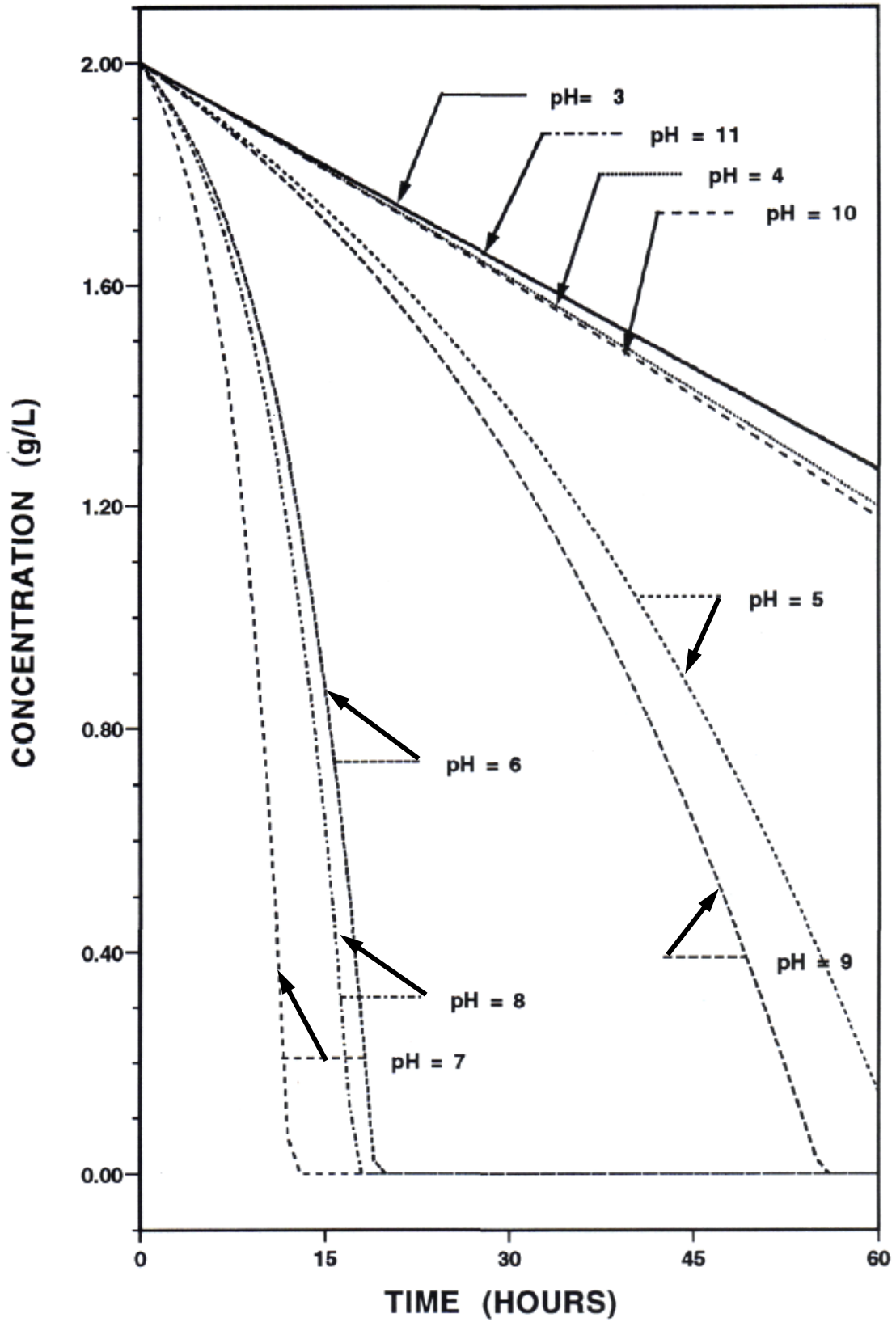


Figure 5.9. Simulation of the Limiting Substrate (C^*) usage under batch solution conditions in a Multigen reactor under conditions of variations in the pH without trace metals.



Figures 5.10 to 5.16 reflect simulations of steady state suspended and surface attached cellular components in a Multigen reactor operated on a continuous flow-through basis over a range of pH levels. In all of the simulations except that shown in Figure 5.15 for surface associated free polymer (P^S), the steady state results for dilution rates less than about 0.23 hr^{-1} are unaffected by the pH conditions. The length of model simulation time to reach steady state at a given dilution rate (not shown herein) did vary with the pH value tested in the simulation. The simulations were run to represent a time period as long as 250 hours with shorter times needed at circumneutral pH and longer times at extreme lower or higher pH values.

The simulations also resulted in approximately the same concentration of each component regardless of the pH value used in the test although the length of time to achieve that value did vary over the range of pH values. As previously discussed in Chapter 2, it could be surmised that while the rate of cellular growth under the more extreme acidic or alkaline conditions might be slower to begin compared to the circumneutral case, over time the cellular growth could show a slow increasing growth trend. Pirt (1975) had noted that many cellular structures vary in response to environmental changes so as to maintain a specific biomass growth rate so that at the steady state condition of the system, the cells should have been able to achieve the same overall final concentration. The results seem to reinforce this observation.

In all cases the circumneutral to alkaline pH simulations (pH 7, 8.5, and 10) allow operation at a slightly higher dilution rate than the acidic pH values (pH 3 and 4.5) before washout of a cellular component is attained. Figure 5.15 shows that there is more surface associated polymer produced at the pH extremes (pH 4, 8.5 and 10) than at the near

Figure 5.10. Simulation of Suspended Cell (A) growth under steady state solution conditions in a Multigen reactor under conditions of variations in the pH without trace metals.

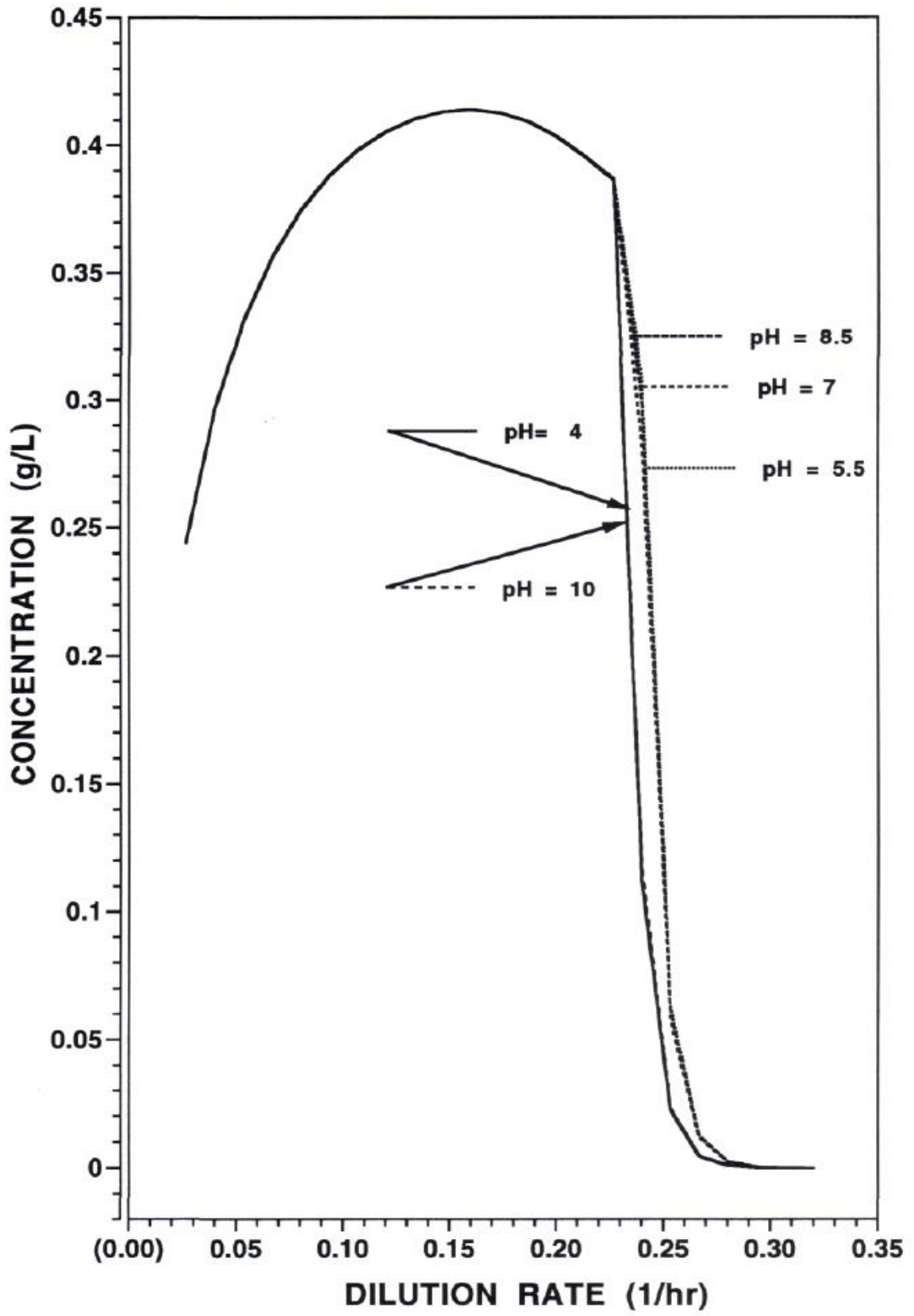


Figure 5.11 Simulation of Suspended Cell Associated Polymer (P) production under steady state solution conditions in a Multigen reactor under conditions of variations in the pH without trace metals.

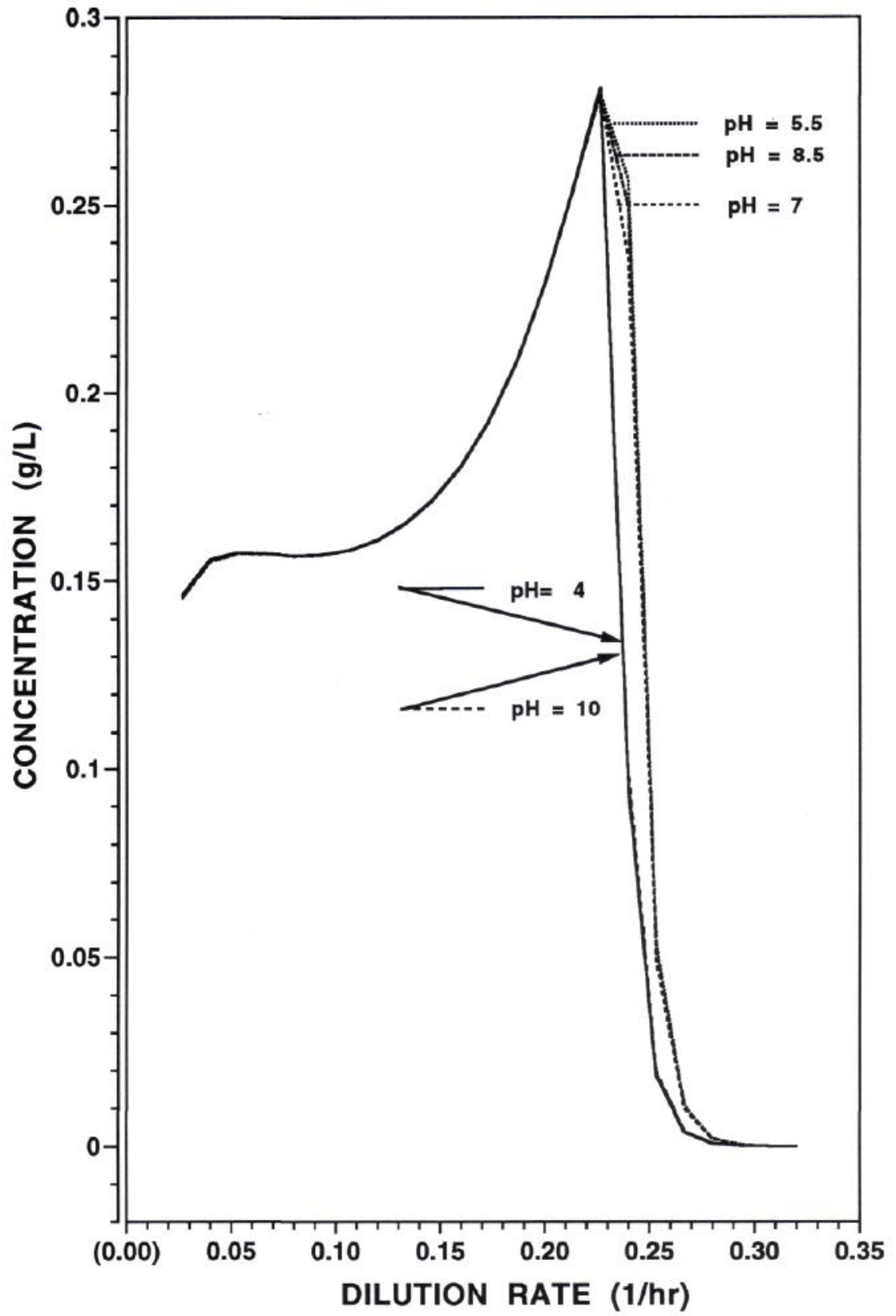


Figure 5.12. Simulation of Surface Attached Cell (A^B) growth under steady state solution conditions in a Multigen reactor under conditions of variations in the pH without trace metals.

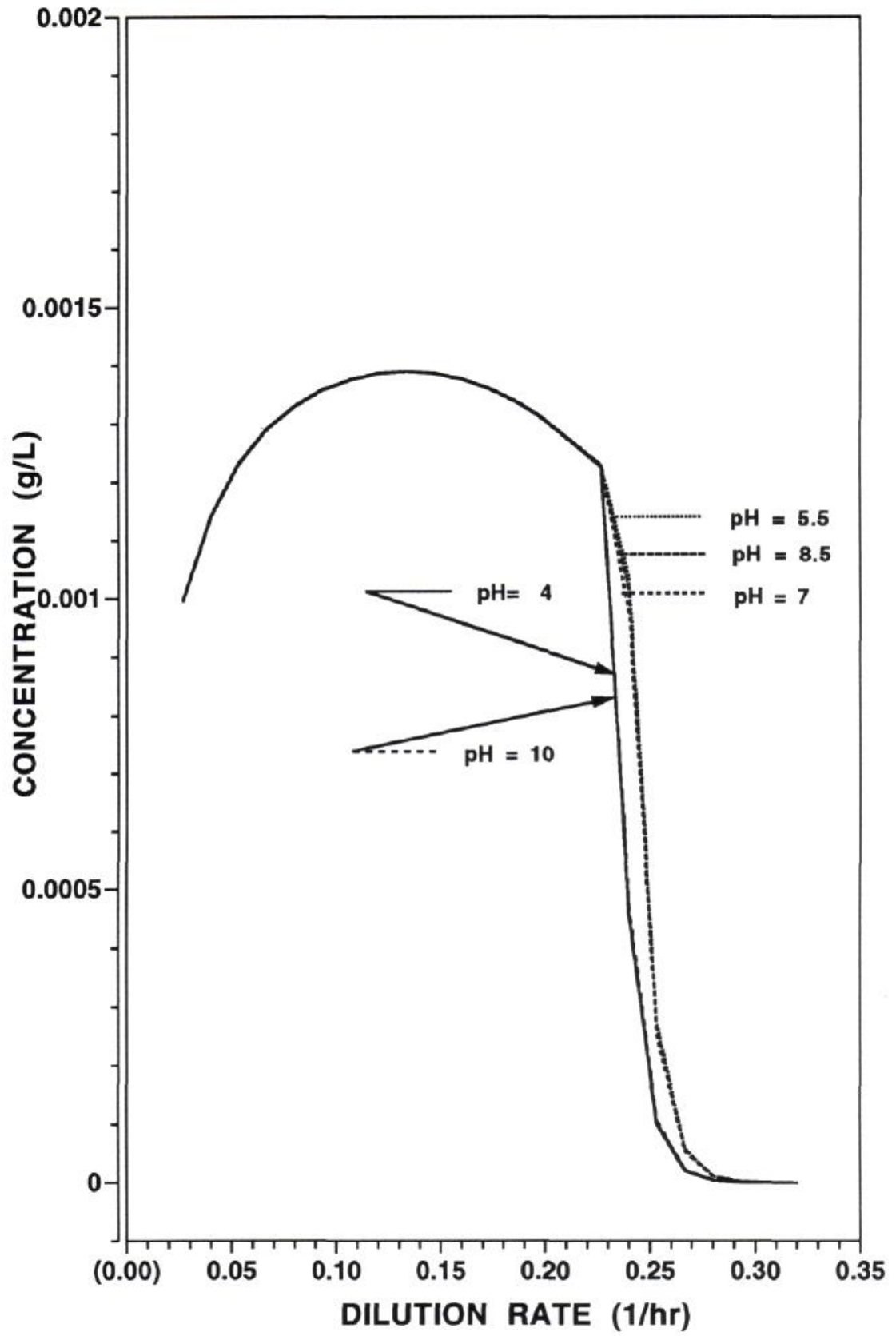


Figure 5.13. Simulation of Surface Attached Cell Associated Polymer (P^B) production under steady state solution conditions in a Multigen reactor under conditions of variations in the pH without trace metals.

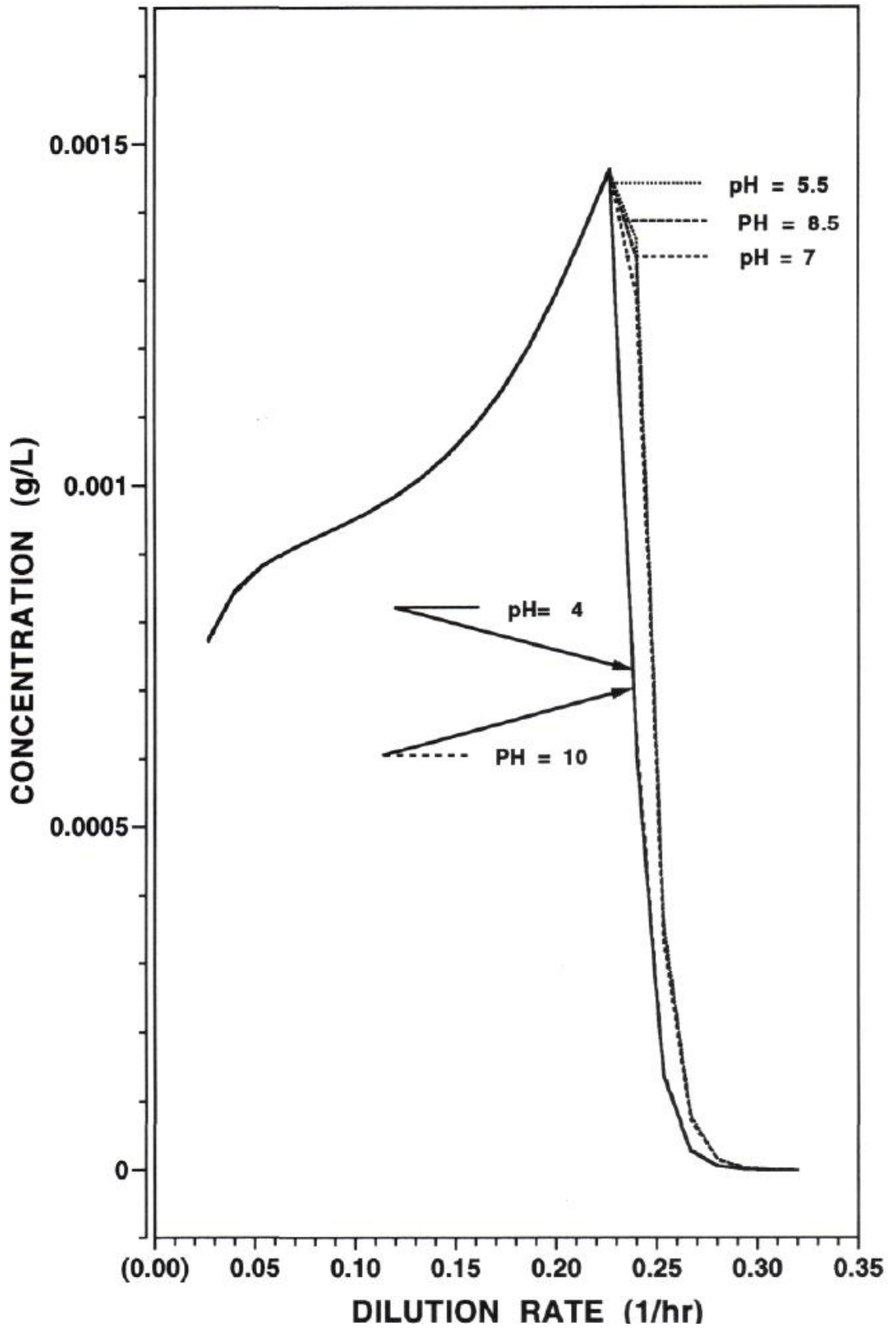


Figure 5.14. Simulation of Free Suspended Polymer (P*) production under steady state solution conditions in a Multigen reactor under conditions of variations in the pH without trace metals.

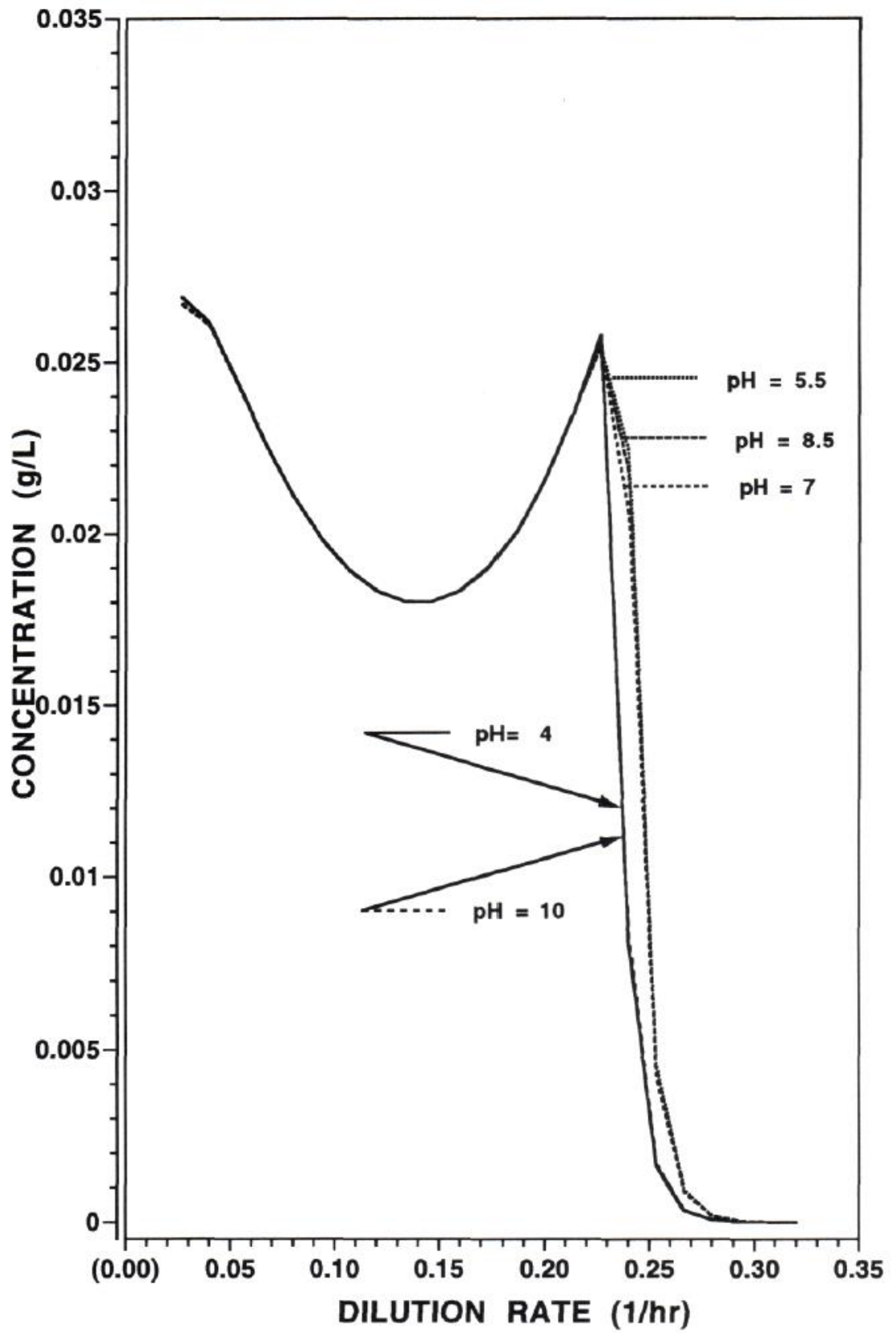


Figure 5.15. Simulation of Surface Associated Free Polymer (P^S) production under steady state solution conditions in a Multigen reactor under conditions of variations in the pH without trace metals.

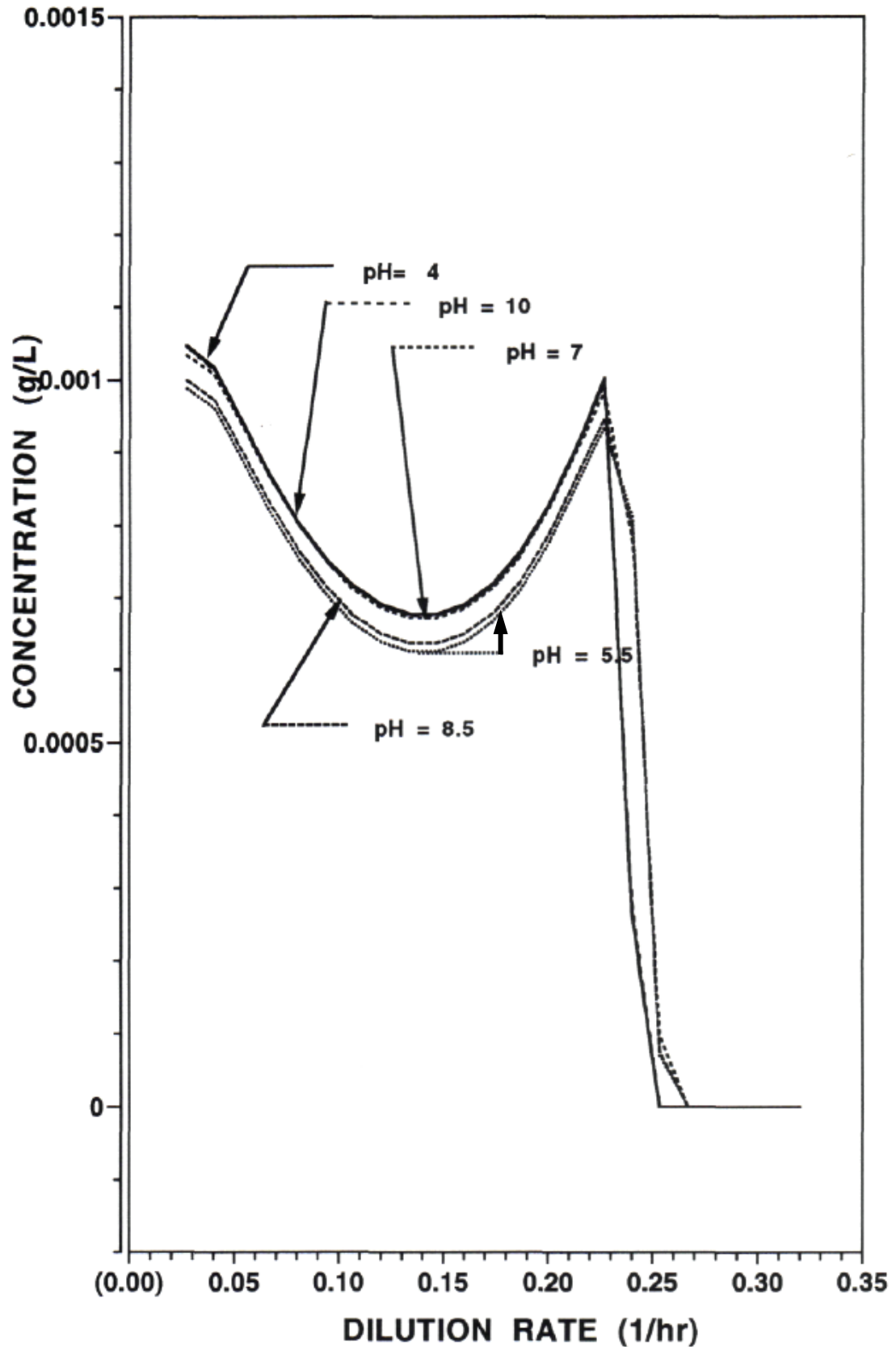
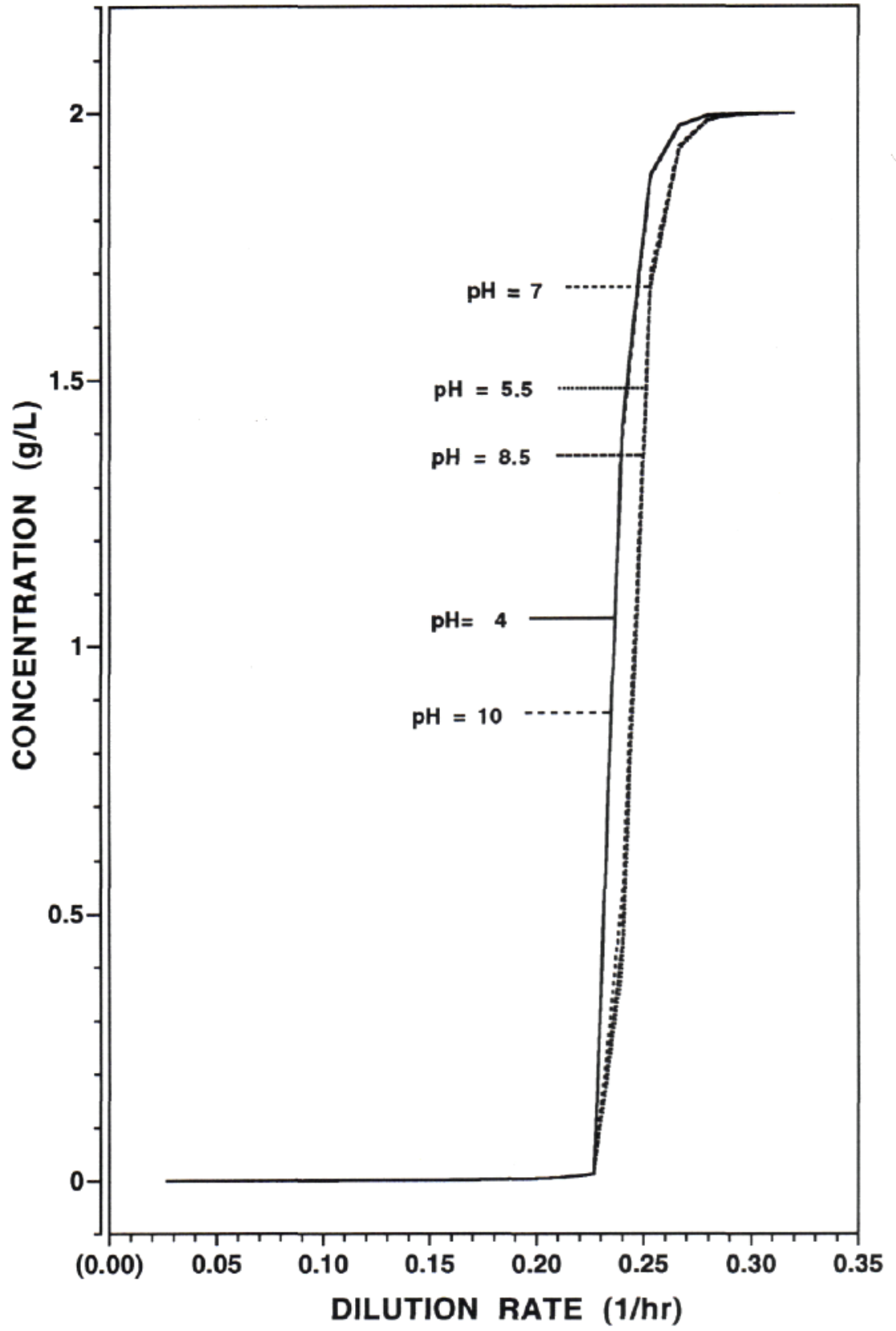


Figure 5.16. Simulation of the Limiting Substrate (C^*) under steady state solution conditions in a Multigen reactor under conditions of variations in the pH without trace metals.



circumneutral pH values (pH 5.5 and 7). The calculated washout in Figures 5.10 to 5.16 (dilution rates of 0.23 to 0.28 hr⁻¹) compare to values measured by Hsieh (1988) (dilution rates of 0.24 to 0.28 hr⁻¹) which were determined at circumneutral pH. This also reinforces the assumption that selection of the *P. atlantica* model parameters used by Hsieh (1988) as similar enough to represent the *P. cepacia* 17616 strain in this modelling effort is realistic.

Figures 5.17 to 5.23 reflect simulations of suspended and surface attached cellular components in a bioreactor (after Hsieh, 1988; Hsieh, 1986) operated under batch growth conditions at variable pH levels. The bioreactor has a volume of 1.42 L with available surfaces comprising 0.321 m² and with mixing achieved at a Re of 300. Relative to the Multigen, the bioreactor has over a 5.5 times higher surface to volume ratio. The same general trends seen in Figures 5.3 to 5.9 for the batch Multigen operation are followed in the batch bioreactor case. The simulated concentration of suspended cells is the same at circumneutral pH, but is about 25 to 30% lower in the bioreactor at other pH values. All of the polymer components (P, P^B, P*, and P^S) in Figures 5.18, 5.20, 5.21 and 5.22, respectively, show larger concentrations in the bioreactor than in the Multigen. The bioreactor results also indicated the components accumulate at a slower rate and take longer to show a concentration reduction compared to the Multigen case. The attached cell components (A^B and P^B) in the bioreactor appear to have a higher initial rate of reduction in concentration compared to the Multigen, and then settle down to a lesser constant rate of detachment after the depletion of the available substrate. The jog in the graphs is an artifact of the data output from the model. The model used a 5-second time step but data was output in 1-hour increments to plot the graph. The transition from the higher rate to a lesser rate

Figure 5.17. Simulation of Suspended Cell (A) growth in a Bioreactor under batch solution conditions without trace metals at variable pH and $Re = 300$.

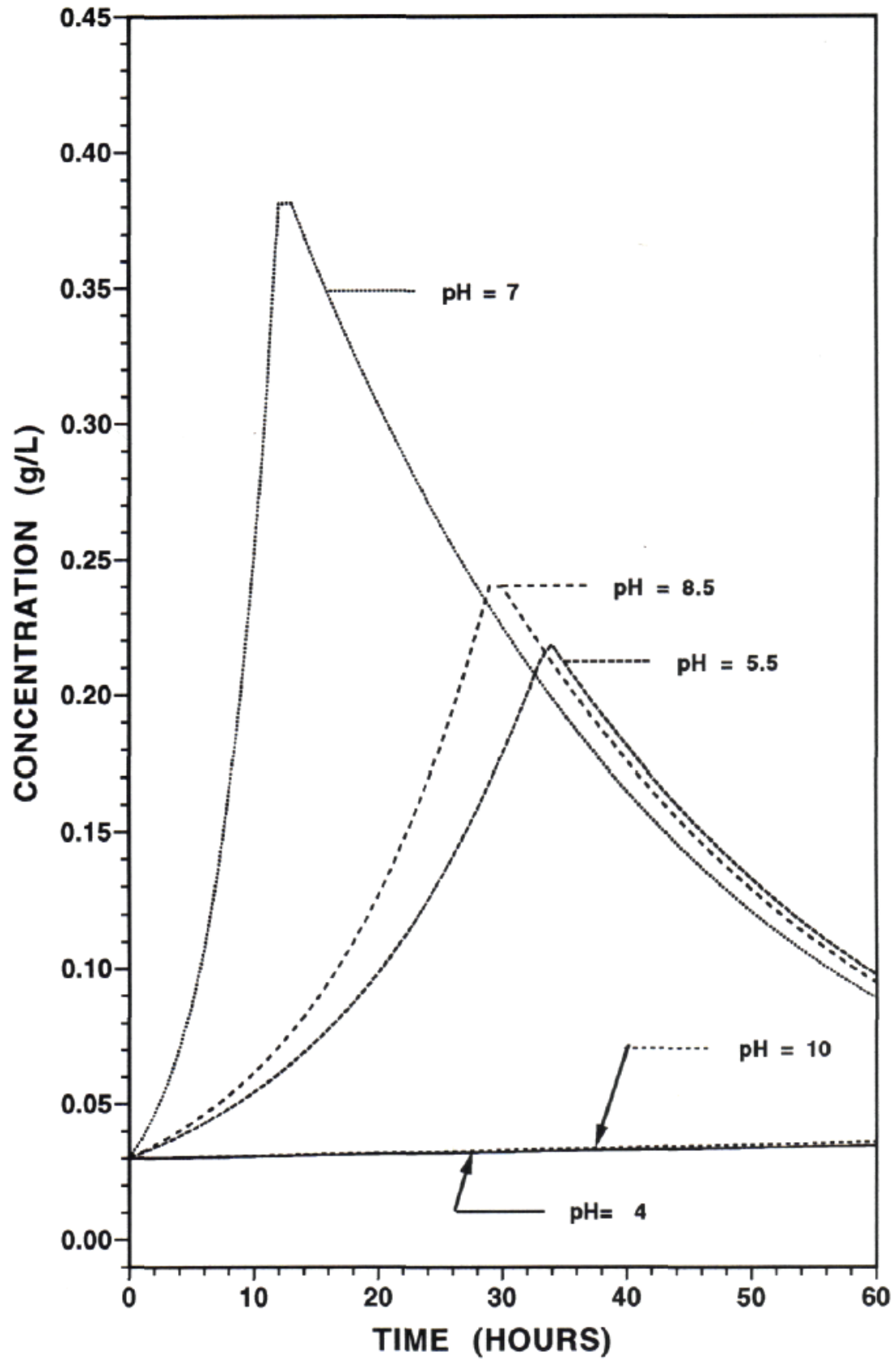


Figure 5.18. Simulation of Suspended Cell Associated Polymer (P) production in a Bioreactor under batch solution conditions without trace metals at variable pH and $Re = 300$.

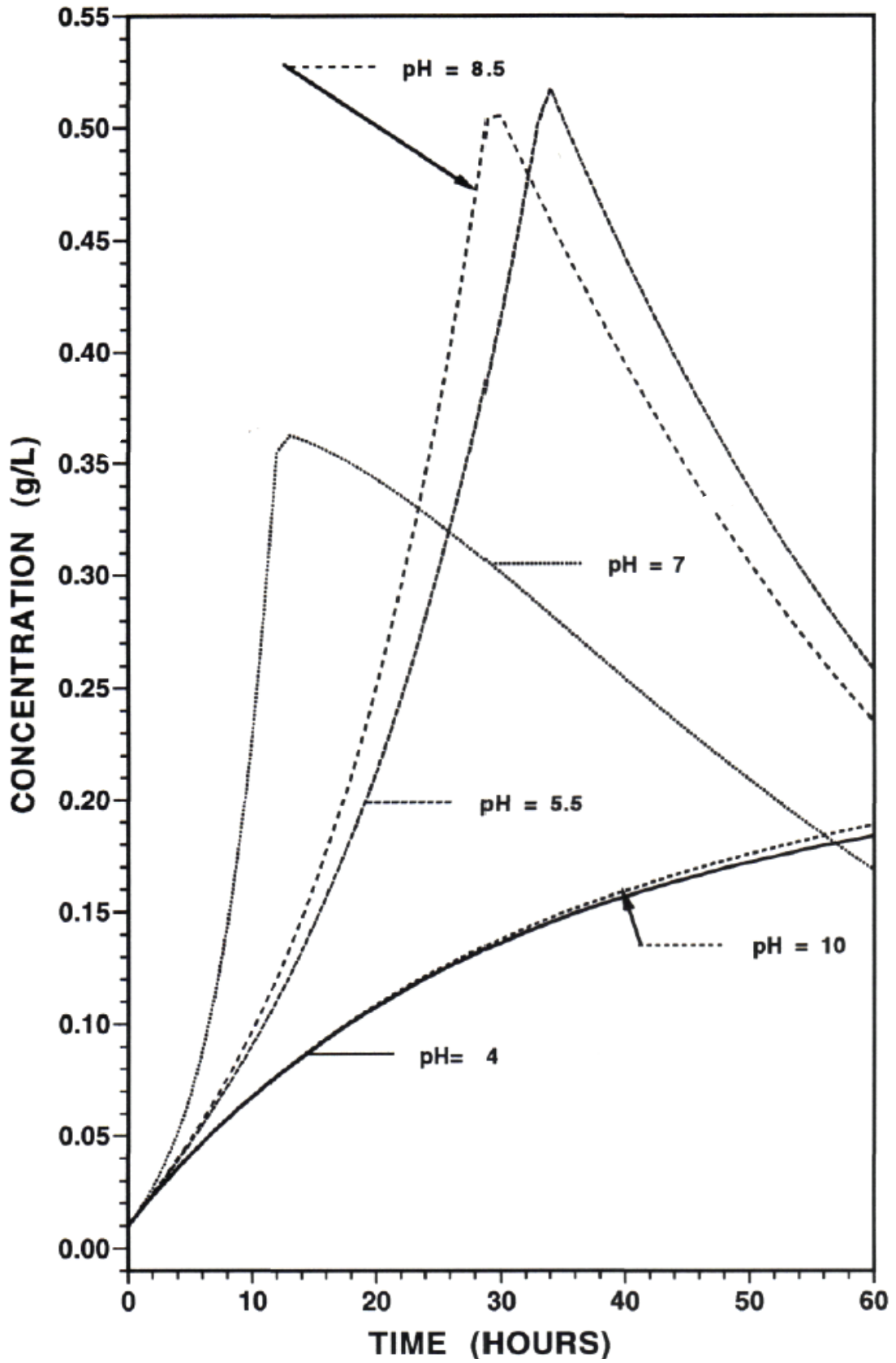


Figure 5.19. Simulation of Surface Attached Cell (A^B) growth in a Bioreactor under batch solution conditions without trace metals at variable pH and $Re = 300$.

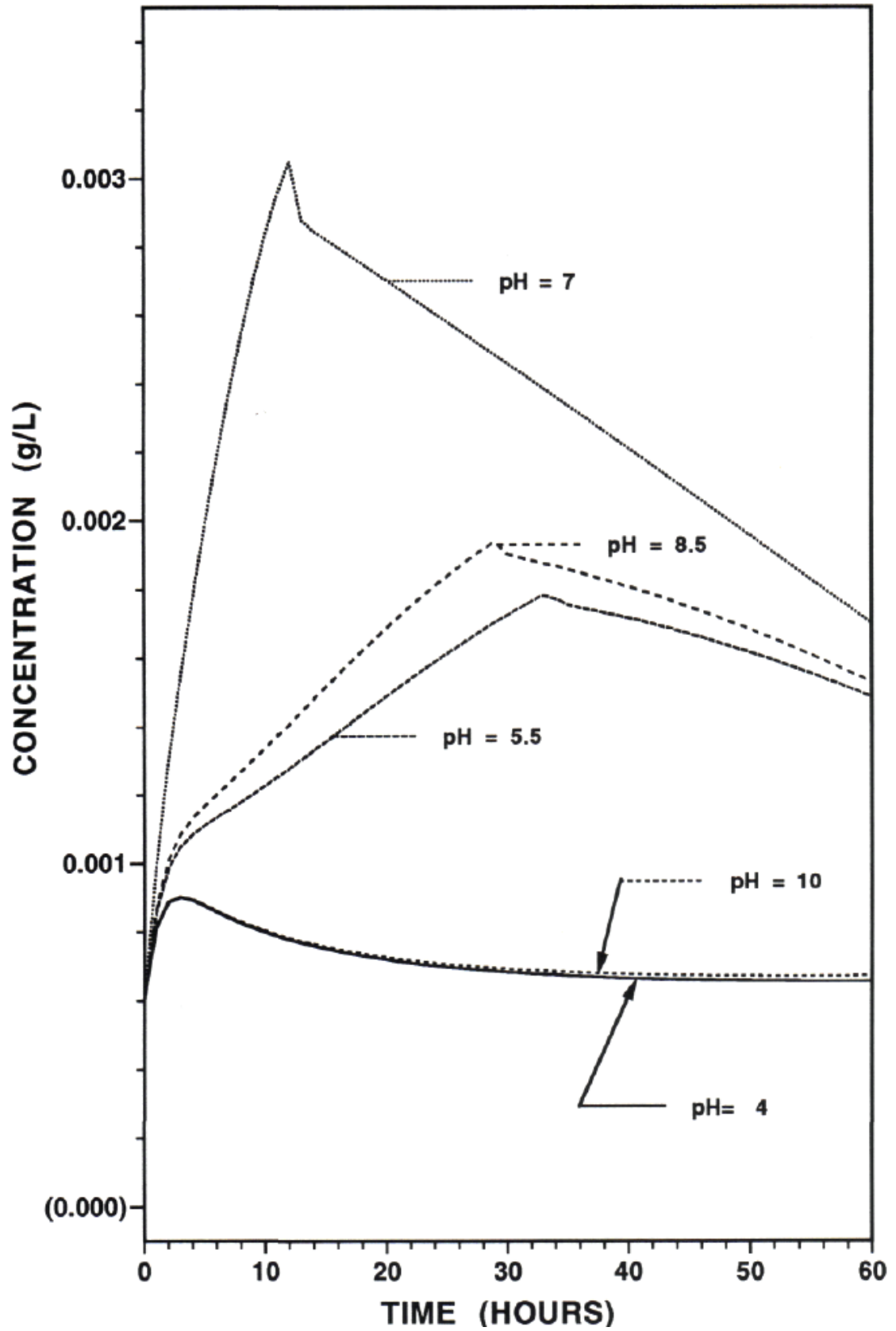


Figure 5.20. Simulation of Surface Attached Cell Associated Polymer (P^B) production in a Bioreactor under batch solution conditions without trace metals at variable pH and $Re = 300$.

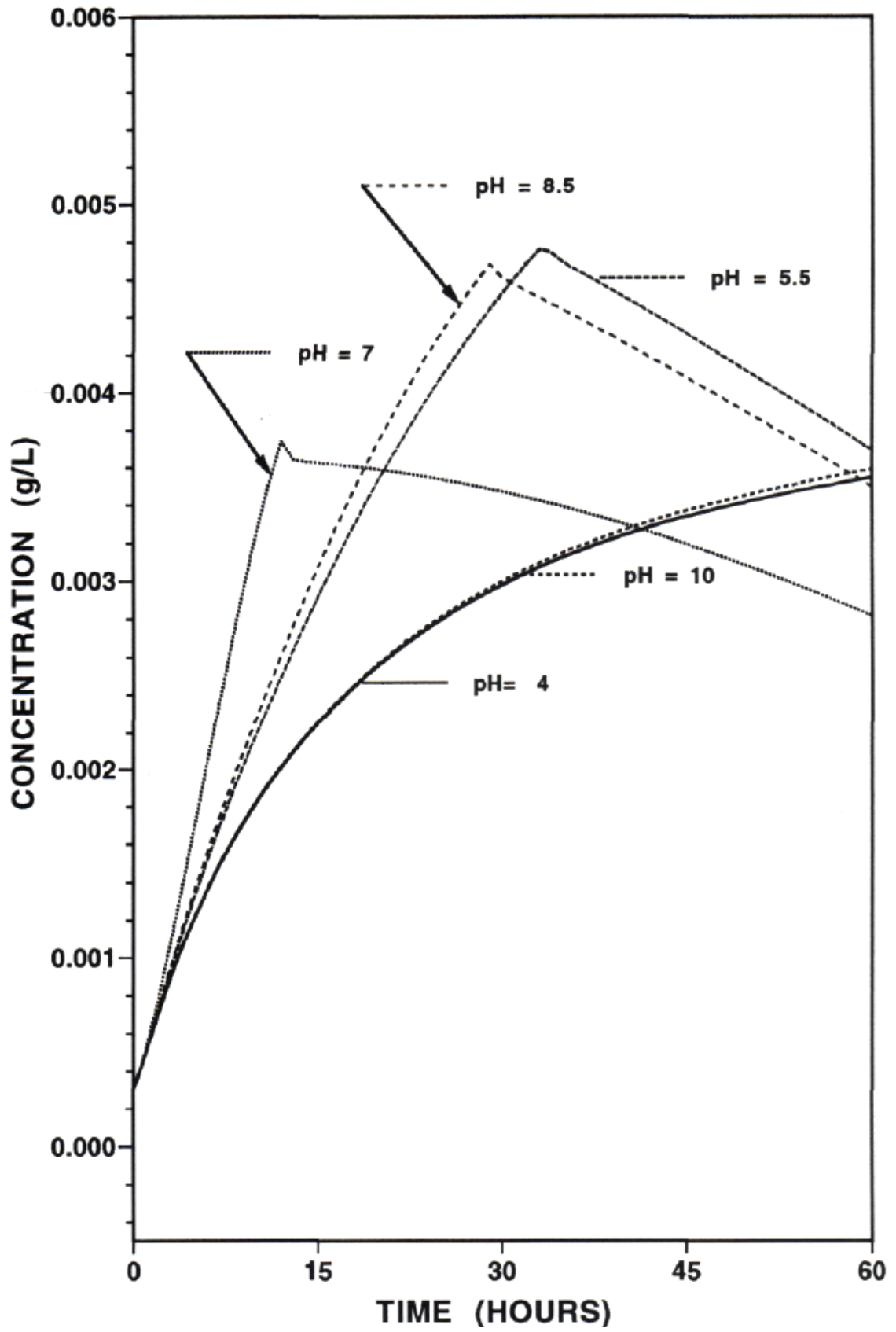


Figure 5.21. Simulation of Free Suspended Polymer (P*) production in a Bioreactor under batch solution conditions without trace metals at variable pH and Re - 300.

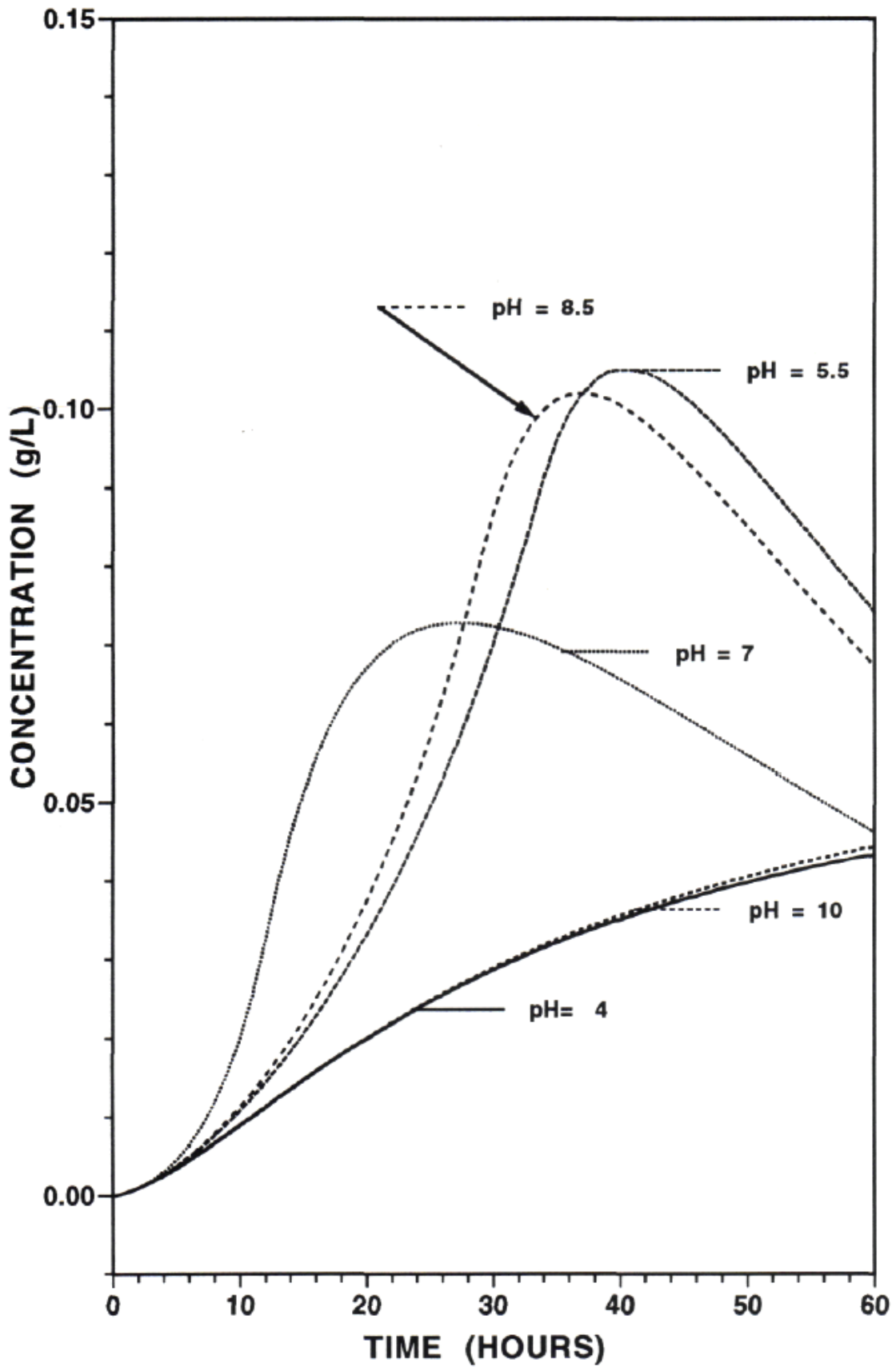


Figure 5.22. Simulation of Surface Associated Free Polymer (P^S) production in a Bioreactor under batch solution conditions without trace metals at variable pH and $Re = 300$.

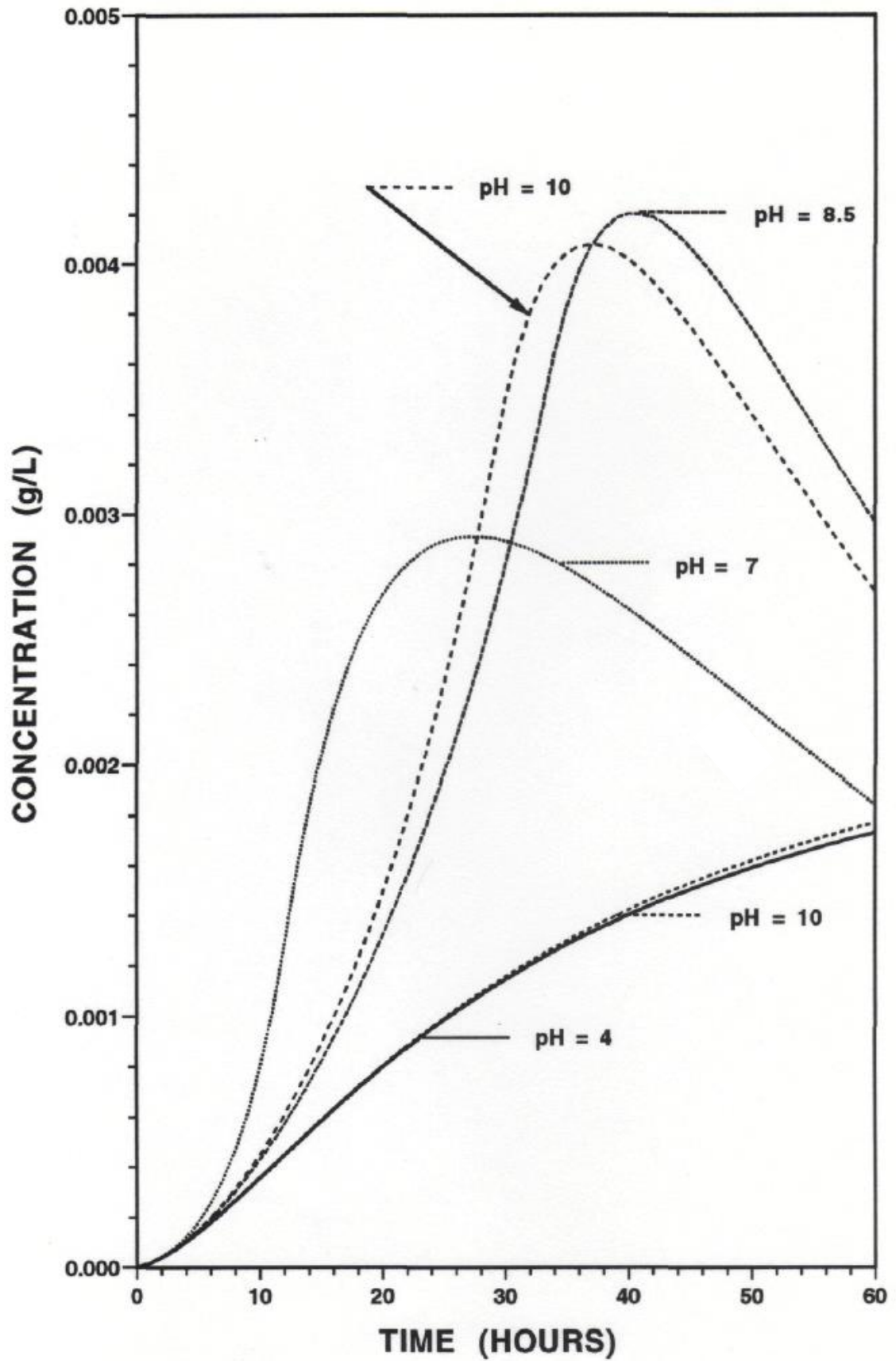
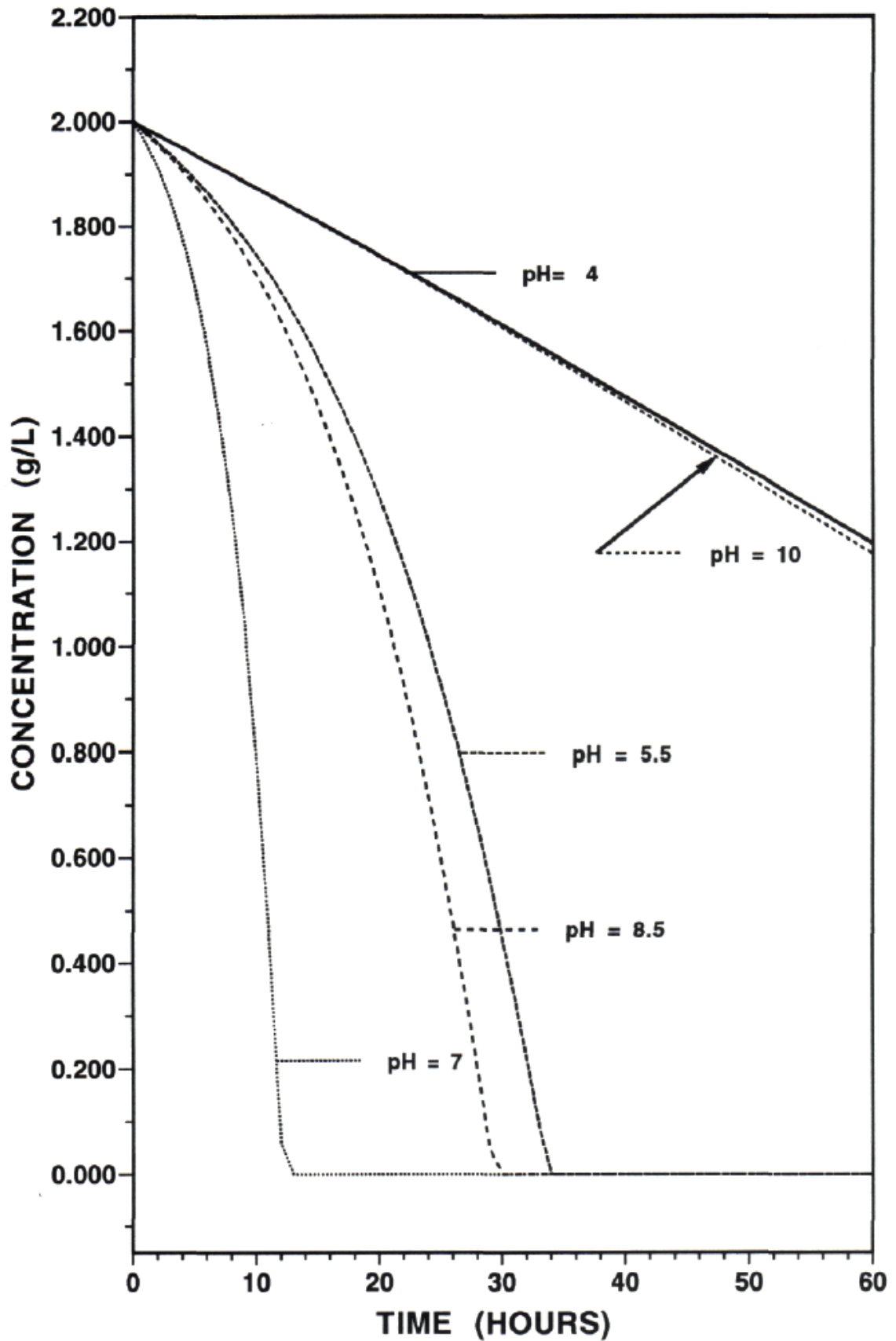


Figure 5.23. Simulation of the Limiting Substrate (C^*) usage in a Bio-reactor under batch solution conditions without trace metals at variable pH and $Re = 300$.



with more data available would be reflected as a curvilinear transition rather than a distinct jog.

Figures 5.24 to 5.30 reflect simulations of the steady state suspended and surface attached cellular components in a bioreactor operated under continuous flow-through growth conditions at variable pH levels. The results for suspended cells (A) and associated polymer (P) in Figures 5.24 and 5.25 are nearly identical to the Multigen case (Figures 5.10 and 5.11 respectively). However, for all other attached cell and polymer components (A^B , P^B , P^* , and P^S), Figures 5.26 to 5.29 show steady state concentrations in the bioreactor several times larger than in the Multigen situations. This is partially explained by the over 5-fold increase in the available surface area between the two cases. The washout of biomass and cell associated components (dilution rates of 0.22 to 0.28 hr^{-1}) appears comparable to the results of Hsieh (1988) for operation of the bioreactor with *P. atlantica*, however, his simulation and experimental results did not show as great a difference in the concentration values of the cellular components.

Figure 5.24. Simulation of Suspended Cell (A) growth in a Bioreactor under steady state continuous flow-through solution conditions without trace metals at variable levels of pH and $Re = 300$.

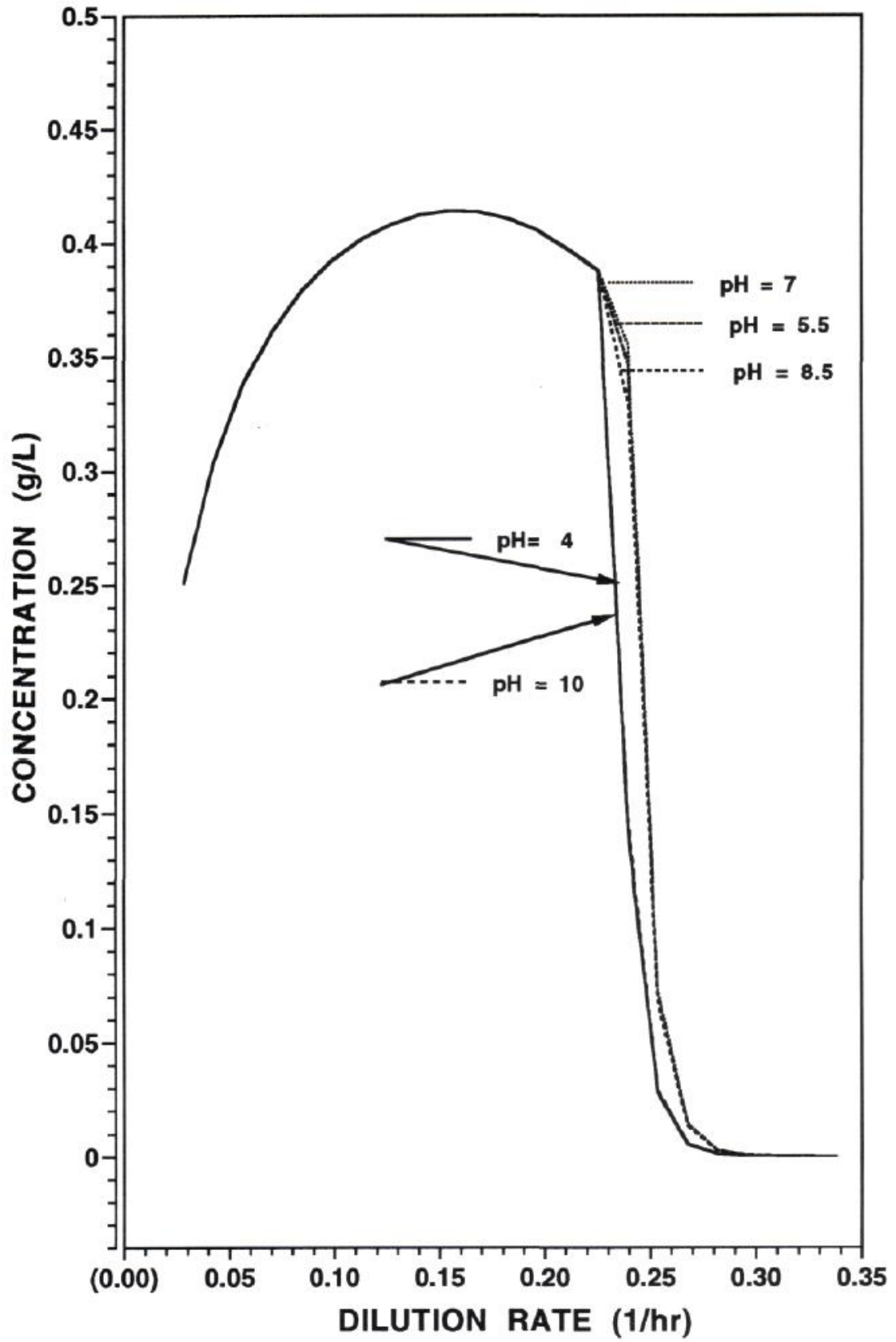


Figure 5.25. Simulation of Suspended Cell Associated Polymer (P) production in a Bioreactor under steady state continuous flow-through solution conditions without trace metals at variable levels of pH and $Re = 300$.

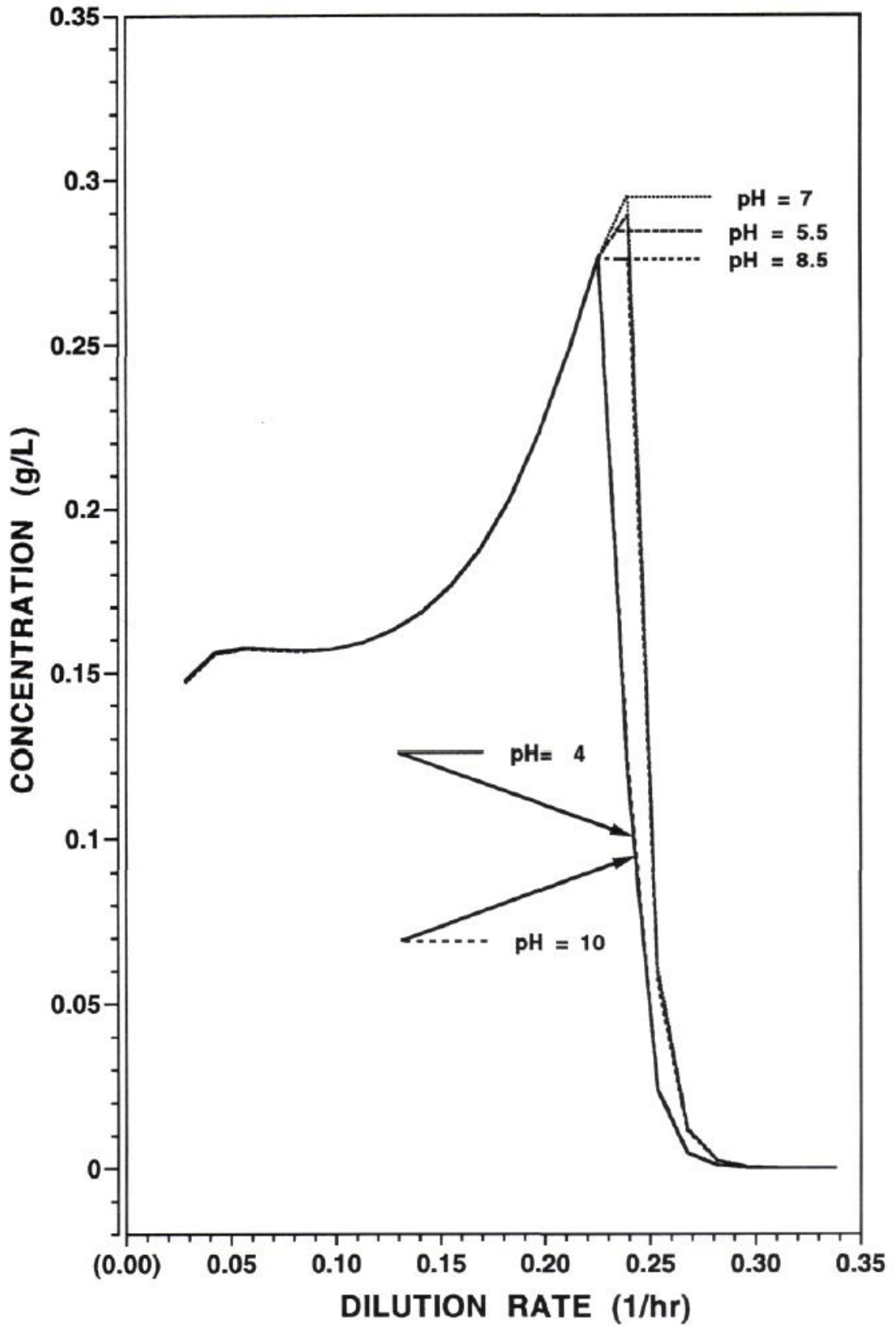


Figure 5.26. Simulation of Surface Attached Cell (A^B) growth in a Bio-reactor under steady state continuous flow-through solution conditions without trace metals at variable levels of pH and $Re = 300$.

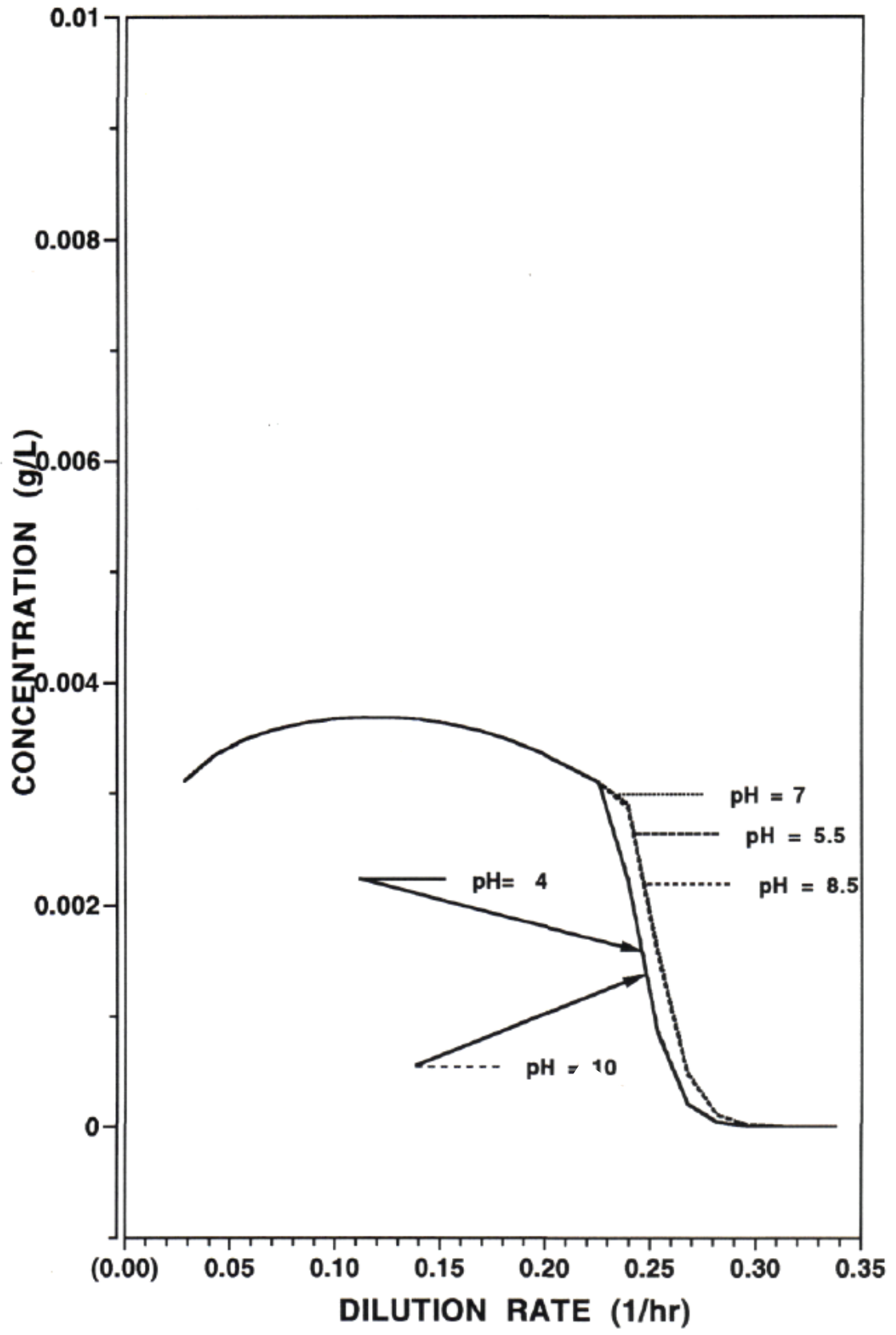


Figure 5.27. Simulation of Surface Attached Cell Associated Polymer (P^B) production in a Bioreactor under steady state continuous flow-through solution conditions without trace metals at variable levels of pH and $Re = 300$.

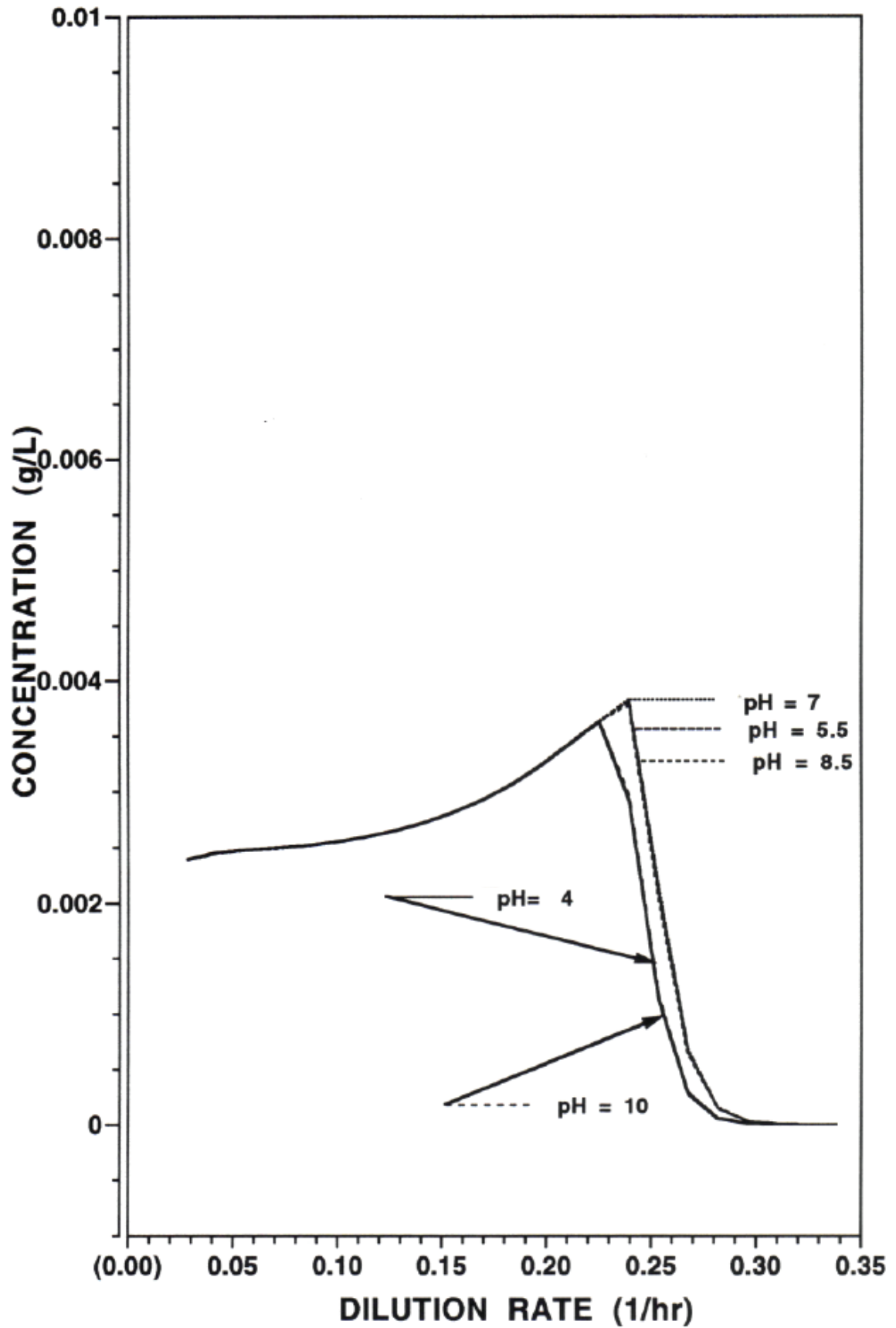


Figure 5.28. Simulation of Free Suspended Polymer (P*) production in a Bioreactor under steady state continuous flow-through conditions without trace metals at variable levels of pH and $Re = 300$.

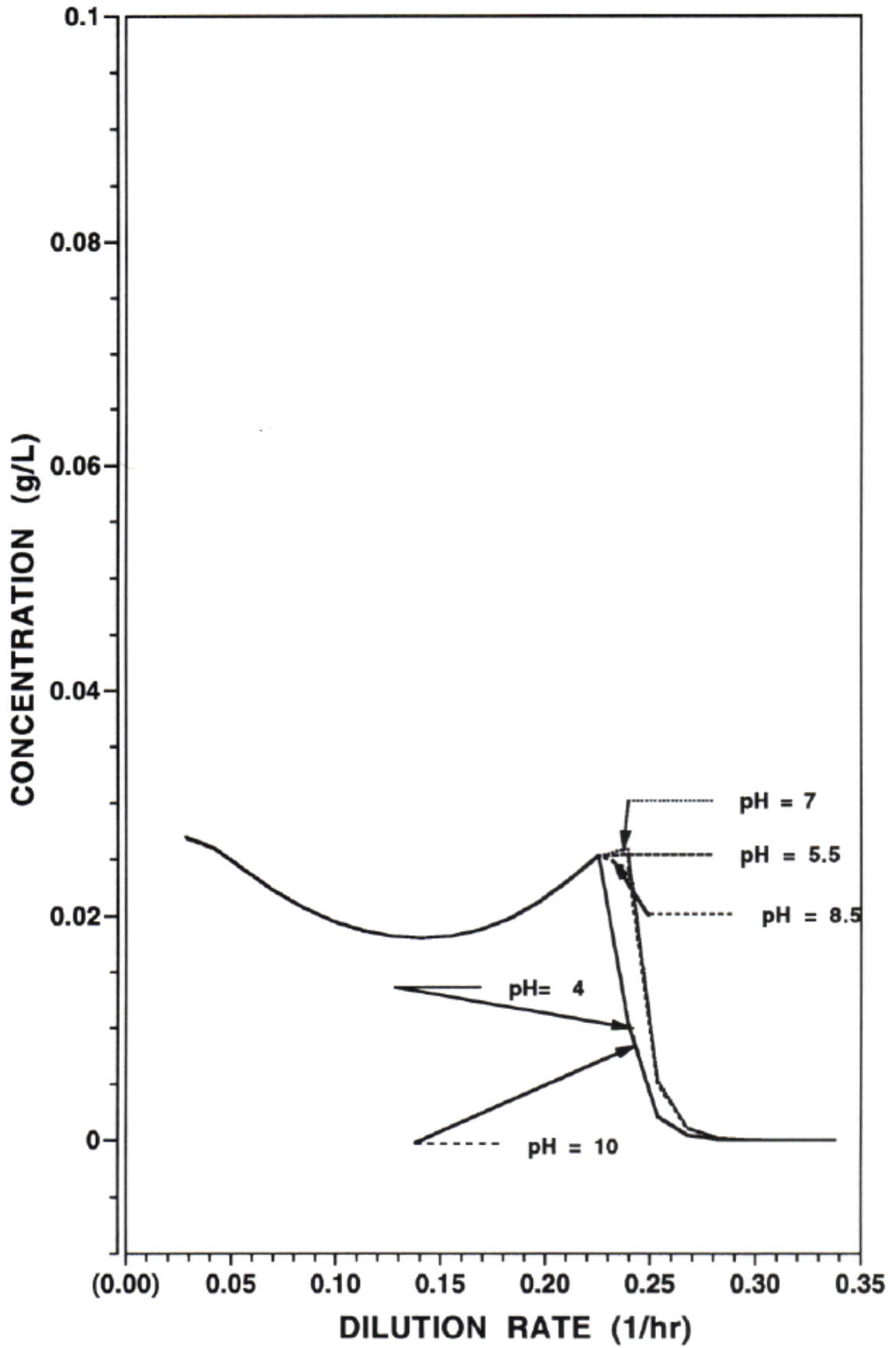


Figure 5.29. Simulation of Surface Associated Free Polymer (P^S) production in a Bioreactor under steady state continuous flow-through conditions without trace metals at variable levels of pH and $Re = 300$.

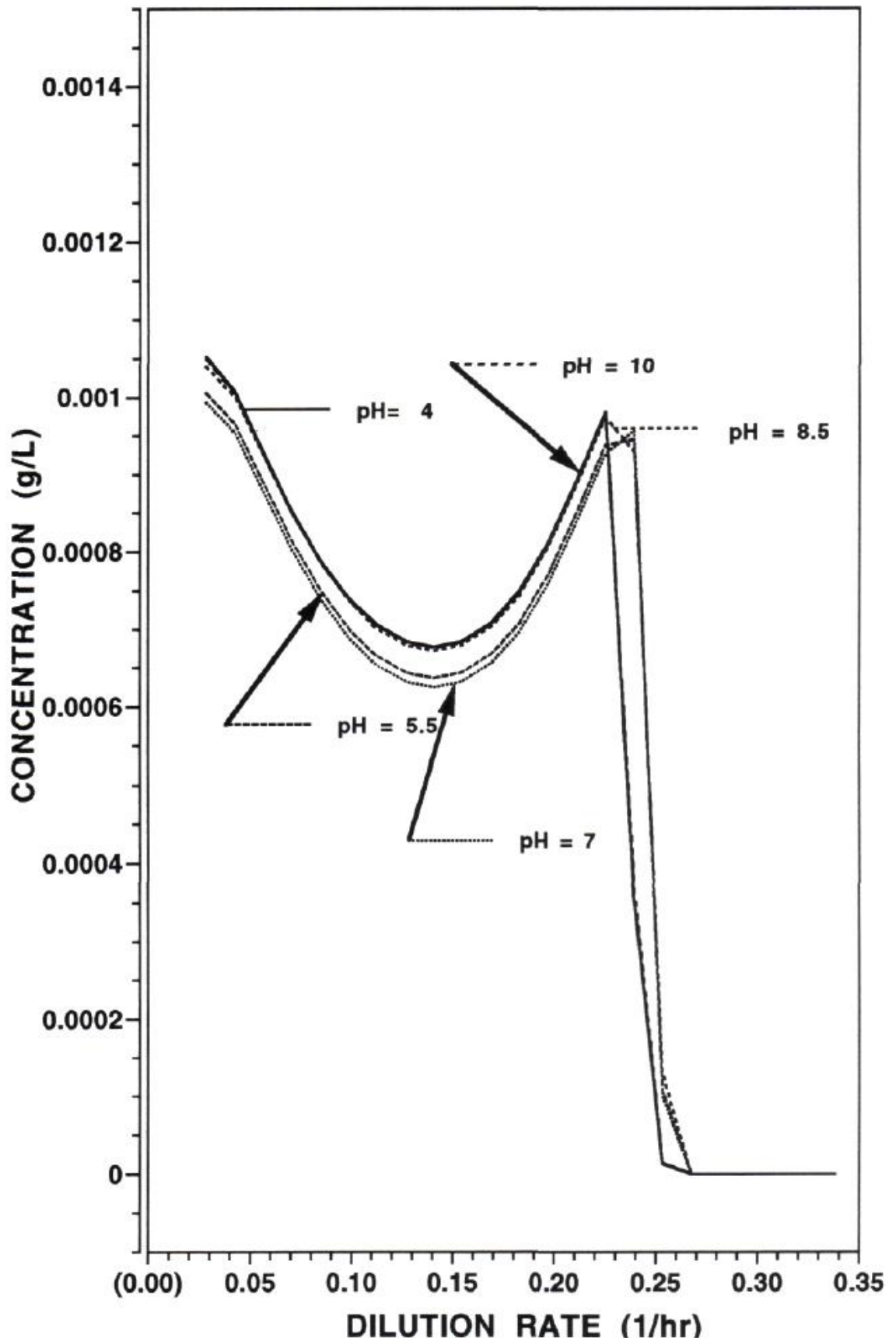
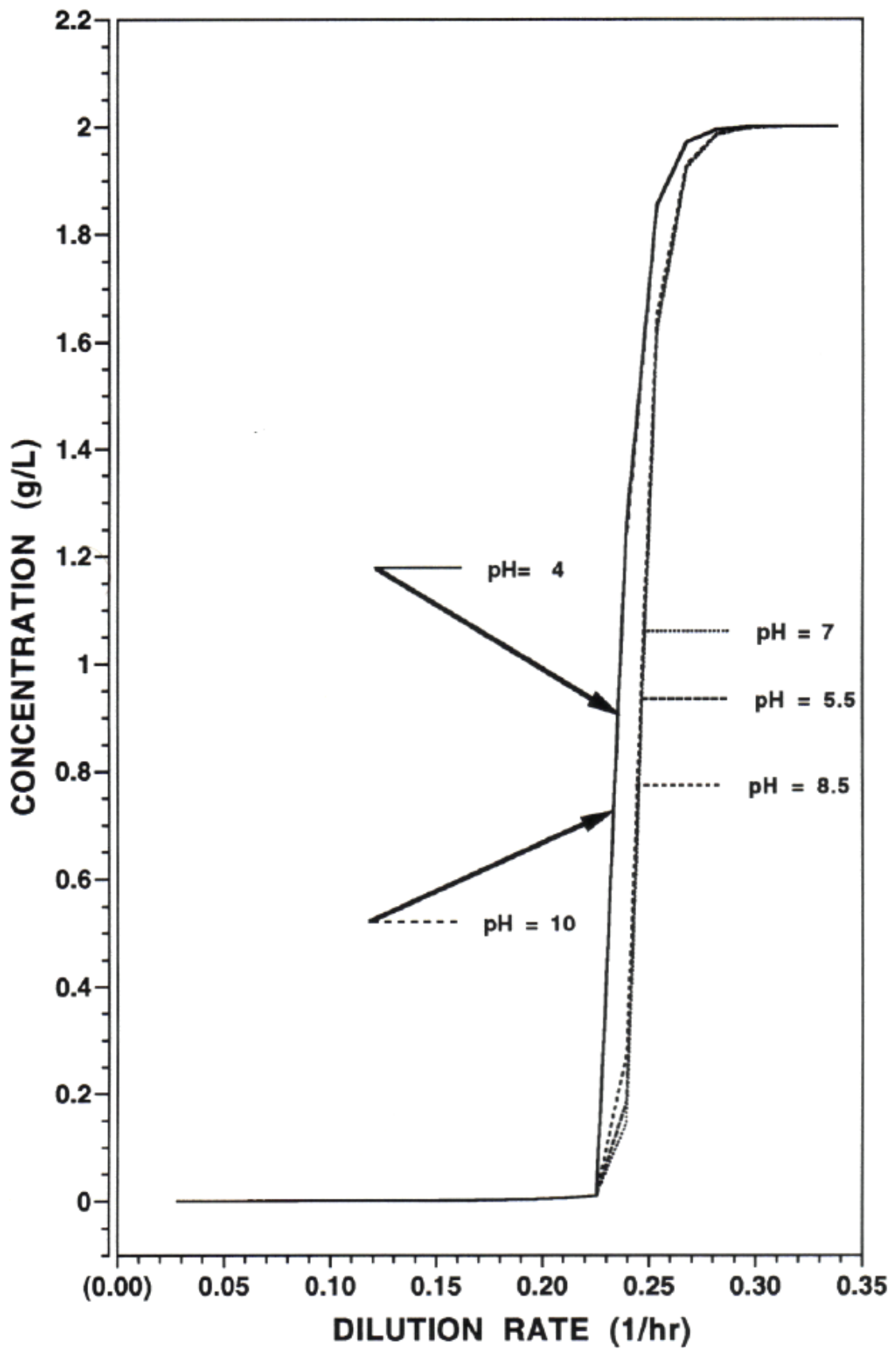


Figure 5.30. Simulation of the Limiting Substrate (C^*) usage in a Bioreactor under steady state continuous flow-through conditions without trace metals at variable levels of pH and $Re = 300$.



CELLULAR GROWTH WITH A TRACE METAL

Simulations in the presence of a trace metal illustrate the model response of the cellular components to the presence of a toxic species and in conjunction with a variation in pH. In the model structure, M^* represents the free metal ion rather than total metal concentration placed in the system. As noted in Chapter 2 and 4 the free ion activity has been shown to be the toxic form of the metal to cells. Table 5.1 tabulates a calculation of the free metal concentration in the MMS medium as a function of pH in the Multigen environment in the absence of cellular components. The free lead ion concentration was calculated using the speciation program MINEQL to be greater than 78 percent of the total metal concentration in all cases of the pH at 7 or below (acidic). For pH values above circumneutral, the free metal concentration dropped off rapidly to less than 1 percent at pH 9. Because of this very low free ion concentration, the fluctuations (relative to the case with no metal present) in concentration of cellular components essentially became zero in a later continuous flow-through simulation.

Estimates were also made in the last column in Table 5.1 of the amount of charged free ion lead and complexed lead species (hydroxides at pH 7 and carbonates at pH 9) that could bind to the glass slide surfaces in the absence of cells and polymer that would be used in later experiments in the reactor. The assumed equilibrium constant for this association of the lead complex with the glass surface was 2.45×10^{-7} . For these simulations, the glass slide surfaces were assumed to not be pH dependent and the same equilibrium constant was assumed for both types of species. As seen in the sample table of values at the end of Appendix II, the divalent lead ion association with cells (4.8×10^{-6}) or exopolymer (pK values ranging from 4.61 to 6.56) compared to glass surfaces had equilibrium constants 20 or more

Table 5.1: Trace Lead Speciation in MMS Medium in a Multigen Reactor under Batch Solution Conditions with Variable pH Levels in The Absence of a Biophase.

Solution pH	Total Metal Concentration (mole/L)	Free Metal Concentration (mole/L)	Surface Adsorbed Metal (% of Total)
5.0	1.0×10^{-5}	8.82×10^{-6}	10
	1.0×10^{-7}	8.82×10^{-8}	10
	1.0×10^{-9}	8.82×10^{-10}	10
7.0	1.0×10^{-5}	4.40×10^{-6}	30
	1.0×10^{-7}	7.75×10^{-8}	30
	1.0×10^{-9}	7.75×10^{-10}	30
9.0	1.0×10^{-5}	1.11×10^{-10}	95
	1.0×10^{-7}	7.39×10^{-12}	95
	1.0×10^{-9}	7.39×10^{-14}	95

times larger. The estimated amount of charged lead complex attachment to the glass slide surfaces at higher pH would more likely occur since the affinity for whatever free ion lead that is available in the solution would be more likely to bind to cells and polymer when present in later simulations. In all cases, the free lead ion form was the dominant species modeled in this effort to bind with cells and polymer. At the high alkaline pH values, the percentage of total lead that can bind to the surface is high due to much of the lead ions forming charged lead carbonate complexes in the medium. Likewise at the acidic pH values the percentages are very low since so much of the lead is in the free-ion form rather than complexed with other components and much more likely to attach to cells or exopolymer. At circumneutral pH, the estimated level of charged lead complexes is lower and is mostly of the lead hydroxide form. This is in turn reflected in a potential glass surface coverage value also in between the two pH extreme coverage values.

Simulated results of free ion lead effects on total suspended biomass X (comprised of suspended active cell mass (A) plus associated attached polymer (P)) in a Multigen operated under batch growth conditions at variable pH levels are shown in Figures 5.31 to 5.33. Simulated results for total attached biomass B [comprised of attached cells (A^B) plus attached cell associated polymer (P^B)] as a function of pH are shown in Figure 5.34 to 5.36. In each graph, the simulation for growth without lead present is compared at 3 levels of total applied lead. Three different pH values are compared in the succession of figures. As the total lead metal added to the solution increases to 10^{-7} M and 10^{-5} M, the general trend shows a marked decrease in the concentration of the biological components and a marked increase in the time to reach maximum values under acidic and circumneutral

Figure 5.31. Simulated effects of variable concentrations of lead on the Total Suspended Biomass (X) [=suspended active cell mass (A) plus associated attached polymer (P)] production in a Multigen reactor under batch growth conditions at pH 5.

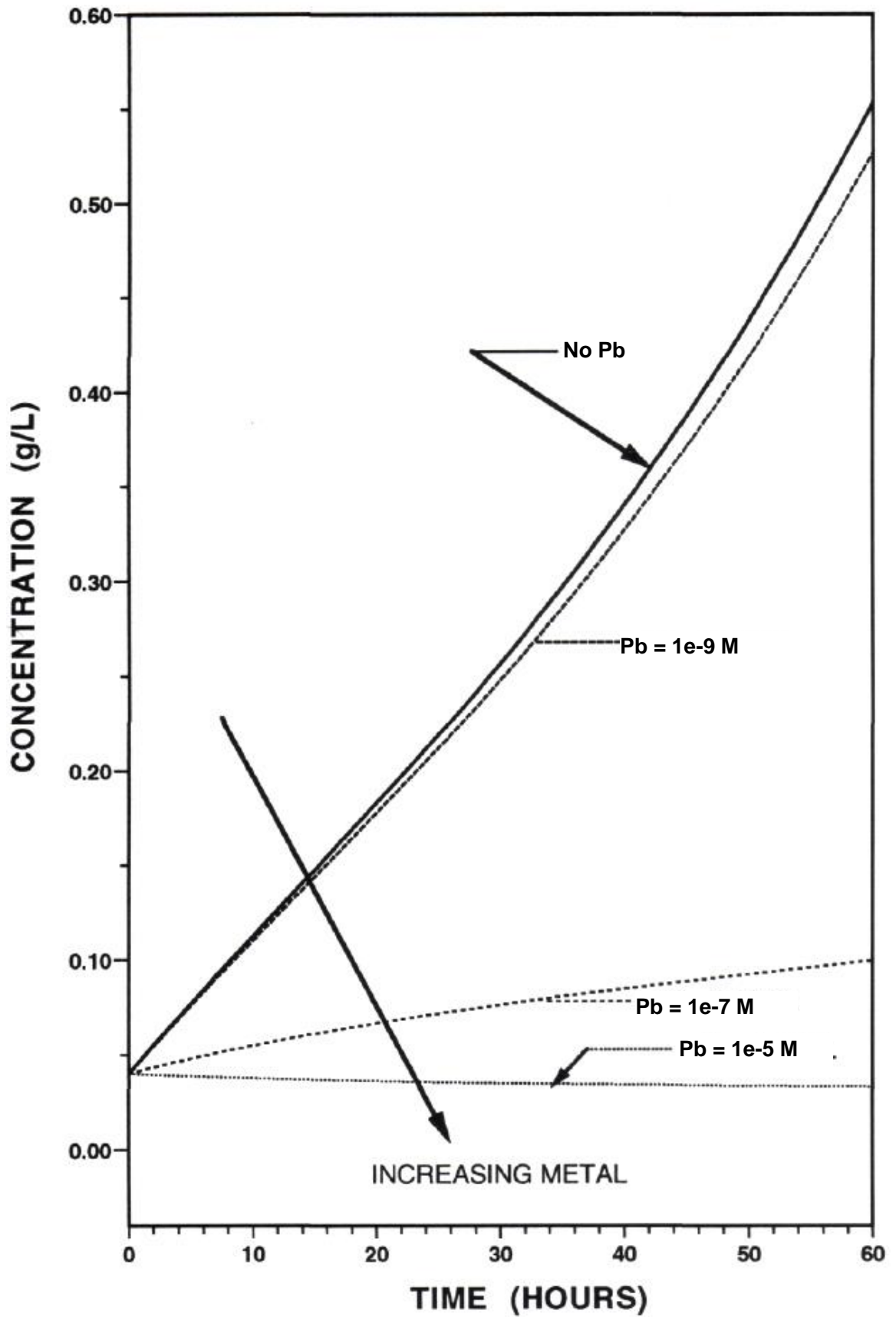


Figure 5.32. Simulated effects of variable concentrations of lead on the Total Suspended Biomass (X) [=suspended active cell mass (A) plus associated attached polymer (P)] production in a Multigen reactor under batch growth conditions at pH 7.

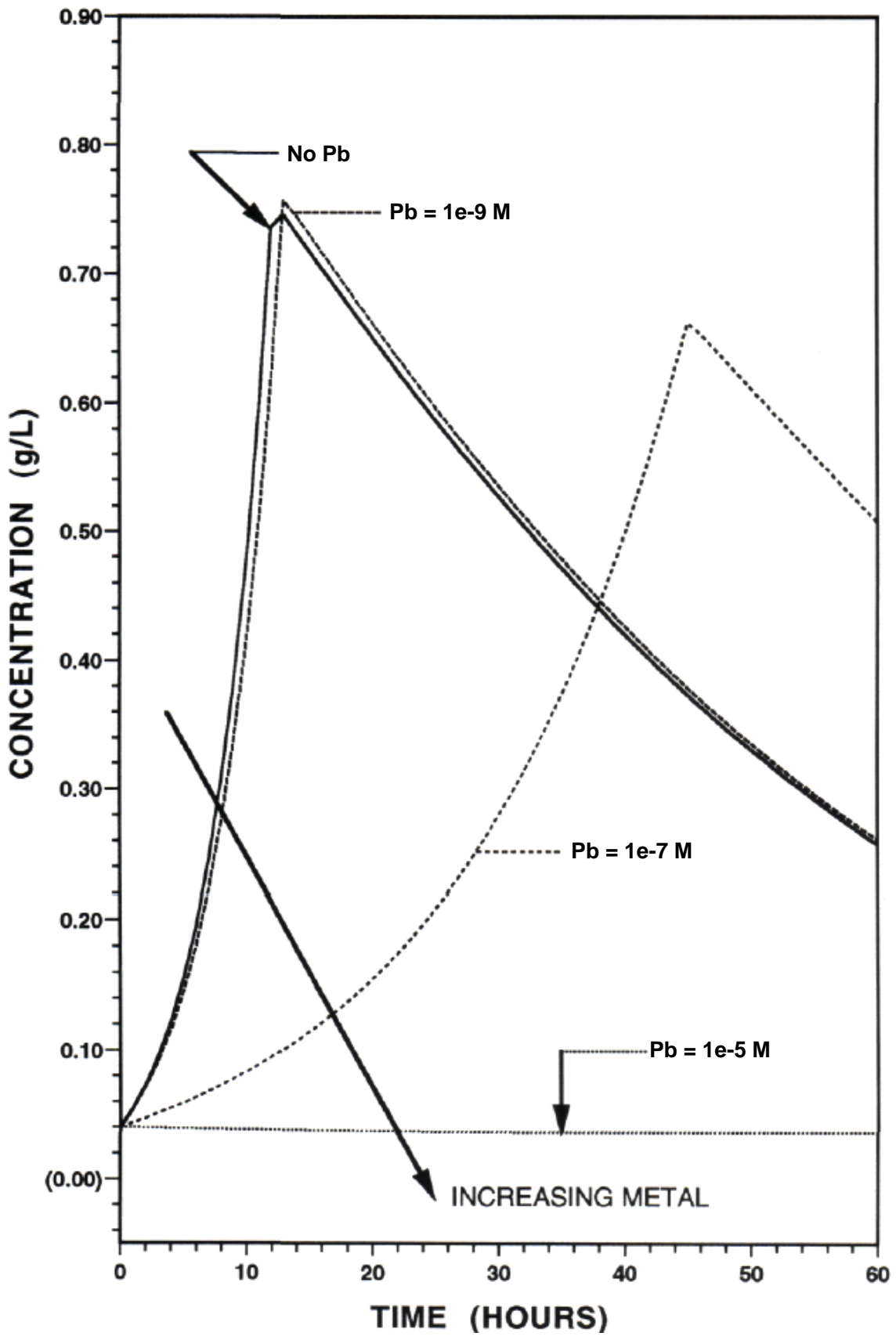


Figure 5.33. Simulated effects of variable concentrations of lead on the Total Suspended Biomass (X) [=suspended active cell mass (A) plus associated attached polymer (P)] production in a Multigen reactor under batch growth conditions at pH 9.

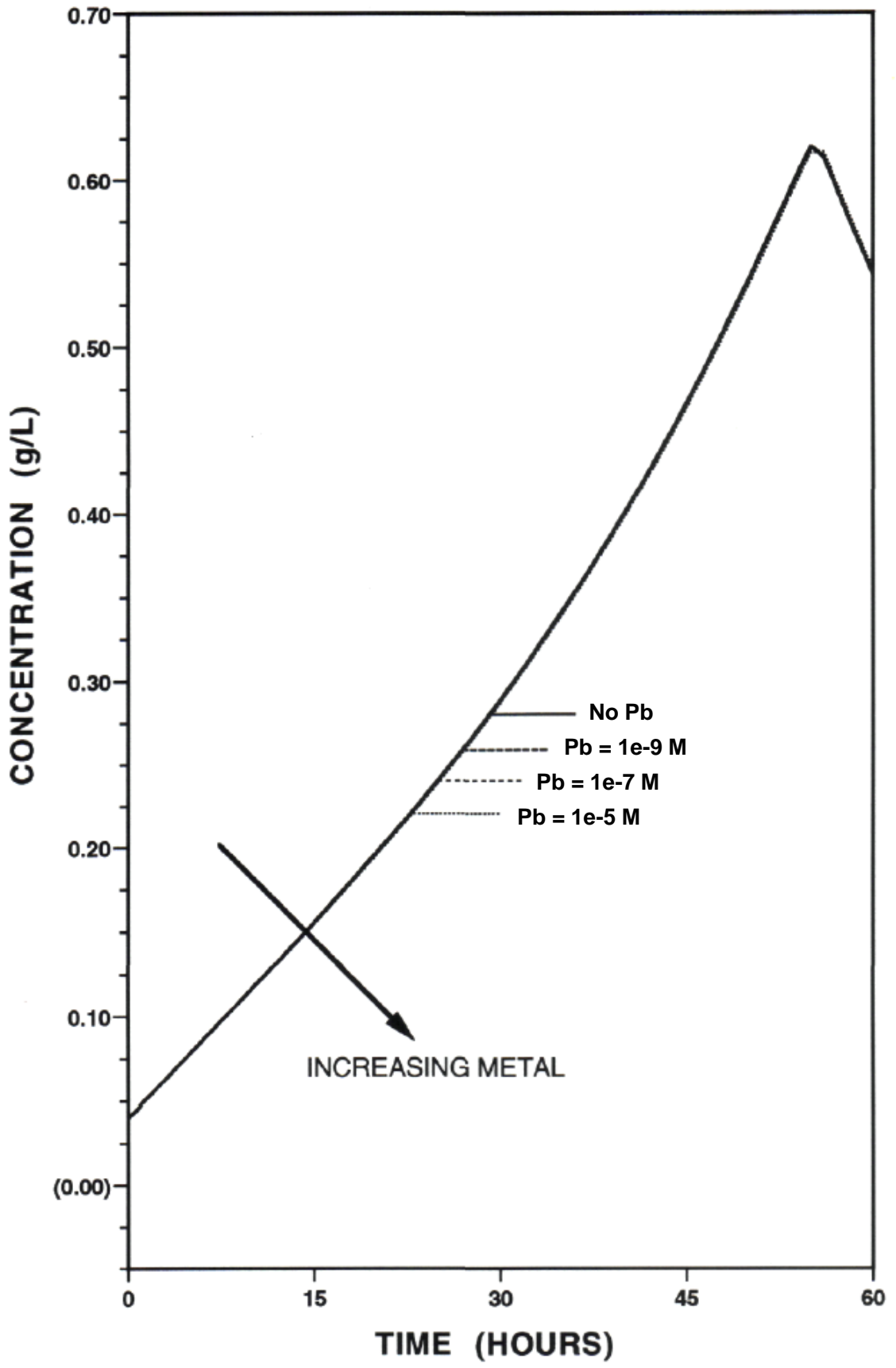


Figure 5.34. Simulated effects of variable concentrations of lead on the Total Attached Biomass (B) [=attached active cell mass(A^B) plus attached associated cell polymer (P^B)] production in a Multigen reactor under batch growth conditions at pH 5.

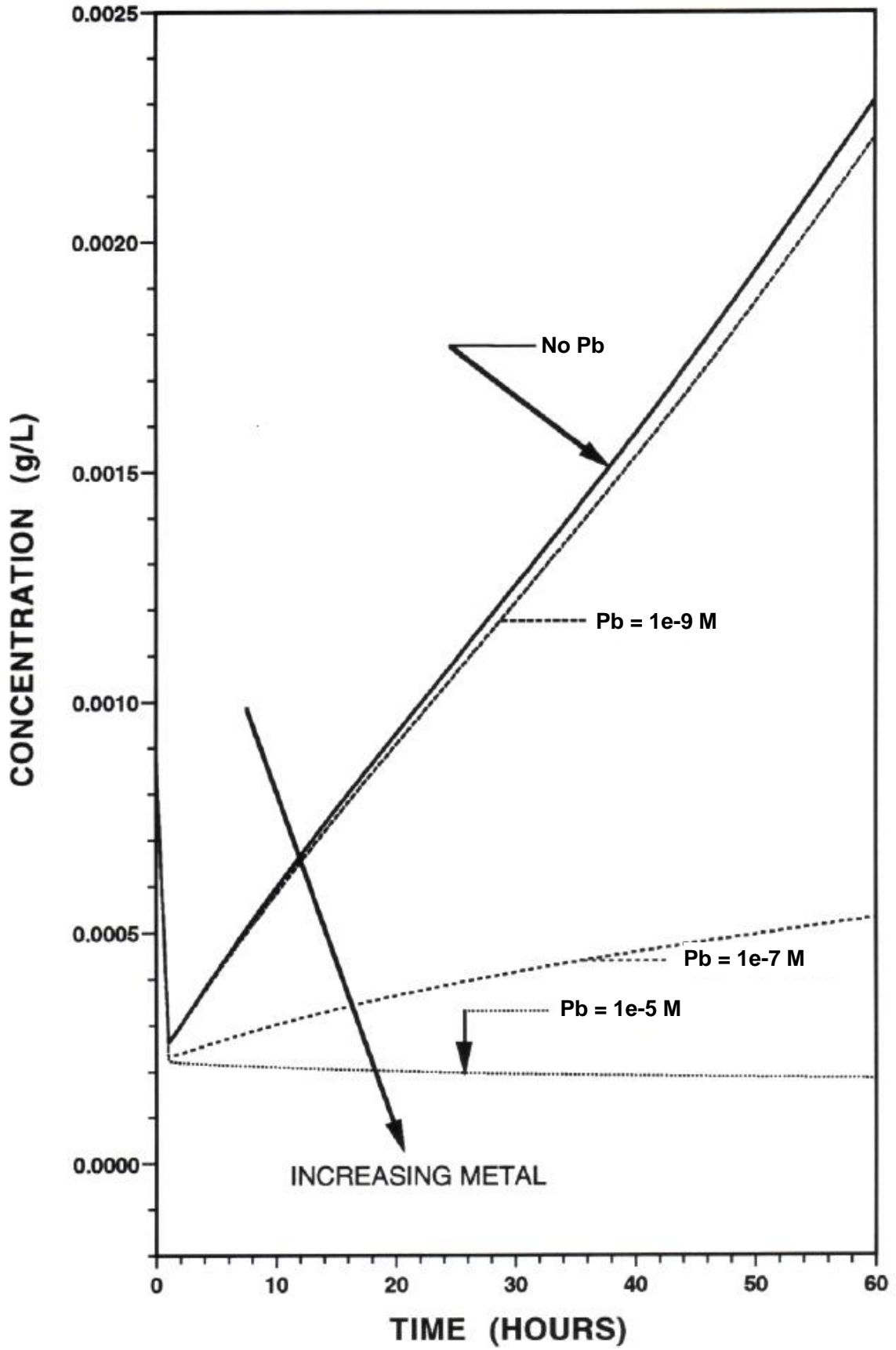


Figure 5.35. Simulated effects of variable concentrations of lead on the Total Attached Biomass (B) [=attached active cell mass (A^B) plus attached associated cell polymer (P^B)] production in a Multigen reactor under batch growth conditions at pH 7.

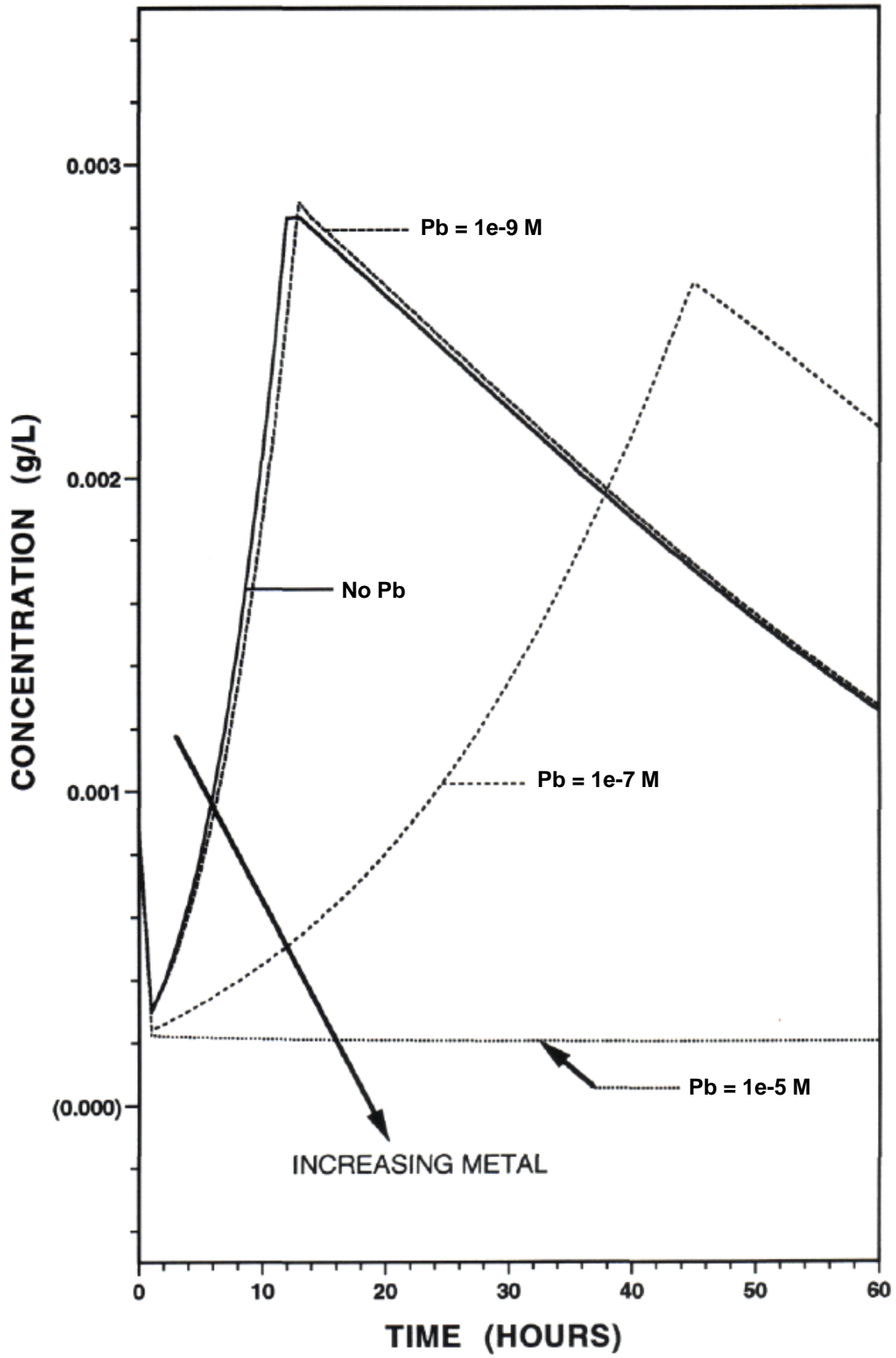
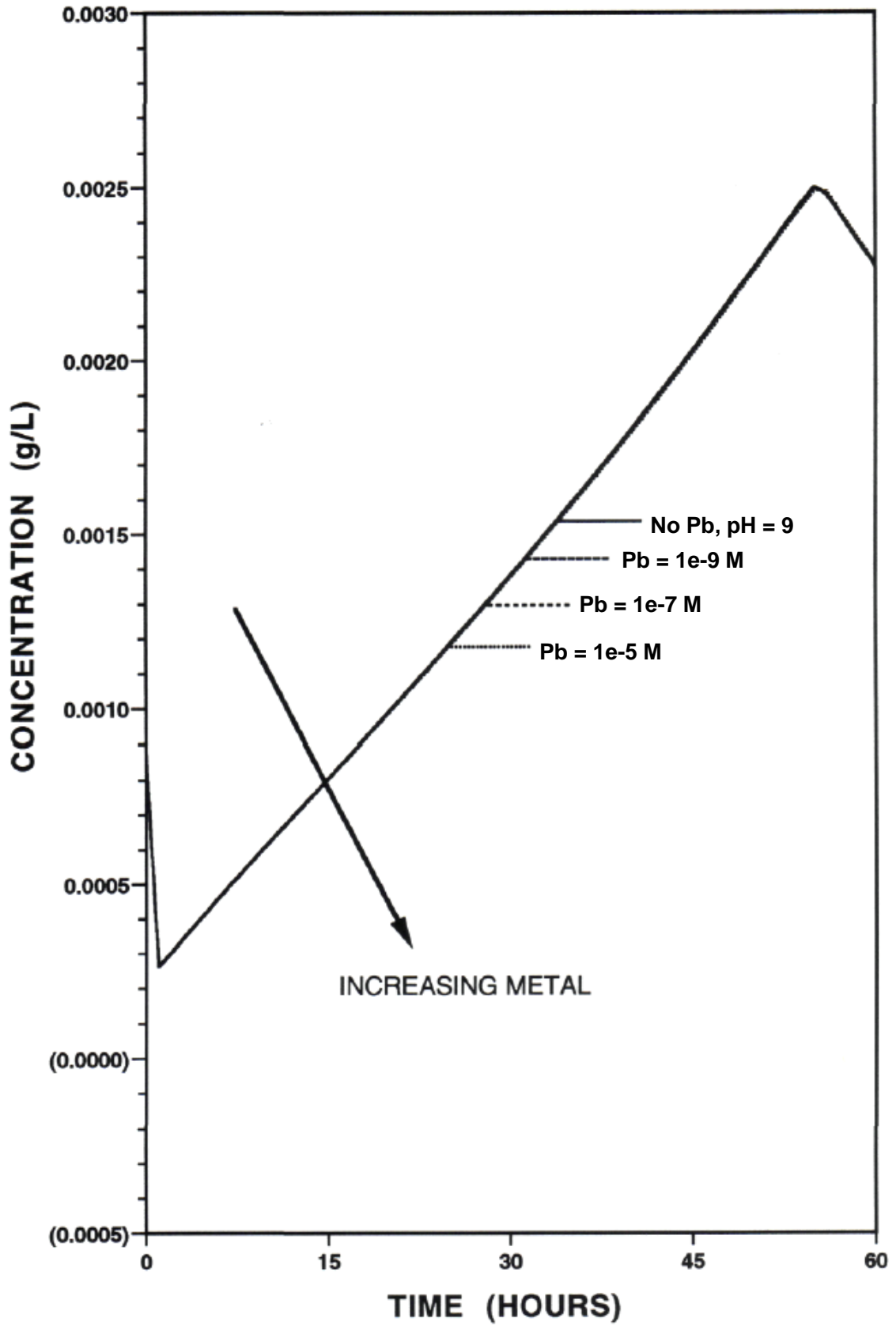


Figure 5.36. Simulated effects of variable concentrations of lead on the Total Attached Biomass (B) [=attached active cell mass (A^B) plus attached associated cell polymer (P^B)] production in a Multigen reactor under batch growth conditions at pH 9.



A total metal concentration of 10^{-9} M under acidic and circumneutral conditions only had a minor effect on the resultant growth curves even though most of the total metal would be in the free ion form. Under extreme alkaline conditions (pH 9) in all cases, all metal concentrations considered had little overall effect on the total suspended or attached biomass and no apparent impact on the shape of the growth curve. This is reasonable as the speciation calculations from MINEQL indicate that much less than 1% of the total metal is in the free ion form at pH 9. This means the metal effects in the bacterial growth equations is negligible and only the variation in pH would change the shape of the simulated curve.

Figures 5.37 to 5.39 show simulated results of free ion lead toxicity (plotted as total applied lead) to total suspended biomass X (comprised of suspended active cell mass (A) plus associated attached polymer (P)) in a bioreactor operated under batch growth conditions at variable pH levels. Figures 5.40 to 5.42 show simulated results for total attached biomass B (comprised of attached cells (A^B) plus attached cell associated polymer (P^B)) as a function of pH. The simulation for X, including the trend at high pH in the presence of the trace metal lead are nearly identical to the results of the batch growth case in the Multigen (Figures 5.30 to 5.32). For the attached biomass B, the model simulations are also similar to that of the Multigen case (Figures 5.34 to 5.36), but the peak concentrations occur at levels several times higher in the bioreactor than in the Multigen.

The model simulations for total suspended biomass X (Figures 5.43 to 5.45) and total attached biomass B (Figures 5.46 to 5.48) in a continuous flow-through low surface area Multigen system indicate the effects of increasing total metal concentration as a

Figure 5.37. Simulated effects of variable concentrations of lead on the Total Suspended Biomass (X) [=suspended active cell mass (A) plus associated attached polymer (P)] production in a Bioreactor under batch growth conditions at pH 5 and $Re = 300$

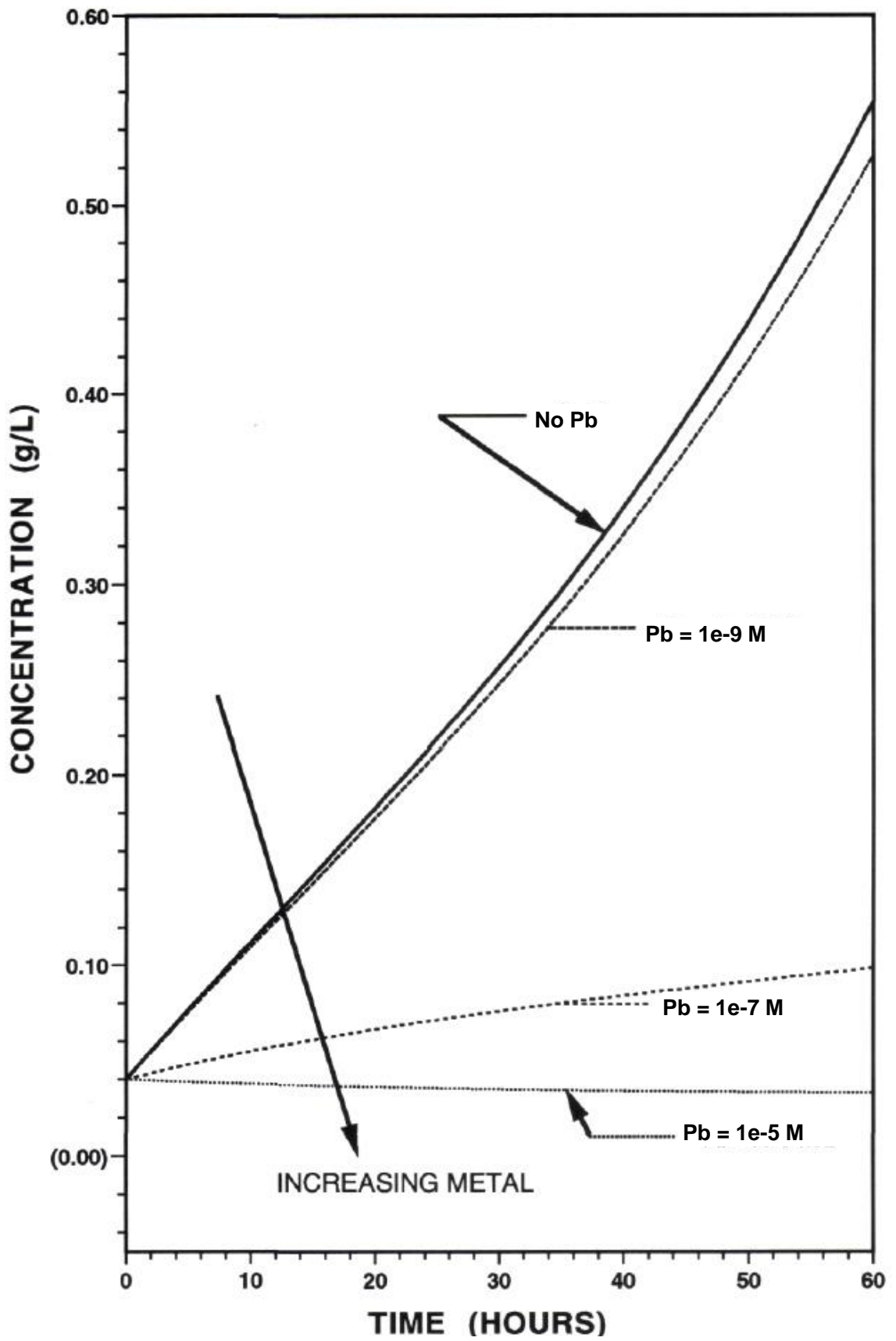


Figure 5.38. Simulated effects of variable concentrations of lead on the Total Suspended Biomass (X) [=suspended active cell mass (A) plus associated attached polymer (P)] production in a Bioreactor under batch growth conditions at pH 7 and $Re = 300$.

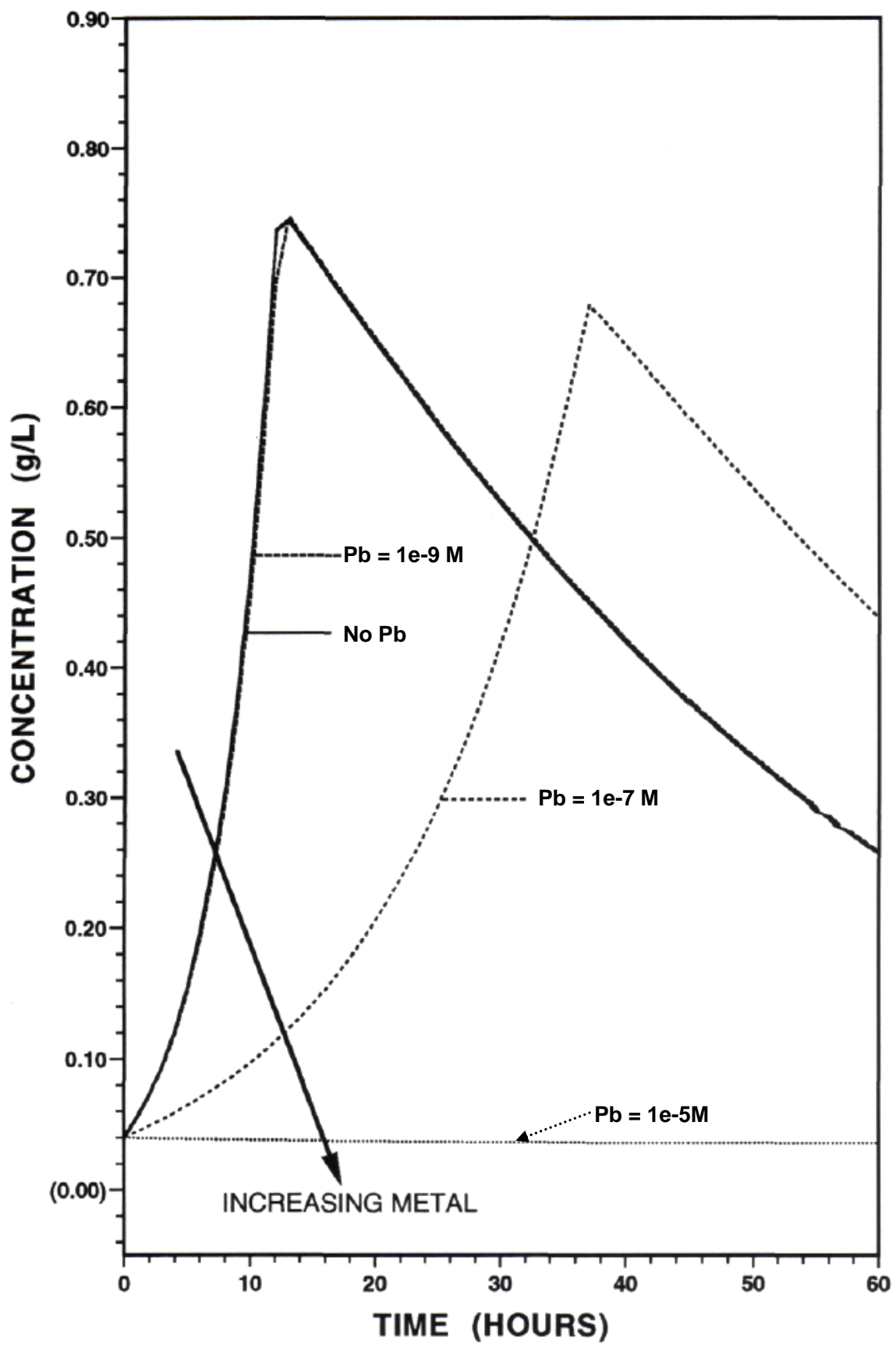


Figure 5.39. Simulated effects of variable concentrations of lead on the Total Suspended Biomass (X) [=suspended active cell mass (A) plus associated attached polymer (P)] production in a Bioreactor under batch growth conditions at pH 9 and $Re = 300$.

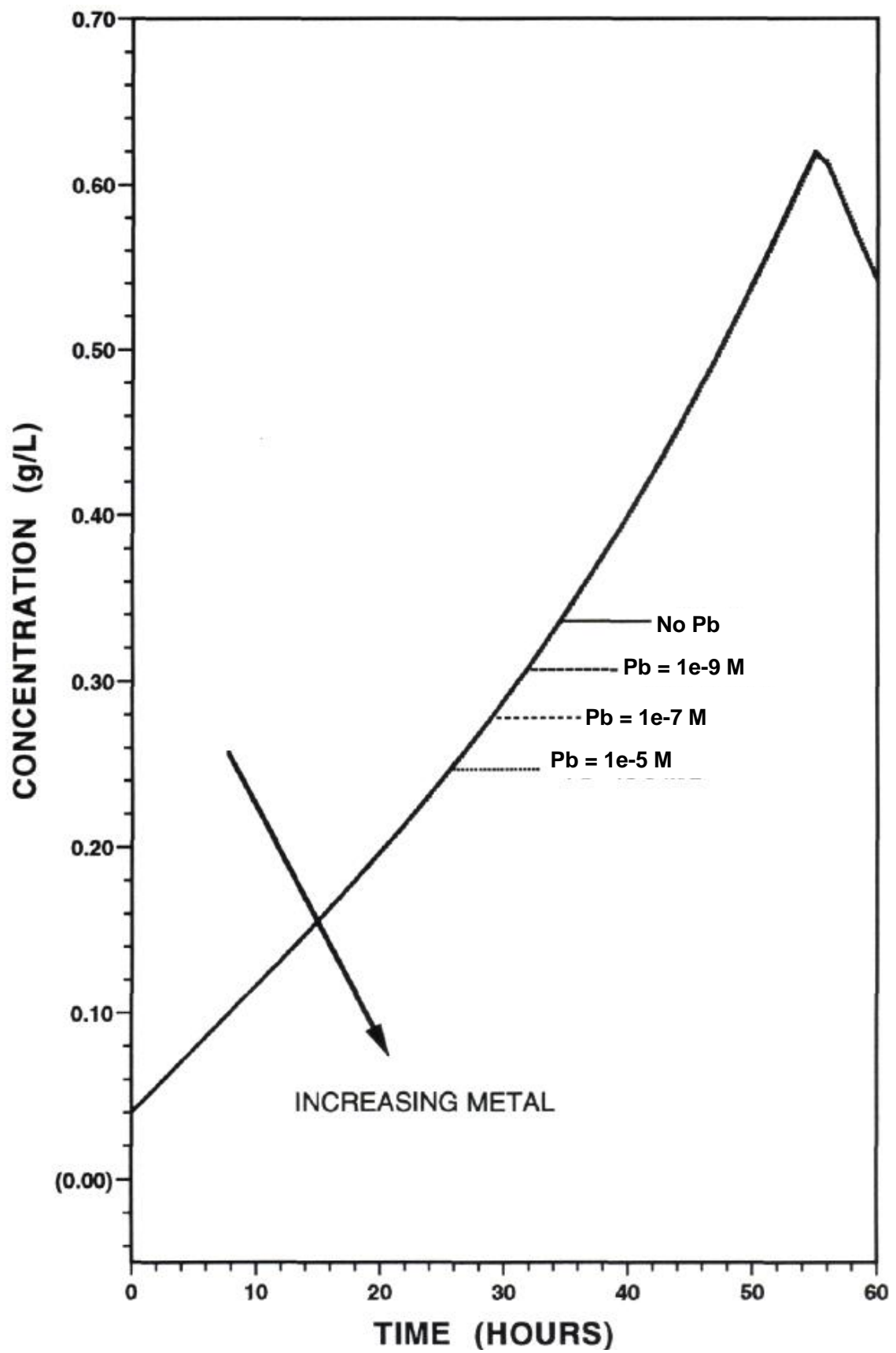


Figure 5.40. Simulated effects of variable concentrations of lead on the Total Attached Biomass (B) [=attached active cell mass (A^B) plus attached associated cell polymer (P^B)] production in a Bioreactor under batch growth conditions at pH 5 and $Re = 300$.

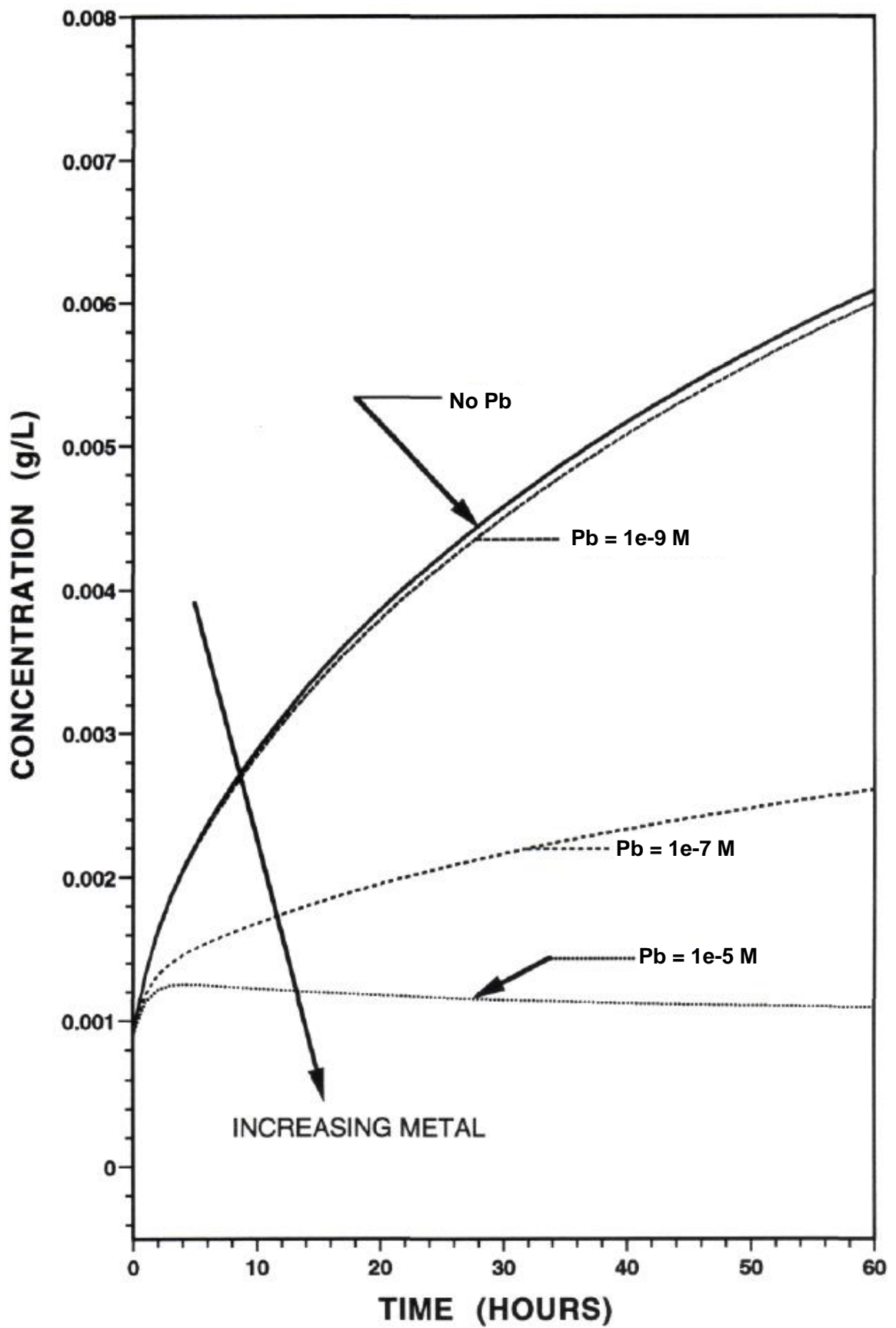


Figure 5.41. Simulated effects of variable concentrations of lead on the Total Attached Biomass (B) [=attached active cell mass (A^B) plus attached associated cell polymer (P^B)] production in a Bioreactor under batch growth conditions at pH 7 and $Re = 300$.

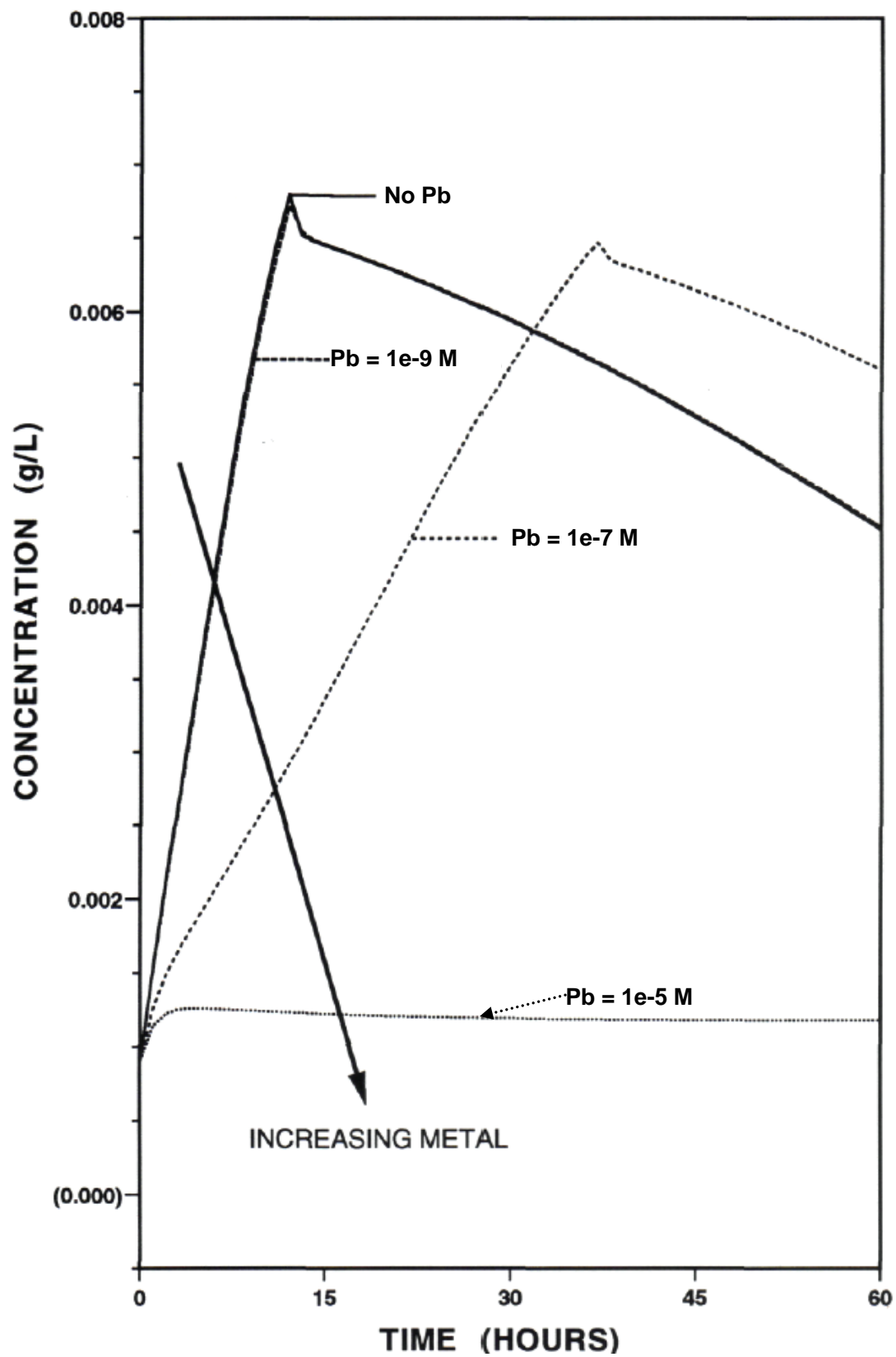


Figure 5.42. Simulated effects of variable concentrations of lead on the Total Attached Biomass (B) [=attached active cell mass (A^B) plus attached associated cell polymer (P^B)] production in a Bioreactor under batch growth conditions at pH 9 and Re - 300.

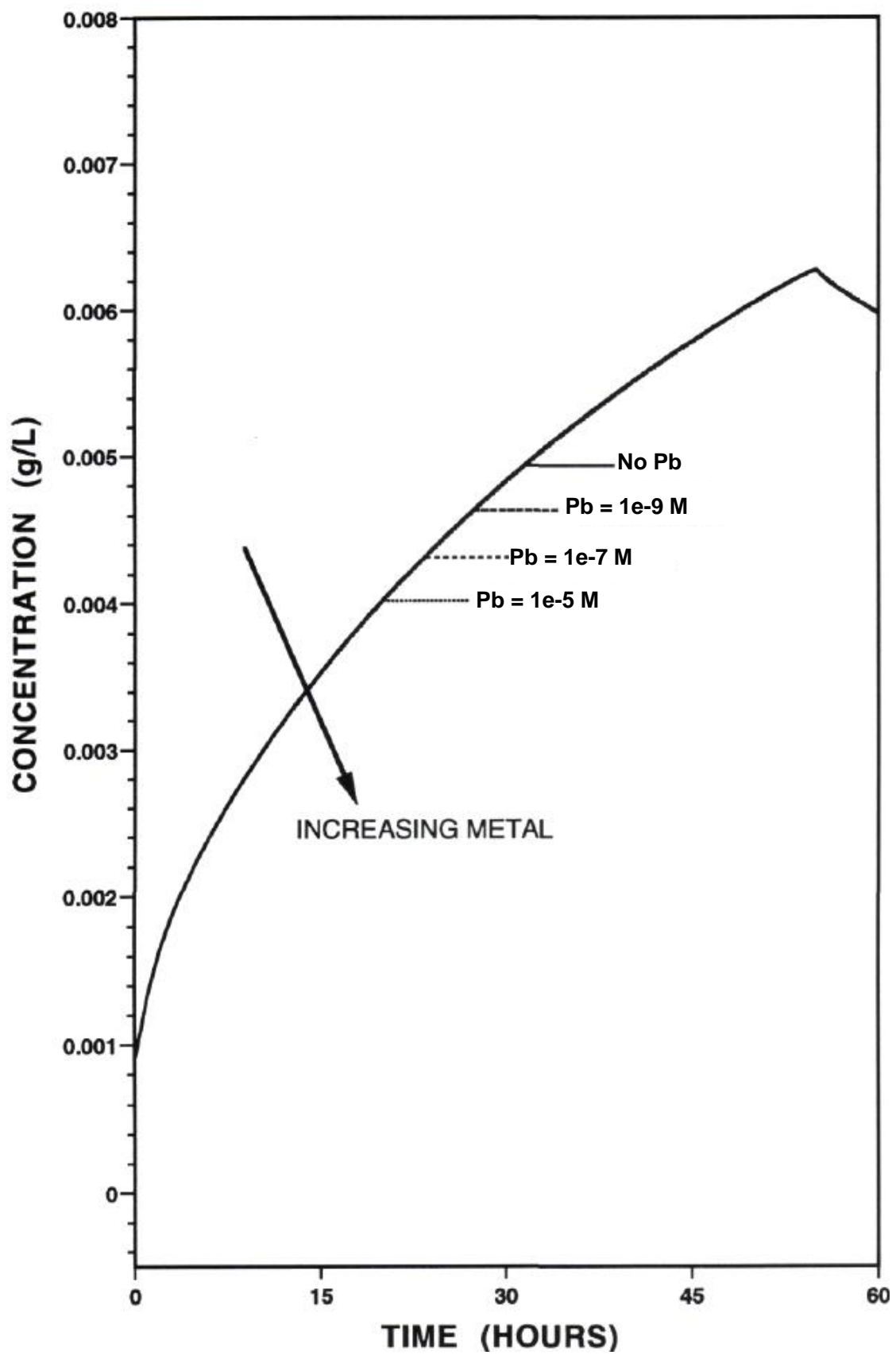


Figure 5.43. Simulated effects of variable concentrations of lead on the Total Suspended Biomass (X) [=suspended active cell mass (A) plus associated attached polymer (P)] production in a steady state continuous flow-through Multigen reactor at pH 5.

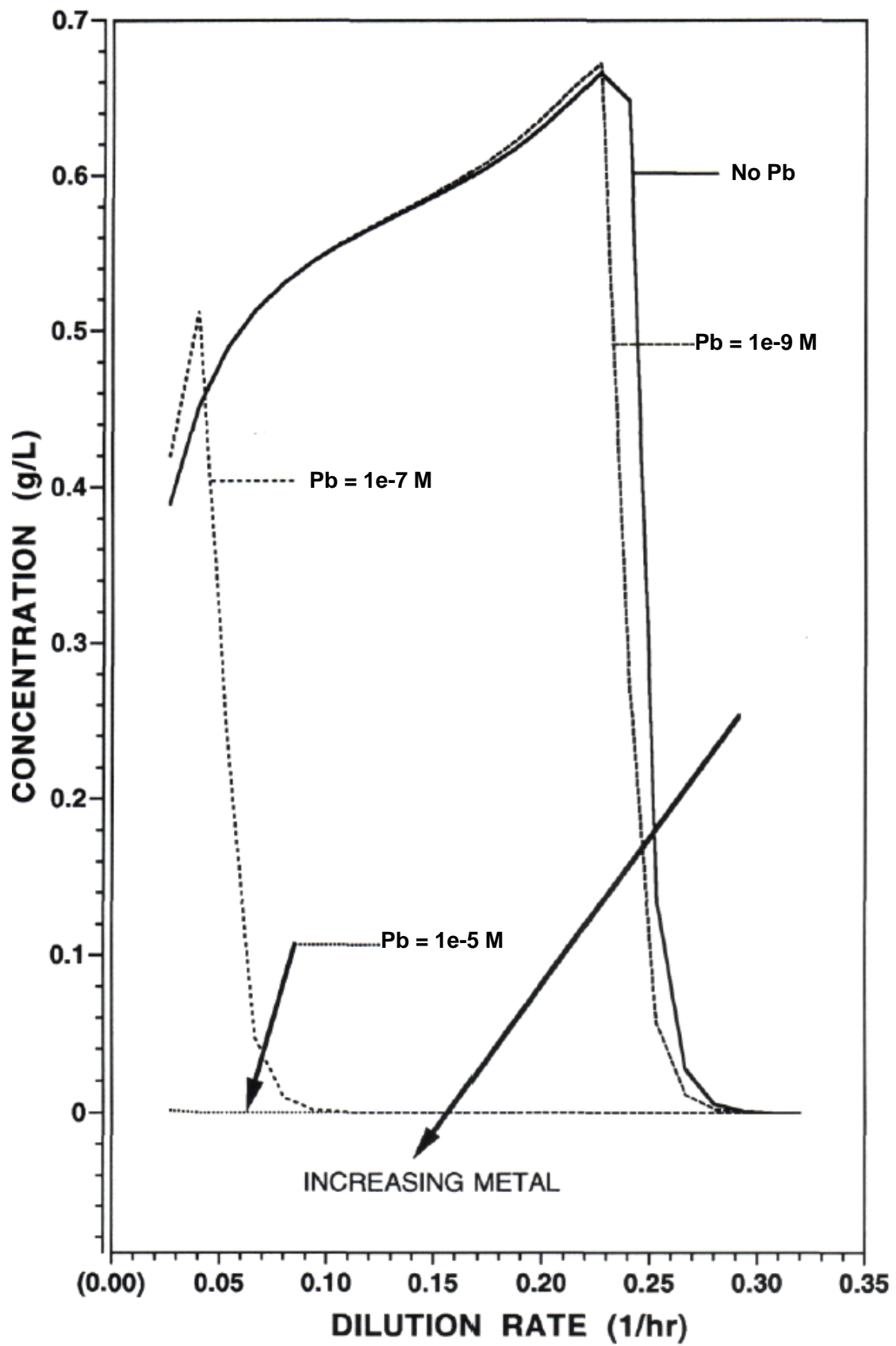


Figure 5.44. Simulated effects of variable concentrations of lead on the Total Suspended Biomass (X) [=suspended active cell mass (A) plus associated attached polymer (P)] production in a steady state continuous flow-through Multigen reactor at pH 7.

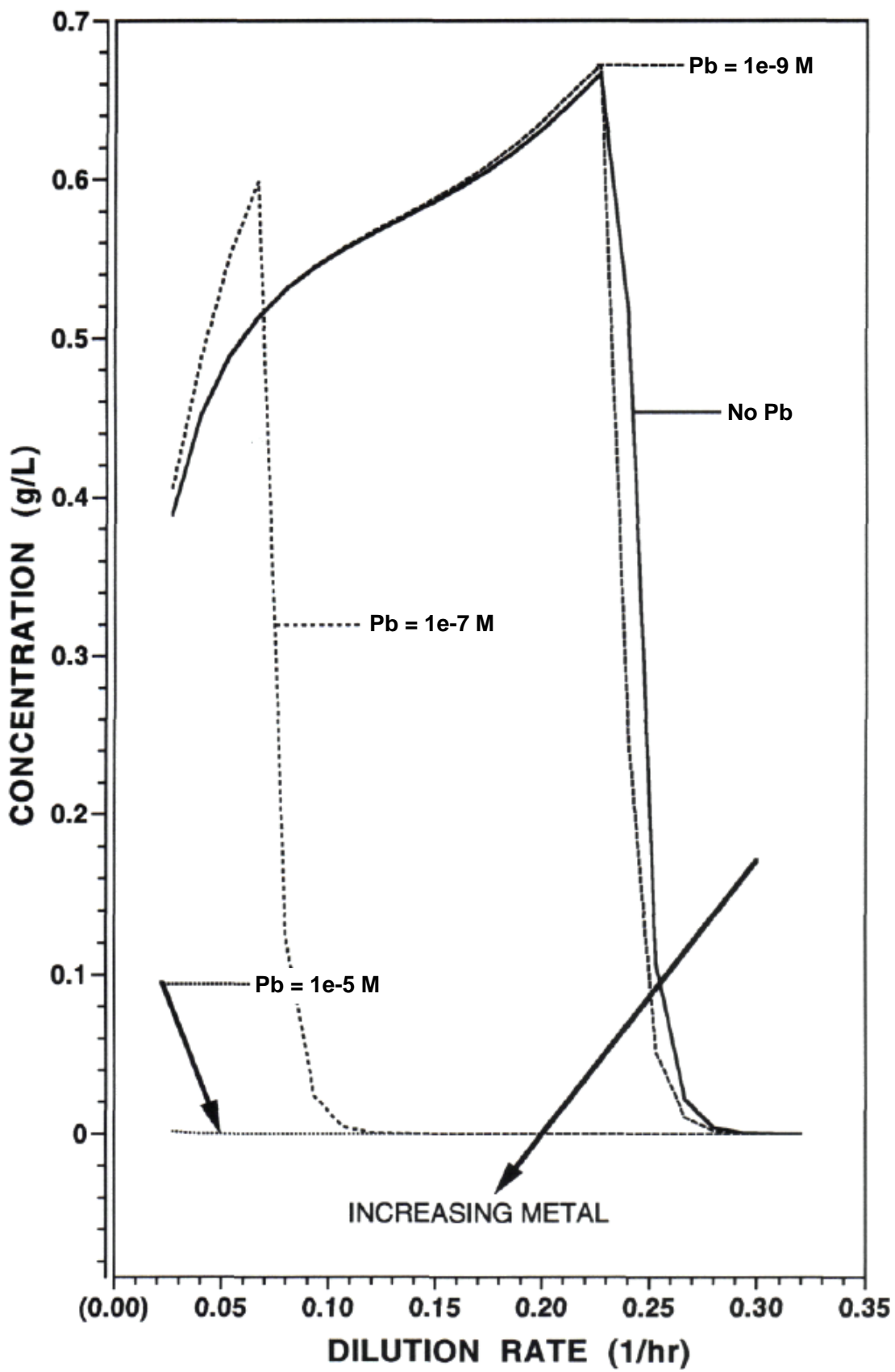


Figure 5.45. Simulated effects of variable concentrations of lead on the Total Suspended Biomass (X) [=suspended active cell mass (A) plus associated attached polymer (P)] production in a steady state continuous flow-through Multigen reactor at pH 9.

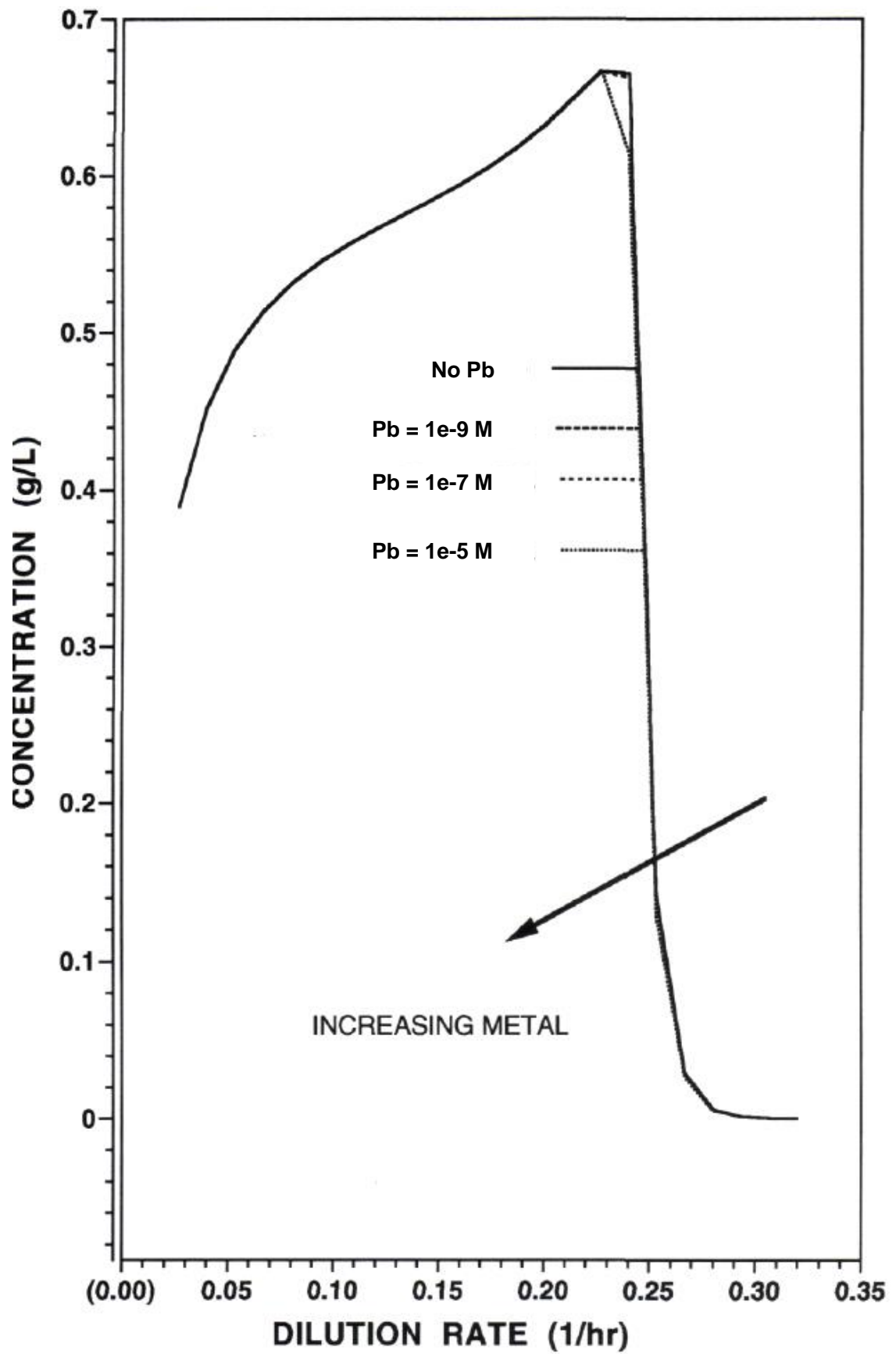


Figure 5.46. Simulated effects of variable concentrations of lead on the Total Attached Biomass (B) [=attached active cell mass (A^B) plus attached associated cell polymer (P^B)] production in a steady state continuous flow-through Multigen reactor at pH 5.

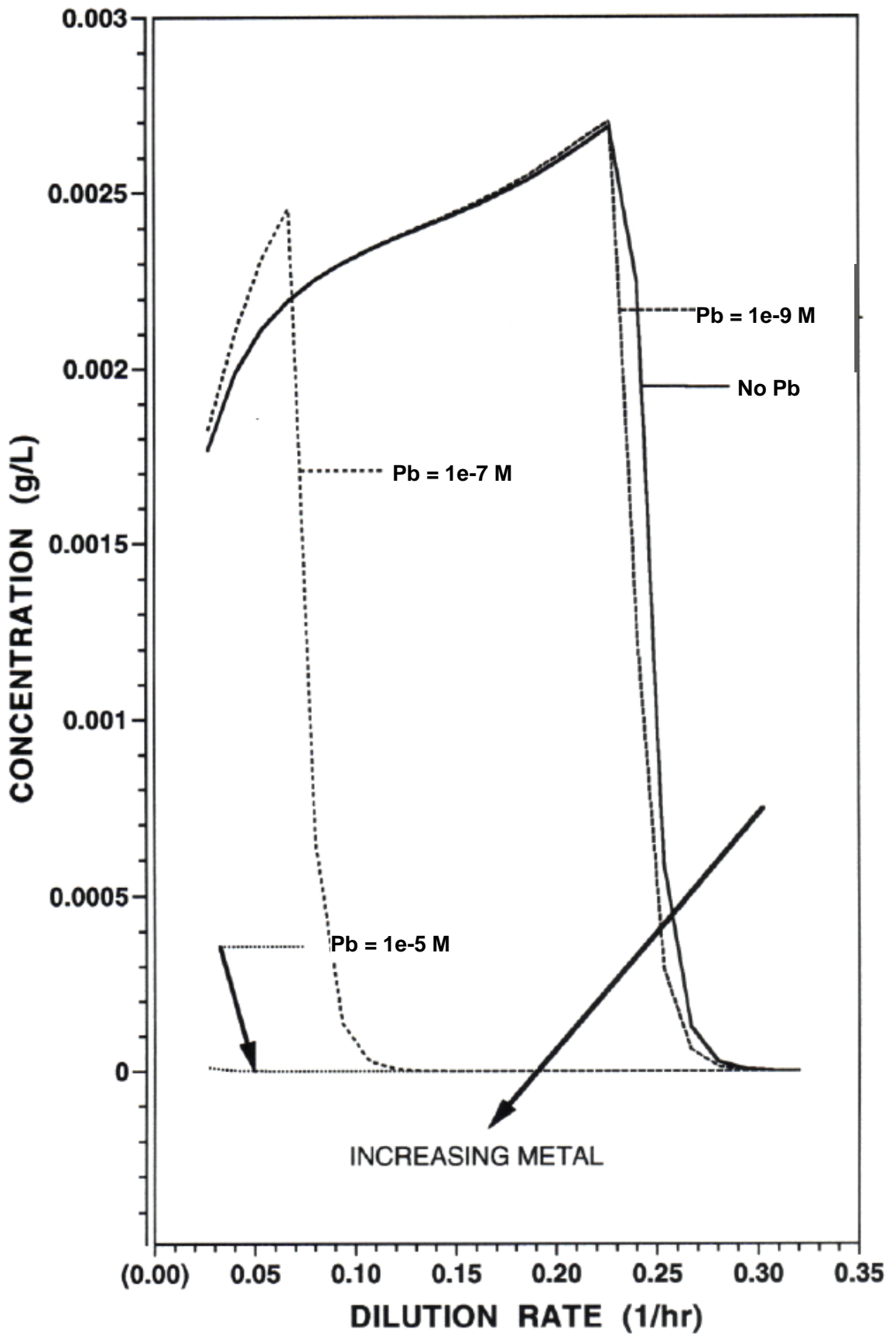


Figure 5.47. Simulated effects of variable concentrations of lead on the Total Attached Biomass (B) [=attached active cell mass (A^B) plus attached associated cell polymer (P^B)] production in a steady state continuous flow-through Multigen reactor at pH 7.

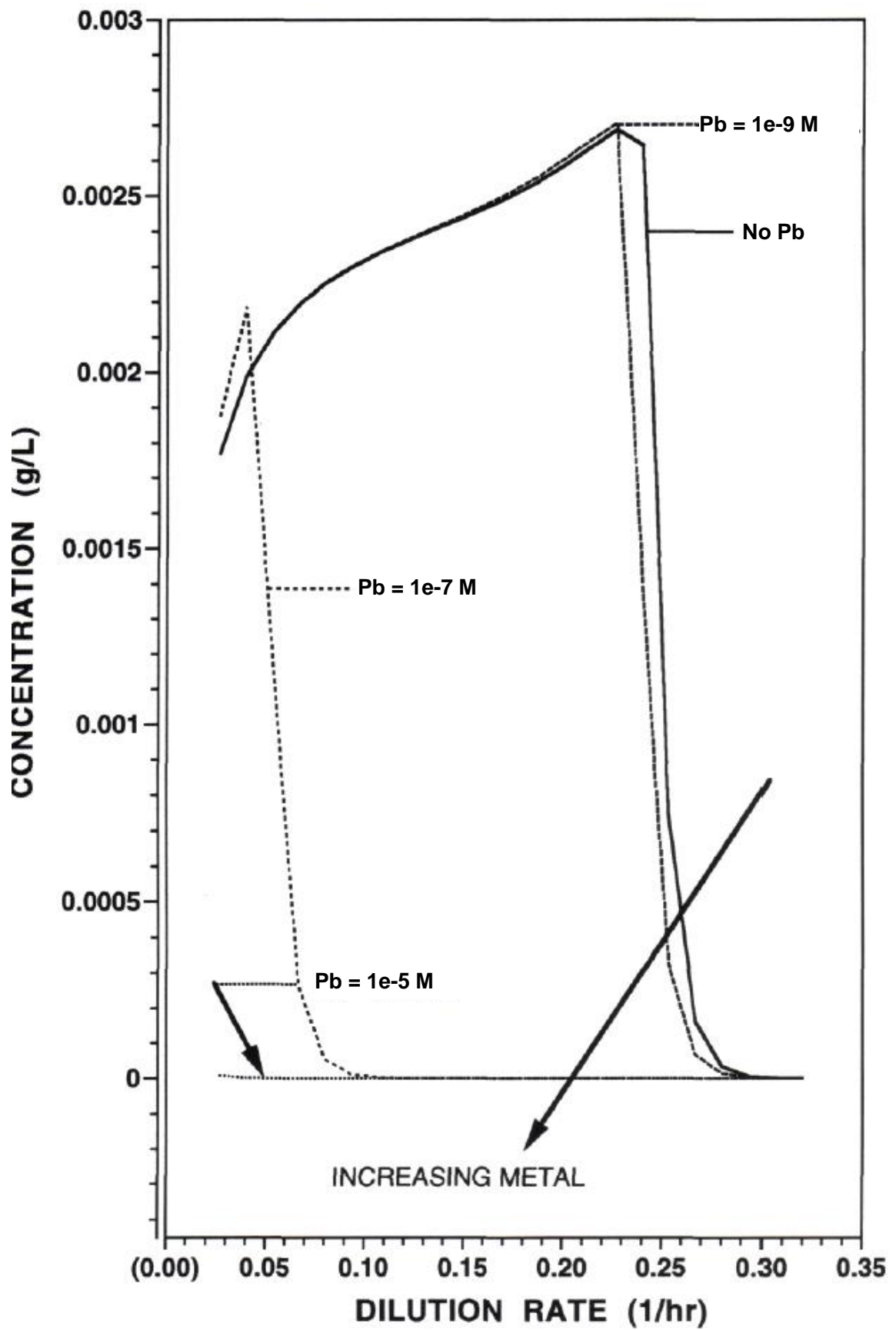
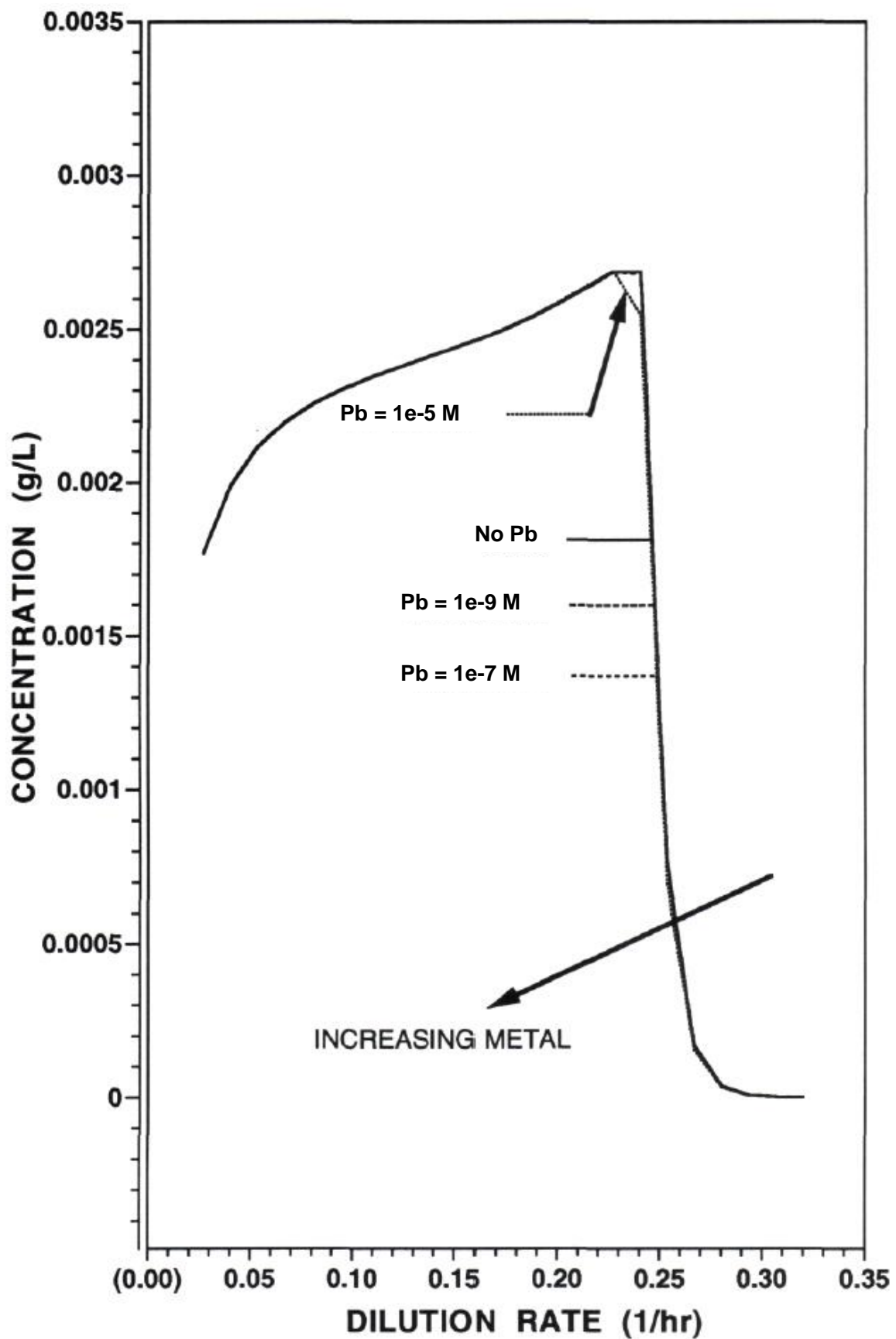


Figure 5.48. Simulated effects of variable concentrations of lead on the Total Attached Biomass (B) [=attached active cell mass (A^B) plus attached associated cell polymer (P^B)] production in a steady state continuous flow-through Multigen reactor at pH 5.



function of variable pH. Total metal concentrations of 10^{-5} and 10^{-7} M at both pH 5 and 7 had washout occurring at a dilution rate of about 0.11 hr^{-1} compared to the 0.27 hr^{-1} for the case of no lead present. The presence of lead at a level of 10^{-9} M at pH 5 and 7 had a washout dilution rate only slightly reduced from that of the case for no metal being present. For both cases of X and B at pH 9 in the presence of the metal, the metal concentration did not affect the washout. This result was expected since the speciation of lead is much less than 1% in the free ion form at a pH of 9.

The model simulations for total suspended biomass X (Figures 5.49 to 5.51) and total attached biomass B (Figures 5.52 to 5.54) in a continuous flow-through bioreactor system indicate the effects of increasing metal concentration as a function of variable pH. For both cases of X and B at pH 9 in the presence of the metal, the metal concentration did not affect the dilution rate at which washout occurred. All curves were identical. Total metal at a level of 10^{-9} M has a negligible effect on washout at pH 5 and 7, as it did in the Multigen case. The dilution rate for washout decreased by only 0.01 to 0.02 hr^{-1} , again due to the low free ion lead form in solution. A total metal concentration of 10^{-7} M at pH 5 had washout occurring at a dilution rate of about 0.09 hr^{-1} compared to the 0.27 hr^{-1} for the case of no lead present. For total metal concentration of 10^{-7} M at pH 7, washout occurred at a dilution rate of about 0.11 hr^{-1} , which was nearly the same as for the Multigen case. A total metal concentration of 10^{-5} M at pH 5 and 7 had washout occurring at all dilution rates. For the total attached biomass B (Figures 5.52 to 5.54), the same trends and washout dilution rate values occur as determined in Figures 5.49 to 5.51, but the maximum steady state concentrations are about 3 times the values found in the Multigen case.

Figure 5.49. Simulated effects of variable concentrations of lead on the Total Suspended Biomass (X) [=suspended active cell mass (A) plus associated attached polymer (P)] production in a steady state continuous flow-through Bioreactor at pH 5 and $Re = 300$.

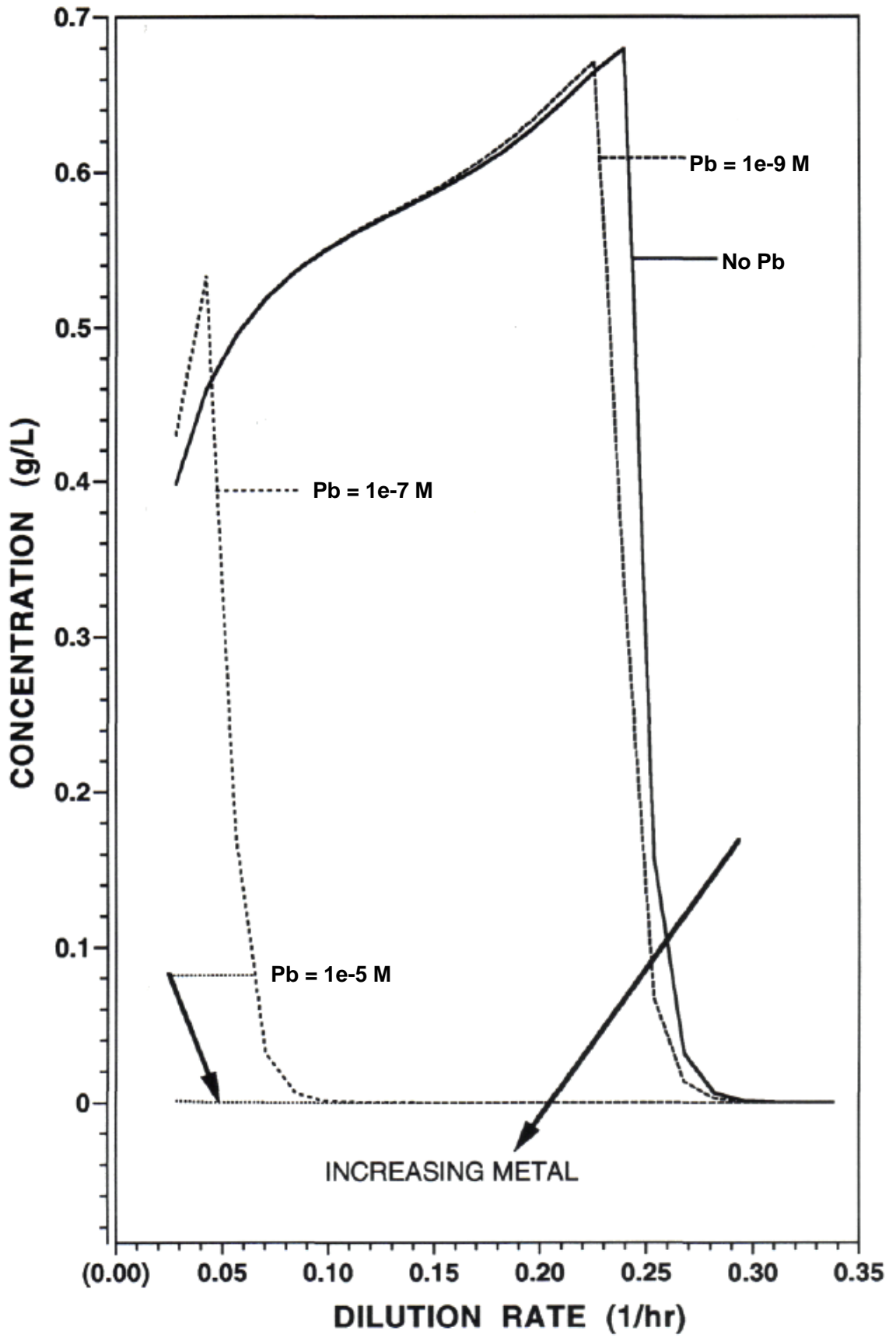


Figure 5.50. Simulated effects of variable concentrations of lead on the Total Suspended Biomass (X) [=suspended active cell mass (A) plus associated attached polymer (P)] production in a steady state continuous flow-through Bioreactor at pH 7 and $Re = 300$.

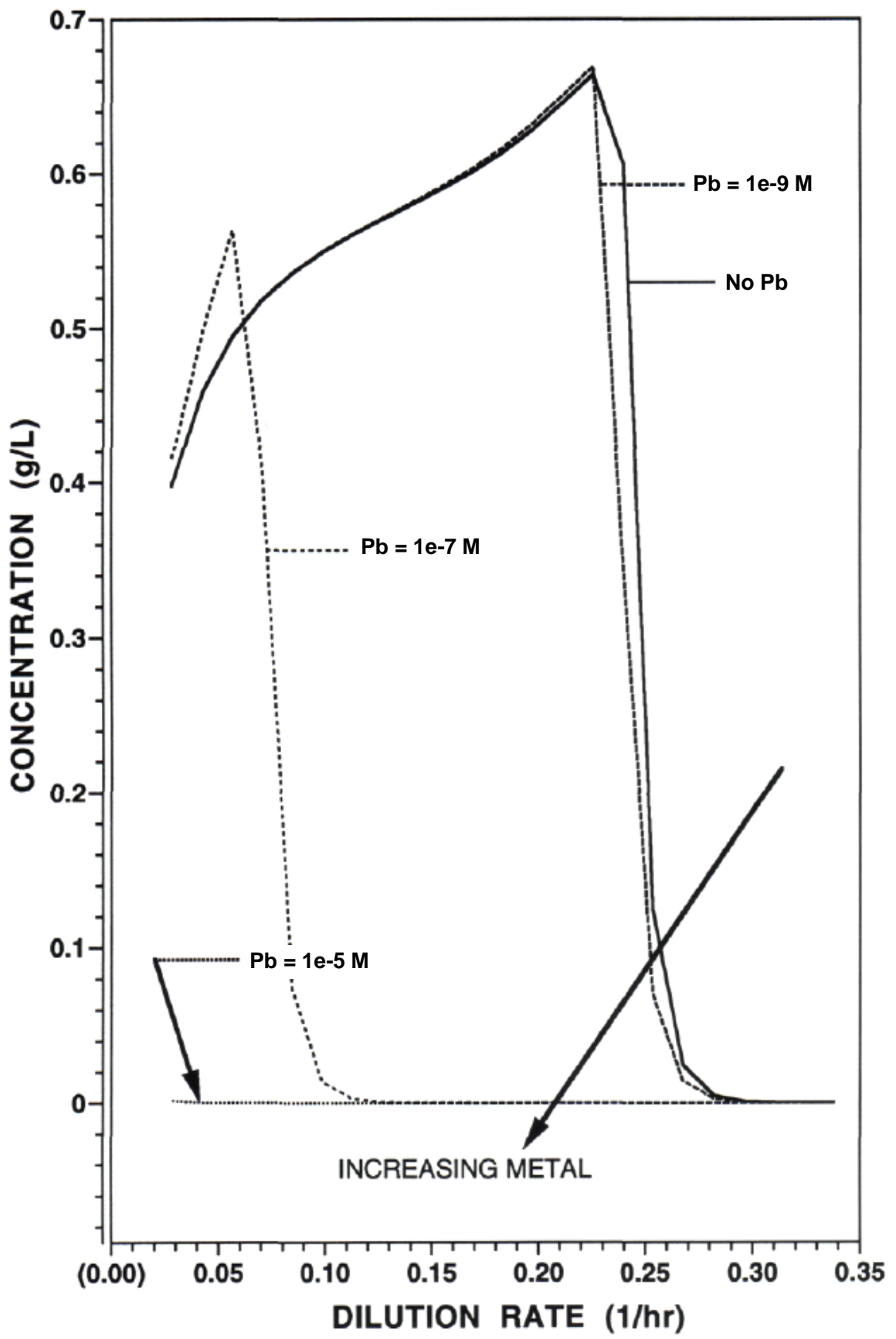


Figure 5.51. Simulated effects of variable concentrations of lead on the Total Suspended Biomass (X) [=suspended active cell mass (A) plus associated attached polymer (P)] production in a steady state continuous flow-through Bioreactor at pH 9 and $Re = 300$.

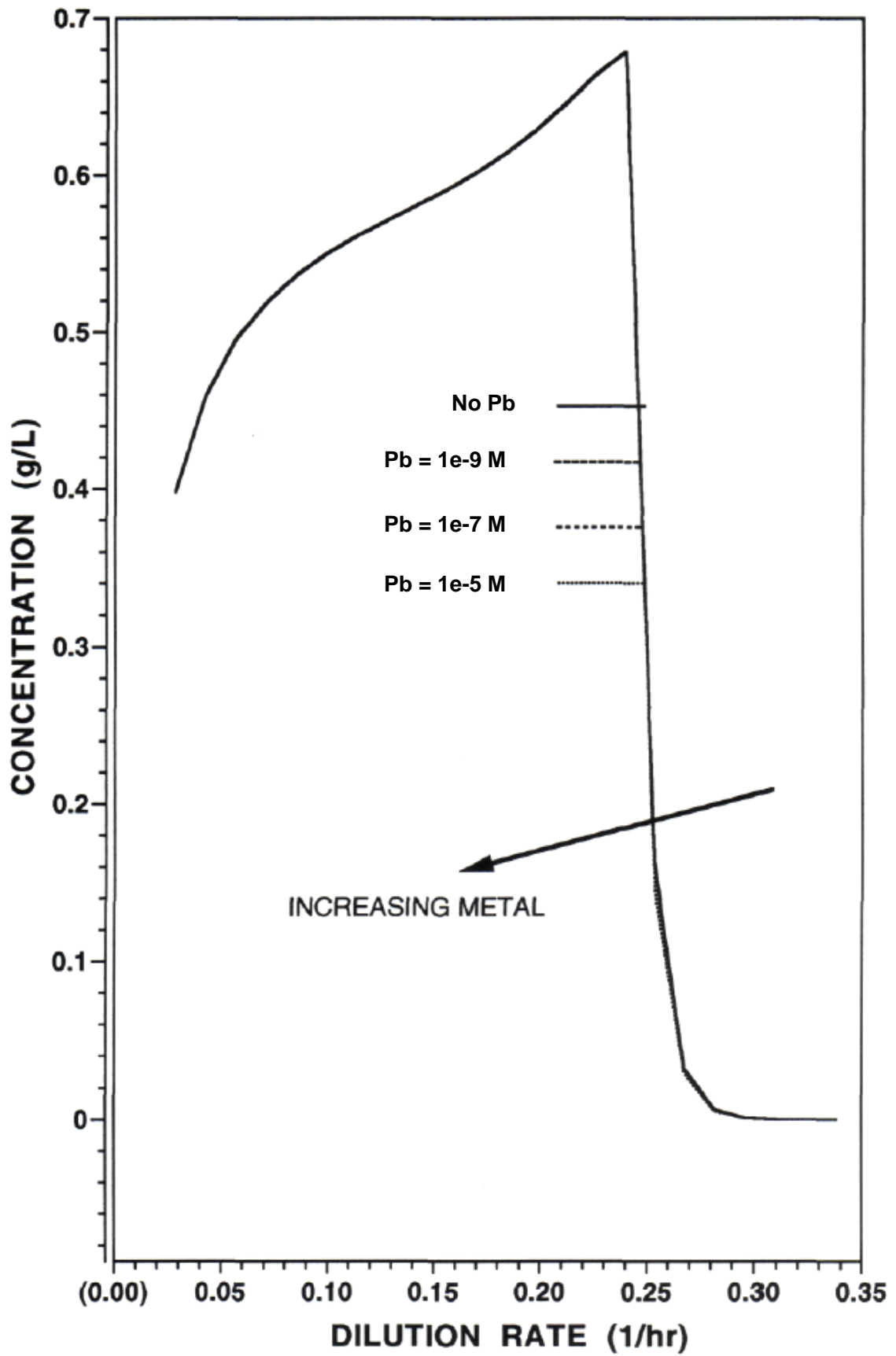


Figure 5.52. Simulated effects of variable concentrations of lead on the Total Attached Biomass (B) [=attached active cell mass (A^B) plus attached associated cell polymer (P^B)] production in a steady state continuous flow-through Bioreactor at pH 5 and $Re = 300$.

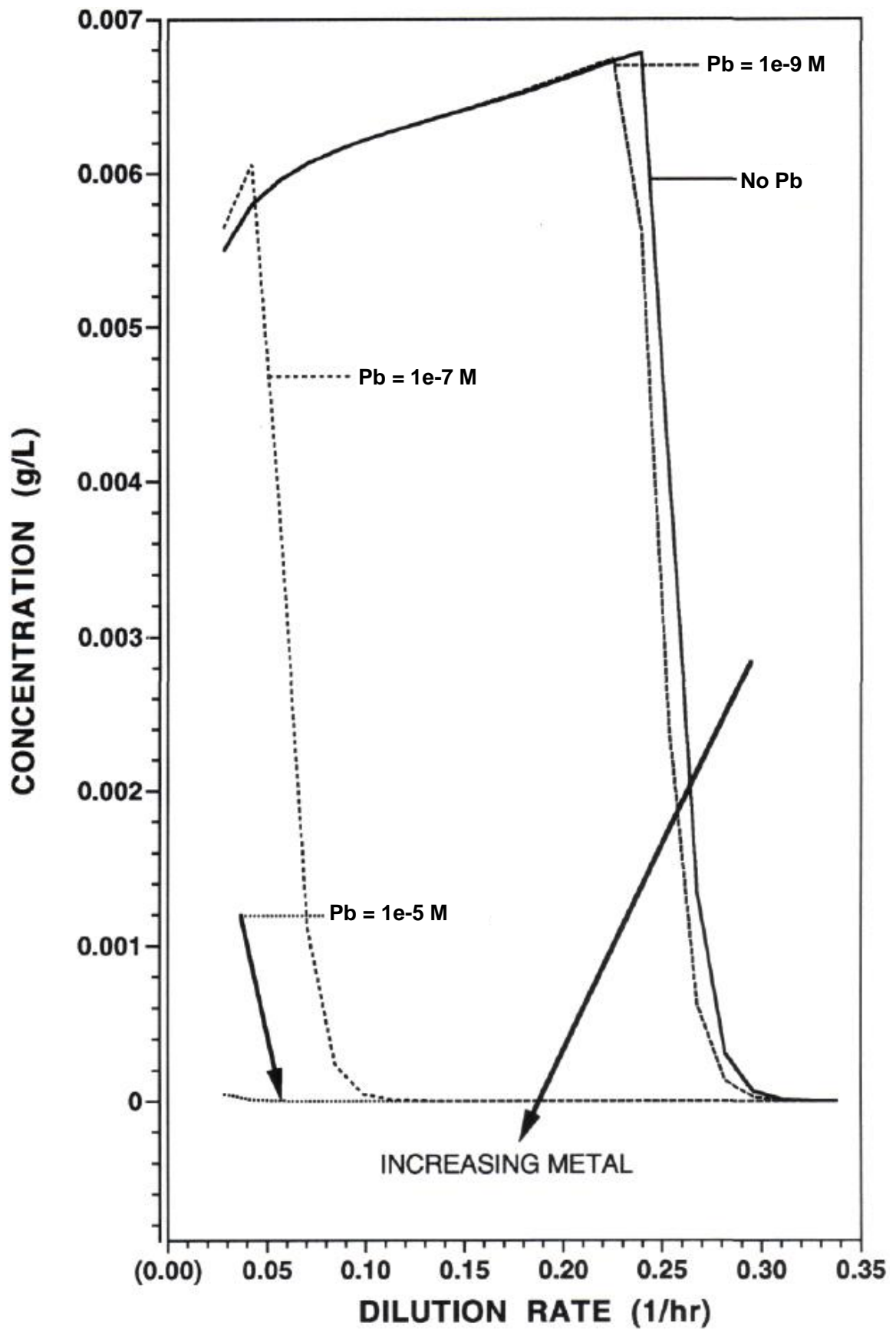


Figure 5.53. Simulated effects of variable concentrations of lead on the Total Attached Biomass (B) [=attached active cell mass (A^B) plus attached associated cell polymer (P^B)] production in a steady state continuous flow-through Bioreactor at pH 7 and $Re = 300$.

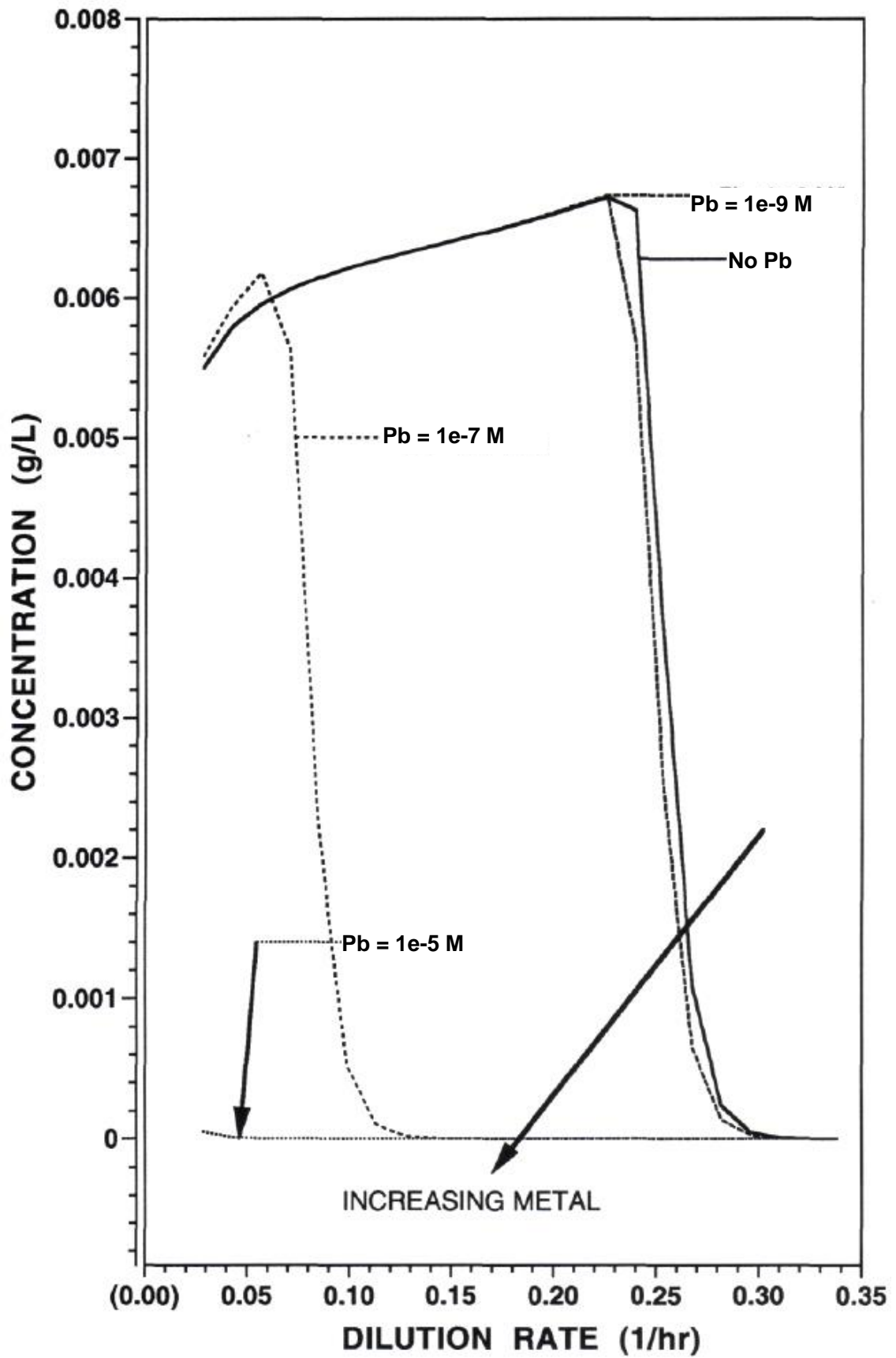
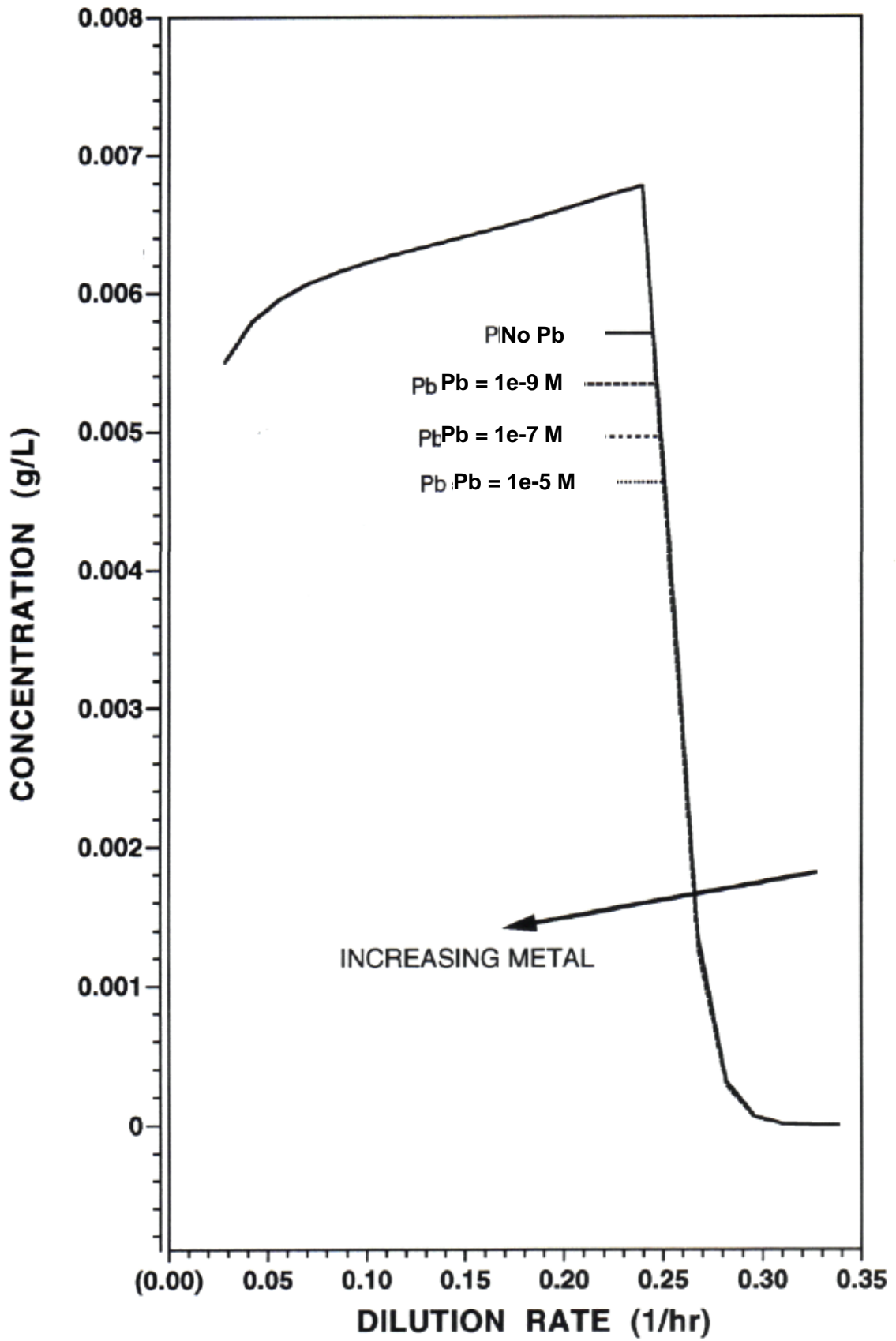


Figure 5.54. Simulated effects of variable concentrations of lead on the Total Attached Biomass (B) [=attached active cell mass (A^B) plus attached associated cell polymer (P^B)] production in a steady state continuous flow-through Bioreactor at pH 9 and $Re = 300$.



To test the transient responses of the model to fluctuations in lead concentrations, step increases in lead levels were studied in the model simulations. A typical transient response is shown in the series of plots in Figures 5.55 to 5.57. Each figure shows the concentration of total suspended active biomass (A), limiting nutrient (C^*) and the dissolved polymer (P^*) system components. The simulation had the cells grown batch-wise to the point of stationary growth, and then switched to continuous mode after reaching stationary phase, all in the absence of lead. When steady-state was achieved (at about 132 hours) total lead was added to a concentration level of 10^{-7} M. The model system was then run as a continuous flow-through reactor until a new equilibrium was reached. The simulation was repeated for three dilution rates (shown in the successive figures) at pH levels of 5, 7, and 9,

At a low dilution rate of 0.07 hr^{-1} (Figure 5.55), the step increase in total lead at pH 9 had little impact on the bacterial growth because of the low level of lead in the free ion form. As the pH level decreased, the effect of the lead in solution caused a slow decrease in X and P^* with time due to the increase in free ion concentration of the lead, and a corresponding increase in C^* as fewer cells were available to make use of the carbon source. At the dilution rate of 0.155 hr^{-1} (Figure 5.56), growth at pH 9 was also unaffected by the presence of the metal. However, the growth of X and P^* was at a slower rate than at the dilution rate of 0.07 hr^{-1} . In the simulation with the dilution rate set to a value of 0.24 hr^{-1} (Figure 5.57), the biomass concentration (X) began to decrease immediately after ending batch reactor operation (hour 12) since the dilution rate was beyond the point of the beginning of washout. The step increase in total metal caused a further decrease in biomass production and washout of the cell population that was able to grow at pH levels of 5 and 7 in the absence of metal. As with both the 0.07 hr^{-1} and

Figure 5.55. Effects of a simulated step increase of lead at steady state from 0 to 1×10^{-7} M at a dilution rate of 0.070 hr^{-1} on the concentration of total suspended biomass (X), free suspended polymer (P*), and the limiting substrate (C*).

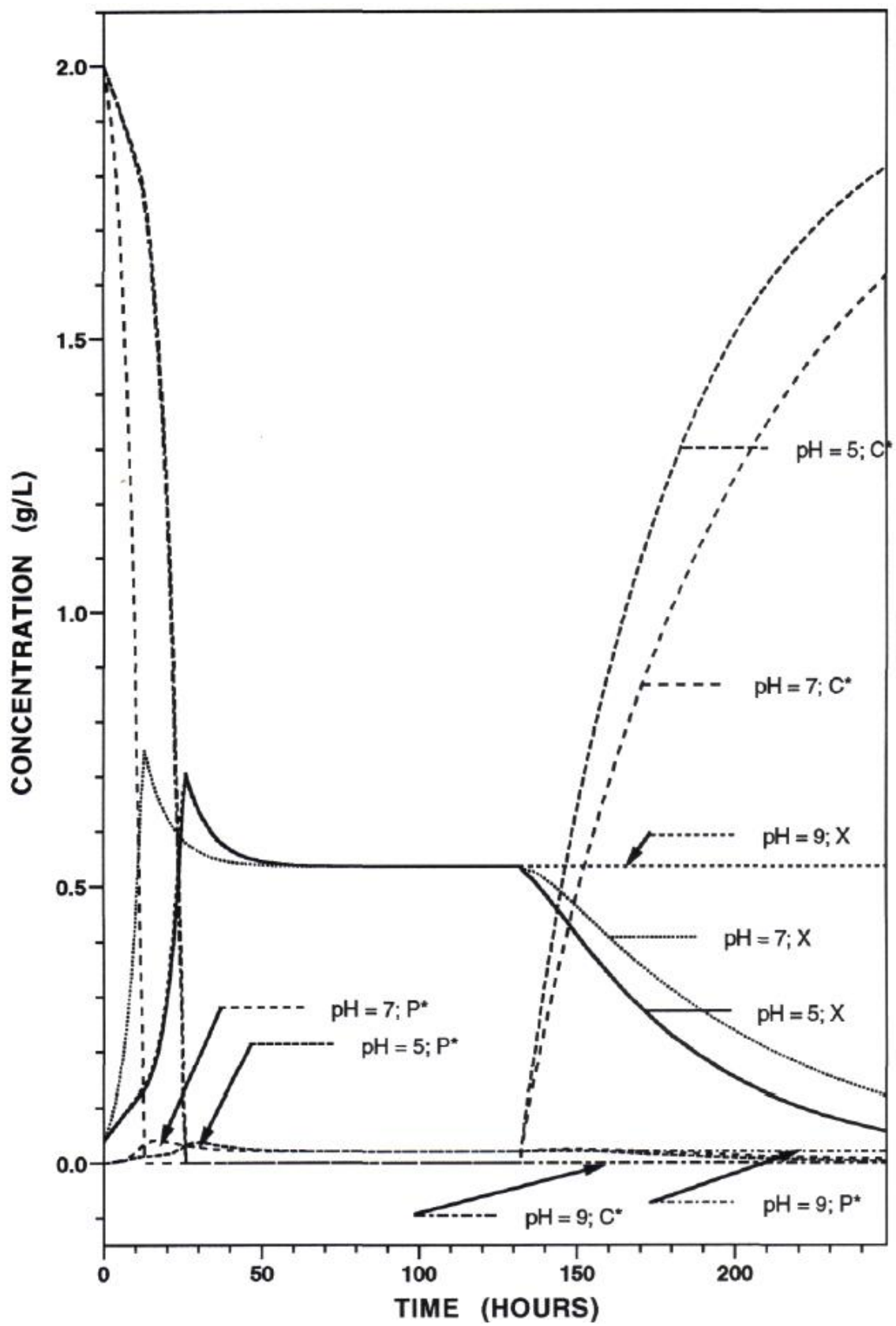
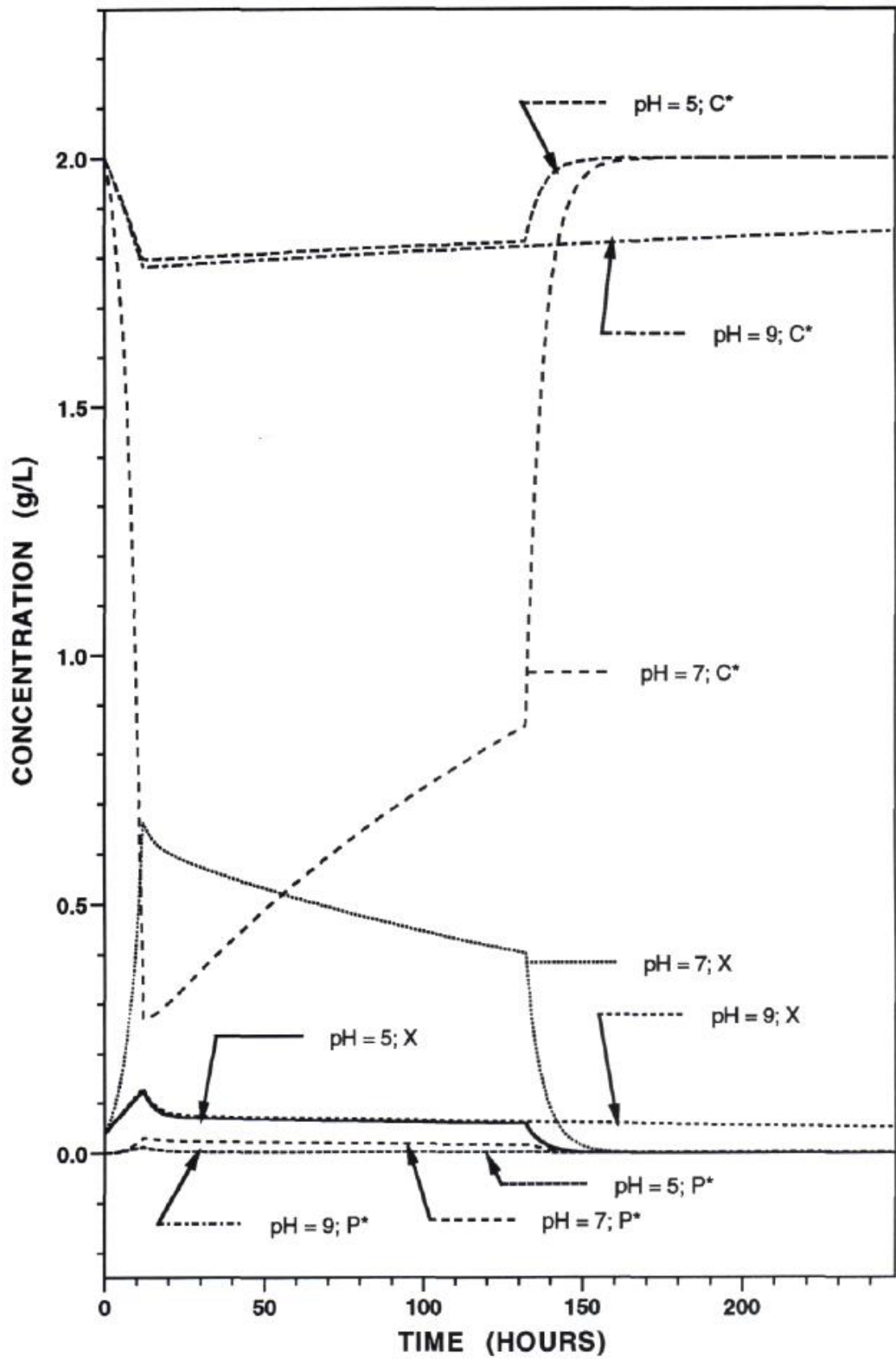


Figure 5.56. Effects of a simulated step increase of lead at steady state from 0 to 1×10^{-7} M at a dilution rate of 0.155 hr^{-1} on the concentration of total suspended biomass (X), free suspended polymer (P*), and the limiting substrate (C*).

Figure 5.57. Effects of a simulated step increase of lead at steady state from 0 to 1×10^{-7} M at a dilution rate of 0.240 hr^{-1} on the concentration of total suspended biomass (X), free suspended polymer (P*), and the limiting substrate (C*).



0.155 hr⁻¹ dilution rates, washout at the higher dilution rate at pH 9 was unaffected by the presence of the trace metal lead. The general trend in these three figures with increasing dilution rate was for lower cell growth rates after a step increase in metal concentration and a corresponding lower level of carbon nutrient (C*) being used at circumneutral and acidic pH levels due to the increasing concentration of the free ion form of the lead in solution.

DISCUSSION

The qualitative results of the simulations suggest that the model predictions are consistent with known behavior of the free ion form of metals and expected growth of cells under variable pH conditions. The apparent conformance of the pH dependent results with the limited prior model results of Hsieh (1988) lends further support to the current model form and function. Information would be required for a specific cellular system to obtain the corresponding model kinetic parameters and experimental results for this system to confirm the complete model validity.

The current model simulations apply to a specific system, a freshwater environment of low ionic strength ($I = 0.05 \text{ M}$) with a single strain of bacteria being present with only one type of inorganic surface (glass). However, the model is conducive to expansion to more complex systems with other types of organisms and/or inorganic surfaces. With sufficient expansion of the robustness of the model, it may be possible one day to enable modeling a biological metals removal treatment system in order to be able to optimize such removals in the system by observing how the model behaves prior to implementing the design/construction process. Such a model would enable a more natural clean-up option for metal contaminated sites in nature compared to the present conventional chemical precipitation treatment options currently in use.

The model modifications necessary to accomplish this expansion would require, however, an analysis of the interactions between existing and new components and sufficient experimental work to ensure proper development of the necessary kinetic parameters for the strains of bacteria that might be considered for use in such a system.

REFERENCES

Hsieh, K.M. 1988. The Growth and Attachment of a Biopolymer Producing *Pseudomonas* Species and the Characterization of its Interactions with a Toxic Trace Metal. Ph.D. Thesis. Cornell University, Ithaca, NY.

Hsieh, K.M., Lion, L. W., and Shuler, M. L. 1985. Bioreactor for the Study of Defined Interactions of Toxic Metals and Biofilms. *Appl. Environ. Microbiol.* 50:1155-1161.

Pirt S. J. 1975. Principles of Microbe and Cell Cultivation. Chapters 14, 15, 17, 23-25. John Wiley & Sons, NY.

Segal, I.H. 1976. Biochemical Calculations: How to Solve Mathematical Problems in General Biochemistry. Second Ed. John Wiley & Sons, NY.

Stumm, W. and Morgan, J.J. 1981. Aquatic Chemistry: An Introduction Emphasizing Chemical Equilibria in Natural Waters. John Wiley & Sons. New York, NY.

CHAPTER 6

SUMMARY AND RECOMMENDATIONS FOR FUTURE RESEARCH

The motivation for this work was to develop a model which could predictively reflect the complex interactions involved between the major biotic and abiotic components, trace metals and pH in an aquatic system. Accomplishing this goal necessitated the development of a conceptual framework from which the approach to the problem could proceed in a logical and orderly manner. The approach used was to take the structured model for a marine environment and extend the system to reflect both a freshwater environment in which hydrogen ion concentration could influence the growth, attachment and speciation of bacterial cellular components and metals within the aqueous environment and the synthesis of information aided by the existing integrated mathematical model for growth and biopolymer production of *Pseudomonas atlantica* at constant pH. The modeling revision, in conjunction with the prior work, prepares the foundation for further experimental work to form the basis of an improved understanding of the interactions between biologically mediated reactions and chemical conditions in aquatic systems.

The initial task required the determination of a mathematical approach that would be useful in describing the interactions of hydrogen ions with cellular components during bacterial growth. Models for pH effects on enzyme activity provided a useful framework and were extended to describe pH effects on whole cells. Conformational changes in the active reaction sites of a cell were attributed to shifts in the ionic form of associated amine and carboxyl functional groups. On a whole cell

basis, pH effects were judged to affect similar functional groups on cellular peptidoglycans comprising the cell envelope. In all cases, it was assumed that the growth variations induced by extracellular pH variations were similar to effects from activators and inhibitors. The selected model mechanism described pH dependence as being governed by the dissociation of a diprotic acid. The resultant dissociation affected the maximum growth rate constant and the half velocity coefficient for cellular growth. In this model, hydrogen ions act as noncompetitive inhibitors of activity. Noncompetitive inhibition terms, expressed in the form of pH dependent Monod constants were incorporated in the revised model.

Extensive simulations were performed to predict the concentrations of biotic components. The results plotted in the Figures of Chapter 5 considered growth in a Multigen (stirred jar fermenter) reactor and the Bioreactor containing glass slides as an attachment surface. The results for batch growth conditions in either reactor indicated that maximum concentrations occurred at circumneutral pH values, with concomitant decreases as the pH became either more acidic or alkaline. The results under continuous flow-through conditions in both reactor showed that the washout dilution rate was not sensitive to the pH level in solution. The data plots in both cases evidenced nearly the same dilution rate as the cut-off point for loss of cellular growth components in each case.

Evaluation of the effects of pH on trace metal speciation in solution was also necessary to gauge the effects of a trace toxic material upon the model microbial system. At low pH levels (3 to 5) metal ions are predominantly in the free ion form which exhibited the greatest toxicity to cellular growth. At high pH levels (8 to 10), the metals would attach to cellular components or readily complex with medium components such as hydroxide,

decreasing the concentration of the toxic free ion species form. The mathematical formulation for model inhibition by metals was previously described (see Appendix I). The addition of the pH-dependency along with the metal inhibition terms resulted in an integrated model able to predict metal distribution in an aquatic system as affected by solution pH and biological components.

The model simulations in Chapter 5 for batch growth conditions showed a general decrease in biotic component concentrations as metal concentrations increased from a level of 10^{-9} M to 10^{-5} M. The simulations for continuous flow-through conditions in either reactor showed that at circumneutral to acidic pH values, an increase in metal concentration lowered the dilution rate at which washout would begin. At alkaline pH values however, the results indicated that biotic components grew independent of the total metal concentration present. The simulations appeared reasonable considering the known effects of pH on bacterial cells and metal speciation available in the literature.

Given the simplified nature of the pH dependent model and its ease of use, a reasonable question is the applicability of the model to complex aquatic environments and engineered treatment systems. Understanding the speciation and phase distribution of toxic metals is useful before any recovery, disposal, or treatment option can be properly designed and implemented. The model discussed in this thesis makes a contribution toward this goal, though it is recognized that its applicability is currently limited to the conditions under which simulations were performed and subject to further experimental verification.

Due to the potential uses of the model, there are a significant number of opportunities for further research and experimental work to both test and expand the boundaries of the model. Each of the major chapters of this thesis provides opportunities for a wide range of additional research topics from experimental in nature to theoretical. Some recommendations for future work are summarized below.

Selection of the freshwater bacterial strain *Pseudomonas cepacia* 17616 requires detailed experimental analyses to more fully characterize cellular growth, polymer production and composition as a function of environmental conditions such as nutrient composition, ionic strength and pH for this bacterial strain. Similar characterizations should also be made with regard to metal binding. Such information will allow determination of the unique maximum growth rate constants, component partitioning and saturation constants, decomposition rates, molecular dissociation constants, attachment and detachment rates and biopolymer degradation and partition coefficients for this strain. Development of these constants for *P. cepacia* 17616 will provide experimental data to use in calibrating the output of the model. Further independent experiments could then serve to confirm the validity of the integrated model for aquatic environments with variable pH.

Questions still remain with regard to the model formulation for cellular attachment mechanisms. In particular, does the pH of the solution play a role in the physico-chemical nature of the cell attraction to a surface? The study of bacterial attachment and detachment process could be extended to provide more in-depth study of the pH-dependent cellular-surface interactions. A model assumption is that rate constants for growth of the attached cells are the same as that of suspended cells. As a biofilm develops, attached cells may become shielded from the pH effects in the bulk solution phase. This in turn implies that the

cellular growth on the surface, transfer of nutrients and release of metabolites may become important in terms of experimental challenges and in performing appropriate model simulations.

Additionally it is known that bacterial cells can form thick biofilms on surfaces. This is well established in wastewater treatment attached growth treatment systems, such as trickling filters or rotating biological contactors (RBCs) where cells will build up until the bottom layer actually attached to the surface loses adhesion when the diffusion of the nutrients and oxygen no longer is able to reach the bottom cell layer and creates a limitation on their ability to grow and survive. Additional experimental work would be necessary to develop diffusion coefficients for transfer of nutrients in a multilayer cell colony and the concomitant diffusion of metals through such a multilayer cellular arrangement. The experimental work should allow for incorporation of the effects of deeper biofilms into the overall model.

The addition of trace metal species to the microbial system poses additional questions. The mechanism of metal toxicity to cells is still not well understood particularly in the case where competing metal cations are present, nor is the specific mechanism and location of uptake of the metal by the cells and the surfaces contained within the system. Experimental work may be able to better define the effect of a metal on cellular growth and biopolymer production rates. Other experimental work focused upon the partitioning of the metal species to reactor surfaces and more specifically the specific forms/species that would bind will also be helpful in better understanding the metal-cell-polymer interactions. The consideration of pH dependency of both cellular growth and metal speciation allows a series of experiments to find optimal metal uptake levels while still maintaining vigorous cell

growth. Knowledge from this work may enable engineering control of reactor systems to enhance metal removal from an aquatic system.

The development of a more generalized mechanistic model for pH-dependent growth and trace metal partitioning by bacterial biofilms is desired. Further refinements in the structured model discussed in this thesis can be expected to better reflect conditions within a natural freshwater aquatic system and to provide more accurate simulations.

Specific modifications recommended for the model developed in this work include the following:

- (1) Refine the nutrient minimal medium to better reflect needed carbon limitations of the selected bacterial strain. The MMS medium was determined to have growth limitations due to phosphorous rather than the expected carbon growth limitation. Iteration between chemical speciation calculations and growth experiments can reveal a composition that provides all needed nutrients and allows sufficient levels of growth for detailed analyses of bacterial components,
- (2) Quantify, through a series of growth experiments, all rate parameters associated with the growth of *P. cepacia* 17616 in suspended culture under optimal nutrient conditions.
- (3) Quantify the effects of pH alterations in the growth rates of suspended cells to develop the cellular dissociation constants for the pH-dependency part of the model.

- (4) Repeat experimental procedures in (2) and (3) above focusing on attached cell metabolic parameters to ascertain whether they are the same as those for suspended cells.
- (5) Investigate the effects of liquid shear on surface attached cellular growth. The model assumed cellular detachment is directly proportional to the Reynold's number. However, model simulations of fluid flow between fixed surfaces indicate that the level of shear at the surface may not be as great as the overall bulk fluid Reynold's number indicates due to the change in the boundary layer thickness at the surface (Bacabac, *et al.*, 2005). The cellular size and/or thickness of the biofilm on the surface may keep growth confined to a laminar sublayer. If the surfaces are spaced close enough together, all fluid flow between the surfaces will be laminar in all situations. If they are spaced too far apart, there may be laminar flow at the surfaces but turbulent flow transport near the center of the surface spacing. Fluid shear may affect detachment rates, but attachment rates may be governed by other mechanisms if only laminar flow conditions exist between surfaces. The possible influence of the fluid flow conditions on the model predictions in laminar versus turbulent regimes should be investigated to reflect the possible disparity or simplifications to the model structure.
- (6) The nature of cellular attachment reflects a perceived two-step process of "reversible" attachment followed by a period of time later when an "irreversible" permanent surface binding occurs. If fluid shear effects differ between true laminar and turbulent flow conditions (as reflected in the system

Reynold's number), the mechanism of attachment of the cells to the surface may be affected. The model needs to reflect this possible change in the governing mechanism by altering the form of the cellular detachment and attachment rate constants.

- (7) The mechanism for the pH-dependency of cellular growth assumed both suspended and attached cells were equally able to interact with hydrogen ions in solution. Further, the mechanism was simplified by assuming the enzyme and enzyme-substrate complex ionizations constants were equal (i.e., substrate binding does not affect the ionization constants). Since it is known that pH is not generally equal to pH_e , experimental work is needed to verify these assumptions and the true noncompetitive nature of the inhibition. If either or both assumptions are incorrect, the model mechanism must be suitable altered to reflect the changes to the saturation constants as well as maximum growth rates.
- (8) The effect of pH and ionic strength on metal adsorption coefficients in the reactor must be characterized. This work would be aided by the medium refinements in (1) above and the repeat of growth experiments in (2) and (3) above in the presence of a metal and with variable pH levels. The results of these experiments would be reflected in changes (if any) in yield coefficients for cell mass and biopolymer productions, especially at low to neutral pH levels. The simulations in Chapter 5 indicated that at high pH levels (9 and above) cellular activity may prove independent of metal concentration,

presumably due to the significant decrease in the free ion form available of the metal. This model result awaits experimental verification.

- (9) The interactions of medium components, including the carbon species, with solid surfaces needs to be investigated. If significant interaction of species is detected, the model equations must be modified to reflect available levels of nutrients at surfaces. This partitioning of a carbon source may result in differing levels available to suspended and attached cells. The model structure may need to be altered to reflect the difference (if any) between available nutrient levels for suspended cells and for attached cells.
- (10) Experimental work by Hsieh (1988) had looked at the partitioning of the metal in solution amongst the cells, polymer and bioreactor surfaces in the sea water medium. Additional investigations are needed to determine the similar interactions in the freshwater medium used for the modeling simulations reflected in this thesis. While it was assumed that the adsorption isotherms were linear and equilibrium was instantaneous, further work is necessary to determine if this is the proper assumption to have made. Further investigation could be used to determine whether or not rate equations for metal binding to the wetted surface or glass are needed to better describe this interaction in the model. The model structure may then need to be altered to reflect the true nature of the interactions with the surface so it better reflects any experimental results that would be obtained.
- (11) The lack of an interactive component of metal speciation as a function of time during execution of the model impedes the operation of the model. Lengthy

computer runs are necessary on a mainframe computer to yield simulations. Metal biophase simulations with the model are cumbersome to operate. Alternate forms of a speciation program should be investigated as a replacement for MINEQL in the model. One of the newer speciation models available might speed up performance. It may also be possible to develop a new numerical solution to metal speciation by utilizing one of the many mathematical techniques available for solving series of simultaneous equations. Work should be directed to altering the program to run in a personal computer environment with allowance for more dynamic interactions especially with metal speciation.

- (11) The revised model needs more vigorous testing through simulation experiments and sensitivity analyses on some of the component parameters.

All of the above considerations were reviewed during the development of the revised model. These items had an impact on the resultant form and function of the model. They require additional detailed investigation to develop a better framework for the model and increase its usefulness for application to natural aquatic systems.

REFERENCES

Bacabac, R.G., Smit, T.H., Cowin, S.C., Van Loon, J. J. W. A., Nieuwstadt, F. T. M., Heethaar, R., and Klein-Nulend, J. 2005. Dynamic Shear Stress in Parallel-Plate Flow Chambers. *Journal of Biomechanics*. 38: 159-167.

Hsieh, K.M. 1988. The Growth and Attachment of a Biopolymer Producing *Pseudomonas* Species and the Characterization of its Interactions with a Toxic Trace Metal. Ph.D. Thesis. Cornell University, Ithaca, NY.

APPENDICES

I. INTERACTIONS OF MICROBIAL BIOFILMS WITH TOXIC TRACE METALS¹

ABSTRACT

Adsorbent surfaces in natural and engineered systems are frequently modified by bacterial attachment, growth of a biofilm and bacterial production of extracellular polymer. Attached cells or adsorbed polymers may alter the metal binding characteristics of the supporting substratum and influence metal partitioning. The interdependent behavior of toxic trace metal partitioning and biofilm development requires description of the interaction between cell growth with its accompanying polymer production and metal speciation. A mechanistic model was developed to describe the growth of a film-forming bacterium which adheres to a substratum through the production of extracellular biopolymers. Each bacterial cell was modeled as a two-component structure consisting of active cell mass and biopolymer. The biopolymer component was further divided into cell-associated and dissolved categories to distinguish biopolymer which remained naturally bound to cell surfaces from that which did not. Use of this structured model permitted independent description of the dynamics of cell growth, and polymer

1. Portions of the following published journal papers are reproduced in this appendix to describe the methodology and modifications performed on the original bacterial model in order to have it working properly, with permission of the coauthors: Lion, L.W., Shuler, M.L., and Hsieh, K.M.

"Interactions of Microbial Biofilms With Toxic Trace Metals: 1. Observation And Modelling Of Cell Growth, Attachment, And Production Of Extracellular Polymer". 1994. *Biotechnology and Bioengineering*. 44: 219-231.

"Interactions of Microbial Biofilms With Toxic Trace Metals: 2. Prediction and Verification of an Integrated Computer Model of Lead (IT) Distribution in the Presence of Microbial Activity". 1994. *Biotechnology and Bioengineering*. 44: 232-239.

production both of which may influence trace metal behavior. The model employs parameters obtained from independent experiments as well as published values to predict experimental observations of bacterial growth, attachment and detachment, biopolymer production, and adsorption of polymer onto solid (glass) surfaces. The model simulates transient and steady-state biofilm systems.

This Structured biofilm model was extended and utilized in conjunction with a chemical speciation model to make predictions of the interfacial interactions of a toxic trace metal, lead (Pb), with a surface modified by a marine film-forming bacterium, *Pseudomonas atlantica*. The extended model simulated behavior of transient and steady-state biofilms systems in the presence of the toxic transition metal (Pb).

1. MODELLING MICROBIAL CELL GROWTH, ATTACHMENT, AND PRODUCTION OF EXTRACELLULAR POLYMER

INTRODUCTION

Microbial attachment to solid surfaces occurs nearly universally in natural and engineered systems where microbes are present. When a cell approaches a surface by either bulk fluid transport or cellular motility, attachment may occur. With subsequent growth, excretion of extracellular polymers and further colonization by other cells, a biofilm is formed on the surface (Characklis, 1981; Trulear & Characklis, 1982).

The presence of biofilms can alter the trace metal partitioning effects of the inorganic surfaces to which cells adhere (Lion, *et al.*, 1988). The description of trace metal solid surface equilibria in natural aquatic systems is, therefore, complicated by the presence of a biofilm. Fixed film reactors such as rotating biological contactors, trickling filters, and

fluidized bed reactors are utilized frequently for wastewater treatment processes. Thus, there is also interest in the modeling of biofilm reactors for the purposes of rational design for removal of trace metals from wastewater.

Numerous theoretical models exist for heterogeneous biofilms (Benefield & Molz, 1985; Bryers, 1984; Droste & Kennedy, 1986, Namkung & Rittman, 1987a; Namkung & Rittman, 1987b; Rittman & McCarty, 1980; Suidan, 1986; Vavilin, 1987; Wanner & Gujer, 1986). These models do not attempt to provide a level of detail that describes the different components of individual cells. However, if description of the effect of a biofilm development on metal partitioning is a desired goal, the transient behavior of both the cellular biomass (which acts as an adsorbing surface) and extracellular polymer (which acts as a complexing ligand) must be defined. This necessitates use of a structured model for the biophase (Fredrickson, *et al.*, 1971).

In this research, the attachment of a common film-forming bacterium onto glass surfaces was studied under defined conditions. An objective was to obtain data for the development of a simulation model for the cells and their polymer. This was accomplished by using a bioreactor system that allowed for independent measurement of attachment and detachment parameters and use of experimental methods which distinguished free polymer from capsular material. A mechanistic model of the growth and attachment of *Pseudomonas atlantica* was developed based on pertinent basic theoretical concepts, experimental observation and independently determined parameters and used to predict reactor performance under batch, and continuous culture conditions.

MODEL DEVELOPMENT

A model derived from actual attachment studies requires systematic examination of the fundamental processes involved. The experiments conducted provided both mechanistic and kinetic information for the construction of the model. Use of the well-defined experimental bioreactor system (Hsieh, *et al.*, 1985) was necessary for obtaining model parameters and for independent verification of simulation results.

Since a predictive, rather than a correlative, model was intended, a structured model was required [see Shuler (1985) for discussion of model structure and the importance of structure in making predictions of transient responses]. The model was designed so that all parameters could be determined independently.

Pseudomonas atlantica is a film-forming marine bacterium. The most commonly described mechanism of bacterial attachment is by means of a matrix of extracellular polymeric substances which extend from the cell surface, termed "glycocalyx" (Costerton, *et al.*, 1978). The adhesive glycocalyx may mediate further attachment of other cells, and as the cells grow and reproduce on the surface, a biofilm is formed. Thus, the model needed to account for both the growth and attachment of cells and the production of biopolymers.

The following basic processes were considered in developing the model:

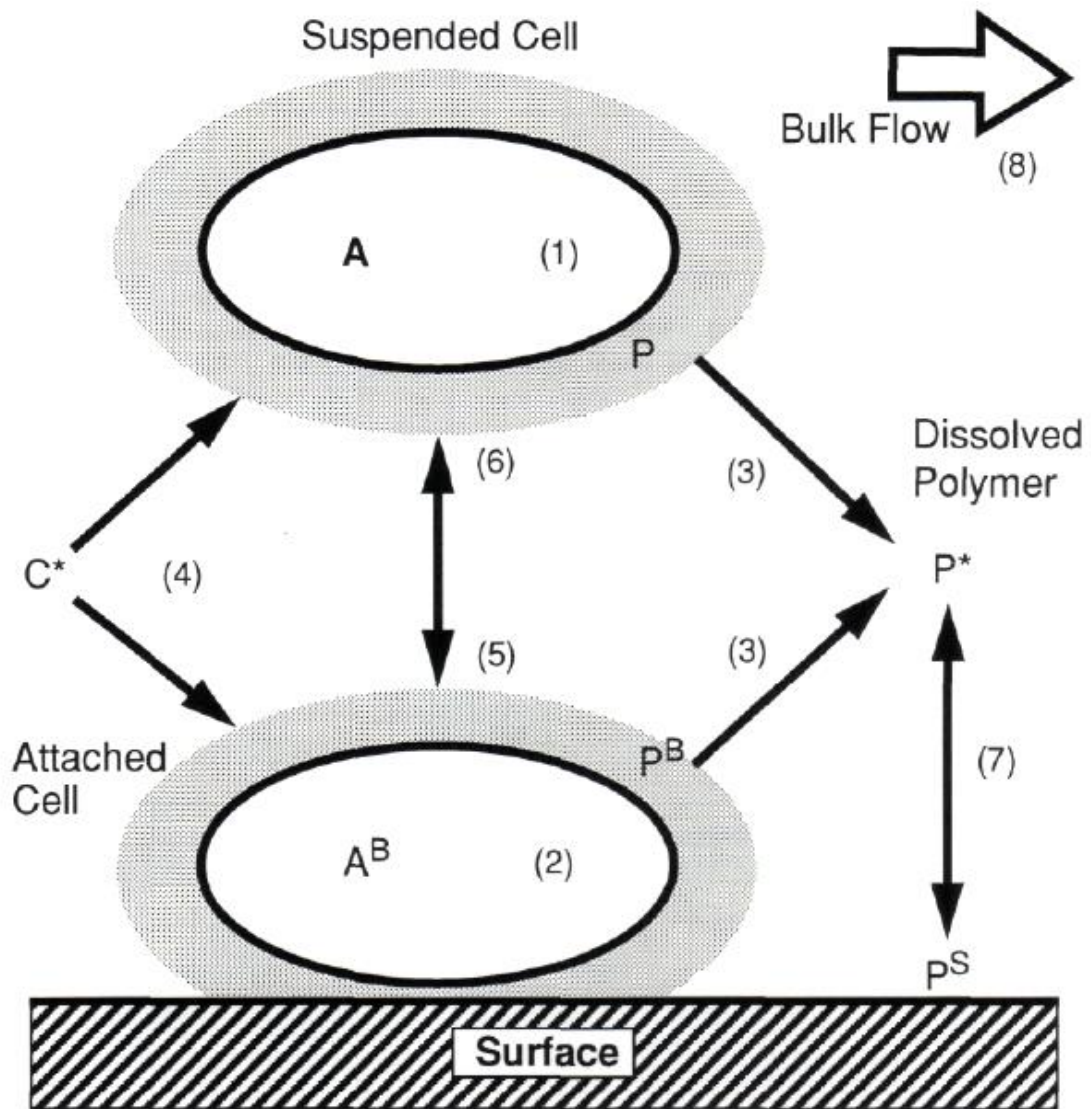
- (1) Growth, decay, and biopolymer production of bacterial cells in suspension.
- (2) Growth, decay, and biopolymer production of attached bacterial cells.
- (3) Release of biopolymer from cell surfaces to solution.
- (4) Utilization of growth-limiting substrate by suspended and attached cells.
- (5) Increase in attached cell density due to attachment and growth.

- (6) Decrease in attached cell density due to detachment and decay.
- (7) Partitioning of dissolved biopolymer by the solid surfaces.
- (8) Effect of fluid shear at the solid surface on cell detachment rate.

Each of these basic processes is shown schematically in Figure A1-1. They combine to simulate the actual biofilm reactor system (Hsieh, *et al.*, 1985), from which the majority of the model input parameters were obtained.

The development of the bacterial attachment model was based on the following general assumptions:

- (1) Each bacterial cell was given a structure consisting of two components, the active (or polymer-free) cell mass (the cellular component within its cell membrane), A [see the accompanying glossary for definition of all terms in the model], and the associated cellular biopolymer (capsular polymeric material as a whole), P . Such a distinction allows for a separate mathematical description of the formation of each component and its dependencies on physical/chemical conditions in the reactor. The bacterium under study, *P. atlantica*, is a producer of extracellular biopolymers which may aid in its attachment to surfaces.
- (2) The single growth-limiting nutrient was organic carbon in the form of glucose, C^* . All other nutrients were present in excess for both suspended and attached cells.
- (3) Growth mechanisms of suspended and attached cells were assumed to be identical. Biosynthetic changes due to a cell's close proximity to a surface are difficult to ascertain and may be impossible to measure. No experimental evidence was found in this study to suggest that growth mechanisms for the attached cells were different from those of the suspended cells. The growth parameter inputs in the model



Schematic of Model Component Interactions

- A = Active biomass, suspended
- P = Biopolymer
- A^B = Active biomass, attached
- P^B = Biopolymers associated with A^B
- P* = Dissolved Biopolymer
- P^S = Surface sorbed biopolymer
- C* = Bulk limiting nutrient concentration

Figure A1.1. Schematic of model component interactions. Each numbered interaction is described in the text.

formulation, however, allow for subsequent incorporation of variations between the two types of cells' physiological requirements. A component of the attached cells is denoted by a superscript B for "Bound". For example, A represents polymer-free cell mass of the suspended culture; A^B represents that of the attached cells.

- (4) No diffusional limitations exist at the solid surface. The requirement for a chemically defined medium in which metal speciation could be calculated, resulted in a solution composition which did not favor production of a dense biofilm. Given that surface coverage by cells was observed to be limited to a monolayer, no diffusional limitations within the film can exist. Further, mass transfer limitations of substrate through the liquid film were calculated to be negligible compared to the maximal rates of glucose uptake at the flow rates used in these experiments.
- (5) The biophase is a pure, homogeneous, and unsegregated culture of *P. atlantica*. Suspended cells were distinguished from the attached cells, but each of the two types was viewed as uniformly distributed throughout the culture or on solid surfaces.

Given the above assumptions along with information obtained through experiments, the equations describing the rate of formation of microbial components were formulated. These equations apply to the batch growth situation. Monod-like expressions were used to represent kinetic changes of the biophase. The rate of formation of the active cell mass of suspended cells, r_A , is given by:

$$r_A = \left[\mu_A' \left(\frac{C^*}{K_{AC^*} + C^*} \right) - k_{dA} \left(\frac{K_{dAC^*}}{K_{dAC^*} + C^*} \right) \right] A \quad (\text{A1.1})$$

where μ_A is the maximum growth rate constant, K_{AC}^* and K_{dAC}^* are saturation constants, and k_{dA} is the maintenance coefficient. Maintenance in this case is defined broadly to include not only energy consumptive reactions but macromolecular turnover that is related to the nutrient status of the cell. Both growth and degradation of A were modeled as functions of the external nutrient concentration.

The rate of formation of the cell associated biopolymer of the suspended culture, r_p , is given by:

$$r_p = \mu_p \left(\frac{C^*}{K_{PC}^* + C^*} \right) A - f_{AP} k_{dA} \left(\frac{K_{dAC}^*}{K_{dAC}^* + C^*} \right) A - \mu_{P^*} \left(\frac{P/A}{K_{P^*P} + P/A} \right) P \quad (A1.2)$$

where μ_p in the first term is the maximum biopolymer production rate constant and K_{PC}^* is the saturation constant. This term assumes the immediate conversion of extracellular glucose into polymer with A as the catalyst. Since the first term in Eq. (A1.2) represents a direct conversion process, it is therefore a "growth" term for P. The second term in Eq. (A1.2) represents the fraction (as indicated by the constant f_{AP}) of A that is converted to P in a "non-growth" associated manner. The use of A as the source for P is necessary since A is unstructured and there is no provision of an intracellular substrate pool in the model. This formulation assumes that part of the cellular maintenance requirements can result in biopolymer formation, as has been previously demonstrated (Robinson, *et al*, 1984). Thus, the maintenance term in Eq. (A1.1) when multiplied by f_{AP} becomes a source term for P. This term represents a non-growth production characteristic of the biopolymer, which is an observable feature in the experimental data (see discussion below). The third term in Eq. (A 1.2) represents the amount of P that is secreted or sheared off from the cell surface to become dissolved biopolymer, P^* . This Monod-like term assumes a maximum

polymer production rate constant, μ_{p^*} , which is modified by the ratio of P to A. It is reasoned that the more P relative to A, or the "thicker" the biopolymer coat around the cell, the more likely that bound polymer will be released into solution.

Equations similar to those for suspended cells [(A1.1) and (A1.2)] are also written for the counterparts of A and P for attached cells, or A^B and P^B :

$$r_A = \left[\mu_A' \left(\frac{C^*}{K_{AC^*} + C^*} \right) - k_{dA} \left(\frac{K_{dAC^*}}{K_{dAC^*} + C^*} \right) \right] A \quad (\text{A1.3})$$

$$r_{P^B} = \mu_{P^B} \left(\frac{C^*}{K_{P^B C^*} + C^*} \right) A^B - f_{A^B P} k_{dA^B} \left(\frac{K_{dA^B C^*}}{K_{dA^B C^*} + C^*} \right) A^B - \mu_{P^* B} \left(\frac{P^B / A^B}{K_{P^* P^B} + P^B / A^B} \right) P^B \quad (\text{A1.4})$$

Increase in the quantity of the dissolved polymer, P^* , is thus due to released biopolymer from P and P^B . The rate of formation of P^* is, then:

$$r_{P^*} = \mu_{P^*} \left(\frac{P / A}{K_{P^* P} + P / A} \right) P - \mu_{P^* B} \left(\frac{P^B / A^B}{K_{P^* P^B} + P^B / A^B} \right) \frac{a}{V} P^B - k_P \left(\frac{a}{V} \right) r_{P^*} - k_{dP^*} P^* \quad (\text{A1.5a})$$

where a is the total available solid surface area and V is the total bioreactor fluid volume. The last term of Eq. (A1.5a) accounts for loss of polymer from solution by microbial degradation or hydrolysis. Although more complicated decay functions could be employed, a first order dependence on P^* was consistent with the observed data. The third term of Eq. (A1.5a) represents the suspended biopolymer that becomes partitioned onto the solid surface. This equation can be explicitly solved for r_{P^*} by rearrangement of the terms to give:

$$r_{p^*} = \frac{\mu_{p^*} \left(\frac{P/A}{K_{p^*P} + P/A} \right) P + \mu_{p^*B} \left(\frac{P^B/A^B}{K_{p^*P^B} + P^B/A^B} \right) \frac{a}{V} P^B - k_{dp^*} P^*}{1 + k_p \left(\frac{a}{V} \right)} \quad (\text{A1.5b})$$

The net rate of formation of sorbed biopolymer on inorganic surfaces, r_{ps} , is simply:

$$r_{ps} = k_p r_p^* \quad (\text{A1.6})$$

Surface bound biopolymer density is considered directly proportional to the suspended biopolymer concentration (by the partition coefficient k_p). The inclusion of a/V in Eq. (A1.5) and (A1.5b) is to maintain correct dimensions. [All suspended components (*e.g.* A and P) have the dimensions of mass per unit volume whereas all surface components (*e.g.* P^B and P^S) have the dimensions of mass per unit area].

The rate of change limiting substrate concentration is given by:

$$r_{C^*} = - \left(\alpha_A r_{A,syn} + \alpha_P r_{P,syn} + \alpha_{A^B} r_{A^B,syn} \frac{a}{V} + \alpha_{P^B} r_{P^B,syn} \frac{a}{V} \right) \quad (\text{A1.7})$$

where:

$$r_{A,syn} = \mu_A \left(\frac{C^*}{K_{AC^*} + C^*} \right) A \quad (\text{A1.8})$$

$$r_{P,syn} = \mu_P \left(\frac{C^*}{K_{PC^*} + C^*} \right) A \quad (\text{A1.9})$$

$$r_{A^B,syn} = \mu_{A^B} \left(\frac{C^*}{K_{A^B C^*} + C^*} \right) A^B \quad (\text{A1.10})$$

$$r_{P^B,syn} = \mu_{P^B} \left(\frac{C^*}{K_{P^B C^*} + C^*} \right) A^B \quad (\text{A1.11})$$

and α_A , α_P , α_{A^B} , and α_{P^B} are stoichiometric coefficients or, effectively, the inverse of the true yield coefficients for each subscripted component. The total suspended biomass (cells plus bound polymer), X, and the total attached biomass, B are therefore defined as:

$$X = A + P \quad (\text{A1.12})$$

$$B = A^B + P^B \quad (\text{A1.13})$$

The rate of formation of X, or r_X , is the sum total of net increases in active cell growth and biopolymer production, and the net increase in suspended biomass due to bacterial attachment and detachment processes. The rate of formation of B, or r_B , is the sum of the net increases in growth of attached cells and polymer production, and the net change in adherent biomass due to attachment and detachment processes. The equations written for r_X and r_B are:

$$r_X = r_B + r_P - k^A (B^{\max} - B) X \frac{a}{V} + k^D \text{Re}(B) \frac{a}{V} \quad (\text{A1.14})$$

$$r_B = r_{A^B} + r_{P^B} - k^A (B^{\max} - B) X + k^D \text{Re}(B) \quad (\text{A1.15})$$

where k^A and k^D are the biomass attachment and detachment rate constants, B^{\max} is the maximum attached biomass concentration, and Re is the Reynolds number.

Cellular attachment in Eqs. (A1.14) and (A1.15) is assumed to depend on the concentration of cells in the bulk liquid and the availability of surface for attachment. Cellular detachment is assumed to depend on attached cell density and the fluid shear at the surface as represented by Re. These assumptions are consistent with the experimental data for $\text{Re} < 2000$ discussed below.

The above equations can easily be placed in overall mass balance equations for a continuous-flow stirred-tank reactor (CSTR) system. For example, the resulting balances on X, A, C*, and P* are:

$$V \frac{dX}{dt} = -Q(X) + Vr_X \quad (\text{A1.16})$$

$$V \frac{dA}{dt} = -Q(A) + Vr_A - k^A (B^{\max} - B) X \left(\frac{a}{V} \right) \left(\frac{A}{XV} \right) V + k^D \text{Re}(B) \frac{a}{V} \left(\frac{A^B}{B} \right) V \quad (\text{A1.17})$$

$$V \frac{dC^*}{dt} = -Q(C_0^* - C^*) + Vr_{C^*} \quad (\text{A1.18})$$

$$V \frac{dP^*}{dt} = -Q(P^*) + Vr_{P^*} \quad (\text{A1.19})$$

Similarly mass balance reactor equations for A^B, P^B, B, and P^S can be written.

MATERIALS

Organism. *Pseudomonas atlantica* NCMB 301 (ATCC 19262) was obtained from the American Type Culture Collection (Rockville, MD). This marine bacterium was originally isolated based on its ability to colonize surfaces. (Corpe, 1970). The organism and extracellular polymer have previously been characterized (Corpe, 1970, Corpe, 1975; Groleau & Yaphe, 1977; Kellems & Lion, 1989; Lion & Rochlin, 1989). The solid medium used for growth on plates and slants was Bacto Marine Agar (Difco Laboratories, Detroit, MI). The liquid medium for inocula was Bacto Marine Broth. Slants and plates were incubated at 25 °C for 25 hours, and slants were stored at 4 °C for several months. Inocula were cultured in 250 mL shake flasks at 25 °C on a rotary shaker at 250 rpm for 10 hours.

Media. The defined artificial seawater medium used in all growth experiments was identical to that described previously by Hsieh, et al., (1985) with the following

exceptions: added nutrients listed previously were replaced with 2 g/L glucose, 0.5 g/L NH_4Cl , 0.1 g/L KH_2PO_4 , and 1.22×10^{-4} g/L $\text{FeCl}_3 \cdot 6\text{H}_2\text{O}$. In addition, $\text{Na}_2\text{H}_2\text{-EDTA}$ (ethylenediaminetetraacetic acid) (1.86×10^{-3} g/L) was added to prevent precipitation of iron. Autoclaved stock solutions of the above components and a filter sterilized vitamin solution (Hsieh, et al., 1985) were added to filter sterilized (0.22 μm , 142 cm diameter Millipore membrane, Bedford, MA) AQUIL synthetic sea salt solution (Morel, et al., 1979). This prevented precipitation of the seawater medium. The combined salt, nutrient, and vitamin solutions will hereafter be referred to simply as the defined medium. The AQUIL salts solution was also used as a suspending medium for the cells. Unlike the Bacto Marine Broth, this medium supported only monolayer (or less) film formation. The use of the medium was necessary to allow calculation of trace metal speciation in experiments in which a toxic trace metal was introduced (see the companion text following).

Batch and Continuous Culture. The fermenter system used was a 2.0 L Multigen (New Brunswick Scientific Co., Edison, NJ) with working volumes ranging from 500 to 1500 mL. Masterflex (Cole Farmer Instrument Co., Chicago, IL) peristaltic pumps provided media addition and withdrawal when used for continuous operation. All stainless steel parts of the Multigen were replaced with machined Teflon parts to minimize bacterial attachment and leaching of metal ions. The wetted fermenter surfaces were either glass or Teflon. Aeration was provided by sparging with filter sterilized air at 2 L/min. These modifications did not compromise the good mixing capabilities that the original Multigen design provided. Culture pH was maintained at 7.0 by the automatic addition of 1 M NaOH. Temperature was maintained at 25 ± 2 °C. In continuous culture experiments with the Multigen and with the bioreactor described

below, steady state conditions were defined by experimental observation of at least three stable measurements of selected parameters (i.e., O.D., glucose, extracellular polymer concentration and the concentration of cell associated polymers) after a minimum of three hydraulic residence times. Values of O.D. were required to vary less than $\pm 5\%$. At lower dilution rates, glucose was barely detectable (<1 mg/L), while at high dilution rates (0.22 to 0.27 h⁻¹), values were easily measured but very sensitive to flow rate. At lower dilution rates, where measurements were near the detection limit, it was difficult to assign a precise deviation. At higher dilution rates, the random variation was $\pm 10\%$. For polymer values, the variation was usually much better than $\pm 10\%$.

Bioreactor Design. The bioreactor system used in bacterial attachment studies has been described previously (Hsieh, *et al.*, 1985; Hsieh, 1985). A schematic of the bioreactor vessel is shown in Figure A 1.2. To summarize, the reactor consists of four 1-inch-thick high-density polyethylene plates clamped together with aluminum supports. The metal parts are not permitted to contact with the reactor fluid to prevent leaching or metal ions. Grooves in the reactor allow for streamlined placement of glass slides as the inorganic solid surface for cellular attachment. A centrifugal pump provided fluid recirculation through the reactor, and constant hydrodynamics was achieved with the use of uniform spacing of glass slides and baffles to distribute inlet flow. From the flow rate, the velocity profile of the reactor fluid past the glass slides and resulting shear forces were calculated (Denn, 1980) given reactor dimensions (spacing between glass slides, hydraulic radius) and fluid properties (density, viscosity). Fluid velocities ranging from laminar to turbulent flow could be easily varied by controlling the recirculation pump. The sampling chamber allowed for medium

addition, product withdrawal, aeration, gas exhaust, thermometer, pH probe, acid/base addition, and fluid sampling. The working reactor volume was 1,420 mL.

Before an experiment the assembled bioreactor was acid cleaned with dilute nitric acid (1:6 volume ratio of acid to distilled, deionized water), rinsed, and autoclaved. The appropriate sterile medium was introduced into the bioreactor through the medium addition port, inoculated with bacteria and the reactor solution was then recirculated over the time course of each batch experiment. The recycle ratio was sufficiently high (>1300) that the reactor could be modeled as a CSTR. The recycle flow rate was typically 8 L/min ($Re = 350$), although it was as high as 50 L/min ($Re = 2,200$) in some experiments. Medium feed rates were under 6 mL/min. Since, for continuous operation, the medium feed and fluid recycle used separate pumps, the fluid hydrodynamics and the degree of substrate conversion were independent of each other with the recirculation pump controlling the hydrodynamics and the feed pump controlling the dilution rate or fluid residence time.

DERIVATION OF MODEL PARAMETERS

Model parameters were derived primarily from experiments. Table A1.1 summarizes the values determined for the model parameters. Initial conditions for experiments are given in Table A1.2.

Although the equations written for the production of various suspended components of the biophase follow the Michaelis-Menton model, the structuring of a cell into A and P prevented the routine application of a linearized form (such as the Lineweaver-Burk plot) to arrive at kinetic constants. Even with this shortcoming, a steady-state mass balance on A may be performed and the results used together with those from batch

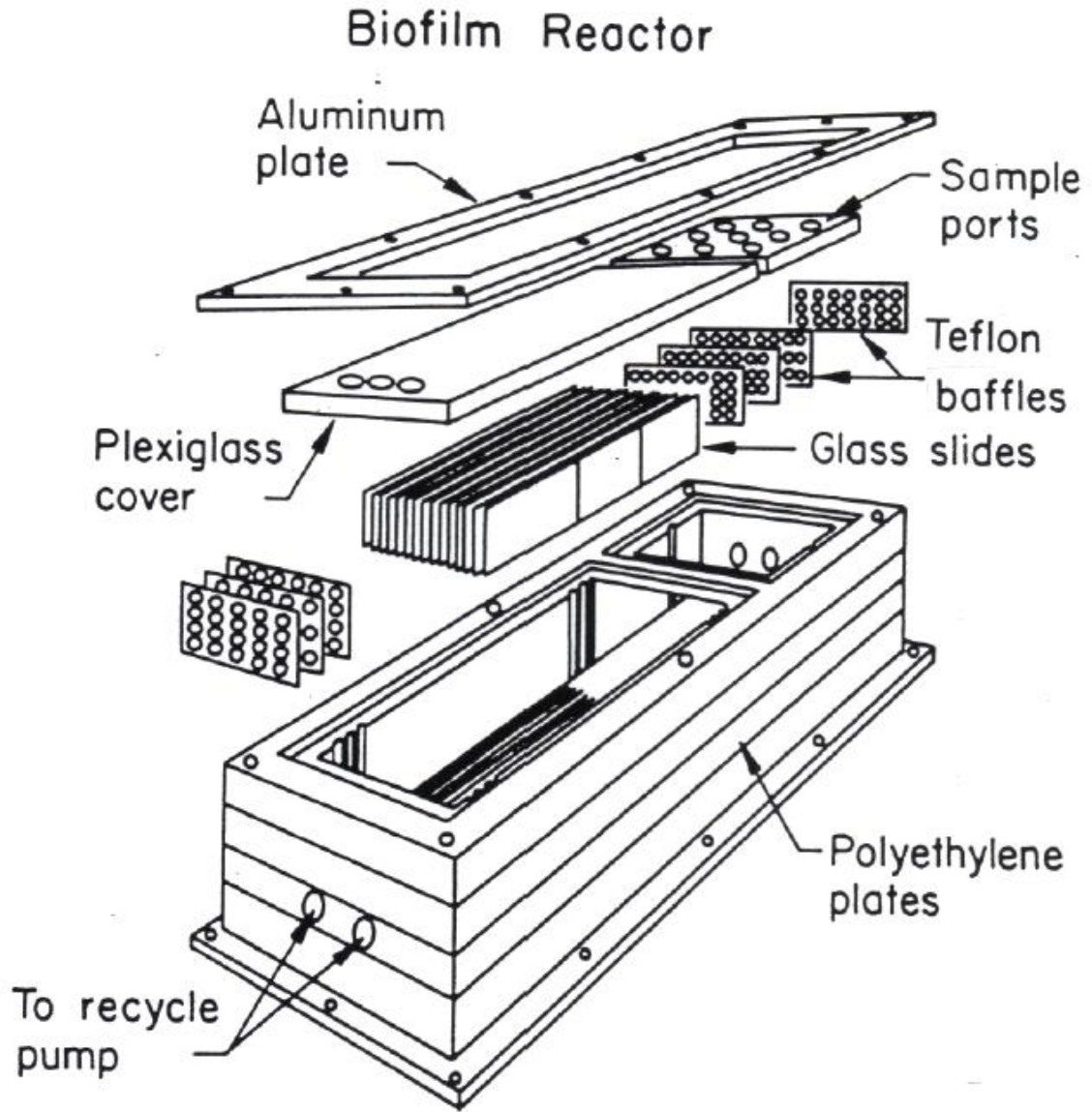


Figure A1.2. Schematic diagram of bioreactor (from Hsieh *et. al.*, 1985).

experiments to generate the kinetic parameters. Mass balance in a Multigen for the polymer free portion of the culture (A) is given by Eq. (A1.17). At steady-state and with no adsorptive surfaces present:

$$DA = r_A \quad (\text{A1.20})$$

where D is the dilution rate or the inverse of the hydraulic residence time (V/Q).

In a similar manner, mass balance for cell-bound polymer (P) and dissolved polymer (P*) in a steady-state Multigen with no adsorptive surfaces gives:

$$DP = r_P \quad (\text{A1.21})$$

$$DP^* = r_{P^*} \quad (\text{A1.22})$$

In the absence of adsorbing surfaces Eq. (A1.5a) becomes:

$$r_{P^*} = \mu_{P^*} \left(\frac{P/A}{K_{P^*P} + P/A} \right) P - k_{dP^*} P^* \quad (\text{A1.23})$$

Substitution of Eqs. (A1.1), (A1.2) and (A1.23) into Eqs. (A1.20), (A1.21) and (A1.22) gives:

$$D = \mu_A \left(\frac{C^*}{K_{AC^*} + C^*} \right) - k_{dA} \left(\frac{K_{dAC^*}}{K_{dAC^*} + C^*} \right) \quad (\text{A 1.24})$$

$$DP = \mu_P \left(\frac{C^*}{K_{PC^*} + C^*} \right) A + f_{AP} k_{dA} \left(\frac{K_{dAC^*}}{K_{dAC^*} + C^*} \right) A - \mu_{P^*} \left(\frac{P/A}{K_{P^*P} + P/A} \right) P \quad (\text{A 1.25})$$

and

$$DP^* = \mu_{P^*} \left(\frac{P/A}{K_{P^*P} + P/A} \right) P - k_{dP^*} P^* \quad (\text{A 1.26})$$

Table A1.1: Values of Model Parameters Associated with Rate Equations.

Active Cell Mass:	suspended:	A	surface attached:	A ^B	
Biopolymer:	suspended:	P*	surface adsorbed:	P ^S	
	associated with suspended cells:	P	associated with attached cells:	P ^B	
Carbon Source:		C*			
		<u>Saturation Constants</u>			
		$K_{AC^*} = 4.7 \times 10^{-4} \text{ g/L}$	<u>Decomposition Rates</u>		
		$K_{PC^*} = 4.4 \times 10^{-3} \text{ g/L}$	$k_{dA} = 0.031 \text{ hr}^{-1}$		
		$K_{ABC^*} = 4.7 \times 10^{-4} \text{ g/L}$	$k_{dAB} = 0.031 \text{ hr}^{-1}$		
		$K_{PBC^*} = 4.4 \times 10^{-3} \text{ g/L}$	<u>Maximum Rates of Synthesis</u>		
		$f_{AP} = 0.95 \text{ gP/gA}$	$\mu_A = 0.25 \text{ hr}^{-1}$		
		$f_{ABP} = 0.95 \text{ gP}^B/\text{gA}^B$	$\mu_{AB} = 0.25 \text{ hr}^{-1}$		
		$K_{P^*P} = 0.1 \text{ gP/gA}$	$\mu_P = 0.24 \text{ hr}^{-1}$		
		$K_{P^*PB} = 0.1 \text{ gP}^B/\text{gA}^B$	$\mu_{PB} = 0.24 \text{ hr}^{-1}$		
		$K_{dAC^*} = 0.01 \text{ g/L}$	$\mu_{P^*} = 0.04 \text{ hr}^{-1}$		
		$K_{dABC^*} = 0.01 \text{ g/L}$	$\mu_{P^*B} = 0.04 \text{ hr}^{-1}$		
		<u>Stoichiometric Coefficients</u>			
			$\alpha_A = 3.6$		
			$\alpha_P = 1.7$		
			$\alpha_{AB} = 3.6$		
			$\alpha_{PB} = 1.7$		

Biopolymer partition coefficient	k_P	=	0.04 L/m^2		
Biopolymer degradation rate const.	k_{dP^*}	=	0.16 hr^{-1}		
Biomass attachment rate constant	k^A	=	4.7 L/g-hr		
Biomass detachment rate constant	k^D	=	0.0035 hr^{-1}		
Maximum attached biomass conc.	B^{\max}	=	$8.5 \times 10^{-3} \text{ g/m}^2$		
Total surface area	a	=	0.321 m^2 (bioreactor), 0.061 m^2 (Multigen)		
Total volume	V	=	1.42 L (bioreactor), 1.5 L (Multigen)		
Reynolds number	Re	=	varies, depending upon recirculation rate (Re = 300 used for bioreactor simulations; Re = 2,000 for Multigen simulations)		

Table A1.2: Initial Conditions for the Bacterial Model.

$A_0 = 0.03 \text{ g/L}$
$P_0 = 0.01 \text{ g/L}$
$A^B_0 = 6.0 \times 10^{-4} \text{ g/m}^2$
$P^B_0 = 3.0 \times 10^{-4} \text{ g/m}^2$
$P^*_0 = 1.0 \times 10^{-6} \text{ g/L}$
$P^S_0 = 1.0 \times 10^{-9} \text{ g/m}^2$
$C^*_0 = 2.0 \text{ g/L}$

Substituting Eq. (A1.26) into Eq. (A1.25) yields:

$$D(P + P^*) = \left(\frac{\mu_p C^*}{K_{pC^*} + C^*} + \frac{f_{AP} k_{dA} K_{dAC^*}}{K_{dAC^*} + C^*} \right) A - k_{dP^*} P^* \quad (\text{A 1.27})$$

From Eq. (A 1.7) and (A 1.18) the substrate balance for a well-mixed reactor at steady-state with no adsorptive surfaces is:

$$D(C^*_0 + C^*) = \alpha_A r_{a,syn} + \alpha_P r_{p,syn} \quad (\text{A 1.28})$$

Substituting the expressions for $r_{A,syn}$ and $r_{P,syn}$ (Eqs. (A1.8) and (A1.9) gives:

$$D(C^*_0 + C^*) = \alpha_A \mu_A \left(\frac{C^*}{K_{AC^*} + C^*} \right) A + \alpha_P \mu_P \left(\frac{C^*}{K_{pC^*} + C^*} \right) A \quad (\text{A 1.29})$$

Substituting Eq. (A 1.27) into Eq. (A 1.29) gives:

$$D(C^*_0 + C^*) = \alpha_A \mu_A \left(\frac{C^*}{K_{AC^*} + C^*} \right) A + \alpha_P \left[D(P + P^*) + k_{dP^*} P^* \left(\frac{f_{AP} k_{dA} K_{dAC^*}}{K_{dAC^*} + C^*} \right) A \right] \quad (\text{A 1.30})$$

Substituting Eq. (A 1.24) into Eq. (A 1.30) and rearranging yields:

$$\frac{(C^*_0 + C^*)}{A} - \frac{\alpha_P (P + P^*)}{A} = \alpha_A + \frac{1}{D} \left(\frac{\alpha_A k_{dA} K_{dAC^*}}{K_{dAC^*} + C^*} - \frac{\alpha_P f_{AP} k_{dA} K_{dAC^*}}{K_{dAC^*} + C^*} \right) + \frac{k_{dP^*} P^*}{AD} \quad (\text{A 1.31})$$

Equation (A1.31) was applied to Multigen data (using the apparatus described above) where the attached population was negligible. Values of α_P , f_{AP} and K_{dAC^*} were estimated (as described below), the value for k_{dA} was obtained from analysis of the declining phase of

batch data (where $dA/dt \approx -k_{dA}A$, in the absence of a surface), and α_A and k_{dP^*} were then obtained by pairwise solution of Eq. (A 1.31) for Multigen results at different dilution rates.

Rearranging Eq. (A 1.30) above gives:

$$\frac{D(C^*_0 + C^*) - \alpha_p D(P + P^*) - k_{dP^*} P^*}{A} = \alpha_A \mu_A \left(\frac{C^*}{K_{AC^*} + C^*} \right) - \left(\frac{f_{AP} k_{dA} K_{dAC^*}}{K_{dAC^*} + C^*} \right) \quad (\text{A 1.32})$$

Here K_{AC^*} and A were obtained from Eq. (A1.32) by pairwise solution of Multigen results for different dilution rates. Alternately, if $C^* \gg K_{dAC^*}$ (as is the case at higher dilution rates), the last term of Eq. (A 1.32) becomes negligible and inverting gives:

$$\left(\frac{D(C^*_0 + C^*) - \alpha_p D(P + P^*) - k_{dP^*} P^*}{A} \right)^{-1} = \frac{1}{C^*} \left(\frac{K_{AC^*}}{\alpha_A \mu_A} \right) + \frac{1}{\alpha_A \mu_A} \quad (\text{A 1.33})$$

Then K_{AC^*} and μ_A can be obtained from a plot of the left-hand side of Eq. (A1.33) versus $1/C^*$. The value of μ_A obtained from Multigen data using Eq. (A 1.32) or (A 1.33) will match μ_A from analysis of A in the exponential growth stage of batch data if α_p is correct (see discussion of α_p below). In addition, μ_A , μ_p and μ_{p^*} can be obtained from the slopes of batch growth data.

The results of Mian, *et al.*, (1978) and Robinson, *et al.*, (1984) were used to estimate α_p , the inverse of biopolymer yield from glucose. Mian, *et al.*, (1978) found the dissolved biopolymer yield of a *Pseudomonas* species under carbon-limited growth at a dilution rate =

0.05 hr⁻¹ to be 33%. Robinson, *et al.*, (1984), in a similar study, showed a polymer conversion of 0.2 mg polymer/mg glucose consumed, or 20% yield. These two yields were averaged and assumed to apply to the experimental strain of *P. atlantica*. The term P represents the cell-associated polymer, which was found to be produced at approximately twice the amount of P* at D = 0.05 hr⁻¹ (Hsieh, 1988). Thus, the average value of 26.5% was doubled, and the inverse was taken to be a trial value of α_p which may be refined by iterative calculation of μ_A from Eq. (A 1.32) or (A 1.33) and comparison to μ_A obtained from batch data. The trial value of α_p (1.9) was found to be quite close to the selected value (1.7) that gave consistent results for μ_A .

The remaining model parameters were estimated as follows. The parameter K_{PC^*} was estimated from a literature survey of saturation constants compiled by Pirt (1975) for growth of bacteria. The parameter K_{dAC^*} was taken from a study by Domach, *et al.*, (1984), of the protein maintenance dependence on intracellular carbon. For f_{AP} , it was reasoned if all of A degraded to P, a maximum of one mass unit of P could be formed for every unit of A, assuming the carbon content of P and A were similar. Since something less than complete conversion is anticipated, a value of $f_{AP} = 0.95$ gP/gA was used in the model. The parameter K_{P^*P} was estimated from the slope of batch data for P*. Sensitivity analyses indicated that, with the exception of f_{AP} and K_{P^*P} , errors in the values of these estimated parameters of several factors did not affect the model's ability to correlate experimental data. For f_{AP} and K_{P^*P} , deviations of $\pm 20\%$ from derived values did not affect the predictions of the model significantly. Once the model parameter estimates were obtained, their values were fixed and used in all subsequent predictions for bioreactor behavior.

From lack of evidence to the contrary, the parameters of the attached cells were treated as being identical to those of the suspended cells. This treatment is supported by the findings of Bakke, *et al.*, (1984), who measured aerobic glucose metabolism by bio-film cultures of *Pseudomonas aeruginosa* at steady-state. These results demonstrated that the same kinetic and stoichiometric coefficients can be used to describe processes in suspended cultures as in biofilms. Prior investigations with *P. atlantica* have shown that the gross chemical characteristics of its extracellular polymer are independent of the physiological state of a culture (Hsieh, et al., 1990).

Biopolymer adsorption onto glass followed a linear isotherm for the range of concentrations studied. A simple mass balance using the equilibrium concentrations in a blank (P^*_0 , no sorbent) and sample (P^*_e , with sorbent present) gives:

$$P^*_0V = P^*_eV + \text{amount adsorbed} \quad (\text{A } 1.34)$$

For a linear isotherm:

$$\frac{\text{amount - adsorbed}}{A} = k_p P^*_e \quad (\text{A } 1.35)$$

Combining the Eqs. (A1.34) and (A1.35) and rearranging gives:

$$\frac{P^*_0}{P^*_e} = 1 + k_p \left(\frac{a}{VP} \right) \quad (\text{A } 1.36)$$

A plot of P^*_0/P^*_e versus a/V yields k_p as shown in Figure A1.3.

Bacterial attachment and detachment were treated as follows. At steady-state, the attachment and detachment rates are equal, or from Eq. (A1.15):

$$k^A (B^{\max} - B) X = k^D (\text{Re}) B \quad (\text{A } 1.37)$$

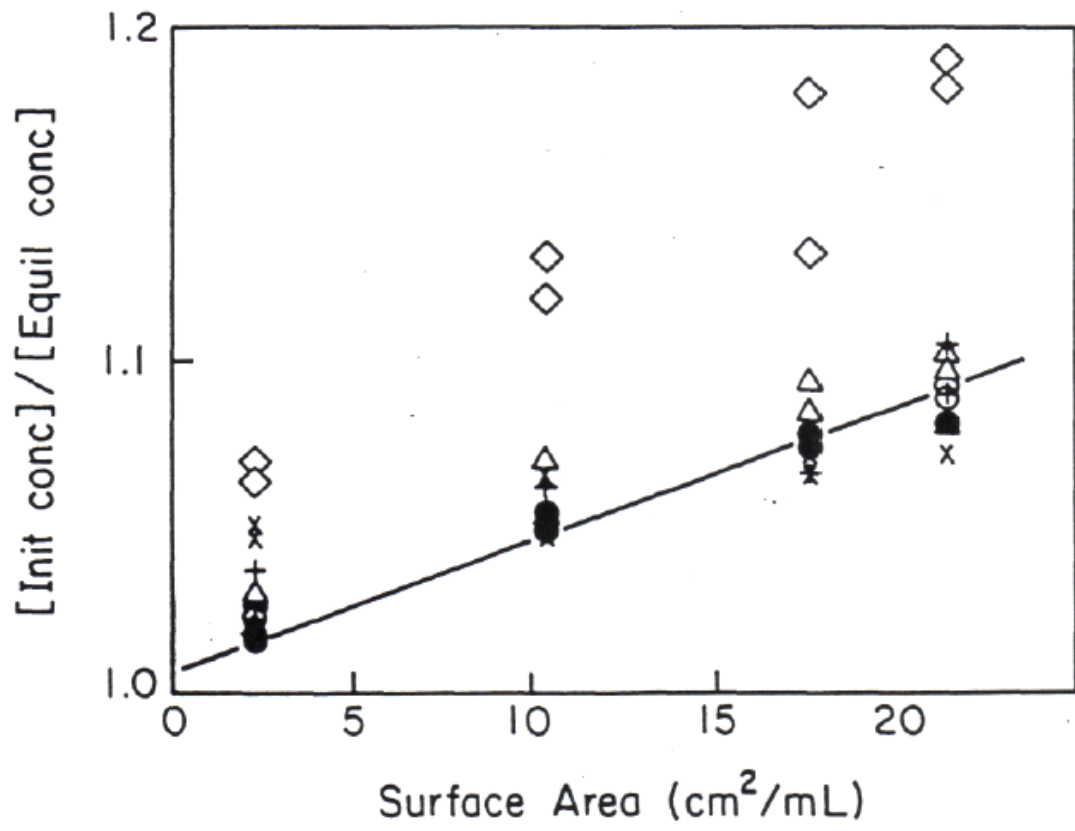
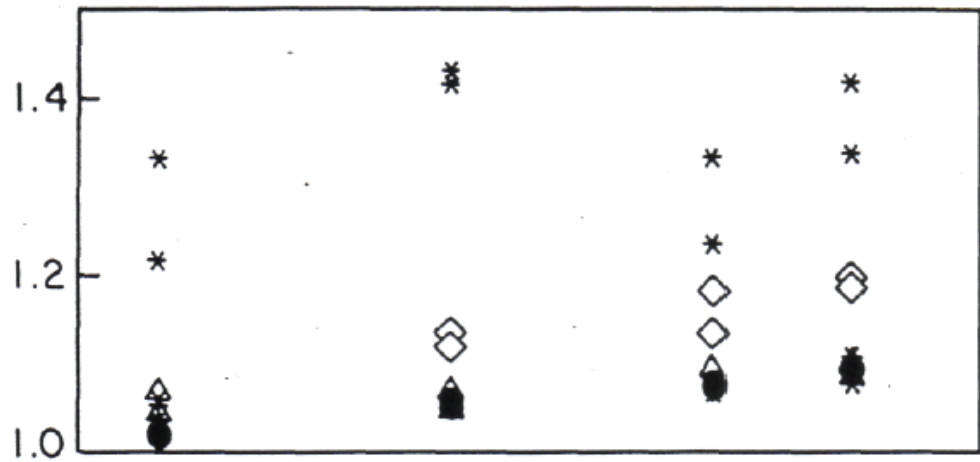
The Reynolds number is included in the detachment term to exclude shear dependence from k^D . A linear correlation between Reynolds number and the density of attached cells was assumed and was consistent with experimental data for conditions of laminar flow (Figure A 1.4). While a more complex, non-linear, dependency could also be justified, the resulting complexity appeared to be unwarranted.

Rearrangement of Eq. (A1.37) gives:

$$\frac{1}{X} = \left(\frac{1}{B} \right) \frac{k^A B^{\max}}{k^D \text{Re}} - \frac{k^A}{k^D \text{Re}} \quad (\text{A 1.38})$$

A plot of $1/X$ versus $1/B$ at known Re (Figure A 1.5) will yield the ratio of k^A and k^D as well as B^{\max} . Either k^A or k^D can be obtained from attachment and detachment kinetic data (see, for example, Figure A 1.6). B^{\max} may also be obtained from equilibrium attachment data which had a hyperbolic form equivalent to that of a Langmuir isotherm (Figure A1.7) (Shuler, 1985). The two estimates of B^{\max} ($8.9 \times 10^{-3} \text{ g/m}^2$ from Figure A1.5, and $8.0 \times 10^{-3} \text{ g/m}^2$ from Figure A1.7) were consistent.

Figure A1.3. Equilibrium biopolymer adsorption onto glass at different dissolved biopolymer concentrations. The Y axis of the bottom graph is enlarged to show overlap of data points. The initial biopolymer concentrations used were (○) 0.0436 g/L, (●) 0.0218 g/L, (Δ) 0.0104 g/L, (+) 0.00246 g/L, (X) 0.000642 g/L, (◇) 0.00017 g/L, and (*) 0.000467 g/L.



DISCUSSION

Despite the relative simplicity of the proposed mechanisms for bacterial growth and attachment, the model predictions agree well with experimental data for both suspended and surface-associated components. The ability of the model to describe transient as well as steady-state behavior indicates the soundness of the mechanisms incorporated. Empirical correlations for model parameters have not been used to improve the goodness of fit.

The partitioning of cellular biomass into a structure consisting of A and P appeared to be a reasonable assumption since A and P each possesses different production characteristics (Hsieh, 1988; Hsieh, et al, 1990) with P having a partial non-growth associated character. The model attributes this behavior to the conversion of A to P (second term in Eq. (A 1.2) which may be conceptually viewed as part of the maintenance requirements of A.

Substantial information was available for the formulation of the mechanisms of bacterial attachment and detachment. The goodness of fit of the attachment and detachment processes to a hyperbolic equation of form equivalent to the Langmuir-adsorption isotherm indicates the plausibility of the proposed dependence on surface coverage. The dependence of detachment on Re is intuitively expected and was confirmed by experiment (Hsieh, 1988). These observations confirm the importance of physicochemical factors associated with the attachment/detachment processes. An agreement between model calculations and the attached biomass B , determined from experiments, indicates that the model dependencies of attachment rate on surface coverage and suspended cell concentration and detachment rate on Re and B work well to describe the observed biofilm formation. The

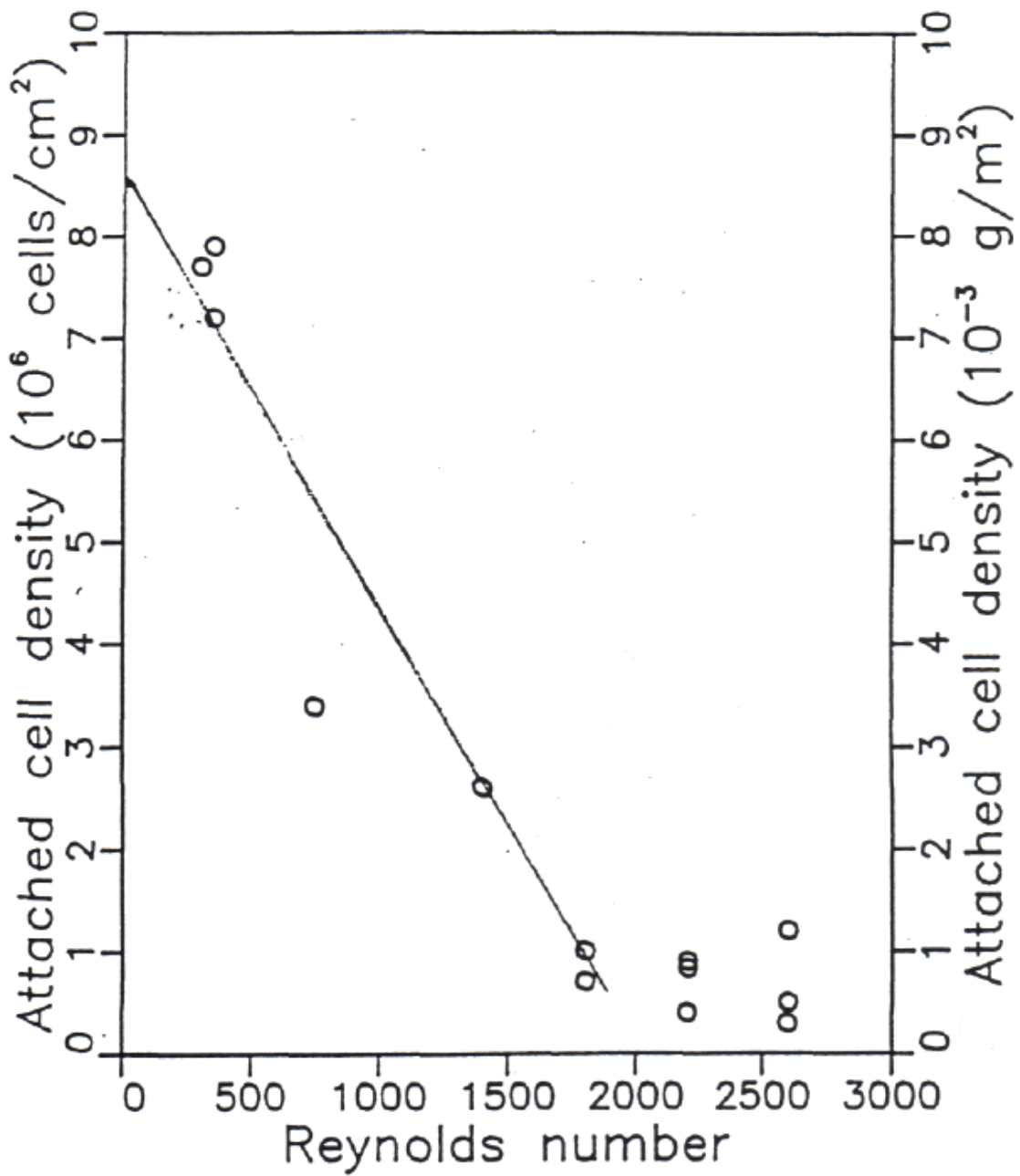


Figure A 1.4. Effect of fluid velocity, as represented by Reynolds number, or equilibrium attached cell density.

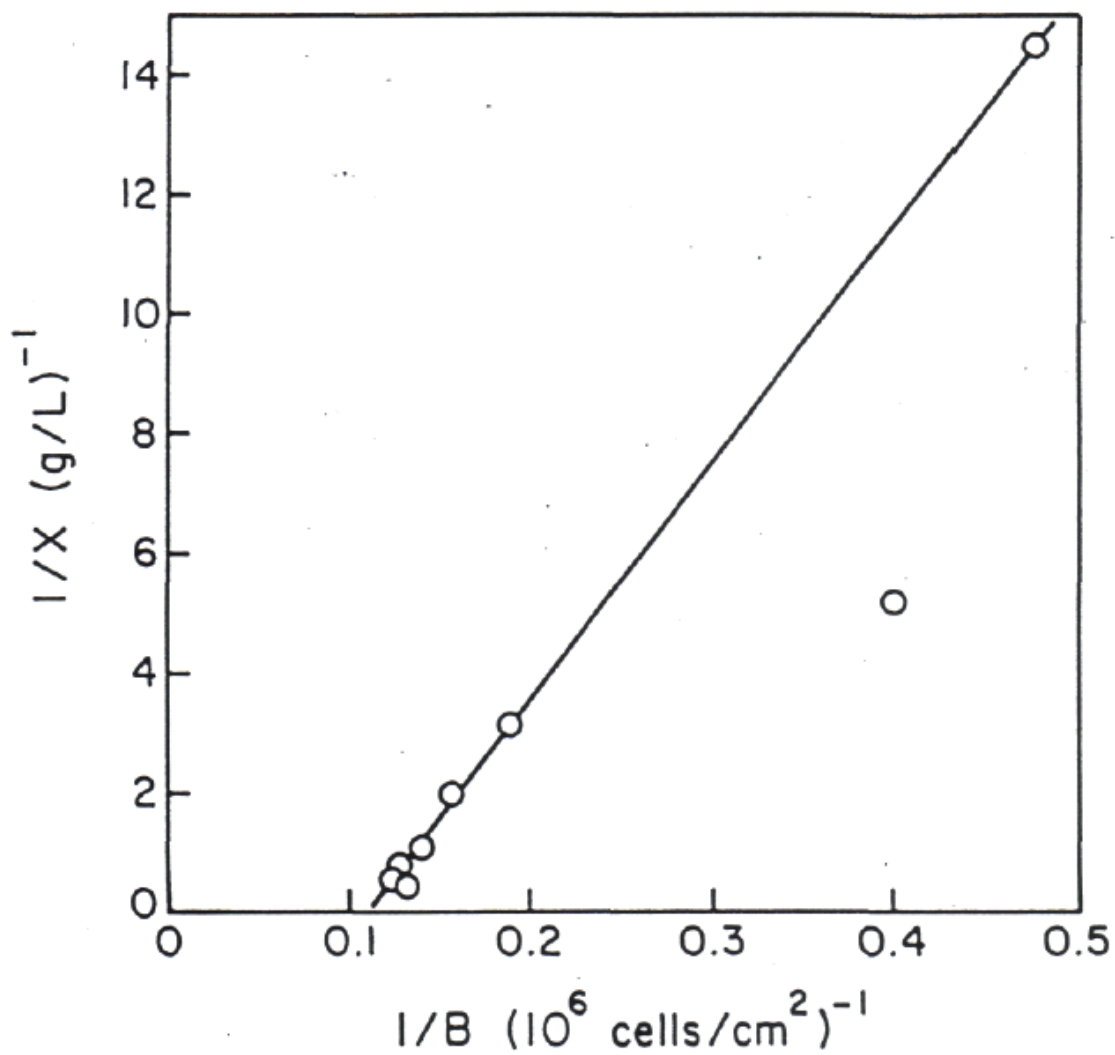


Figure A1.5. Linear plot for cell attachment parameters at low fluid velocity (Reynolds number is 300).

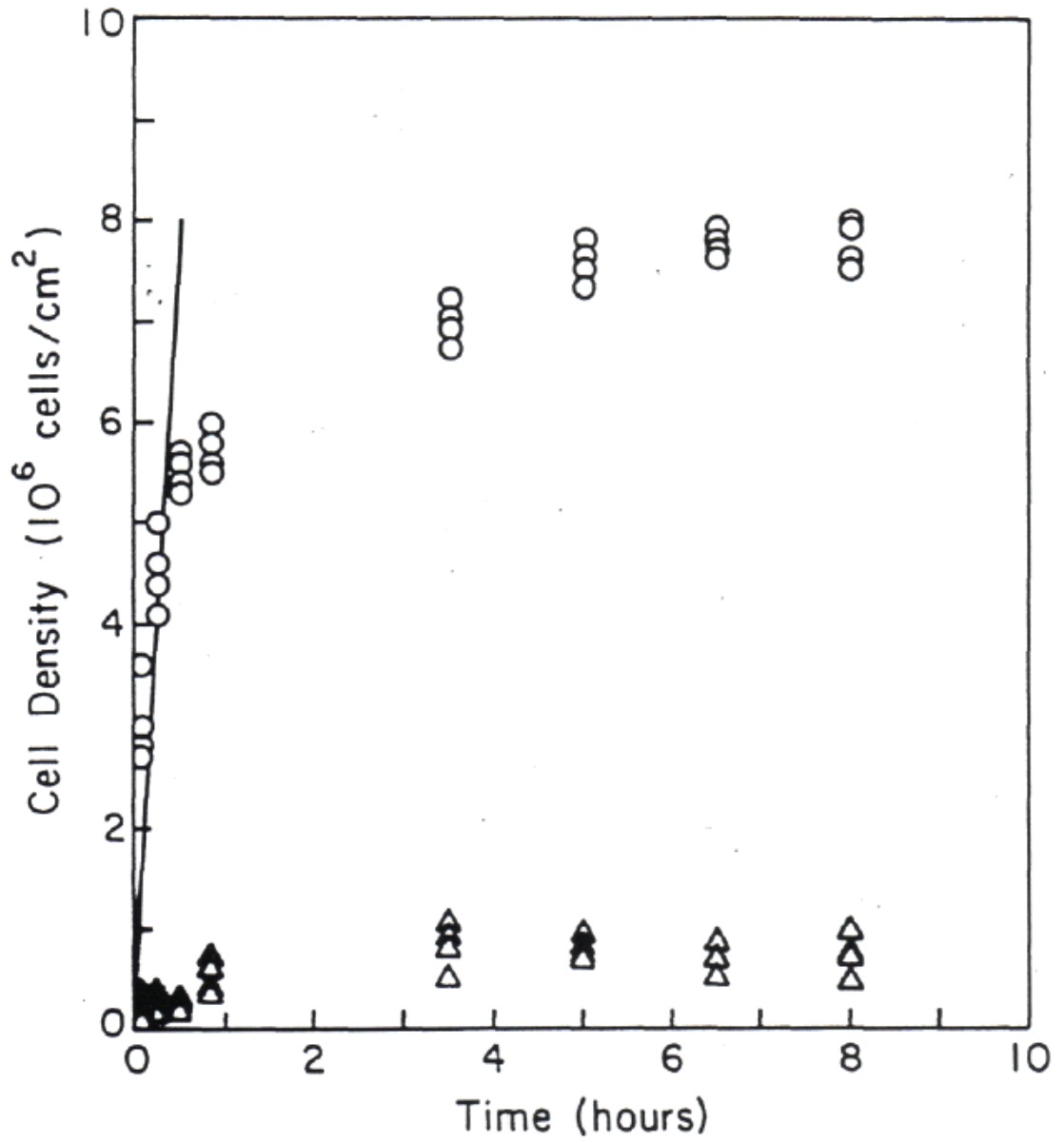


Figure A 1.6. Attachment of *P. atlantica* onto clean glass slides from a culture of constant OD = 2. Cellular attachment rate can be estimated from the initial slope as shown: (o) recirculation flow = 8 L/min, Re = 350; (Δ) recirculation flow = 50 L/min, Re = 2200.

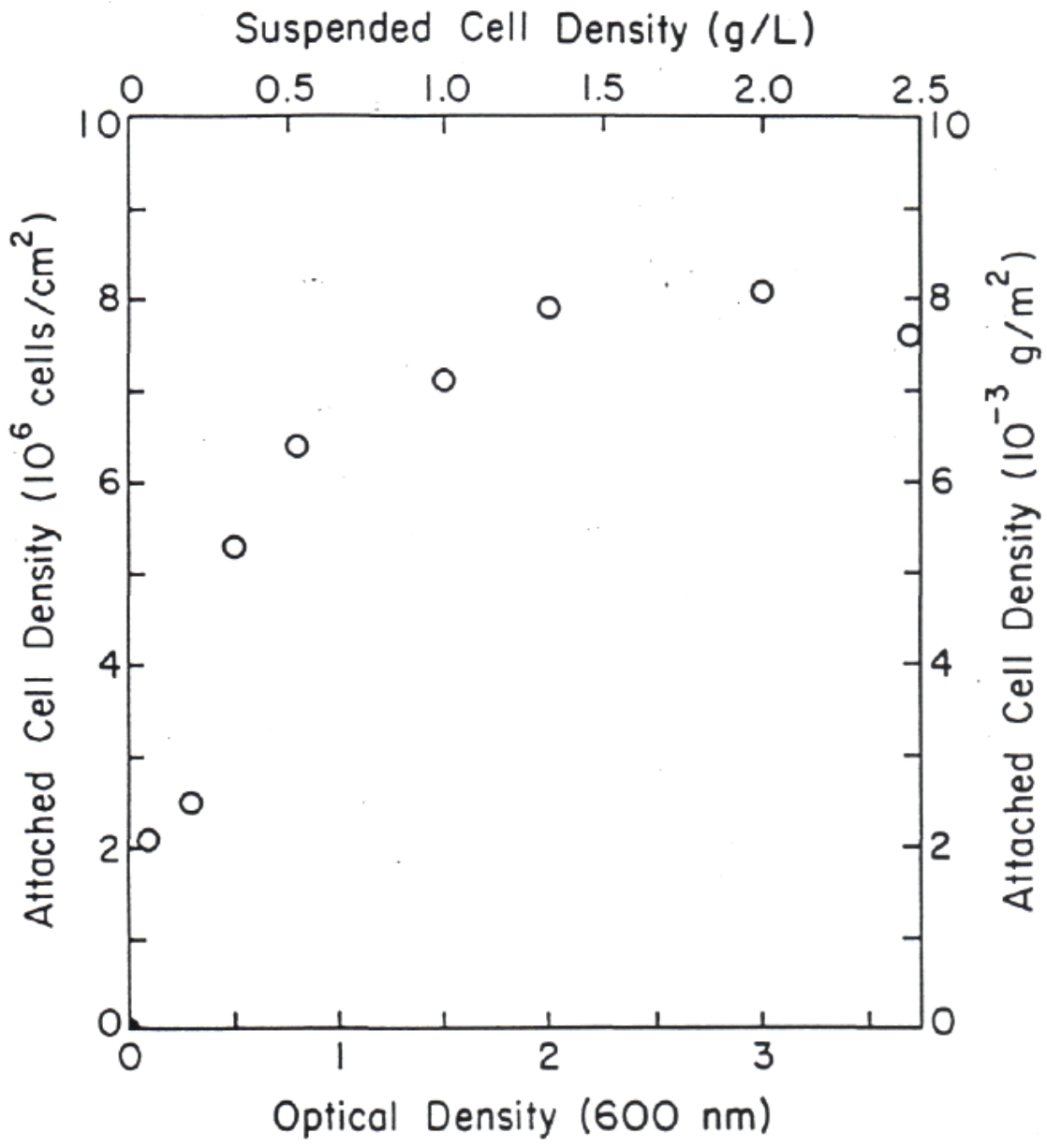


Figure A 1.7. Equilibrium attached cell density as a function of suspended cell concentration at Reynolds number of 300.

fact that attached cells do not wash out permits an adherent population to maintain itself in the reactor system.

The proposed dependence of biopolymer loss from the cell surface as a function of the relative amounts of P to A also seems plausible [see Eqs. (A1.2) and (A1.4)]. Although experimental results did not unequivocally prove the existence of a saturation constant, the model certainly corroborated well with qualitative observations. Batch growth data showed that as a cell grew, the amount of P increased relative to A, but after reaching a maximum, P/A subsequently decreased. In effect, in the model P and A "compete" for the limiting nutrient. A consequence of this formulation is that at higher dilution rate (0.2 vs. 0.25/hr) the slight increase in C^* and decrease in A result in a predicted increase in P that appears to be consistent with observations. The model assumes release of P produces P^* . In batch growth, accumulation of P^* should occur to a greater extent than observed unless a degradation term for P^* is included in the model. Metabolic degradation of P^* by cells of *P. atlantica* in the stationary growth stage has been observed (Hsieh, 1988).

As might be expected, the disparity between model predictions and data is greatest at the extremes, i.e., at long times during batch growth and at extremely low dilution rates during continuous growth. A model with higher degrees of structure or more complexity within the degree of structure employed would likely be necessary to more accurately predict data in these regimes as well as to simulate more complex attachment or biofilm systems. The progression of the model to one with higher degrees of structure was curbed by the objective of equal and concurrent development with experimental work. In other words, it was desired that any formulated mechanism and proposed parameter be measured or estimated from experiments. Because of the current novel (Structured) approach to

modeling bacterial attachment, the existence of supporting data in the literature is sparse. A more detailed model formulation was, therefore, not deemed appropriate at the present.

2. MODELLING LEAD(II) DISTRIBUTION IN THE PRESENCE OF MICROBIAL ACTIVITY

INTRODUCTION

A mechanistic understanding of trace metal removal processes has important implications both in natural aquatic systems, where the ability to predict the movement and fate of toxic species is desired, and in engineered systems, where such knowledge can aid in the design of water or wastewater treatment processes to maximize metal removal.

Adherent microorganisms are common in both natural and engineered aquatic systems. Their presence complicates the description of adsorption reactions between metals and solid surfaces by modifying surfaces through cellular growth and production of metal complexing agents such as extracellular polymers. Trace metals, in turn, affect microbial growth through their toxicity. Interactions between biofilms and trace metals have been reviewed by Lion, *et al.*, (1988).

The purpose of this paper is to experimentally characterize the interactions of a toxic trace metal and bacterial component at the solid-solution interface and to predict these interactions with a mechanistically based model. Separate models of microbial growth and metal speciation were integrated to make predictions without the use of adjustable parameters. Accomplishing these objectives necessitated fundamental studies of major system components which include the bacterium and associated microbial products, the solid surface, and the trace metal. The experimental apparatus (bioreactor) described by Hsieh, *et al.* (1985), allowed for independent study of the reactions between these major components under defined physical/chemical conditions.

MATERIALS

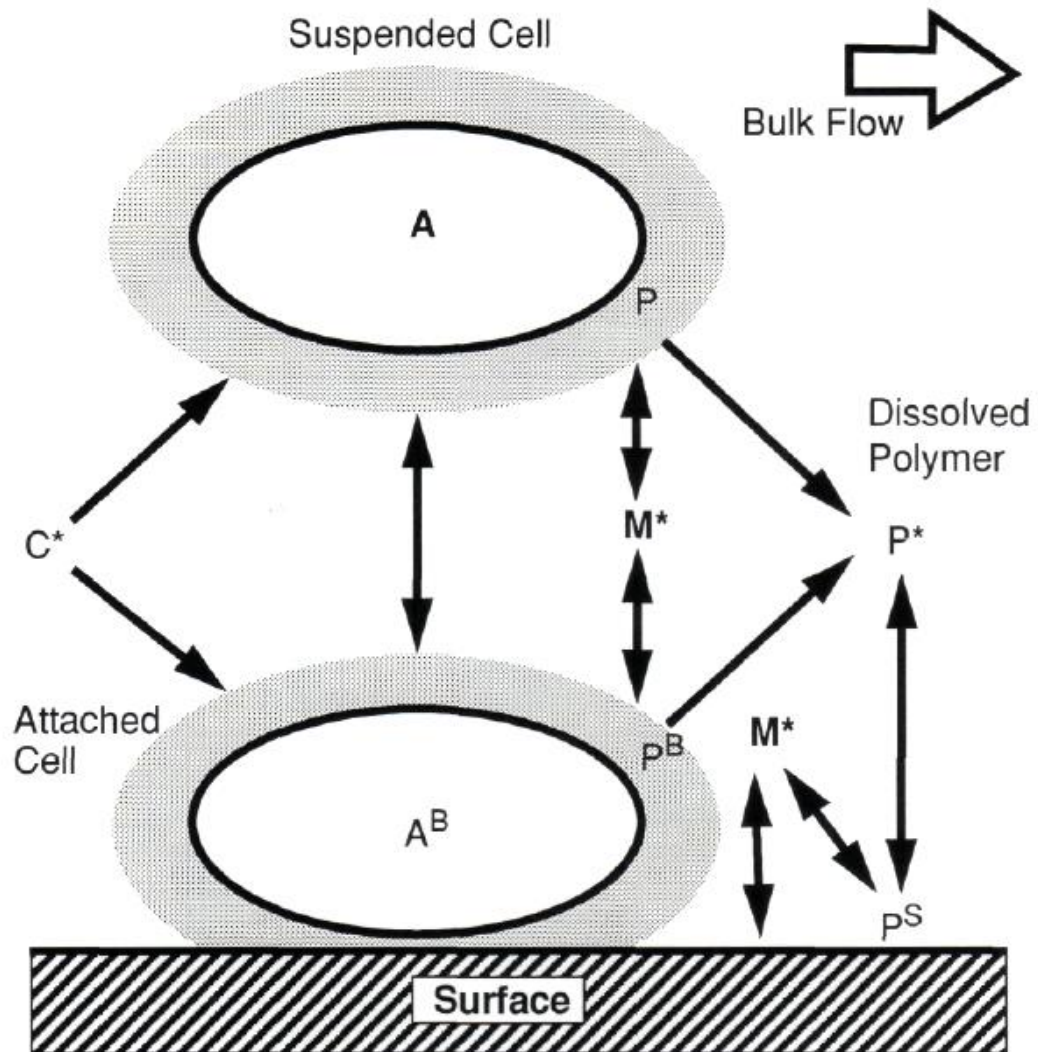
The experiments described here made extensive use of methods previously developed for characterization of a polymer forming bacterium and its interaction with a toxic trace metal. The bioreactor system and methods for analysis of cell and polymer concentrations as discussed in Hsieh, *et al.* (1985; 1990; 1994), Kellems and Lion (1989) and Lion and Rochlin (1989) describe analysis methods for ^{210}Pb and measurement of its binding constants with cells and extracellular polymer.

The experiments were performed using the marine film-forming bacterium *Pseudomonas atlantica* NSMB 301 (ATCC 19262). The composition of artificial seawater growth medium for the organism was that described by Hsieh, *et al.* (1985), with the modifications noted in Hsieh, *et al.* (1994).

The bioreactor system described by Hsieh, *et al.* (1985), was used to provide a controlled environment for either batch or continuous growth conditions. The reactor construction is of glass, polyethylene, and Teflon to minimize the possibility of trace metal contamination. Separate pumps for recirculation and medium addition permitted independent regulation of fluid residence time and the fluid velocity profile relative to the attachment substratum. Reactor preparation for experimental runs was described in Hsieh, *et al.* (1985).

MODEL DEVELOPMENT AND DERIVATION OF MODEL PARAMETERS

The presence of lead adds one additional variable, *i.e.*, metal ion toxicity, to the bacterial model described in Hsieh, *et al.* (1994). Interactions of the model components are illustrated in Figure A1.8. In addition to the toxic effect of lead (Pb) on the biophase,



Schematic of Model Component Interactions in the Presence of Metal

- A = Active biomass, suspended
- P = Biopolymer
- A^B = Active biomass, attached
- P^B = Biopolymers associated with A^B
- P* = Dissolved Biopolymer
- P^S = Surface sorbed biopolymer
- C* = Bulk limiting nutrient concentration
- M* = Free trace metal ion concentration

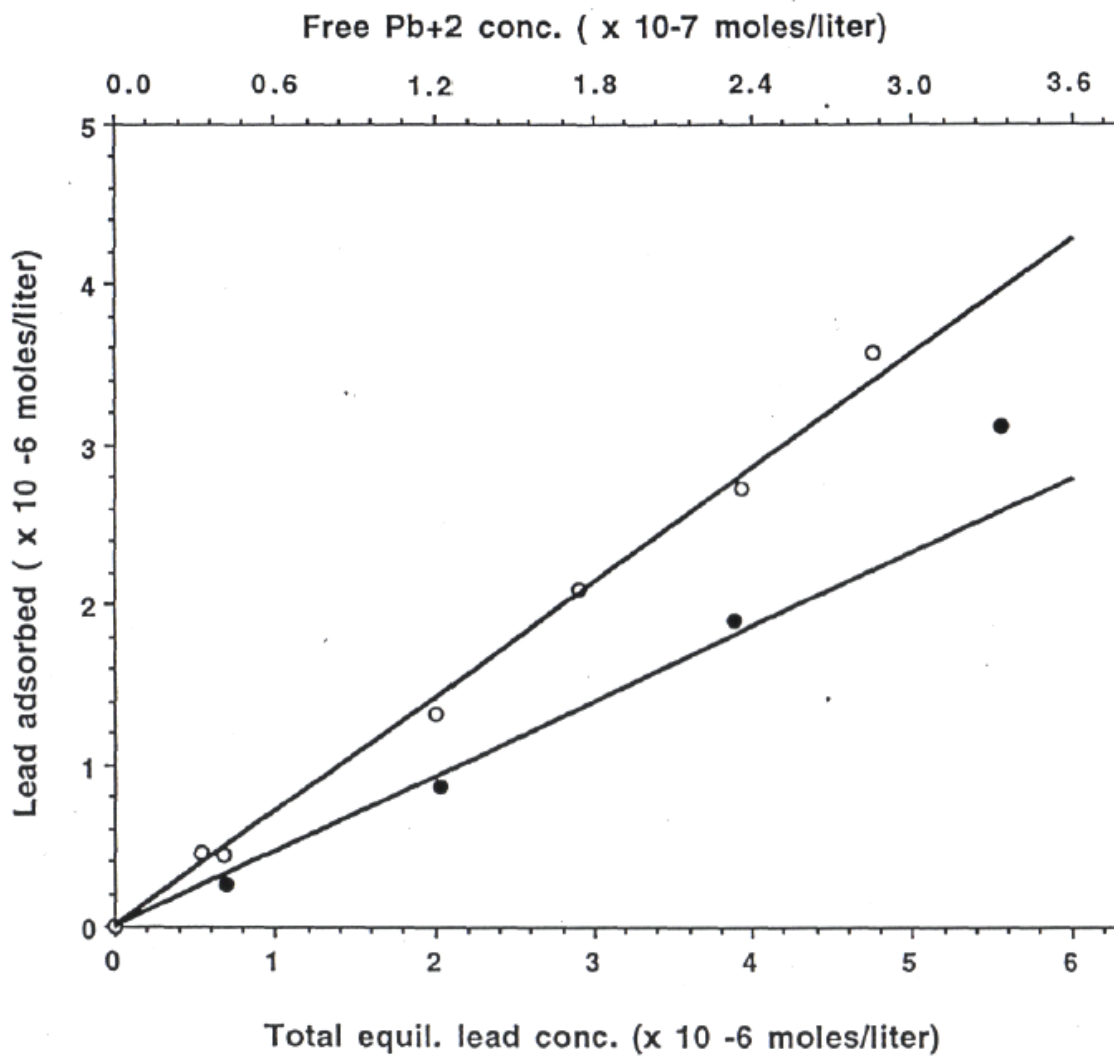
Figure A1-8. Schematic of model component interactions in the presence of metal. The arrows associated with M* represent binding with each component.

the biophase can influence metal speciation and partitioning through complexation and adsorption reactions. Experiments were carried out to determine the threshold and extent of Pb toxicity to *P. atlantica*. At a total lead concentration of 10^{-6} M (corresponding to 5×10^{-8} M Pb^{+2}/L) the extent of growth of *P. atlantica* was uninhibited (Hsieh, *et al.*, 1985). Beyond the threshold concentration, concentration of bacteria decreased logarithmically with increasing $[\text{Pb}^{+2}]$.

Before any simulation of lead distribution can be performed, lead binding constants with various solution components and experimental surfaces must be obtained. In the experimental system, Pb speciation was dictated by the concentration of inorganic ligands in the defined seawater media plus lead binding to the bioreactor surface (glass), bacterial cells, and bacterial biopolymer. Equilibrium lead adsorption to the bioreactor wall surfaces and with glass slides was previously evaluated by Hsieh, *et al.* (1985), and is shown in Figure A1.9. Lead adsorption by reactor walls and glass slides appeared to be reasonably linear with equilibrium total lead concentrations up to 5×10^{-6} M.

Equilibrium lead adsorption to bacterial cell surfaces was studied by Lion and Rochlin (1989). Equilibrium data, after correction for lead binding by dissolved polymer, are shown in Figure A1.10 (the Langmuir isotherm has been linearized by plotting the inverse of the amount adsorbed to cells the inverse of lead concentration). Based on a *P. atlantica* surface area of $467 \text{ cm}^2/10^{+10}$ cells (Corpe, 1975) and a measured solution concentration of $1.3 \times 10^{+12}$ cells/g, the calculated maximum adsorption density Γ_{maxC} and equilibrium adsorption constant, KC , are 9.75×10^{-8} M Pb/g cell and $4.84 \times 10^{+8}$ L/M Pb, respectively. Lion and Rochlin (1989) discuss the measurement of the equilibrium adsorption constants and the influence of dissolved bacterial polymer.

Figure A 1.9. Equilibrium lead adsorption onto glass and bioreactor walls. (From Hsieh, *et al.*, 1985). (○) adsorption onto glass and bioreactor walls (●) adsorption onto walls only



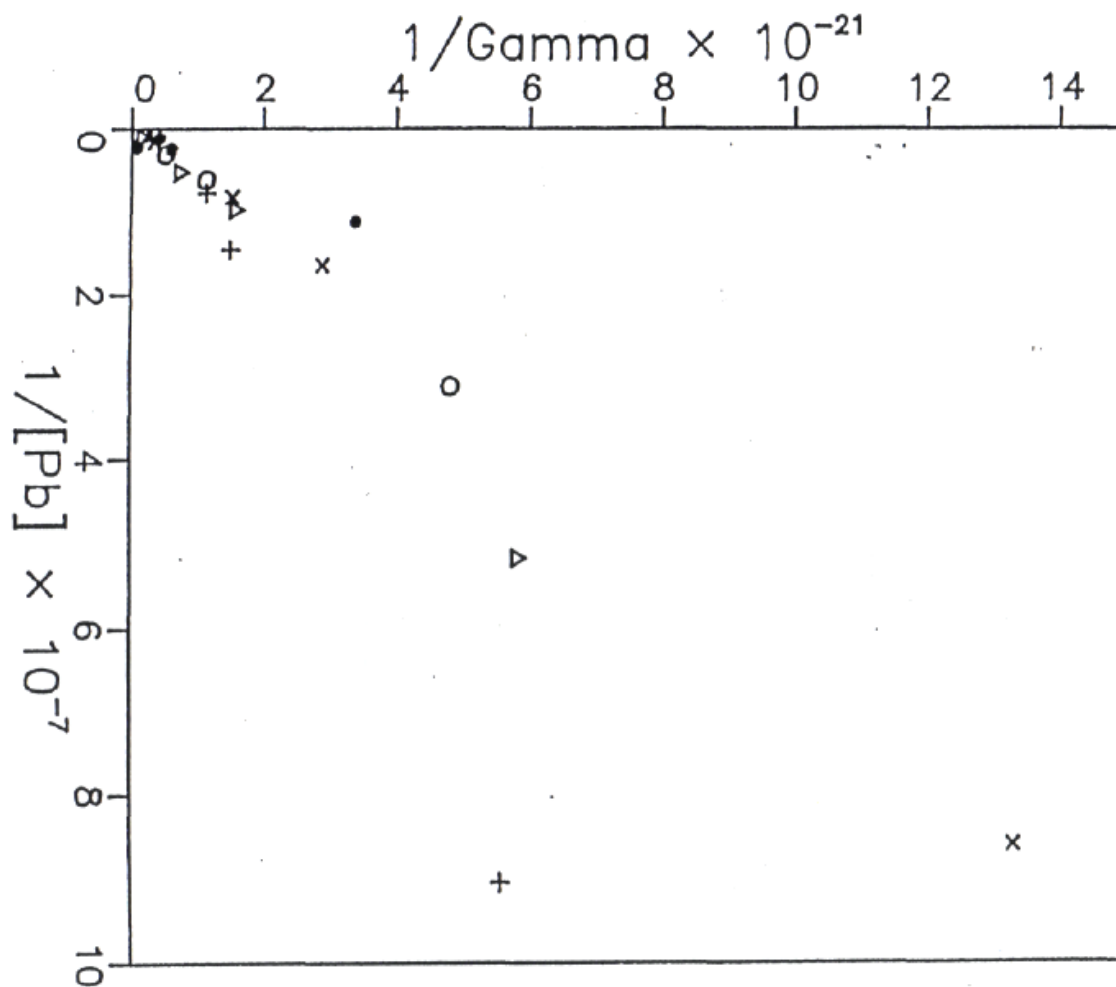


Figure A1.10. Equilibrium lead adsorption onto bacterial cells. Γ is adsorbed lead in moles per cell. Data are corrected for lead binding to dissolved organics (see Lion & Rochlin, 1989). Original data were obtained from Rochlin, 1986.

Kellems and Lion (1989) report lead binding constants for *P. atlantica* bacterial biopolymers. Their observed bimodal distribution fit of the polymer binding constants was used in the Pb speciation calculations performed here. The polymer Pb binding site density of 0.7×10^{-4} M Pb/g polymer reported by Corpe (1975) was employed for model calculations. This value provided a better fit to the observed data than did the value of 1.3×10^{-4} M Pb/g polymer reported by Harvey (1981) or the value of 1.9×10^{-4} M Pb/g polymer reported by Kellems and Lion (1989). For glass surfaces, a single binding site type was modeled (i.e., a Langmuir isotherm). A calculation using data from Figure A 1.9 yielded the linear region of the isotherm with a slope equal to the product of the maximum adsorption density, $\Gamma_{\max S}$, and the binding constant, K_S . A value of $\Gamma_{\max S}$ equal to 7.6×10^{-7} M Pb/m² for the surface of glass slides agreed best with subsequent observations in the bioreactor system and was in reasonable agreement with the value of 8.3×10^{-6} M Pb/ m² determined by Armistead, et al. (1969) for pure SiO₂. The resulting value for K_S was $2.4 \times 10^{+7}$ L/M (based on the product of $\Gamma_{\max S}$ and K_S determined from Figure A1.9). It should be noted that the Langmuir fit to the data in Figure A 1.10 was a matter of convenience, since $\Gamma_{\max S}$ and K_S were used as parameters input for spoliation calculations using the chemical equilibrium model MINEQL (Westall, *et al.*, 1976). An accurate estimate of $\Gamma_{\max S}$ can only be obtained from data that include the plateau region of the adsorption isotherm. A retrofit using the above values of $\Gamma_{\max S}$ and K_S agreed with data in Figure A 1.9.

The information on lead binding gathered above can be coupled with a structured model for the biophase (described in the article by Hsieh et al., 1994) and used to calculate lead distribution in a model aquatic system. The basic processes considered in the model and interactions with the addition of lead to the system are shown in schematic form in Figure

A1.8. It was assumed that lead is equally inhibitory to the growth of active cell mass of both suspended and attached cells. The equations for the net growth rate of suspended and attached cells described by Hsieh, et al. (1994), were modified to include the effects of metal toxicity and are given by:

$$r_A = \left[\mu_A \left(\frac{C^*}{K_{AC^*} + C^*} \right) \left(\frac{K_{AM^*}}{K_{AM^*} + M^*} \right) - k_{dA} \left(\frac{K_{dAC^*}}{K_{dAC^*} + C^*} \right) \right] A \quad (\text{A1.39})$$

$$r_{A^B} = \left[\mu_{A^B} \left(\frac{C^*}{K_{A^B C^*} + C^*} \right) \left(\frac{K_{A^B M^*}}{K_{A^B M^*} + M^*} \right) - k_{dA^B} \left(\frac{K_{dA^B C^*}}{K_{dA^B C^*} + C^*} \right) \right] A^B \quad (\text{A1.40})$$

The term of the form $K/(K + M^*)$ accounts for metal ion inhibition of cell growth and was initially formulated by Aiba, *et al.* (1968; 1969) for product inhibition. The value of K_{AM^*} and $K_{A^B M^*}$ was estimated to be 1.5×10^{-7} M Pb^{+2}/L , based on the observed toxicity threshold (Aiba, *et al.*, 1968) and subsequent bioreactor systems experiments.

Within the model structure, M^* represents free metal ion rather than total metal concentration. It has been shown that metal toxicity is related to free ion activity and metal which is adsorbed or complexed with inorganic or organic ligands is not toxic (e.g., Sunda & Gillespie, 1979; Zevenhuizen, *et al.*, 1979). Thus the distinction between total metal concentration and free metal ion concentration is important, particularly in transient systems where the quantities of agents which bind trace metals such as biopolymers, and bacterial cells can vary. In conjunction with a computer program (MINEQL) for the calculation of chemical equilibrium composition of aqueous systems developed initially by Westall, *et al.* (1976), the speciation of lead was calculated for the bioreactor system given the metal binding constants to polymers, cells, and the glass surface presented above. In a fully integrated model, interactions between the chemical speciation program and the model of

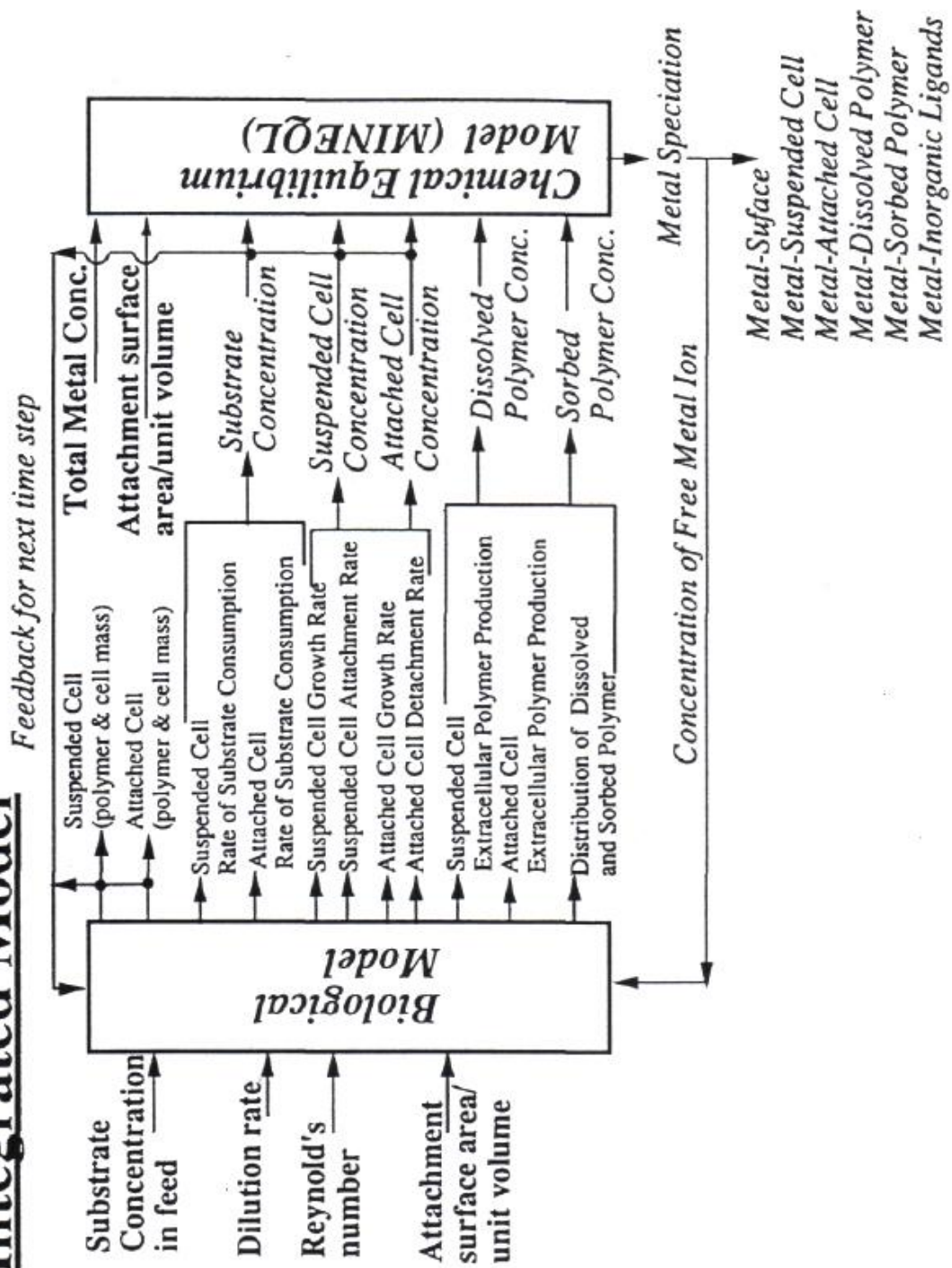
the biological components of the reactor system would occur to determine lead speciation at each time step. Given the status of cell and polymer concentrations, the chemical speciation program would yield the free lead ion concentration which would serve as an input into the bacterial model for the next iteration. The intended flow of information through the integrated models for the biophase and chemical speciation is illustrated in Figure A1.11. For the conditions considered in the experiments reported here, lead speciation was insensitive to changes in the concentration of cells and extracellular polymer. Therefore, computer time was saved by performing the simulations of the biological system with a constant free metal concentration and by using separate calculations with the speciation program to determine the concentrations of cell and polymer-bound lead.

MODEL PREDICTIONS AND COMPARISON TO EXPERIMENT

To test the validity of the combined bacterial and chemical speciation models, simulated results were compared to experiments. Initial experiments were carried out in a 2 L Multigen fermenter (New Brunswick, NJ) with a usable volume of 1.5 L. The Multigen was operated at a Reynolds number of 2000 and the wetted surface area of the reactor vessel (0.061 m^2) was used as an input in model simulations of results. Due to lead toxicity ($5 \times 10^{-7} \text{ M}$) in a continuous flow Multigen system, the maximum growth rate or washout occurred at a lower dilution rate (about 0.21 hr^{-1}) as compared to a system without lead (0.27 hr^{-1}) (see Hsieh, *et al.*, 1990). At a lower total lead concentration ($1 \times 10^{-7} \text{ M}$), the effect of lead on the biophase was predicted to be essentially negligible (Hsieh, 1985). At a higher total lead concentration ($1 \times 10^{-6} \text{ M}$), washout was predicted to occur at about 0.19 hr^{-1} (Hsieh, 1988). Lead binding by bacterial cells and biopolymers coincided with increases in these microbial components. Lead adsorption onto glass surfaces reached equilibrium after about 10 hours

Figure A1.11. Schematic of information flow in the integrated model.

Integrated Model



although the simulation assumed instantaneous equilibrium. The present form for the combined model does not consider chemical kinetics for adsorption and complexation reactions.

Effects on overall lead speciation in the experimental system due to attached bacteria and adsorbed biopolymer were negligible because of their sparse surface densities relative to suspended concentrations. Therefore, contributions to equilibrium lead distribution from bacterial components on the solid surfaces were substantially smaller than their counterparts in solution. Furthermore, lead partitioning coefficients for both bacterial cells and biopolymer were smaller than that for the solid (glass) surface. Thus significant contribution to metal partitioning arising from microbial components as reported previously was difficult to observe in the model experimental system (Brown & Lester, 1982a; Brown & Lester, 1982b; Chang, *et al.*, 19851; Corpe, 1975; Davis, 1984; Friedman & Dugan, 1968; Norberg & Persson, 1984). This was a result of the experimental necessity for use of a chemically defined medium in which lead speciation could be calculated. Metals such as Fe and Cu which are commonly added to enhance bacterial growth were excluded to prevent competition for dissolved ligands and surface sites. In addition, organic substances such as yeast, or peptone and vitamins which do not have defined metal binding constants were also excluded. As a result, the growth rate of the test organism was slow and its ability to form a thick biofilm was impaired.

To test the transient responses of the model to fluctuations in lead concentrations, step increases in lead levels were studied, both in experiments in the bioreactor and in computer simulation. The bacteria were first grown batch-wise, and then switched to

continuous mode after reaching stationary phase, all in the absence of lead. When steady state was reached (at about 132 hr), lead was added to the desired level. The system was then allowed to reach a new steady state. With increasing dilution rate, the effect of lead became noticeable. Model predictions indicated that due to lead toxicity, the active cell mass concentration, A , decreased, and that the biopolymer concentration, P , increased. An increase in biopolymer concentration as a result of the presence of toxic molecules has been observed previously (Jones, 1970).

CONCLUSIONS

A relatively simple structured model was adopted to describe the dynamic behavior of adherent cells and their extracellular polymer. Model structure was necessitated by the fact that cell and polymer concentrations do not covary but display their own unique production characteristics. Use of structure is also necessitated since both the concentrations of suspended and attached cells as well as dissolved and sorbed polymer can influence metal phase distribution. Given this model, which describes the temporal behavior of metal adsorbing surfaces (*i.e.*, cells) and dissolved ligands (*i.e.*; extracellular polymer), it is a relatively straight forward process to modify the model to predict the effects of these variations on trace metal concentration.

Overall, model simulation results correspond relatively well with experiments. The soundness of the combined model depends on the mechanisms of the bacterial model as well as the accuracy of lead partitioning coefficients derived for the various bacterial and surface components. Thus a lack of information on the mechanism of the effect of lead on biopolymer production ultimately affects predicted lead partitioning

due to biopolymers even if the coefficients were reliably obtained through independent experiments.

The overall high degree of qualitative correlation between the model and observation suggests the validity of the model mechanisms. Further experimental information and potential additions to the model structure would be required to better correlate the transient behavior and to enable the model to apply to a wider range of operating conditions. For example, polymer production rate is at present only indirectly influenced by metal toxicity through its effect on cell concentration. Since the polymer is produced in the absence of cell growth a direct metal influence of polymer metal on production could be included as a future modification to the model. This modification would be desirable only if independent experiments could be designed to obtain the necessary inhibition constants.

The predictive capability of lead distribution in a bioreactor demonstrated above was the objective of this work. Although the model, in its current form, is applicable to a specific system, i.e., to a single bacterium, extracellular polymer, trace metal, and solid surface, the model can be extended to describe a more complex aquatic system. The nature of the modifications would depend upon the interactions which were to be considered. For example, use of a marine bacterium in the seawater matrix permitted use of conditional binding constants (i.e., constant ionic strength and pH) which would not be necessarily pertinent in a dilute fresh water electrolyte. Incorporation of pH dependence for the chemical and biological reactions would then be necessary.

ACKNOWLEDGEMENTS

This research was supported, in part, by NSF grants CEE-8304120 and BCS-8617408.

NOMENCLATURE

a	Total surface area
A	"Active" cell mass concentration; i.e., the concentration of cell mass stripped of its extracellular polymer
A^B	The concentration of attached or bound active cell mass
B	Total attached biomass ($= A^B + P^B$)
B^{\max}	Maximum attached biomass concentration
C^*	Substrate (glucose) concentration
D	Dilution rate (inverse of hydraulic retention time)
f_{AP}	The fraction of active cell mass (A) which is converted to cell-bound polymer (P) as active cell mass degrades
f_A^B	The fraction of attached active cell mass (A) which is converted to attached cell-bound polymer (P^B) as active cell mass degrades
k_{dA}	Maximum decomposition rate of active cell mass in suspension
k_{dA}^B	Maximum decomposition rate of attached active cell mass
k_P	Biopolymer partition coefficient
k_{dP^*}	Biopolymer degradation rate constant
k^A	Rate of biomass attachment
k^D	Rate of biomass detachment
K_{AC^*}	Saturation, or half-velocity, coefficient for growth of suspended cells
K_A^B	Saturation, or half-velocity, coefficient for growth of attached cells

K_{PC^*}	Saturation, or half-velocity, coefficient for production of polymer associated with suspended cells
$K_{P^B C^*}$	Saturation, or half-velocity, coefficient for production of polymer associated with attached cells
K_{P^*P}	Saturation, or half-velocity, coefficient for production of dissolved polymer, (P^*), from cell-bound polymer of suspended cells, (P)
$K_{P^*P^B}$	Saturation, or half-velocity, coefficient for production of dissolved polymer, (P^*), from cell-bound polymer of attached cells, (P^B)
K_{dAC^*}	Saturation, or half-velocity, coefficient for decomposition of suspended cells
$K_{dA^B C^*}$	Saturation, or half-velocity, coefficient for decomposition of attached cells
Q	Volumetric flow rate of nutrients into a continuous bioreactor system
P	The concentration of polymer associated with suspended cells
P^*	The concentration of dissolved polymer
P^S	The concentration of surface sorbed polymer
P^B	The concentration of polymer associated with attached cells
r_A	Net rate of change of active cell concentration in suspension
$r_{A, \text{syn}}$	Rate of growth of active cell mass in suspension
r_A^B	Net rate of change of attached cell mass
$r_{A^B, \text{syn}}$	Rate of growth of attached cell mass
r_B	Net rate of change of attached biomass (attached cells plus attached cell-bound polymer) concentration
r_{C^*}	Rate of change of growth limiting substrate concentration
r_{p^*}	Net rate of change of dissolved polymer concentration

r_p	Net rate of change of suspended cell-bound polymer concentration
$r_{p,\text{syn}}$	Rate of production of suspended cell-bound polymer
r_p^B	Net rate of change of attached cell-bound polymer
$r_{p,\text{syn}}^B$	Rate of production of attached cell-bound polymer
r_p^S	Net rate of change of sorbed polymer
r_X	Net rate of change of suspended biomass (cells plus cell-bound polymer) concentration
Re	Reynolds number
V	Total reactor volume
X	Total suspended biomass (= A + P)
α_A	Stoichiometric coefficient (inverse yield) for synthesis of suspended cells from substrate
α_A^B	Stoichiometric coefficient (inverse yield) for synthesis of attached cells from substrate
α_P	Stoichiometric coefficient (inverse yield) for synthesis of bound polymer on suspended cells from substrate
α_P^B	Stoichiometric coefficient (inverse yield) for synthesis of bound polymer on attached cells from substrate
μ_A	Maximum growth rate for suspended cells
μ_A^B	Maximum growth rate for attached cells
μ_P	Maximum rate for production of cell-bound polymers on suspended cells
μ_P^B	Maximum rate for production of cell-bound polymers on attached cells
μ_{P^*}	Maximum production rate of dissolved polymer from suspended cells

$\mu_{P^*}^B$

Maximum production rate of dissolved polymer from attached cells

REFERENCES

Aiba, S., Shoda, M. and Nagatani, M. 1968. Kinetics of Product Inhibition in Alcohol Fermentation. *Biotechnol. Bioeng.* 10: 845-864.

Aiba, S. and Shoda, M. J. 1969. Reassessment of the Product Inhibition in Alcohol Fermentation. *J. Ferment. Technol. Jpn.* 47: 790-794.

Armistead, C.G., Tyler, A.J., Hambleton, F.H., Mitchell S.A. and Hockey, J.A. 1969. Surface Hydroxylation of Silica. *Phys. Chem.*, 73: 3947-3953.

Bakke, R., Trulear, M.G., Robinson, J.A. and Characklis, W.G. 1984. Activity of *Pseudomonas aeruginosa* in Biofilms: Steady State. *Biotechnol. Bioeng.* 26: 1418-1428.

Benfield, L. and Molz, F. 1985. Mathematical Simulation of a Biofilm Process. *Biotechnol. Bioeng.* 27: 921-931.

Brown, M.J. and Lester, J.N. 1982a. Role of Bacterial Extracellular Polymers in Metal Uptake in Pure Bacterial Culture and Activated Sludge. I. Effects of Metal Concentration. *Water Res.* 16: 1539-1548.

Brown, M.J. and Lester, J.N. 1982b. Role of Bacterial Extracellular Polymers in Metal Uptake in Pure Bacterial Culture and Activated Sludge. II. Effects of Mean Cell Residence Time. *Water Res.* 16: 1549-1560.

Bryers, J.D. 1984. Biofilm Formation and Chemostat Dynamics: Pure and Mixed Culture Considerations. *Biotechnol. Bioeng.* 26: 948-958.

Chang, S.-Y., Huang, J.-C. and Liu, Y.-C. 1985. Heavy Metal Removal in a Fixed-Film Biological System, pp. 103-108. In: R.W. Peters and B.M. Kim (Eds.), *Separation of Heavy Metals and Other Trace Contaminants*. Vol. 81. AIChE Symposium Series No. 243. American Institute of Chemical Engineers, New York.

Characklis, W.G. 1981. Fouling Biofilm Development: A Process Analysis. *Biotechnol. Bioeng.* 23: 1923-1960.

Corpe, W.A. 1970. An Acid Polysaccharide Produced by a Primary Film Forming Marine Bacterium. *Dev. Ind. Microbiol.* 11: 402-412.

Corpe, W.A. 1975. Metal-Binding Properties of Surface Materials From Marine Bacteria. *Dev. Ind. Microbiol.* 16: 249-255.

Costerton, J.W., Geesey, G.G. and Cheng, KJ. 1978. How Bacteria Stick. *Sci. Am.* 238: 86-95

Davis, J.A. 1984. Complexation of Trace Metals by Adsorbed Natural Organic Matter. *Geochim. Cosmochim. Acta.* 48: 679-691.

Denn, M.M. 1980. *Process Fluid Mechanics*, Prentice Hall, Inc.; Englewood Cliffs, N.J.

Domach, M.M., Leung, S.K., Cahn, R.E., Cocks, G.G. and Shuler, M.L. 1984. Computer Model for Glucose-Limited Growth of a Single Cell of *Escherichia coli* B/r-A. *Biotechnol. Bioeng.* 26: 203-216.

Droste, R.L. and Kennedy, K.J. 1986. Sequential Substrate Utilization Factor in Fixed Biofilms. *Biotechnol. Bioeng.* 28: 1713-1720.

Fredrickson, A.G., Ramkrishna D. and Tsuchiya, H.M. 1971. Necessity of Including Structure in Mathematical Models of Unbalanced Microbial Growth. *Chem. Engr. Symp. Series.* 67: 53-59.

Friedman, B.A. and Dugan, P.R. 1968. Concentration and Accumulation of Metallic Ions by the Bacterium *Zoogloea*. *Dev. Ind. Microbiol.* 9: 381-388.

Groleau, D. and Yaphe, W. 1977. Enzymatic Hydrolysis of Agar: Purification and Characterization of β -Neoagarotetraose Hydrolase From *Pseudomonas atlantica*. *Can. J. Microbiol.* 23: 672-679.

Harvey, R.W. 1981. Lead-Bacterial Interactions in an Estuarine Salt Marsh Microlayer. Ph.D. Dissertation. Stanford University, Stanford, CA.

Hsieh, K.M. 1985. Design of a Bioreactor System for the Study of the Interactions of Trace Metals and Microbial Cells at the Solid Solution Interface. M.S. Thesis. Cornell University, Ithaca, NY.

Hsieh, K.M. 1988. The Growth and Attachment of a Biopolymer Producing *Pseudomonas* Species and the Characterization of its Interactions with a Toxic Trace Metal. Ph.D. Dissertation. Cornell University, Ithaca, NY.

Hsieh, K.M., Lion, L.W. and Shuler, M.L. 1985. Bioreactor for the Study of Defined Interactions of Toxic Metals and Biofilms. *Appl. Environ. Microbiol.* 50: 1155-1161.

Hsieh, K.M., Lion, L.W. and Shuler, M.L. 1990. Production of extracellular and Cell-Associated Biopolymers by *Pseudomonas atlantica*. *Biotechnol. Let.* 12: 449-454.

Hsieh, K.M., Murgel, G.A., Lion, L.W. and Shuler, M.L. 1994. Interactions of Microbial Biofilms With Toxic Trace Metals: 1. Observation and Modeling of Cell Growth, Attachment and Production of Extracellular Polymer. *Biotechnol. Bioeng.*, to appear.

Jones, G.E. 1970. Metal Organic Complexes formed by Marine Bacteria. In: D.W, Hood (Ed.), Organic Matter in Natural Waters. Occasional Pub. No. 1, Inst. of Mar. Sci, College, Alaska, pp. 301-319.

Kellems, B. and Lion, L.W. 1989. Effect of Bacterial Exopolymer on Lead (II) Adsorption by $\gamma\text{Al}_2\text{O}_3$ in Seawater. Est., Coast. and Shelf Sci. 28: 443-457.

Lion, L.W., Hsieh, K.M., Shuler, M.L. and Ghiorse, W.C. 1988. Trace Metal Interactions with Microbial Biofilms in Natural and Engineered Systems. CRC Critical Rev. in Env. Control. 17: 273-306.

Lion, L.W. and Rochlin, K.L. 1989. Adsorption of Pb(II) by a Marine Bacterium, the Effect of Cell Concentration and pH. Est., Coast. and Shelf Sci. 29: 11-22.

Mian, F.A., Jarman T.R. and Righelato, R.C. 1978. Biosynthesis of Exopolysaccharide by *Pseudomonas aeruginosa*. J. Bacteriol. 134: 418-422.

Morel, F.M.M., Rueter, J.G., Anderson, D.M. and Guillard, R.R.L. 1979. AQUIL: A Chemically Defined Phytoplankton Culture Medium for Trace Metal Studies. J. Phycol. 15: 135-141.

Namkung, E. and Rittmann, B.E. 1987a. Modeling Bisubstrate Removal by Biofilms, Biotechnol. Bioeng. 29: 269-278.

Namkung, E. and Rittmann, B.E. 1987b. Evaluation of Bisubstrate Secondary Utilization Kinetics by Biofilms. *Biotechnol. Bioeng.* 29: 335-342.

Norberg, A.B. and Persson, H. 1984. Accumulation of Heavy-Metal Ions by *Zoogloea ramigera*. *Biotechnol. Bioeng.* 26: 239.

Pirt, S.J. 1975. Principles of Microbe and Cell Cultivation. Blackwell Scientific Publications, Oxford, England.

Rittmann, B.E. and McCarty, P.L. 1980. Model of Steady-State Biofilm Kinetics. *Biotechnol. Bioeng.* 22: 2343-2357.

Robinson, J.A., Trulear, M.G. and Characklis, W.G. 1984. Cellular Reproduction and Extracellular Polymer Formation by *Pseudomonas aeruginosa* in Continuous Culture. *Biotechnol. Bioeng.* 26: 1409-1417.

Shuler, M.L. 1985. Dynamic Modeling of Fermentation Systems. In: Comprehensive Biotechnology, Vol. 2., M. Moo-Young (Ed). Pergamon Press, Oxford, England.

Suidan, M.T. 1986. Performance of Deep Biofilm Reactors. *J. Environ. Engr.* 112: 78-93.

Sunda, W. and Gillespie, P.A. 1979. The Response of a Marine Bacterium to Cupric Ion and Its Use to Estimate Cupric Ion Activity in Seawater. *J. Mar. Res.* 37; 7(51-777).

Trulear, M.G. and Characklis, W.G. 1982. Dynamics of Biofilm Processes. *J. Water Poll. Control Fed.* 54: 1288-1381.

Vavilin, V.A. 1987. A Model of Spatial separation of Heterogeneous Biomass in Fixed-Film Reactor for Biological Treatment. *Biotechnol. Bioeng.* 29: 142-145.

Warner, O. and Gujer, W. 1986. A Multispecies Biofilm Model. *Biotechnol. Bioeng.* 28: 314-328.

Westall, J.C., Zachary, J.L. and Morel, F.M.M. 1976. MINEQL, a Computer Program for the Calculation of Chemical Equilibrium Composition of Aqueous Systems. Technical Note No. 18, Department of Civil Engineering, MIT, Cambridge, MA.

Zevenhuizen, L.P.T.M., Dolfig, J., Eshuis, E.J. and Scholten-Koerselman, I.J. 1979, Inhibitory Effects of Copper on Bacteria Related to the Free Ion Concentration. *Microb. Ecol.* 5: 139-146.

APPENDIX II
DESCRIPTION OF THE INTEGRATED MODEL WITH pH-DEPENDENT
GROWTH ROUTINES

The derivation of the bacterial model was described in Chapter 4. The actual programming structure is discussed here. The program discussed evolved from the original model of Hsieh (1988). The revised program was written in structured FORTRAN 77 and run in a DEC VAX 6310 under VMS 6.0.

The revised program combined previously separated programs into a single master program with subroutines. Provisions have been made to allow for batch and continuous modes of operation and to allow for simulating system perturbations, *i.e.*, transient model behavior can be observed by altering operating conditions at any time during continuous operation. To perform these different operating modes, the main program calls subroutines BATCH6, CTN6, and CTN6STEP, where necessary.

The program also contains the chemical speciation program MINEQL. The routine used was a revision of the version implemented initially by Westall *et al.* (1976). This part of the program was used with minimal modifications made to tailor it to the needs of the current research. The modifications made were mainly to allow its execution within the limitations of the VAX 6310. Changes in output formats and internal data transfer from files into arrays for use in the program were implemented to improve the efficiency and decrease CPU time to complete an analysis. This latter adjustment was essential because the program is designed to allow an input call from the main bacterial model at each time the bacterial model outputs new system component concentrations.

The model algorithm can be briefly summarized as follows:

- (1) Main program module BIO_MOD initializes several variables necessary to control selection of needed subroutines called for desired analysis with exclusion of all unneeded routines. Initial call is to the bacterial model MOD6CTN3.
- (2) Input parameters, initial conditions and sequence constants are read from CONST7CTN.DAT.
- (3) Initial check is whether a metal species is present. If there is no metal, biophase components are allowed to increase growth in a batch mode by calculating appropriate rate equations including corrections for specified solution pH. The entire batch growth data are written to file OUTP6.DAT.
- (4) At a specified point during batch growth (where initial conditions are redefined), the system may be switched to continuous mode. OUT6BAT.DAT contains batch growth data up to the onset of continuous feed. Biophase components are allowed to continue to increase growth in the continuous mode by calculating appropriate rate equations including corrections for specified solution pH. The entire continuous growth data for specified durations are written to file OUT6CTN.DAT.
- (5) A step change in operating conditions may be performed after steady State is reached in the continuous growth phase. Changed parameter values are read from CONST7CTN2.DAT. Again, continuous growth data calculated from appropriate rate equations including corrections for specified solution pH with time following the step change are written to OUT6STEP.DAT.
- (6) Continuous data as a function of dilution rate before the step change are written to OUT6.DAT and continuous data after the step change are written to OUT62.DAT.

- (7) If the initial check for a metal species indicates one is present, the program MOD6CTN3 calls subroutine CONVERT2.DAT. The necessary conversion factors were provided from this file to prepare the input concentration data in MMSTESTMETAL.DAT to be input into the array OSYS_DAT. Subroutine MINEQL is called for a speciation calculation, including correction for ionic strength greater than zero, using the data in the array OSYS_DAT and returns the value of the free-metal concentration for use in the bacterial growth calculations.
- (8) With a metal present during batch and continuous growth calculations, the corresponding subroutines will call subroutine CONVERT3.DAT at preselected time intervals to perform a recalculation of the free metal concentration to discern the effects of the bacterial growth on the speciation of the metal. The necessary conversion factors were provided from CONVERT3.DAT to prepare the input concentration data in MMSTEST.DAT to be input into the array OSYS_DAT. Subroutine MINEQL is called for a speciation calculation, including correction for ionic strength greater than zero, using the data in the array OSYS_DAT and returns the value of the free-metal concentration for use in the next iteration of the bacterial growth calculations.
- (9) If the metal is only present in the step change in operating conditions, the program MOD6CTN3 performs batch and continuous growth phases as if there were no metal present (steps 2 to 4 above). The step change subroutine OUT6STEP then performs the iterative calculations previously described in steps 7 and 8 above.
- (10) Upon completion of calculations for all of the above steps, if included, program control returns to BIO_MOD where it checks whether calculations of metal surface

adsorption are needed. Subroutine READAT is called to perform the calculations. Data in CONVERT1.DAT indicates the source of output data from the bacterial growth model. This data is combined with the output data from MINEQL contained in the array DATA_DAT. Calculated surface adsorption results are output in the file PLOTLTN.DAT.

- (11) The speciation results contained in any of the output files OUTP6.DAT, OUT6.DAT, OUT62.DAT, OUT6CTN.DAT, OUT6STEP.DAT, or OUT6BAT.DAT can be read by a plotting routine and shown in graphical form, as all the figures in Chapter 5 were plotted.

Examples of plots shown in this thesis as a function of solution pH made from program output files are as follows: Batch growth data as shown in Figure 5.2 through 5.9 were plotted from OUTP6.DAT. Continuous data for Figure 5.10 through 5.16 were plotted from OUT6.DAT. Continuous data as shown in Figures 5.43 to 5.48 were obtained from several data files. OUT6BAT.DAT contains data from time = 0 to about 12 hr. OUT6CTN.DAT contains data from time = 12 to about 132 hr. OUT6STEP.DAT contains data from time = 132 to about 250 hr. Different versions of the above three files correspond to the different dilution rates used. For example, if Figure 5.56 at $D = 0.155$ were plotted from OUT6BAT.DAT; 10, OUT6CTN.DAT; 10, and OUT6STEP.DAT; 10, Figure 5.57 at $D = 0.24$ may have been plotted from version 17, and so on.

A listing of BIO_MOD with its entire attendant subroutines including MINEQL are shown below. Sample input files CONST7CTN.DAT, CONST7CTN2.DAT, CONVERT1.DAT, CONVERT2.DAT, CONVERT3.DAT, MMSTESTMETAL.DAT, and MMSTEST.DAT are shown below after the program listing. The program reads these input

files with a fixed format, meaning that the parameter values must be entered in the indicated standard or exponential notation with a decimal point present. Each parameter occupies a line. The parameter name, units, and other variables required by the program are also listed. The parameter names correspond to those used in previous chapters. For example, KACR is K_{AC}^* , MUA is μ_A , and so on.

Comment lines within the program detail programming steps with logic rationale and list all input files read and output files created. The program listed below includes the metal toxicity and pH dependencies. The presence of the metal dependency does not affect the execution of the bacterial program in the absence of metal, as long as the initial metal concentration is set to zero. The program user is referred to the MINEQL documentation for further information on running MINEQL.

REFERENCE

Hsieh, K.M. 1988. The Growth and Attachment of a Biopolymer Producing *Pseudomonas* Species and the Characterization of its Interactions with a Toxic Trace Metal. Ph.D. Thesis. Cornell University, Ithaca, NY.

Westall, J.C., J.L. Zachary, and F.M.M. Morel. July 1976. MINEQL-A Computer Program for the Calculation of Chemical Equilibrium Composition of Aqueous Systems. Technical Note No. 18, Water Quality Laboratory. Department of Civil Engineering, Massachusetts Institute of Technology, Cambridge, MA.

C Program -- pHMODEL.for;16 Operational II/ 4/94

PROGRAM BIO_MOD

* THIS BIOFILM PROGRAM IS DESIGNED FOR MORE ORDERLY AND QUICKER EXECUTION
* IN RUNNING POSSIBLE COMBINATIONS OF BATCH, CONTINUOUS, STEP INCREASE/DE-
* CREASE MODES WITH OR WITHOUT METALS PRESENT AND WITH pH-DEPENDENCY OF
* BACTERIAL, GROWTH.
* CHARACTER STRING ARRAY TO REPLACE SEPARATE FILES IN RAM MEMORY FOR FASTER
* ACCESS.

CHARACTER *80 OSYS_DAT(10000)
COMMON/OSYBDAT/OSYS_DAT, IROW

*

* DEFINING A VARIABLE TO RETURN FREE METAL VALUES FROM MINIQL.

DOUBLE PRECISION FM
COMMON/FM_DAT/FM

*

* DEFINING THE COUNTER FOR ALLOWING METAL CALCULATIONS OR OMITTING THEM.

COMMON/METAL/IMETAL

*

* DEFINE A VARIABLE TO ALLOW OR OMIT SURFACE ADSORPTION CALCULATIONS.

COMMON/SURFACE/ISURF

*

* DEFINE A VARIABLE FOR OUTPUT OF MINEQL DATA FOR READAT ROUTINE IF NOT
* SUCCESSFUL GENERATING THE DATA FILES FROM THE FULL PROGRAM DUE TO
* STOPPING WITH DIVIDE BY ZERO ERRORS AS SOME COMPONENTS BECOME NEGLIGIBLY
* SMALL.

INTEGER DAT_ROW
COMMON/DATROW/DAT_ROW

*

* CHARACTER STRING ARRAY FOR RETURNING CELL/POLYMER SPECIATION WITH METALS
* FROM MINIQL FOR SURFACE ADSORPTION ANALYSIS.

CHARACTER *9 DAT_DAT(10)
COMMON/DATDAT/DAT_DAT

*

CHARACTER *9 DATA_DAT(256)
COMMON/DATADAT/DATA_DAT

*

* CALL FOR THE BIOFILM GROWTH MODEL OPERATION.

PRINT *, ''
PRINT *, 'MOD6CTN3 executing ... '

*

CALL MOD6CTN3

*

* RETURN FROM BIOFILM MODEL.

PRINT *, 'Ok ... MOD6CTN3 terminated normally !'

*

* CHECK WHETHER SURFACE METAL SPECIATION CALCULATIONS ARE NEEDED.

* PROCESSING WILL BE DONE IN A BATCH ROUTINE RATHER THAN CALLS TO MINIQL

* DURING THE RUNNING OF THE BIOFILM MODEL WITH METAL PRESENT.

IF (ISURF.EQ.O) THEN
GO TO 100

```

ELSE
ENDIF
*
OPEN (UNIT=11,NAME='PLOTILN.DAT',TYPE='NEW',FORM='FORMATTED',
1  CARRIAGECONTROL='LIST')
*
PRINT *,''
PRINT *,'READAT executing ...'
*
CALL READAT
*
PRINT *,'Ok ... READAT terminated normally!'
PRINT *,''
*
CLOSE (UNIT = 11)
*
100 STOP 'BIO_MOD execution is now complete ... check output!'
END
*****
*****
SUBROUTINE MOD6CTN3
*****
* BIOFILM PROGRAM CONTAINING BOTH BATCH AND CONTINUOUS MODES
* OF OPERATION.
* CALLS SUBROUTINES BATCH6, CTN6, CTN6STEP, AND CTN6EQNS
* BATCH6 OUTPUTS BATCH GROWTH DATA TO OUTP6.DAT OVER ENTIRE
* BATCH GROWTH TIME PERIOD, AND OUTPUTS TO OUT6BAT.DAT
* DATA IN BATCH (TO GROW UP CELLS) BEFORE CONTINUOUS MODE
* BEGINS AS SPECIFIED IN DATA FILE: CONST7CTN.DAT
* CTN6 BEGINS CONTINUOUS OPERATION USING CONCENTRATIONS AT
* THE END OF OUT6BAT.DAT AND RUNS TILL DESIRED TIME WHEN
* EQUILIBRIUM IS REACHED
* CTN6STEP CONTINUES WITH CONTINUOUS OPERATION BUT WITH OPERATIONAL
* CONDITIONS SPECIFIED BY CONST7CTN2.DAT (STEP CHANGE OCCURRING)
* MOD6CTN2 (MAIN PROGRAM) LOOPS OVER DESIRED DILUTION RATES AND
* OUTPUTS CONTINUOUS DATA (OF SUBROUTINE CTN6; I.E. EQUILIBRIUM
* DATA BEFORE STEP CHANGE) TO OUT6.DAT
* CTN6EQNS ROUTINE CONTAINS THE MAIN EQUATIONS FOR THE CONTINUOUS
* PART
*
* 3/26/87: PS is made equal or greater than 0 in subroutines
* BATCH6 and CTN6EQNS.
* 5/2/91: Revisions made by G.A.Murgel TO get original model to work.
* 10/8/94: Revisions made by G.A.Murgel to add pH dependency.
C
IMPLICIT REAL (K,M)
C
DOUBLE PRECISION A,P,AB,PB,PR,PS,CR,MR,X,B
C
COMMON /PARAM1/KACR,KPCR,KABCR,KPBCR,FAP,FABP,KPRP,KPRPB,KDACR,KDABCR
COMMON / PARAM2 /MUA,MUAB,MUP,MUPB,MUPR ,MUPBR,KDA,KDAB ,KDPR,HPLUS
COMMON /PARAM3/KAMR,KABMR,ALPHA,ALPHP,ALPHAB,ALPHPB,KM,KMB,KP,KA,KD
COMMON /PARAM4/BMAX,AREA,VOL,RE,TIM,TCTNO,KE1,KES1,KE2,KES2
COMMON /CTN1/CRF,TIMCTN,TIMCTN2,PRINT,IDENTIM,FO,FC,FF,DELF
COMMON /VAR1/A,P,AB,PB,PR,PS,CR,MR,X,B
COMMON DI,ISTEP,ICONT
COMMON /INI2/AOCTN,POCTN,ABOCTN,PBOCTN,PROCTN,PSOCTN,CROCTN,MROCTN

```

```

COMMON /METAL/IMETAL
COMMON /SURFACE/ISURF
C
INTEGER DAT_ROW COMMON/DATROW/DAT_ROW
C
INTEGER ISTEP,ICONT,IMETAL,ISURF
C
DOUBLE PRECISION FM
COMMON /FM_DAT/FM
C
CHARACTER *80 OSYS_DAT(10000) COMMON/OSYSDAT/OSYS_DAT,IROW
C
CHARACTER *9 DAT_DAT(10)
COMMON/DATDAT/DAT_DAT
C
CHARACTER *9 DATA_DAT(256)
COMMON/DATADAT/DATA_DAT
C
INTEGER MCOUNTER
COMMON/COUNTER/MCOUNTER
C
C Define all variables
C Read values of variables and kinetic constants from CONST7CTN.DAT
C UNIT=4 is an acronym for the file name specified.
C
OPEN (UNIT=4,NAME='CONST7CTN.DAT',FORM='FORMATTED',TYPE='OLD')
READ (4,*) KACR
READ (4,*) KPCR
READ (4,*) KABCR
READ (4,*) KPBCR
READ (4,*) FAP
READ (4,*) FABP
READ (4,*) KPRP
READ (4,*) KPRPB
READ (4,*) KDACR
READ (4,*) KDABCR
READ (4,*) MUA
READ (4,*) MUAB
READ (4,*) MUP
READ (4,*) MUPB
READ (4,*) MUPR
READ (4,*) MUPBR
READ (4,*) KDA
READ (4,*) KDAB
READ (4,*) KDPR
READ (4,*) KAMR
READ (4,*) KABMR
READ (4,*) ALPHA
READ (4,*) ALPHIP
READ (4,*) ALPHAB
READ (4,*) KM
READ (4,*) KMB
READ (4,*) KP
READ (4,*) KA
READ (4,*) KD

```

```

READ (4,*) BMAX
READ (4,*) AREA
READ (4,*) VOL
READ (4,*) RE
READ (4,*) TIM
READ (4,*) TCTN0
READ (4,*) A0
READ (4,*) P0
READ (4,*) AB0
READ (4,*) PB0
READ (4,*) PR0
READ (4,*) PS0
READ (4,*) CR0
READ (4,*) MR0
READ (4,*) CRF
READ (4,*) TIMCTN
READ (4,*) KE1
READ (4,*) KES1
READ (4,*) KE2
READ (4,*) KES2
READ (4,*) HPLUS
READ (4,*) PRINT
READ (4,*) IDTIM
READ (4,*) F0
READ (4,*) FF
READ (4,*) DELF
READ (4,*) ISTEP
READ (4,*) ICONT
READ (4,*) IMETAL
READ (4,*) ISURF

CLOSE (UNIT=4)

C
C Initialize concentrations
C
      A=A0
      P=P0
      AB=AB0
      PB=PB0
      PR=PR0
      PS=PS0
      X=A+P
      B=AB+PB

C
C Check if a metal is present in the medium rather than simply as a step
C change of operation.
C
      IF (IMETALEQ) THEN

C
C Routine call to use subroutine of speciation program MINEQL in order to
C calculate the free metal concentration before beginning any calculations.
C
      CALL CONVERT2

C
* PRINT *, 'Created speciation file, calling MINEQL...'
C
      OPEN (UNIT = 10, FILE = 'THERMO.DAT', STATUS = 'OLD')

```

```

*      OPEN (UNIT = 6, FILE = 'BATNISYS. OUT', STATUS = 'NEW,
* & CARRIAGECONTROL='LIST')
C
      CALL MINIQL
C
      CLOSE (UNIT = 10)
C
      MR=FM
C
      ELSE
      MR=MRO
      END IF
C
C Start batch growth
C
      CALL BATCH6(ICONI)
C
C Query whether need these files for a continuous run.
C
      IF(ICONI.EQ.1) THEN
      GO TO 200
      ELSE
C
C Initialize limiting nutrient concentration for continuous run
C
      DUMBFF=FF*100.+0.0001
      IFF=DUMBFF
      DUMBDELFI=DELF*100.+0.0001
      IDELF=DUMBDELFI
      DUMBF0=F0*100.+0.0001
      IFO=DUMBF0
C
C Open output files that will contain data from continuous run
C
      OPEN (UNIT=3,NAME='OUT6.DAT',FORM='FORMATTED',TYPE='NEW',
1 CARRIAGECONTROL='LIST')
C
      ENDIF
C
IF (METALEQ.1) THEN
      OPEN (UNIT=14,NAME='FOR09.DAT',FORM='FORMATTED',TYPE='NEW'
1 CARRIAGECONTROL='LIST')
      ELSE
      ENDIF
C
      IF (ISTEP.EQ.1) THEN
      GO TO 15
      ELSE
      OPEN (UNIT=8,NAME='OUT62.DAT',FORM='FORMATTED',TYPE='NEW',
1 CARRIAGECONTROL='LIST')
C
      OPEN (UNIT=15,NAME='FOR962.DAT',FORM='FORMATTED',TYPE='NEW'
1 CARRIAGECONTROL='LIST')
C
      ENDIF
C

```

```

C Continuous run looping over nutrient feed concentrations
C
  15 DO 20 I=IFO, IFF, IDELF
C
C Initialize concentrations at where batch mode ended
C
  A=AOCIN
  P=POCTN
  AB=ABOCTN
  PB=PBOCTN
  PR=PROCTN
  PS=PSOCTN
  CR=CROCTN
  MR=MR0TIN
  X=A+P
  B=AB+PB

  DUMBI=I
  FC=DUMBI/100
  DI=FC/VOL

C
C Subroutine CTN6 for continuous operation. Note query whether desire to
C use the continuous portion of the program.
C
  CALL CTN6

C
  WRITE (3,150) DI,A,P,AB,PB,PR,PS,CR,X,B,MR

C
C Subroutine CTN6STEP for continuous operation but using input data
C from CONST7CTN2.DAT, or after step change. Note query whether desire
C to use the step change option in the program.
C
  IP (ISTEP.EQ. 1) THEN
    GO TO 20
  ELSE

C
  CALL CTN6STEP

C
  END IF

C
  WRITE (8,150) DI,A,P,AB,PB,PR,PS,CR,X,B,MR

C
20 CONTINUE

C
  CLOSE (UNIT=3)

C
  IF (IMETALEQ.I) THEN
    CLOSE (UNIT=14)
  ELSEIF (ISTEP.EQ.O) THEN
    CLOSE (UNIT=8)
    CLOSE (UNIT=15)
  ELSE
  END IF

C
150 FORMAT (' ',G10.4, 10(' ',G10.4))

C
200 RETURN
  END

```

```

*****
*****
SUBROUTINE BATCH6(ICONT)
*****
*       SUBPROGRAM TO MOD6CTN3 FOR BATCH SYSTEM OPERATION.
*
*       PROGRAM GIVES COMPONENT CONCENTRATIONS WHERE CONTINUOUS RUN BEGINS.
*       THE PARAMETER FILE NAME IS CONST7CTN.DAT
*
*       3/26/87: PS is made equal or greater than 0.
*       8/8/94 : pH-DEPENDENCY ADDED BY G.A. MURGEL
*
*       IMPLICIT REAL (K,M)
*
*       DOUBLE PRECISION A,P,AB,PB,PR,PS,CR,MR,X,B
C
COMMON /PARAM1/KACR,KPCR,KABCR,KPBCR,FAP,FABP,KPRP,KPRPB,KDACR,KDABCR
COMMON /PARAM2/MUA,MUAB,MUP,MUPB,MUPR,MUPBR,KDA,KDAB,KDPR,HPLUS
COMMON /PARAM3/KAMR,KABMR,ALPHA,ALPH,ALPHAB,ALPHPB,KM,KMB,KP,KA,KD
COMMON /PARAM4/BMAX,AREA,VOL,RE,TIM,TCTN0,KE1,KES1,KE2,KES2
COMMON /CTN1/CRF,TIMCTN,TIMCTN2,PRINT,IDENTIM,F0,FC,FF,DELF
COMMON /VAR1/A,P,AB,PB,PR,PS,CR,MR,X,B
COMMON /INI2/A0CTN,P0CTN,AB0CTN,PB0CTN,PR0CTN,PS0CTN,CR0CTN,MR0CTN
COMMON /METAL/IMETAL
COMMON /SURFACE/ISURF
C
DOUBLE PRECISION FM
COMMON /FM_DAT/FM
C
INTEGER DAT_ROW
COMMON/DATROW/DAT_ROW
C
CHARACTER *80 OSYS_DAT(10000)
COMMON/OSYSDAT/OSYS_DAT,IROW
C
CHARACTER *9 DAT_DAT(10)
COMMON/DATDAT/DAT_DAT
C
CHARACTER *9 DATA_DAT(256)
COMMON/DATADAT/DATA_DAT
C
INTEGER MCOUNTER
COMMON/COUNTER/MCOUNTER
C
C Convert run time to seconds
C
RTIM=TIM*3600.
ITIM=RTIM
C
C pH-DEPENDENT CORRECTIONS OF MUA, MUAB, KACR AND KABCR
PRMUA=MUA/(1+(HPLUS/KES1)+(KES2/HPLUS))
PRMUAB=MUAB/(1+(HPLUS/KES1)+(KES2/HPLUS))
PRKACR=KACR*((1+(HPLUS/KE1)+(KE2/HPLUS))/(1+(HPLUS/KES1)+
1 (KES2/HPLUS)))
PRKABCR=KABCR*((1+(HPLUS/KE1)+(KE2/HPLUS))/(1+(HPLUS/KES1)+
1 (KES2/HPLUS)))
C
C Open output files, OUTF6.DAT for batch growth data

```

```

C OUT6BAT.DAT for batch growth data up to when continuous operation starts
C
      OPEN (UNIT=1,NAME='OUTP6.DAT',FORM='FORMATTED',TYPE='NEW',
1     CARRIAGECONTROL='LIST')
2     C
      IF(ICONT.EQ.J) THEN
          GO TO 3
      ELSE
C
      OPEN (UNIT=5,NAME='OUT6BAT.DAT',FORM='FORMATTED',TYPE='NEW',
1     CARRIAGECONTROL='LIST')
C
      END IF
C
C Loop over total run time in batch
C
2     DO 5 I=0,ITIM,IDTIM
C
C Kinetic equations for all components.
C
C Cells
      RA1=CR/(PRKACR+CR)
C
C Metal Retardation factor ignored in equations if MR=0
      RA2 = KAMR/(KAMR +MR)
      RA3=KDACR/(KDACR+CR)
      RA=(PRMUA*RA1*RA2-KDA*RA3)*A
C
C Substrate
      RASYN=(PRMUA*RA1*RA2)*A
C
C Attached Cells
      RAB1=CR/(PRKABCR+CR)
C
C Metal Retardation factor ignored in equations if MR=0
      RAB2=KABMR/(KABMR+MR)
      RAB3=KDABCR/(KDABCR+CR)
      RAB=(PRMUAB*RAB1*RAB2-KDAB-RAB3)*AB
C
      RABSYN=(PRMUAB*RAB1*RAB2)*
C
C Free Polymer
      RPR1=(P/A)/(KPRP+P/A)
      RPR2=(PB/AB)/(KPRPB+PB/AB)
      RPR4=KDPR*PR
      RPR=((MUPR*RPR1*P)+(MUPBR*RPR2*(AREA/VOL)*PB)-RPR4)/(1+KP*
1     (AREA/VOL)))
C
C Bound Polymer
      RP1=CR/(KPCR+CR)
      RP=((MUP*RP1*RA2)+(FAP*KDA*RA3))*A-MUPR*RPR1*P
C
      RPSYN=MUP*RP1*RA2*A
C
C Surface Attached Bound Polymer
      RPB1=CR/(KPBCR+CR)
      RPB=((MUPB*RPB1*RAB2)+(FABP*KDAB*RAB3))*AB-MUPBR*RPR2*PB
C

```

```

RPBSYN=MUPB*RPB1*RAB2*AB
C
RCR=-((ALPHA*RASYN+ALPHP*RPSYN+(ALPHAB*RABSYN+ALPHPB*RPBSYN)*
1 (AREA/VOL))
C
ATT=KA*(BMAX-B)*X*(AREA/VOL)
DET=KD*RE*B*(AREA/VOL)
C
C Calculate incremental changes in concentrations
C
DDTIM=IDTIM
D'TIM=DDTIM/3600. C
DA=RA*D'TIM
DP=RP*D'TIM
DAB=RAB*D'TIM
DPB=RPB*D'TIM
DPR=RPR*D'TIM
DPS=RPR*KP*D'TIM
DCR=RCR*D'TIM
DSORP=(ATT-DET)*D'TIM
C
C Sum up the incremental changes in concentrations before next loop
C
A=A+DA
P=P+DP
AB=AB+DAB
PB=PB+DPB
PR=PR+DPR
PS=PS+DPS
IF(PS,LT.0.0)PS=0,
CR=CR+DCR
IP(CR,LT.0.0)CR=U.
C
C Net Surface Change
X=A+P-DSORP
B=AB+PB+DSORP/(AREA/VOL)
C
A=X*A/(A+P)
P=X*P/(A+P)
C
AB=B*AB/(AB+PB)
PB=B*PB/(AB+PB)
C
TI = I/60.
THOUR = TI/60.
C
C Output at greater time intervals than used in calculation loop
C If difference in THOUR and print interval is zero, then can output
C results to files; else bypass and iterate loop.
C
IF (AMOD(THOUR,PRINT).EQ. 0.0) THEN
C
C Check if metal is not present in batch data, then just write output to files .
If (IMETAL.EQ.0) THEN
GO TO 50
ELSEIF (I.EQ.O) THEN
GO TO 50
ELSE

```

```

        END IF
C
C If outputting data to files, call MINEQL to recalculate the free metal
C concentration for use in the next hour of calculations.
C
        CALL CONVERT3
C
        OPEN (UNIT = 10, FILE = 'THERMO.DAT', STATUS = 'OLD')
C
        CALL MINIQL
C
        CLOSE (UNIT = 10)
C
        MR=FM
C
        50 WRITE (1,110) THOUR,A,P,AB,PB,PR,PS,CR,X,B,MR
        110 FORMAT ('F5.0, 10(', 'G10.4)
C
C Output batch data up to TCIN0, time when continuous operation starts
C Also initialize values for continuous run
C
        IF (THOUR.GT.TCIN0) THEN
            GO TO 60
        ELSEIF (ICONT.EQ.0) THEN
            WRITE (5,110) THOUR,A,P,AB,PB,PR,PS,CR,X,B,MR
        ELSE
            GO TO 60
        END IF
C
        60 A0CTN=A
        P0CTN=P
        AB0CTN=AB
        PB0CTN=PB
        PR0CTN=PR
        PS0CTN=PS
        CR0CTN=CR
        MR0CTN=MR
C
        END IF
C
        5 CONTINUE
C
        IF(ICONT.EQ.1) THEN
            GO TO 200
        ELSE
            CLOSE(UNIT=5)
        END IF
C
        200 RETURN
        END
*****
*****
SUBROUTINE CIN6
*****

```

```

C
C Routine for continuous operation
C
      IMPLICIT REAL (K,M)
C
      DOUBLE PRECISION A,P,AB,PB,PR,PS,CR,MR,X,B
C
      COMMON /PARAM1/KACR,KPCR,KABCR,KPBCR,FAP,FABP,KPRP,KPRPB,KDACR,KDABCR
      COMMON /PARAM2/MUA,MUAB,MUP,MUPB,MUPR,MUPBR,KDA,KDAB,KDPR,HPLUS
      COMMON /PARAM3/KAMR,KABMR,ALPHA,ALPH,ALPHAB,ALPHPB,KM,KMB,KP,KA,KD
      COMMON /PARAM4/BMAX,AREA,VOL,RE,TIM,TCTN0,KE1,KES1,KE2,KES2
      COMMON /CTN1/CRF,TIMCTN,TIMCTN2,PRINT,IDTIM,F0,FC,FF,DELF
      COMMON /VAR1/A,P,AB,PB,PR,PS,CR,MR,X,B
      COMMON /METAL/IMETAL
      COMMON /SURFACE/ISURF
C
      DOUBLE PRECISION FM
      COMMON /FM_DAT/FM
C
      INTEGER DAT_ROW
      COMMON/DATROW/DAT_ROW
C
      CHARACTER *80 OSYS_DAT(10000)
      COMMON/OSYSDAT/OSYS_DAT, IROW
C
      CHARACTER *9 DAT_DAT(10)
      COMMON/DATDAT/DAT_DAT
C
      CHARACTER *9 DATA_DAT(256)
      COMMON/DATADAT/DATA_DAT
C
      INTEGER MCOUNTER
      COMMON/COUNTER/MCOUNTER
C
C Read input data
C
      OPEN (UNIT=4,NAME='CONST7CTN.DAT',FORM='FORMATTED',TYPE='OLD')
      READ (4,*) KACR
      READ (4,*) KPCR
      READ (4,*) KABCR
      READ (4,*) KPBCR
      READ (4,*) FAP
      READ (4,*) FABP
      READ (4,*) KPRP
      READ (4,*) KPRPB
      READ (4,*) KDACR
      READ (4,*) KDABCR
      READ (4,*) MUA
      READ (4,*) MUAB
      READ (4,*) MUP
      READ (4,*) MUPB
      READ (4,*) MUPR
      READ (4,*) MUPBR
      READ (4,*) KDA
      READ (4,*) KDAB
      READ (4,*) KDPR
      READ (4,*) KAMR
      READ (4,*) KABMR

```

```

READ (4,*) ALPHA
READ (4,*) ALPHP
READ (4,*) ALPHAB
READ (4,*) ALPHPB
READ (4,*) KM
READ (4,*) KMB
READ (4,*) KP
READ (4,*) KA
READ (4,*) KD
READ (4,*) BMAX
READ (4,*) AREA
READ (4,*) VOL
READ (4,*) RE
READ (4,*) TIM
READ (4,*) TCTN0
READ (4,*) A0
READ (4,*) P0
READ (4,*) ABO
READ (4,*) PBO
READ (4,*) PRO
READ (4,*) PS0
READ (4,*) CR0
READ (4,*) MR0
READ (4,*) CRF
READ (4,*) TIMCTN
READ (4,*) KE1
READ (4,*) KES1
READ (4,*) KE2
READ (4,*) KES2
READ (4,*) HPLUS
READ (4,*) PRINT
READ (4,*) IDTIM
*
      CLOSE (UNIT=4)
C
C Initialize or change run time units
C
      RTIMCTN=(TIMCTN+TCTN0)*3600.
      ITIMCTN=RTIMCTN
      RTIMCTN0=(TCTN0)*3600.
      ITIMCTN0=RTIMCTN0
C
      TJ = (TCTN0+40.0)*60.0
C
C Open output file
C
      OPEN (UNIT=2,NAME='OUT6CTN.DAT',FORM='FORMATTED',TYPE='NEW',
1      CARRIAGECONTROL='LIST')
C
C Start loop over time intervals
C
      DO 10 I=ITIMCTN0,ITIMCTN,ITIMCTN
C
C Subroutine CTN6EQNS has the kinetic equations for continuous operation
C
      CALL CTN6EQNS
C
      TI = I/60.

```

```

C
C PRINT EVERY 4 HOURS INSTEAD OF EVERY HOUR IF MORE THAN 40 HOURS INTO A RUN.
C
      IF (I1.GT.T1) THEN
        THOUR = T1/240.
      ELSE
        THOUR = T1/60.
      ENDIF

C
C Output at greater time intervals than used in calculation loop
C If difference in THOUR and print interval is zero, then can output
C results to files; else bypass and iterate loop.
C
      IF (AMOD(THOUR,PRINT).EQ.0.0) THEN

C
C Check if metal not present in continuous, then just write output to files.
      IF (IMETAL.EQ.0) THEN
        GO TO 50
      ELSE

C
      IF (I.EQ.ITIMCTIN0) THEN
        GO TO 50
      ELSE
        END IF

C
      END IF

C
C If outputting data to files, call MINEQL to recalculate the free metal
C concentration for use in the next hour of calculations.
C
      CALL CONVERT3

C
      OPEN (UNIT = 10, FILE = 'THERMO.DAT', STATUS = 'OLD')

C
      CALL MINIQL

C
      CLOSE (UNIT = 10)

C
      MR=FM

C
      IF (I.EQ.ITIMCTIN) THEN
        N=DAT_ROW - 7
        DO 70 J=N,DAT_ROW
          WRITE (14,12345) DAT_DAT(J)
12345  FORMAT(1X,A9)
          70  CONTINUE

C
          L=DAT_ROW-7
          NI=(MCOUNTER*8)+1

C
          DATA_DAT(NI)=DAT_DAT(L)
          DATA_DAT(NI+1)=DAT_DAT(L+1)
          DATA_DAT(NI+2)=DAT_DAT(L+2)
          DATA_DAT(NI+3)=DAT_DAT(L+3)
          DATA_DAT(NI+4)=DAT_DAT(L+4)
          DATA_DAT(NI+5)=DAT_DAT(L+5)
          DATA_DAT(NI+6)=DAT_DAT(L+6)
          DATA_DAT(NI+7)=DAT_DAT(L+7)

```

```

C
          GO TO 10
          ELSE
          END IF
C
50  THOUR=TI/60
    WRITE (2,120) THOUR,A,P,AB,PB,PR,PS,CR,X,B,MR
120  FORMAT ('F5.0, 10(', 'G10.4)
C
    MCOUNTER=MCOUNTER+1
    ELSE
    END IF
C
10  CONTINUE
C
    CLOSE(UNIT=2)
    RETURN
    END
*****
*****
SUBROUTINE CTN6STEP
*****
C
C Subroutine for continuous operation after step change addition of a trace
C metal. Routine will calculate an initial free metal value, initial it to
C the variable MR and start from there to do calculations.
C
    IMPLICIT REAL (K,M)
C
    DOUBLE PRECISION A,P,AB,PB,PR,PS,CR,MR,X,B
C
    COMMON /PARAM1/KACR,KPCR,KABCR,KPBCR,FAP,FABP,KPRP,KPRPB,KDACR,KDABCR
    COMMON /PARAM2/MUA,MUAB,MUP,MUPB,MUPR,MUPBR,KDA,KDAB,KDPR,HPLUS
    COMMON /PARAM3/KAMR,KABMR,ALPHA,ALPHI,ALPHAB,ALPHIP,KM,KMB,KP,KA,KD
    COMMON /PARAM4/BMAX,AREA,VOL,RE,TIM,TCTN0,KE1,KES1,KE2,KES2
    COMMON /CTN1/CRF,TIMCTN,TIMCTN2,PRINT,IDTIM,F0,FC,FF,DELF
    COMMON /VAR1/A,P,AB,PB,PR,PS,CR,MR,X,B
    COMMON /METAL/IMETAL
    COMMON/SURFACE/ISURF
C
    DOUBLE PRECISION FM
    COMMON /FM_DAT/FM
C
    INTEGER DAT_ROW
    COMMON/DATROW/DAT_ROW
C
    CHARACTER *80 OSYS_DAT(10000)
    COMMON/OSYSDAT/OSYS_DAT,IROW
C
    CHARACTER *9 DAT_DAT(10)
    COMMON/DATDAT/DAT_DAT
C
    CHARACTER *9 DATA_DAT(256)
    COMMON/DATADAT/DATA_DAT
C
    INTEGER MCOUNTER
    COMMON/COUNTER/MCOUNTER
C

```

C Read input data

C

```
OPEN (UNIT=6,NAME='CONST7CTN2.DAT',FORM='FORMATTED',TYPE='OLD')
READ (6,*) KACR
READ (6,*) KPCR
READ (6,*) KABCR
READ (6,*) KPBCR
READ (6,*) FAP
READ (6,*) FABP
READ (6,*) KPRP
READ (6,*) KPRPB
READ (6,*) KDACR
READ (6,*) KDABCR
READ (6,*) MUA
READ (6,*) MUAB
READ (6,*) MUP
READ (6,*) MUPB
READ (6,*) MUPR
READ (6,*) MUPBR
READ (6,*) KDA
READ (6,*) KDAB
READ (6,*) KDPR
READ (6,*) KAMR
READ (6,*) KABMR
READ (6,*) ALPHA
READ (6,*) ALPHP
READ (6,*) ALPHAB
READ (6,*) ALPHPB
READ (6,*) KM
READ (6,*) KMB
READ (6,*) KP
READ (6,*) KA
READ (6,*) KD
READ (6,*) BMAX
READ (6,*) AREA
READ (6,*) VOL
READ (6,*) RE
READ (6,*) TIM
READ (6,*) TCIN0
READ (6,*) A0
READ (6,*) P0
READ (6,*) AB0
READ (6,*) PB0
READ (6,*) PR0
READ (6,*) PS0
READ (6,*) CR0
READ (6,*) MR0
READ (6,*) CRF
READ (6,*) TIMCTN2
READ (6,*) KE1
READ (6,*) KES1
READ (6,*) KE2
READ (6,*) KES2
READ (6,*) HPLUS
READ (6,*) PRINT
READ (6,*) IDTIM
```

*

```
CLOSE (UNIT=6)
```

```

C
C Initialize metal concentration
C
      CALL CONVERT2
C
      OPEN ( UNIT = 10, FILE = 'THERMO.DAT', STATUS = 'OLD')
C
      CALL MINIQL
C
      CLOSE ( UNIT = 10)
C
      MR=FM
C
C Change time unit of loop intervals
C
      RTIMCTN2=(TIMCTN2+TIMCTN+TCIN0)*3600.
      ITIMCTN2=RTIMCTN2
      RITIMCTN02=(TIMCTN2+TCIN0)*3600.
      IITIMCTN02=RITIMCTN02
C
      TJ = (TCIN0 + TIMCTN + 40.0) * 60.0
C
C Open output file for after step change
C
      OPEN (UNIT=12,NAME='OUT6STEP.DAT',FORM='FORMATTED',TYPE='NEW',
1      CARRIAGECONTROL='LIST')
C
C Start loop
C
      DO 10 I=IITIMCTN02,ITIMCTN2,ITIM
C
C CIN6EQNS has kinetic equations for continuous operation
C
      CALL CIN6EQNS
C
      TI=I/60
C
C PRINT EVERY 4 HOURS INSTEAD OF EVERY HOUR.
C Check to widen output data interval into steady state.
      IF (TI.GT.TJ) THEN
          THOUR=TI/240 .
      ELSE
          THOUR=TI/60
      END IF
C
C If difference in THOUR and print interval is zero, then can output
C results to files; else bypass and iterate loop.
C
      IF (AMOD(THOUR,PRINT).EQ.0.0) THEN
C
C Check if metal not present in continuous, then must write output to files.
      IF (I.EQ.IITIMCTN02) THEN
          GO TO 50
      ELSE
          END IF
C
C If outputting data to files, call MINEQL to recalculate the free metal
C concentration for use in the next hour of calculations.

```

```

C
CALL CONVERT3
*
OPEN (UNIT = 10, FILE = 'THERMO.DAT', STATUS = 'OLD')
C
CALL MINIQL
C
CLOSE (UNIT = 10)
C
MR=FM
C
IF (LEQ(ITIMCTIN2) THEN
N=DAT_ROW-7
DO 70 J=N,DAT_ROW
WRITE (15,12345) DAT_DAT(J)
12345 FORMAT(1X,A9)
70 CONTINUE
C
L=DAT_ROW-7
NI=(MCOUNTER*8)+1
C
DATA_DAT(NI)=DAT_DAT(L)
DATA_DAT(NI+1)=DAT_DAT(L+1)
DATA_DAT(NI+2)=DAT_DAT(L+2)
DATA_DAT(NI+3)=DAT_DAT(L+3)
DATA_DAT(NI+4)=DAT_DAT(L+4)
DATA_DAT(NI+5)=DAT_DAT(L+5)
DATA_DAT(NI+6)=DAT_DAT(L+6)
DATA_DAT(NI+7)=DAT_DAT(L+7)
C
GO TO 10
ELSE
END IF
C
50 THOUR = TI/60.
WRITE (12,120) THOUR,A,P,AR,PR,PR,PS,CR,X,R, MR
120 FORMAT ('F5.0, 10(',G10.4)
C
MCOUNTER=MCOUNTER+1
C
ELSE END IF
C
10 CONTINUE
C
CLOSE(UNIT=12)
RETURN
END
*****
*****
SUBROUTINE CTIN6EQNS
*****
*
3/26/87: PS is made equal or greater than 0.
C
IMPLICIT REAL (K,M)
C
DOUBLE PRECISION A,P,AB,PB,PR,PS,CR,MR,X,B
C

```

```

COMMON /PARAM1/KACR,KPCR,KABCR,KPBCR,FAP,FABP,KPRP,KPRPB,KDACR,KDABCR
COMMON /PARAM2/MUA,MUAB,MUP,MUPB,MUPR,MUPBR,KDA,KDAB,KDPR,HPLUS
COMMON /PARAM3/KAMR,KABMR,ALPHA,ALPH,ALPHAB,ALPHPB,KM,KMB,KP,KA,KD
COMMON /PARAM4/BMAX,AREA,VOL,RE,TIM,TCTN0,KE1,KES1,KE2,KES2
COMMON /CTN1/CRF,TIMCTN,TIMCTN2,PRINT,IDTIM,F0,FC,FF,DELF
COMMON /VAR1/A,P,AB,PB,PR,PS,CR,MR,X,B
COMMON D1,ISTEP,ICONT
COMMON /METAL/IMETAL
COMMON/SURFACE/ISURF

C
DOUBLE PRECISION FM
COMMON /FM_DAT/FM

C
CHARACTER *80 OSYS_DAT(10000)
COMMON/OSYS DAT/OSYS_DAT, IROW

C
INTEGER DAT_ROW
COMMON/DATROW/DAT_ROW

C
CHARACTER *9 DAT_DAT(10)
COMMON/DATDAT/DAT_DAT

C
CHARACTER *9 DATA_DAT(256)
COMMON/DATADAT/DATA_DAT

C
INTEGER MCOUNTER
COMMON/COUNTER/MCOUNTER

C
C ph-Dependent corrections of MUA, MUAB, KACR and KABCR.
C
PRMUA=MUA/(1+(HPLUS/KES1)+(KES2/HPLUS))
PRMUAB=MUAB/(1+(HPLUS/KES1)+(KES2/HPLUS))
PRKACR=KACR*((1+(HPLUS/KE1)+(KE2/HPLUS))/(1+(HPLUS/KES1)+
1 (KES2/HPLUS)))
PRKABCR=KABCR* ((1+ (HPLUS/KE1) + (KE2/HPLUS) ) / (1 +(HPLUS/KES1) +
1 (KES2/HPLUS)))

C
C KINETIC EQUATIONS
C
C Cell Mass
RA1=CR/(PRKACR+CR)

C
C Metal retardation ignored if MR=0; Then RA2=1
RA2=KAMR/(KAMR+MR)
RA3=KDABCR/(KDABCR+CR)
RA=(PRMUA*RA1*RA2-KDA*RA3)*A-(DI*A)

C
C Substrate
RASYN=(PRMUA*RA1*RA2)*A

C
C Attached cells
RAB1=CR/(PRKABCR+CR)

C
C Metal retardation ignored if MR=0; Then RA2=1
RAB2=KABMR/(KABMR+MR)
RAB3=KDABCR/(KDABCR+CR)
RAB=(PRMUAB*RAB1*RAB2-KDAB*RAB3)*AB

C

```

```

RABSYN= ((PRMUAB*RAB1*RAB2)*AB
C
C Free Polymer
RPR1=(P/A)/(KPRP+P/A)
RPR2=(PB/AB)/(KPRPB+PB/AB)
RPR4=KDPR*PR
RPR=( ( (MUPR*RPR1*P) + (MUPBR*RPR2*(AREA/VOL)*PB) - (DI*PR)-RPR4)/(1
1 +KP*(AREA/VOL)))
C
C Bound Polymer
RP1=CR/(KPCR+CR)
RP=( (MUP*RP1*RA2) + (FAP*KDA*RA3) ) *A-(MUPR*RPR1*P)-(DI*P)
C
RPSYN=MUP*RP1*RA2*A
C
C Attached Cell Bound Polymer
RPB1=CR/(KPBCR+CR)
RPB=( (MUPB*RPB1*RAB2)+FABP*KDAB*RAB3) *AB-MUPBR*RPN2*PB
C
RPBSYN=MUPB*RPB1 *RAB2*AB
C
C Substrate
RCR = - ( (ALPHA*RASYN) + (ALPHP*RPSYN) + ( (ALPHAB *RABSYN) +
1 (ALPHPB*RPBSYN))*(AREA/VOL) )+(DI*(CRF-CR))
C
C Attachment/Detachment calculations
ATT=KA*(BMAX-B)*X*(AREA/VOL)
DET=KD*RE*B*(AREA/VOL)
C
DDTIM=IDTIM
DTIM=DDTIM/3600.
C
C Incremental changes
DA=RA*DTIM
DP=RP*DTIM
DAB=RAB*DTIM
DPB=RPB*DTIM
DPR=RPR*(1.0-KP)*DTIM
DPS=RPR*KP*DTIM
DCR=RCR*DTIM
DSORP=(ATT-DET)*DTIM
C
C Summing incremental changes in concentrations before next loop
A=A+DA
P=P+DP
AB=AB+DAB
PB=PB+DPB
PR=PR+DPR
PS=PS+DPS
IF(PS.LT.0.0)PS=0.
CR=CR+DCR
IF(CR.LT.0.0)CR=0
C
C Net surface change
X=A+P-DSORP
B=AB+PB+DSORP/(AREA/VOL)
C
A=X*A/(A+P)

```

```

C      P=X*P/(A+P)
C
C      AB=B*AB/(AB+PB)
C      PB=B*PB/(AB+PB)
C
C      RETURN
C      END
*****
*****
      SUBROUTINE CONVERT2
*****
C This routine takes the initial mineral medium concentrations and outputs
C these concentrations into a file in the format that CHEM.FOR
C recognizes. The return allows MINEQL to calculate the free metal
C concentration at the point just prior to the introduction of the
C cellular components. This routine is used only once at that point
C in time in the batch routine or in the step routine.
C
C INPFIL is name of file containing Freshwater defined medium concentrations
C and kinetic constants for MINEQL. File named MMSTESTMETAL.DAT.
C
C unit string array (OSYS.DAT) contains converted concentrations and
C kinetic constant to be input into MINEQL.
C
C      IMPLICIT NONE
C
C      INTEGER I,J,N1COMP,N2OTHR
C      INTEGER L_COUNTER,IROW
C
C      CHARACTER*42 DATN1(25),DATN2(250)
C      CHARACTER*16 INPFIL
C
C      DOUBLE PRECISION FM
C      COMMON /FM_DAT/FM
C
C      CHARACTER * 80 OSYS_DAT(10000)                                !BY TP
C      COMMON /OSYSDAT/OSYS_DAT,IROW                                !BY TP
C
C      CHARACTER *9 DAT_DAT(10)
C      COMMON/DATDAT/DAT_DAT
C
C      CHARACTER *9 DATA_DAT(256)
C      COMMON/DATADAT/DATA_DAT
C
C      INTEGER MCOUNTER
C      COMMON/COUNTER/MCOUNTER
C
C --- Input conversion parameters and names of medium speciation data.
C
C      OPEN (UNIT=7,NAME='CONVERT2.DAT',TYPE='OLD',FORM='FORMATTED')
C
C      READ (7,33) INPFIL
C      READ (7,*) N1COMP
C      READ (7,*) N2OTHR
C
C      33 FORMAT (A16)
C      CLOSE (UNIT=7)

```

```

C
C --- Input Freshwater defined medium components concentrations and
C kinetic parameters in INPFIL
C
C       J=1
C
C       OPEN(UNIT=9,NAME=INPFIL,TYPE='OLD',FORM='FORMATTED')
C
C File 'INPFIL' = MMSTESTMETAL.DAT.
C
C       DO I=1,N1COMP
C       READ (9,251) DATN1 (I)
C       END DO
C
C       DO I=1,N20THR
C       READ (9,253) DATN2 (I)
C       END DO
C
C 251  FORMAT (A30)
C 253  FORMAT (A42)
C
C       CLOSE (UNIT=9)
C
C Write all necessary input for MINIQL into RAM file OSYS.DAT
C
C       L_COUNTER = (N1COMP + 8 + N20THR) * (J-1)                                !BY TP
C
C       DO I = 1, N1COMP                                                            !BY TP
C           OSYS_DAT (L_COUNTER + 1) = DATN1 (I)                                  !BY TP
C           L_COUNTER = L_COUNTER + 1                                             !BY TP
C       END DO                                                                      !BY TP
C
C       DO I = 1, N20THR                                                            !BY TP
C           OSYS_DAT (L_COUNTER + 1) = DATN2 (I)                                  !BY TP
C           L_COUNTER = L_COUNTER + 1                                             !BY TP
C       END DO                                                                      !BY TP
C
C File building complete. Return to calling program.
C
C       RETURN
C       END
*****
*****
SUBROUTINE CONVERT3
*****
C This program takes components in growth medium and converts them into
C stoichiometric concentrations for MINIQL, then outputs these
C concentrations into a file in the format that CHEM.FOR recognizes.
C
C CONVERT3.DAT contains parameters for converting components into
C stoichiometric concentrations.
C INPFIL is name of file containing Freshwater defined medium concentrations
C and kinetic constants for MINIQL. (Actual file name is MMSTEST.DAT) .
C Unit string array (OSYS.DAT) contains converted concentrations and
C kinetic constants to be input into MINIQL.
C
C       IMPLICIT NONE

```

```

C
C --- define variables to be used
C
      REAL AMASS(60),PMASS(60),ABMASS(60),PBMASS(60)
      REAL PRMASS(60),PSMASS(60),CRMMASS(60)
      REAL GMAXP,GMAXC,GMAXS
      REAL FPR1,FPR2,FPR3,FPR4,FS1,FS2,FS3
      REAL AREA,VOL,CELLSURF
      REAL PR1(60),PR2(60),PR3(60),PR4(60)
      REAL CELL1(60),SURF1(60),SURF2(60),SURF3(60)
      REAL XMASS(60),BMASS(60)

C
      DOUBLE PRECISION A,P,AB,PB,PR,PS,CR,MR,X,B
      COMMON /VAR1/  A,P,AB,PB,PR,PS,CR,MR,X,B

C
INTEGER IJ,N1COMP,N2OTHR
INTEGER L_COUNTER,IROW
C
      CHARACTER *11 INPFIL
      CHARACTER *42 DATN1(25),DATN2(250)
      CHARACTER *14 DATNNI(10)
      CHARACTER * 13 A_PR1(1000), A_PR2(1000),           !BY TP
&                A_PR3(1000), A_PR4(1000), A_CELL1(1000), ! BY TP
&                A_J3URF1(1000), A_SURF2(1000), A_SURF3(1000) ! BY TP

C
      DOUBLE PRECISION PM
      COMMON /FM_DAT/FM

C
      CHARACTER * 80 OSYS_DAT(10000)           !BY TP
      COMMON /OF3Y3DAT/OSYS_DAT, IROW        ! BY TP

C
      CHARACTER * 9 DAT_DAT(10)
      COMMON/DATDAT/DAT_DAT

C
      CHARACTER * 9 DATA_DAT(256)
      COMMON/ DATA DAT/ DATA_DAT

C
      INTEGER MCOUNTER
      COMMON/COUNTER/MCOUNTER

C
C --- input conversion parameters and names of medium speciation data.
C
      OPEN (UNIT=7,NAME='CONVERT3.DAT',TYPE='OLD',FORM='FORMATTED')

C
      READ (7,*) N1COMP
      READ (7,*) N2OTHR
      READ (7,*) GMAXP
      READ (7,*) GMAXC
      READ (7,*) GMAXS
      READ (7,33) INPFIL
      READ (7,*) FPR1
      READ (7,*) FPR2
      READ (7,*) FPR3
      READ (7,*) FPR4
      READ (7,*) FS1
      READ (7,*) FS2
      READ (7,*) FS3
      READ (7,*) AREA

```

```

        READ (7,*) VOL
        READ (7,*) CELLSURF
C
    33  FORMAT (A11)
C
        CLOSE (UNIT=7)
C
C --- Do loop for each time period
C --- Input batch growth components and convert
C
        J=1
C
C Set array values equal to values of variables from common.
C
        AMASS(J)=A
        PMASS(J)=P
        ABMASS(J)=AB
        PBMASS(J)=PB
        PRMASS(J)=PR
        PSMASS(J)=PS
        CRMASS(J)=CR
C
        PR1(J)=GMAXP*FPR1*(PRMASS(J)+PSMASS(J)*AREA/VOL)
        PR2(J)=GMAXP*FPR2*(PRMASS(J)+PSMASS(J)*AREA/VOL)
        PR3(J)=GMAXP*FPR3*(PRMASS(J)+PSMASS(J)*AREA/VOL)
        PR4(J)=GMAXP*FPR4*(PRMASS(J)+PSMASS(J)*AREA/VOL)
        XMASS(J)=AMASS(J)+PMASS(J)
        BMASS(J)=ABMASS(J)+PBMASS(J)
        CELL1(J)=GMAXC*(XMASS(J)+BMASS(J)*AREA/VOL)
        SURF1(J)=GMAXS*FS1*(AREA/VOL)*(1.0-BMASS(J)*CELLSURF)
        SURF2(J)=GMAXS*FS2*(AREA/VOL)*(1.0-BMASS(J)*CELLSURF)
        SURF3(J)=GMAXS*FS3*(AREA/VOL)*(1.0-BMASS(J)*CELLSURF)
C
C --- Input Freshwater defined medium components concentrations and
C kinetic parameters on INPFIL
C
        OPEN (UNIT=9,NAME=INPFIL,TYPE='OLD',FORM='FORMATTED')
C
        DO I=1,N1COMP
        READ (9,251) DATN1(I)
        END DO
C
        DO I=1,8
        READ (9,252) DATNN1(I)
        END DO
C
        DO I=1,N2OTHR
        READ (9,253) DATN2(I)
        END DO
C
    251  FORMAT (A30)
    252  FORMAT (A14)
    253  FORMAT (A42)
C
        CLOSE (UNIT=9)
C
C Write all necessary input for MINIQL into RAM file OSYS.DAT C

```

```

L_COUNTER = (N1COMP + 8 + N2OTHR) * (J-1) ! BY TP
C
DO I = 1, N1COMP ! BY TP
OSYS_DAT ( L_COUNTER + 1 ) = DATN1 ( I ) ! BY TP
L_COUNTER = L_COUNTER + 1
END DO ! BY TP
C
WRITE (A_PR1(J), FMT=' (1X,E10 .3) ' ) PR1 (J) ! BY TP
WRITE (A_PR2(J), FMT=' (1X,E10 .3) ' ) PR2 (J) ! BY TP
WRITE (A_PR3(J), FMT=' (1X,E10 .3) ' ) PR3 (J) ! BY TP
WRITE (A_PR4(J), FMT=' (1X,E10 .3) ' ) PR4 (J) ! BY TP
WRITE (A_CELL1 (J), FMT=' ( 1X, E10 . 3 ) ' ) CELL1 (J) ! BY TP
WRITE (A_SURF1 (J), FMT=' ( 1X, E10 . 3 ) ' ) SURF1(J) ! BY TP
WRITE (A_SURF2 (J), FMT=' ( 1X, E10 . 3 ) ' ) SURF2 (J) ! BY TP
WRITE (A_SURF3(J), FMT=' ( 1X, E10.3 ) ' ) SURF3 (J) ! BY TP
C
OSYS_DAT ( L_COUNTER + 1 ) = DATNN1 (1)//A_PR1 (J) ! BY TP
OSYS_DAT ( L_COUNTER + 2 ) = DATNN1 (2)//A_PR2 (J) ! BY TP
OSYS_DAT ( L_COUNTER + 3 ) = DATNN1 (3)//A_PR3 (J) ! BY TP
OSYS_DAT ( L_COUNTER + 4 ) = DATNN1 (4)//A_PR4 (J) ! BY TP
OSYS_DAT ( L_COUNTER + 5 ) = DATNN1 (5)//A_CELL1 (J) ! BY TP
OSYS_DAT ( L_COUNTER + 6 ) = DATNN1 (6)//A_SURF1 (J) ! BY TP
OSYS_DAT ( L_COUNTER + 7 ) = DATNN1 (7)//A_SURF2 (J) ! BY TP
OSYS_DAT ( L_COUNTER + 8 ) = DATNN1 (8)//A_SURF3 (J) ! BY TP
C
L_COUNTER = L_COUNTER +8 ! BY TP
C
DO I = 1, N2OTHR ! BY TP
OSYS_DAT (L_COUNTER + 1 ) = DATN2 ( I ) ! BY TP
L_COUNTER = L_COUNTER + 1 ! BY TP
END DO
C
C Return to program to run MINEQL . Speciation file created. ! BY TP
C
RETURN
END
*****
*****
* Speciation program--MINIQL--for use in freshwater speciation for free metal
* determination and in determining concentrations of selected components
* within the bacterial medium.
*
* Line after SLV 9870: 1.0 D-60 changed to 1.0 D-38 due to VAX's capability
* double spacing in output changed to single spacing
* Subroutine GRAPH deleted from original version since it is not. usefl here.
*
* Added lines in OUTPUT to write essential data to DAT. DAT
*
* certain output to unit 6 (SYS. OUT) is disabled, only important outout
* remains. Those write lines disabled are commented by using '!'.
*****
SUBROUTINE MINIQL
*****
COMMON/VAR/GX(25),X(25),C(250),GC(250),Y(25),Z(25,25),
1 GK(250),A(250,25),IDX(25),IDY(250)
DOUBLE PRECISION GX,X,Y,Z,C,GC
C

```

```

DOUBLE PRECISION FM
COMMON/FM_DAT/FM
C
CHARACTER *80 OSYS_DAT(10000)
COMMON/OSYSDAT/OSYS_DAT
C
INTEGER DAT_ROW
COMMON/DATROW/DAT_ROW
C
CHARACTER *9 DAT_DAT(10)
COMMON/DATDAT/DAT_DAT
C
CHARACTER *9 DATA_DAT(256)
COMMON/DATADAT/DATA_DAT
C
INTEGER MCOUNTER
COMMON/COUNTER/MCOUNTER
C
DAT_ROW=0
C
CALL INDATA
C
      ITER=0
      XMU=0.05
CALL IONCOR(XMU)
C
CALL CHEMEQ
CALL OUTPRT
C
RETURN
END
*****
*****
*****
      SUBROUTINE CHEMEQ
***** CHEMEQ; INDATA; OUTPRT; ERROR(I) *****
*****
COMMON/PARM/IADS,EPS,TEMP,ET,ETSF,ETFSC,NNN,NSP,NN(6),ITER,ITRPR
COMMON/VAR/GX(25),X(25),C(250),GC(250),Y(25),Z(25,25),
1 T(25),GK(250),A(250,25),IDX(25),IDY(250)
COMMON/VPHP/IONIT,XIS,GFO,IONPH,IPHA,IPHB,PHACT,HBA,HB,HA,IPHFX
COMMON/COND/IONZ(200),SPION(250,2),CAPPA0(200),SIZE(200),DELH(250)
COMMON/CYCLE/ICYCLE(2),ITITL,IPCP,ICND,THRSH,NXDIM,NYDIM,ITMAX,TSPC
C
DOUBLE PRECISION FM
COMMON/FM_DAT/FM
C
CHARACTER *80 OSYS_DAT(10000)
COMMON/OSYSDAT/OSYS_DAT, IROW
C
INTEGER DAT_ROW
COMMON/DATROW/DAT_ROW
C
CHARACTER *9 DAT_DAT(10)
COMMON/DATDAT/DAT_DAT
C
CHARACTER *9 DATA_DAT(256)
COMMON/DATADAT/DATA_DAT

```

C	INTEGER MCOUNTER COMMON/COUNTER/MCOUNTER	
C	DOUBLE PRECISION GX,X,Y,Z,C,GC	CEQ 80
C	INTEGER MSG(40) /	CEQ 90
*	1 'COMP', 'PONE', 'NTS', '> NX', 'DIM',	CEQ 100
*	2 'SPEC', 'IES', '> NY', 'DIM', ' ',	CEQ 110
*	3 'ID', 'NOT', 'FOUN', 'D: I', 'NPUT',	CEQ 120
*	4 'ID', 'NOT', 'FOUN', 'D: I', 'ADY',	CEQ 130
*	5 'ID', 'NOT', 'FOUN', 'D: I', 'ADX',	CEQ 140
*	6 'PHAS', 'E RU', 'LE V', 'IOLA', 'TION',	CEQ 150
*	7 'TER', 'ATIO', 'NS >', 'TMA', 'X',	CEQ 160
*	8 'SING', 'ULAR', 'Z M', 'ATRI', 'X' /	CEQ 170
C	ITER=0	CEQ 180
	XMU= 0.0	CEQ 190
	IF(IONPH.EQ.0) GO TO 5	CEQ 200
	TPH=T(IADX(50))	CEQ 210
	TPHA=T(IADX(IPHA))	CEQ 220
	TPHB=T(IADX(IPHB))	CEQ 230
	HA=0.0	CEQ 240
	HB=0.0	CEQ 250
	5 IF(IPHFX.EQ.0) GO TO 10	
	GK(IADY(50))	
	GX(IADX(50))	
10	CALL SOLID	CEQ 260
	CALL SOLVE	CEQ 270
	CALL SOLID X(K)	CEQ 280
	IF (K.NE. 0) GO TO 10	CEQ 290
	IF (IONPH.EQ. 0) GO TO 70	CEQ 300
	JPH=IADX(50)	CEQ 310
	JPHA=IADX(IPHA)	CEQ 320
	JPHB=IADX(IPHB)	CEQ 330
	HR=SNGL (C (IADY (50)) -X(JPH))	CEQ 340
	IF (HR.EQ.0.0) GO TO 80	CEQ 350
	T(JPH)-T(JPH) -IIR	CEQ 360
	IF(HR.GT.O.) GO TO 40	CEQ 370
	IF(HB.NE.0.0) GO TO 20	CEQ 380
	T(JPHA) =T(JPHA) + HR/IONZ(IPHA)	CEQ 390
	HA=HA-HR	CEQ 400
	GO TO 80	CEQ 410
20	IF((HB+HR).LT.0.0) GO TO 30	CEQ 420
	T(JPHB) =T(JPHB) +HR/IONZ (IPHB)	CEQ 430
	HB=HB+HR	CEQ 440
	GO TO 80	CEQ 450
30	T(JPHB)=T(JPHB) -HB/IONZ (IPHB)	CEQ 460
	T(JPHA) =T(JPHA) +(HR+HB) /IONZ(IPHA)	CEQ 470
	HA=HA- (HR+HB)	CEQ 480
	HB=0.0	CEQ 490
	GO TO 80	CEQ 500
40	IF(HA.NE.0.0) GO TO 50	CEQ 510
	T (JPHB) =T(JPHB) +HR/IONZ (IPHB)	CEQ 520
	HB=HB+HR	CEQ 530

GO TO 80	CEQ 540
50 IF{(HA-HR).LT.0.0) GO TO 60	CEQ 550
T(JPHA)=T(JPHA) + HR/IONZ(IPHA)	CEQ 560
HA=HA-HR	CEQ 570
GO TO 80	CEQ 580
60 T(JPHA)=T(JPHA)+HA/IONZ{IPHA)	CEQ 590
T(JPHB)=T(JPHB)+(HR-HB)/IONZ(IPHB)	CEQ 600
HB=HB+(HR-HB)	CEQ 610
HA=0.0	CEQ 620
GO TO 80	CEQ 630
70 IF(IONIT.EQ.0) RETURN	CEQ 640
80 CALL IONCAL(XMUC)	CEQ 650
IF((ABC((XMUC-XMU)/XMUC).LT.O.0005).OR.XMUC.GT.0.5) GOTO 90	CEQ 660
XMU = XMUC	CEQ 670
CALL IONCOR(XMU)	CEQ 680
IF(IPHFX.EQ.0) GO TO 10	
GX(IADX(50)) = -(PHACT+GFO)	
GK(IADY(50)) = PHACT+GFO	
GO TO 10	CEQ 690
90 XTS = SQRT(XMUC)	CEQ 700
* IF(IONIT.EQ.-1.OR.IONPH.EQ.-1) WRITE(6,122) XMUC	CEQ 705
* IF(IPHFX.GE.1) WRITE(6,123) GX(IADX(50))	
PHACT = -(GX(IADX(50))+GFO)	
IF(IONPH.EQ.0) RETURN	
HBA = HB-HA	CEQ 720
T(JPH) = TPH	CEQ 740
T(JPHA) = TPHA	CEQ 750
T(JPHB) = TPHB	CEQ 760
IF(IONPH.LE.-1) RETURN	
* IF (HA.NE.0.0) WRITE(6,110) HA	CEQ 770
* IF (HB.NE.0.0) WRITE(6,120) HB	CEQ 780
* WRITE(6,100) PHACT	CEQ 790
100 FORMAT('0',4X, 'ACTIVITY CORRECTED PH = ',F7.3)	CEQ 800
110 FORMAT('0',4X, 'ACID REQUIRED TO FIX PH = '1PE14.6, ' EQUIV./L')	CEQ 810
120 FORMAT('0',4X, 'BASE REQUIRED TO FIX PH = '1PE14.6, ' EQUIV./L')	CEQ 820
122 FORMAT('0',6X, 'TONIC STRENGTH = ',1PE9.3)	CEQ 822
123 FORMAT('0',4X, 'LOG H CONCENTRATION = ',F8.3)	
RETURN	CEQ 830

C INPUT DATA	CEQ 840
ENTRY INDATA	CEQ 850
CALL INPUT	CEQ 860
CALL OINCMP	CEQ 870
CALL OTNSPC	CEQ 880
CALL INION	CEQ 890
XMU = 0.0	
IF(IADS.NE.O.AND.(IONIT.NE.0.OR.IONPH.NE.0)) CALL IONCOR(XMU)	
RETURN	CEQ 900

C PRINT DATA	CEQ 10
ENTRY OUTPRT	CEQ 920
CALL OUTCMP	CEQ 930
CALL OUTSPC	CEQ 940
IF (IPCP.LE.0) CALL OUTPC	CEQ 950
IF (ICND.EQ.0) CALL CONDUCT	CEQ 960
RETURN	CEQ 970

C ERROR IN DATA	

```

ENTRY ERROR ( I ) CEQ 990
I1=(I-1)*5+1 CEQ 1000
I2=I*5 CEQ 1010
WRITE (6, 130) I, (MSG(I),I1=I1,I2) CEQ 1020
IF (I.LE.5) STOP '@ CEQ 1030' CEQ 1030
CALL OUTCMP CEQ 1040
CALL OUTSPC CEQ 1050
STOP '@ CEQ 1060' CEQ 1060
130 FORMAT ( 2x, '**** EXECUTION TERMINATED ** ERROR ',13,' ** ',5A4) CEQ 1070
C
END CEQ 1080
*****
FUNCTION IADY(IDYT) IDY 1090
***** IADY(IDYT) ,IADX(IDXT) ***** IDY 1100
*****
COMMON/PARM/IADS,EPS,TEMP,ET,ETSF,ETFSC,NNN,NSP,NN(6),ITER,ITRPR IDY 1110
COMMON/VAR/GX(25),X(25),C(250),GC(250),Y(25),2(25,25), IDY 1120
1 T(25),GK(250),A(250,25),IDX(25),IDY(250) IDY 1130
C
DOUBLE PRECISION FM
COMMON/FM_DAT/FM
COMMON /DATDAT/DAT_DAT ! BY TP
DOUBLE PRECISION GX, X, Y, Z , C , GC IDY 1140
C IDY 1150
DO 10 I=1,NSP IDY 1160
IF(IDY(I).EQ.IDYT) GO TO 20 IDY 1170
10 CONTINUE IDY 1170
CALL ERROR(4) IDY 1180
20 IADY=I IDY 1210
RETURN IDY 1220
***** IDY 1230
ENTRY IADX(IDXT) IDY 1240
DO 30 J=1,NNN IDY 1250
IF(IDX(J).EQ.IDXT) GOTO 40 IDY 1260
30 CONTINUE IDY 1270
WRITE(6,50) IDXT IDY 1280
CALL ERROR(5) IDY 1290
40 IADX=J IDY 1300
C
RETURN IDY 1310
50 FORMAT('0' , '????????? ID =',I5,' ??????????') IDY 1320
C
END IDY 1330
*****
FUNCTION CSOLN(IDCMP) CGS 1340
***** CSOLN,GSOLN(IDCMP); CSOLID,GSOLID(IDSPC); PCSC(IDSPC,IDCMP) ***** CGS 1350
*****
COMMON/FARM/IADS,EPS,TEMP,ET,ETSF,ETFSC,NNN,NSP,NN(6),ITER,ITRPR CGS1360
COMMON/VAR/GX(25),X(25),C(250),GC(250),Y(25),Z(25,25), CGS1370
1 T(25),GK(250),A(250,25),IDX(25),IDY(250) CGS 1380
C
DOUBLE PRECISION FM
COMMON/FM_DAT/FM
COMMON /DATDAT/DAT_DAT ! BY TP
DOUBLE PRECISION GX,X,Y,Z,C,GC CGS 1390
C
C COMP. CONC. IN SOLN. CGS 1400

```

```

IW=0 CGS 1410
GO TO 10 CGS 1420
*****
ENTRY GSOLN(IDCMP) CGS 1430
IW=1 CGS 1440
10 I1=NN(1)+1 CGS 1450
I2=NN(1)+NN(2) CGS 1460
JJ=IADX(IDCMP) CGS 1470
SUM=X(JJ) CGS 1480
DO 20 1=11,12 CGS 1490
20 IF (A (I, JJ).NE.O) SUM=SUM+A(I, JJ) *C(I) CGS 1500
IF(IW.EQ.1) GO TO 30 CGS 1510
CSOLN=SUM CGS 1520
RETURN CGS 1530
30 GSOLN = ALOG10 (SUM) CGS 1540
RETURN CGS 1550
*****
ENTRY CSOLID(IDSPC) CGS 1560
IW = 0 CGS 1570
GO TO 40 CGS 1580
*****
ENTRY GSOLID(IDSPC) CGS 1590
IW = 1 CGS 1600
40 ,JJ = IADY(IDSPC) CGS 1610
I1=NN(1)+NN(2)+NN(3)+1 CGS 1620
I2=I1+NN(4)-1 CGS 1630
SUM=0.0 CGS 1640
IF(IW.EQ.1) GO TO 50 CGS 1650
IF(JJ.GE.I1.AND.JJ.LE.I2) SUM = C(JJ) CGS 1660
CSOLID = SUM CGS 1670
RETURN CGS 1680
50 IF(JJ.GE.I1.AND.JJ.LE.I2) SUM = GC(JJ) CGS 1690
GSOLID=SUM CGS 1700
RETURN CGS 1710
*****
C PERCENT SPECIES IN COMPONENT CGS 1720
ENTRY PCSC(IDSPC, IDCMP) CGS 1730
IW - IADY(IDSPC) CGS 1740
JJ = IADX( IDCMP) CGS 1750
SUM=T(JJ) CGS 1760
IF(NN(3).EQ.0) GO TO 70 CGS 1770
I1=NN(1)+NN(2)+1 CGS 1780
I2=NN(1) +NN(2) +NN(3) CGS 1790
DO 60 1 = I1,I2 CGS 1800
60 SUM=SUM-A(I,JJ)*C(I) CRS '181D
70 PCSC=0.0 CGS 1820
IF(SUM.NE.0.0) PCSC=A(IW,JJ) *C (I1)/SUM CGS 1830
C
RETURN CGS 1840
END CGS 1850
*****
SUBROUTINE INION ION 1860
***** INION; IONCOR(XMU) ; IONCAL(XMU) ; CONDUCT***** ION 1870
COMMON/ PARM/ IADS, EPS, TEMP, ET, ETSF, ETFSC, NNN, NSP, NN(6), ITER, ITRPR ION 1880
COMMON/ VAR/ GX(25), X(25), C(250), GC(250), Y(25), Z(25,25), ION 1890
1 (25), GK(250), A(250,25), IDX(25), IDY(250) ION 1900

```

```

COMMON/VPHF/IONIT,XIS,GFO,IONPH,IPHA,IPHB,PHACT,HBA,HB,HA,IPHFX ION 1910
COMMON/COND/IONZ(200),SPION(250,2),CAPPA0(200),SIZE(200),DELH(250) ION1920
COMMON/VSURF/PSID,PSI0,PSIB,SIGD,SIG0,SIGB,AREA,C1,C2,ZEL ION 1930
C
DOUBLE PRECISION FM
COMMON/FM_DAT/FM
COMMON /DATDAT/DAT_DAT ! BY TP
DOUBLE PRECISION GX,X,Y,Z,C,GC,PSID,PSI0,PSIB,SIGD,9IG0,SIGB ION 1940
DIMENSION ACON(25) ION 1950
C
GFO=0.0 ION 1960
ETSF=0.05915 ION 1970
ETFSC = 19.46 ION 1980
ET=0.5116 ION 1990
XIS=-1.0 ION 2000
READ(10,170) (IONZ(J),J=1,200)
READ(10,180) (CAPPA0(J),J=1,200),(SIZE{J},J=1,200)
DO 20 I=1,NSP ION 2030
VI = 0.0 ION 2040
VJ = 0.0 ION 2050
DO 10 J=1,NNN ION 2060
VI = VI+A(I,J)*IONZ(IDX(J)) ION 2070
10 VJ = VJ+A(I,J)*IONZ(IDX(J))*2 ION 2080
SPION(I,1) =VI ION 2090
20 SPION(I,2) =VJ ION 2100
C TEMPERATURE CORRECTION ION 2110
IF(TEMP.EQ.25.0) GO TO 40 ION 2120
ET = 87.74 - .4008*TEMP + 9.398E-4*TEMP**2 - 1.141E-6*TEMP**3 ION 2130
ET = 1.82483E6*(ET*(273.15 + TEMP))**(-3./2.) ION 2140
TEMCOR = (1000./ (2.303*1.987) )*((1./(273.15+TEMP))-1./298.15) ION 2150
* WRITE(6,150) TEMCOR,ET ION 2160
DO 30 I=1,NSP ION 2170
30 GK(I) = GK(I) - TEMCOR*DELH(I) ION 2180
IP(IADS.EQ.0) GO TO 40 ION 2190
ETSF=0.05915*(273.15+TEMP)/298.15 ION 2200
ETFSC = 5802./(273.15+TEMP) ION 2210
* WRITE (6,160) ETSF ION 2220
40 RETURN ION 2230
***** ION 2240
ENTRY IONCOR(XMU) ION 2250
TF(XMU.NE.O.O) GO TO 60 ION 2260
DO 50 I=1, NNN ION 2270
50 XMU=XMU+ABS (T(I) *IQNZ (IDX( I) ))* ION 2280
XMU = 0. 5*XMU ION 2290
60 XIS=SQRT(XMU) ION 2300
GF=-ET* (XIS/ (1.0+XIS) -0.2*XMU) ION 2310
DGF=GF-GFO ION 2320
GF0=GF ION 2330
IF(IADS.GE.0) GO TO 65
IPO = IADX(161)
IPB = IADX(160)
*
* 65 IF( .NOT. (IONIT.LE.-1. OR. IONPH. LE.-1) ) WRITE(6,190) XMU.GFO ION 2340
65 CONTINUE
*
DO 70 I=1, NSP ION 2350
IF(IADS.GE.O) GO TO 68

```

```

      IF(A(I,IPO).NE.O.O.OR.A(I,IPB).NE.0.0) GO TO 70
68  GK(I)=GK(I) + DGF*(SPION(I,2)-SPION(I,1)**2)          ION 2360
70  CONTINUE
      RETURN ION 2370
***** ION 2380
      ENTRY IONCAL(XMUC)          ION 2390
      XMUC=0.0                    ION 2400
      DO 80 J=1,NNN              ION 2410
80  XMUC = XMUC + X(J)*IONZ(IDX(J))**2          ION 2420
      IF(IADS.EQ.O) GO TO 90      ION 2430
      IPO = IADX(161)            ION 2440
      IPB = IADX(160)           ION 2450
90  I1 = NN(1)+1                ION 2460
      I2 = NN(1)+NN(2)          ION 2470
      DO 110 I=1,12             ION 2480
      IF(IADS.EQ.O) GO TO 100     ION 2400
      IF(A(I,IPO).NE.O.O.OR.A(I,IPB).NE.0.0) GO TO 110 ION 2500
100 XMUC = XMUC + C(I)*SPION(I,1)**2          ION 2510
110 CONTINUE                    ION 2520
      XMUC = 0.5*XMUC           ION 2530
      RETURN                     ION 2540
*****
C   CONDUCTIVITY CALCULATIONS          ION 2550
      ENTRY CONDUCT              ION 2560
      IF(XIS.EQ.-1.0) RETURN      ION 2570
      CAPP=0.0                    ION 2580
      DO 120 I = 1 ,25           ION 2590
120  ACON(I)=0.0                ION 2600
C   CONDUCTIVITY OF COMPONENTS CALCULATED ION 2610
      DO 130 J=1,NNN            ION 2620
      IDJ=IDX(J)                 ION 2630
      B1=0.23*CAPP0(IDJ)*X(J)+30.32*IABS(IONZ(IDJ))*X(J) ION 2640
      D=XIS/(1.+0.3291*SIZE(IDJ)*XIS)          ION 2650
      ACON(J)=IABS(IONZ(IDJ))*(CAPP0(IDJ)*X(J)-D*B1)/1000. ION 2660
130  CAPP=CAPP+ACON(J)         ION 2670
C   CONDUCTIVITY OF OH(-) CALCULATED   ION 2680
      B1=(0.23*198.3+30.32)*C(IADY(13595) )    ION 2690
      D=XIS/(1.+0.3291*1.38*XIS)                ION 2700
      ACON(NNN+1)=(198.3*C(IADY(13595))-D*B1)/1000. ION 2710
      CAPP=CAPP+ACON(NNN+1)                    ION 2720
      WRITE(6,200)                             ION 2730
      DO 140 J=1,NNN                            ION 2740
*
* 140 WRITE(6,210) IDX(J),ACON(J)              ION 2750
140 continue
*
      IDJ=13595                                ION 2760
C
* WRITE(6,210) IDJ,ACON(NNN+1)                 ION 2770
* WRITE(6,220) CAPP                             ION 2780
C
      RETURN                                    ION 2790
150 FORMAT('0',10X,'FORMATION CONSTANTS CORRECTED FOR TEMPERATURE',/ ION2800
      '10',' TEMP.CORR.FACTOR = ',OPF8.4,5X,'IONIC STR. CORR. FACTOR= ' ION2810
      20PF8.3)                                  ION 2820
160 FORMAT('0',10X,'D.L.EXP.CONSTANT' =',F9.5) ION 2830
170 FORMAT(40I2)                                ION 2840
180 FORMAT(8(F7.2,3X))                          ION 2850

```

```

190 FORMAT('0,' IONIC STRENGTH = ', 1PE9 . 3,5X,' LOG F(Z=1) =', 0PF7 . 4      ION 2860
200 FORMAT('0,' CONDUCTIVITY OF COMPONENTS  ')                                ION 2870
210 FORMAT('0',2X,15,2X, 1PE10.3)                                             ION 2880
220 FORMAT('0,' TOTAL CONDUCTIVITY OF SOLUTION = ',1PE9.3)                    ION 2890
C
      END                                                                    ION 2900
*****
      SUBROUTINE EXCOL(J0,JJ)                                                  EXC 2910
***** EXCOL(J0, JJ) ; EXROW{I0,II} ***** EXC 2920
*****
      COMMON/ FARM/ IADS, EPS, TEMP, ET, ETSF,ETFSC,NNN,NSP,NN( 6 ),ITER,ITRPREXC 2930
      COMMON /VAR/GX (25),X(25),C(250),GC(250),Y(25),Z(25,25) ,                EXC 2940
1 T(2B) ,GK(250) ,A(250,25) ,IDX(25) ,IDY(250)                                EXC 2950
      COMMON/CYCLE/ICYCLE(2),ITITL,IPCP,ICND,THRSH,NXDIM,NYDIM,ITMAX,TSPEION 2960
      COMMON /COND/IONZ(200),SPION(250,2),CAPPA0(200),SIZE(200),DELH(250)    ION 2970
C
      DOUBLE PRECISION FM
      COMMON/FM_DAT/FM
      COMMON /DATDAT7DAT_DAT
      DOUBLE PRECISION GX,X, Y, Z,C,GC,V
      ! BY TP
C
      IV=IDX(JJ)                                                                EXC 2980
      IDX (T,T) =TDX(J0)                                                        EXC 2990
      IDX(J0)=IV                                                                EXC 3000
      V=X(J0)                                                                    EXC 3010
      X(J0)=X(JJ)                                                                EXC 3020
      X(JJ)=V                                                                    EXC 3030
      V=GX(J0)                                                                    EXC 3040
      GX(J0)=GX(JJ)                                                             EXC 3050
      GX(JJ)=V                                                                    EXC 3060
      V=T(J0)                                                                    EXC 3070
      T(J0)=T(JJ)                                                                EXC 3080
      T(JJ)=V                                                                    EXC 3090
      DO 10 I=1,NYDIM                                                            EXC 3100
      VB=A(I,J0)                                                                EXC 3110
      A(I,J0)=A(I,JJ)                                                            EXC 3120
10 A(I,JJ)=VB                                                                    EXC 3130
      RETURN                                                                    EXC 3140
***** EXC 3150
      ENTRY EXROW(IO,II)                                                        EXC 3160
      IV=IDY(II)                                                                EXC 3170
      IDY(II) =IDY(IO)                                                           EXC 3180
      IDY(IO)=IV                                                                EXC 3190
      DO 20 J=1, NXDIM                                                           EXC 3200
      VB=A(IO,J)                                                                EXC 3210
      A(IO,J)=A(II, J)                                                           EXC 3220
20 A(II,J)=VB                                                                    EXC 3230
      VB=GK(IO)                                                                  EXC 3240
      GK(IO)=GK(II)                                                             EXC 3250
      GK(II)=VB                                                                  EXC 3260
      VB=DELH(IO)                                                                EXC 3270
      DELH(IO) = DELH(II)                                                        EXC 3280
      DELH(II)=VB                                                                EXC 3290
      VB = SPION(IO,1)                                                           EXC 3300
      SPION(IO,1) = SPION(II,1)                                                 EXC 3310
      SPION(II,1) = VB                                                           EXC 3320
      VB = SPION(IO,2)                                                           EXC 3330

```

```

        SPION(IO,2) = SPION(II,2;                                EXC 3360
        SPION(II,2) = VB                                        EXC 3370
C
        RETURN                                                EXC 3380
        END                                                    EXC 3390
*****
SUBROUTINE INPUT'                                           INP 3400
***** INPUT' *****                                       INP 3410
*****
        COMMON/FARM/IADS,EPS,TEMP,ET,ETSF,ETFSC,NNN,NSP,NN(6),ITER,ITRPR    INP3420
        COMMON/VAR/GX(25)/X(25)/C(250),GC(250),Y(25),Z(25,25),              INP 3430
1 T(25), GK(250),A(250,25),IDX(25),IDY(250)                               INP 3440
        COMMON/CYCLE/ICYCLE(2),ITITL,IPCP,ICND,THRSH,NXDIM,NYDIM,ITMAX,TSP    INP 3450
        COMMON/VPHF/IONIT,XIS,GFO,IONPH,IPHA,IPHB,PHACT,HBA,HB,HA,IPHFX      INP 3460
        COMMON/COND/IONZ(200),SPION(250,2),CAPPA0(200),SIZE(200),DELH(250)  INP 3470
        COMMON/VSURF/PSID,PSI0,PSIB,SIGD,SIG0,SIGB/AREA,C1,C2,ZEL           INP 3480
*
        DOUBLE PRECISION FM
        COMMON/FM_DAT/FM
        COMMON /DATDAT/DAT_DAT'                                           ! BY TP
*
        CHARACTER * 80 BUFFER                                             ! BY TP
*
        CHARACTER * 80 OSYS_DAT(100000)                                  ! BY TP
        COMMON /OSY2DAT/OSYS_DAT, IROW                                    ! BY TP
        DATA IROW/0/                                                    ! BY TP
*
        DIMENSION IADXT(200), AT(6),IDT(6),IAT(6)                        INP 3490
        DOUBLE PRECISION GX,X,Y,Z,C,GC,PSID,PSI0,PSIB,SIGD,SIG0,SIGB,GXT    INP 3500
*
* Statements for MINEQL print out of normal file of speciation results.
* WRITE(6,248)                                                           INP 3505
* WRITE(6,400)
C
        irow = 0
C INITIALIZE ADDRESS                                                    INP 3510
        DO 10 J=1,200                                                    INP 3520
10 IADXT(J)=0                                                            INP 3530
        C INPUT PROBLEM DATA PARAMETERS                                INP 3540
        C
        IROW = IROW + 1                                                  ! BY TP
        READ (OSYS_DAT( IROW), FMT=' (A80) ') BUFFER                    ! BY TP
        READ (BUFFER ( 1 :5) , FMT = ' (F5.1) ') TEMP                    ! BY TP
        READ (BUFFER ( 6 :7) , FMT = ' (I2) ') IADS                       ! BY TP
        READ (BUFFER ( 8 :14) , FMT = ' (F7.1 ) ') AREA                  ! BY TP
        READ (BUFFER (15 :16) , FMT = ' (I2) ') IONIT'                   ! BY TP
        READ (BUFFER (17 :18) , FMT = ' (I2) ') IONPH                    ! BT TP
        READ (BUFFER (19 :22) , FMT = ' (I4) ') IPHA                     ! BY TP
        READ (BUFFER (23 :26) , FMT = ' (I4) ') IPHB                     ! BY TP
        READ (BUFFER (27 :29) , FMT = ' (I3) ') ICYCLE (1)                ! BY TP
        READ (BUFFER (30 :32) , FMT = ' (I3) ') ICYCLE (2)                ! BY TP
        READ (BUFFER (33 :34) , FMT = ' (I2) ') ITITL                    ! BY TP
        READ (BUFFER (35 :40) , FMT = ' (E6.1) ') EPS                     ! BY TP
        READ (BUFFER (41 :42) , FMT = ' (I2) ') IPCP                     ! BY TP
        READ (BUFFER (43 :44) , FMT = ' (I2) ') ICND                     ! BY TP
        READ (BUFFER (45 :49) , FMT = ' (F5.2) ') THRSH                  ! BY TP
        READ (BUFFER (50 :52) , FMT = ' (I3) ') ITRPR                    ! BY TP
        READ (BUFFER (53 :56) , FMT = ' (I4) ') ITMAX                    ! BY TP

```

	READ (BUFFER(57 : 60) , ' (I4) ')	NXDIM	! BY TP
	READ (BUFFER(61 : 64) , ' (I4) ')	NYDIM	! BY TP
	READ (BUFFER (65 : 66) ' (I2) ')	IPHFX	! BY TP
	READ (BUFFER(67 : 72) , ' (E6.1)	') TSP	! BY TP
C	IF (TEMP. EQ.0.0) TEMP =25.0		INP 3570
	IF (NXDIM. EQ.0) NXDIM =25		INP 3580
	IF (NYDIM. EQ.0) NYDIM = 100		INP 3590
	IF (ITMAX. EQ.0) ITMAX = 100		INP 3600
	IF(EPS.EQ.0.0) EPS = 1.0E-4		INP 3610
	IF(THRSH.EQ.0.0) THRSH = 0.01		INP 3620
	ITRPR = ITMAX- ITRPR		INP 3630
	ZEL=1.0		
C	J=0		INP 3640
			INP 3650
C	20 IROW = IROW + 1		! BY TP
	READ (OSYS_DAT(IROW), FMT = '(A80)') BUFFER		! BY TP
	READ (BUFFER(1:5) , FMT = '(I5)') IDXT		! BY TP
	READ (BUFFER(8:14), FMT= '(F7.2)') GXT		! BY TP
	READ (RUFFER(16:25), PMT= '(E.10.3)') TT		! BY TP
C	IF(IDXT.EQ.0) GO TO 30		INP 3670
	J=J+1		INP 3680
	IDX(J)= IDXT		INP 3690
	GX(J)=GXT		INP 3700
	T(J)=TT		INP 3710
	X(J)=10.**GXT		INP 3720
	IADXT(IDXT)=J		INP 3730
	GO TO 20		INP 3740
	30 IF (J.GT.NXDIM) CALL ERROR(1)		INP 3750
	IF(J.GT.10.AND.NYDIMEQ.100) NYDIM = 250		INP 3760
	NNN=J		INP 3770
C	INITIALIZE NN ; A AND B		INP 3780
	DO 40 L=1,6		INP 3790
	40 NN(L) = 0		INP 3800
	DO 50 I=1,NYDIM		INP 3810
	DO 50 J=1,NXDIM		INP 3820
	50 A(I,J)=0.0		IMP 3830
	DO 60 I=1,250		INP 3840
	SPION(I,1) =0.0		INP 3850
	60 SPION(I,2) =0.0		INP 3860
C	INPUT BASIS IN A MATRIX		IMP 1070
	DO 70 I=1,NNN		INP 3880
	IDY(I)=IDX(I)		INP 3890
	A(I,I)=1.0		TNP 5900
	DELH(I) =0.0		INP 3910
	70 GK(I)=0.0		INP 3P20
	NN(1)=NNN		INP 3930
C	INPUT THERMODYNAMIC DATA		TNP 3940
	I=NN(1)		INP 3950
	DO 110 L=2,6		INP 3960
	IO=I		INP 3970
	READ(10,260) IN		INP 3980
	IF(IN.EQ.0) GO TO 110		INP 3990
	DO 100 II=1,IN		INP 4000
	READ(10,260) IDYT,GKT,(IDT(J),IAT(J),J=1,4),DELHT		INP 4010
	DO 80 J=1,4		INP 4020

JTEST=IDT(J)	INP 4030
IF(JTEST.EQ.0) GO TO 80	INP 4040
IF(IADXT(JTEST).EQ.0) GO TO 100	INP 4050
80 CONTINUE	INP 4060
I = I + 1	INP 4070
IDY(I)=IDYT	INP 4080
DELH(I) = DELHT	INP 4090
GK(I)=GKT	INP 4100
DO 90 J=1,4	INP 4110
JTEST=IDT(J)	INP 4120
IF(JTEST.EQ.0) GO TO 90	INP 4130
A(IADXT(JTEST))=IAT(J)	INP 4140
90 CONTINUE	INP 4150
100 CONTINUE	INP 4160
NN(L)=1-I0	INP 4170
110 CONTINUE	INP 4180
C READ SPECIES MODIFICATION & TYPE SPECIFICATIONS	INP 4190
ENTRY INTYPE	INP 4200
C	
120 IROW = IROW + 1	! BY TP
READ (OSYS_DAT(IROW) , FMT = '(A80)') BUFFER	! BY TP
READ (BUFFER (1 : 5) , FMT = '(15) ') LTYPE	! BY TP
C	
IF(LTYPE.EQ.0) GO TO 240	INP 4220
C	! BY TP
130 IROW = IROW + 1	! BY TP
READ (OSYS_DAT(IROW) , FMT=(A80)') BUFFER	! BY TP
IF (IADS .NE. 0) THEN	! BY TP
READ (BUFFER (1 : 5) , FMT='(15)') IDYT	! BY TP
READ (BUFFER (8 : 14) , FMT=' (F7.2) ') GKT	! BY TP
READ (BUFFER (15 : 18) , FMT=' (14) ') IDT(1)	! BY TP
READ (BUFFER (19 :22) , FMT=' (F4.1) ') AT (1)	! BY TP
READ (SUPPER (23 :26) , FMT=' (14) ') IDT (2)	! BY TP
READ (BUFFER (27 :30) , FMT=' (F4.1) ') AT (2)	! BY TP
READ (BUFFER (31 :34) , FMT=' (14) ') IDT (3)	! BY TP
READ (BUFFER (35 :38) , FMT=' (F4.1) ') AT (3)	! BY TP
READ (BUFFER (39 :42) , FMT=' (14) ') IDT (4)	! BY TP
READ (BUFFER (43 :46) , FMT=' (F4.1) ') AT (4)	! BY TP
READ (BUFFER (47 :50) , FMT=' (14) ') IDT (5)	! BY TP
READ (BUFFER (51 :54) , FMT=' (F4.1) ') AT (5)	! BY TP
READ (BUFFER (55 :58) , FMT=' (14) ') IDT (6)	! BY TP
READ (BUFFER (59 :62) , FMT=' (F4.1) ') AT (6)	! BY TP
READ (BUFFER (63 :70) , FMT=' (F8.3) ') DELHT	! BY TP
ELSE	! BY TP
READ (BUFFER (1 : 5) , FMT='(15)') IDYT	! BY TP
READ (BUFFER (8: 14) , FMT='(F7.2)') GKT	! BY TP
READ (BUFFER (15 :18) , FMT='(14)') IDT(I)	! BY TP
READ (BUFFER (19 :21) , FMT='(13)') IAT (1)	! BY TP
READ (BUFFER (22 :25) , FMT='(14)') IDT (2)	! BY TP
READ (BUFFER (26 :28) , FMT='(13)') IAT (2)	! BY TP
READ (BUFFER (29 :32) , FMT='(14)') IDT (3)	! BY TP
READ (BUFFER (33 :35) , FMT='(13)') IAT (3)	! BY TP
READ (BUFFER (36 :39) , FMT='(14)') IDT (4)	! BY TP
READ (BUFFER (40 :42) , FMT='(13)') IAT (4)	! BY TP
READ (BUFFER (43 :46) , FMT='(14)') IDT (5)	! BY TP
READ (BUFFER (47 :49) , FMT='(13)') IAT (5)	! BY TP
READ (BUFFER (50 :53) , FMT='(14)') IDT (6)	! BY TP

	READ (BUFFER (54 : 56; FMT='(13)') IAT(6) FMT='(F8.3)')	! BY TP
	READ (BUFFER (57 : 64), DELHT	! BY TP
	END IF	! BY TP
C		
	IF(IDYT.EQ.O) GO TO 120	INP 4250
	SEARCH	INP 4260
	II = 0	INP 4270
	DO 150 L=1,6	INP 4280
	IF(NN(L).EQ.O) GO TO 150	INP 4290
	I0=II+1	TNP 4300
	II=II+NN(L)	INP 4310
	DO 140 I = I0, II	IMP 4320
	IF(IDY(I).NE.IDYT) GO TO 140	INP 4330
	IF(DELHT.NE.0.0) DELH(I) = DELHT	INP 4340
	IF(GKT.NE.0.0) GK(I)=GKT	INP 4350
	GO TO 200	INP 4360
	140 CONTINUE	INP 4370
	150 CONTINUE	INP 4380
C	SEARCH UNSUCCESSFUL: ENTER NEW SPECIES	INP 4390
	IALL0=0	INP 4400
	DO 170 J=1,6	INP 4410
	JTEST=IDT (J)	INP 4420
	IF (JTEST.EQ.O) GO TO 170	INP 4430
	IF(IADXT(JTEST).NE.0) GO TO 160	INP 4440
	WRITE(6,300) IDYT,JTEST	INP 4450
	CALL ERROR(3)	INP 4460
	160 IALLO=1	INP 4470
	170 CONTINUE	INP 4480
	IF(IALLO.NE.0) GO TO 180	INP 4490
	WRITE(6,300) IDYT	INP 4500
	CALL ERROR(3)	INP 4510
	180 I=NN(1)+NN(2)+NN(3)+NN(4)+NN(5)+NN(6)+1	INP 4520
	NN(6)=NN(6) + 1	INP 4530
	L=6	INP 4540
	IDY(I)=IDYT	INP 4550
	DELH(I) = DELHT	INP 4560
	GK(I)=GKT	INP 4570
	DO 190 J=1,6	INP 4580
	JTEST=IDT(J)	INP 4590
	IF(JTEST.EQ.0) GO TO 190	INP 4600
	IF(IADS.EQ.0) A(I,IADX(JTEST)) = IAT(J)	INP 4610
	IF(IADS.NE.0) A(I,IADX(JTEST))= AT(J)	INP 4620
	190 CONTINUE	INP 4630
C	MOVE SPECIES I FROM TYPE L TO LTYPE	INP 4640
	200 IF(L.EQ.LTYPE) GO TO 130	INP 4(550
	K=1	INP 4(560
	II = 0	INP
	DO 210 LL=1,L	INP
	210 II=II+NN(LL)	INP 4 ft go
	IF(LTYPE.GT.L) GO TO 220	INP 4700
	K=-1	INP 4710
	II=II-NN(L)+1	INP 4720
	220 NN(L)=NN(L)-1	TNP 4730
	NN(LTYPE)=NN(LTYPE)+1	INP 4740
	230 CALL EXROW(I,II)	INP 4750
	L=L + K	INP 4760
	I = II	INP 4770
	II=II+NN(L)*K	INP 4780

```

IF(L.NE.LTYPE) GO TO 230
GO TO 130
C
240 NSP = NN(1)+NN(2)+NN(3)+NN(4)+NN(5)+NN(6)
RETURN
248 FORMAT ('0'////,15X,')*****
$***',/0',16X,'THE MINEQL+STANFORD COMPUTER PROGRAM FOR SOLVING',
$/0',17X,'SOLUTION-SURFACE CHEMICAL EQUILIBRIUM PROBLEMS',
$/0',21X,'WAS LAST MODIFIED ON JANUARY 7,1983 ',
$/0',21X,'BY DHARMA IYER,','0',21X,
$'DEPARTMENT OF CIVIL ENGINEERING, SYRACUSE UNIVERSITY.','','
/0',18X, 'IF YOU ENCOUNTER ANY ERRORS IN THE COMPUTER PRINTOUT',//
/0',20X, MAKE SURE YOU HAVE : ' , /
/0',20X, ' 1. READ THE MANUAL CAREFULLY, ' , /
/0',20X, ' 2. CHECKED YOUR JCL CARDS,','/
/0',20X, ' 3. CHECKED THE MAIN PROGRAM,','/
/0',20X, ' 4. CHECKED THE DATA CARDS,','/
/0',20X, ' 5. USED REASONABLE GUESSES FOR CONCENTRATIONS(GX),','/
/0',20X, ' 6. REVIEWED YOUR EQUILIBRIUM PROBLEM AND DATA',/
/0',15X, '*****')
250 FORMAT(I5,2X,F7.2,E7.2)
260 FORMAT(I5,2X,F7.2,4(I4,I3)/14X,F8.3)
270 FORMAT(I5,2X,F7.2,6(I4,F4.1),F8.3)
280 FORMAT(15, 2X,F7.2,6(I4,I3) , F8.3)
290 FORMAT(F5.1,I2,F7.1,2I2,2I4,2I3,I2,E6.1,2I2,F5.2,I3,3I4,I2,E6.1)
300 FORMAT(/'0','SPECIES ID - ',15,' $$ COMPONENT ID = ',15)
400FORMAT(/'0',15X,'NOTE: WHERE DOUBLE LAYER CALCULATIONS ARE ',
1'INCLUDED,','0',19X,IADS = 1 (IN PROGRAM PARAMETER CARD) WILL ',
2'ALLOW SURFACE CONSTANTS TO BE CORRECTED FOR IONIC STRENGTH',
3/'0',19X,'IF YOU DO NOT WANT SURFACE CONSTANTS TO BE CORRECTED,',
4' SPECIFY IADS = -1')
C
END
*****
SUBROUTINE OUTPUT
***** OUTPUT; OINCOMP; OINSPC; OUTCMP; OUTS PC; OUTPC* *
*****
COMMON/PARM/IADS,EPS,TEMP,ET,ETSF,ETFSC,NNN,NSP,NN (6),ITER,ITRPR
COMMON/VAR/GX(25) ,X(25) ,C(250) , GC (250) , Y(25) ,Z(25,25),
1T(25) ,GK(250) ,A(250,25) , IDX(25) , IDY(250)
COMMON/CYCLE/ICYCLE(2),ITITL,IPCP,ICND,THRSH,NXDIM,NYDIM,ITMAX,TSP
COMMON/VPHF/IONIT,XIS,GFO,IONPH,IPHA,IPHB,PHACT,HBA,HB,HA,IPHF
COMMON/COND/IONZ (200),SPION(250,2),CAPPA0(200),SIZE(700),DELH (250)
COMMON/VSURF/PSID,PSI0,PSIB,SIGD,SIG0,SIGB,AREA,C1,C2,ZEL
C
DOUBLE PRECISION
GX,X,Y,Z,C,GC,PSID,PS 10,PSIB,SIGD,SIGO,SIGB,CTSPOUT5000
C
INTEGER NAME(200)/
1'CA ','MG ','SR ','K ','NA ','FE3 ','FE2 ','MN2 ','CU2 ',
2'BA ','CD ','ZN ','NI ','HG ','PB ','CO2 ','CO3 ','AG ',
3'CR ','AL ','CS ','LI ','BE ','SC ','TIO ','SN2 ','SN4 ',
4'LA ','CE3 ','AU1 ','TH4 ','UO2 ','CU1 ','X34 ','X35 ','X36 ',
5'X37 ','X38 ','X39 ','X40 ','9*' ','H ','48*' ',
@'E- ' ',
6'COS-',SO4','CL ','F ','BR ','I ','NH3','S ','PO4',
7'P207','PO10','SIO3','S2O3','CN ','AC ','ACAC','CIT ','OX ',
8'SAL ','TART','EN ','DIP ','SUSA','GLY ','GLU ','PIC ','NTA ',

```

```

9'EDTA','DCTA','CYST','NOR ','PHTH','ARG ','ORN ','LYS ','HIS ',      OUT 5110
&'ASP ','SER ','ALA ','TYR ','MET ','VAL ','THR ','PHE ','ISO ',      OUT 5120
1'LEU ','PRO ','BOH4','S03 ','SCN ','NHOH','M004','W04 ','AS04',      OUT 5130
2'V04 ','SE04','N03 ','TRIS ','SOH ','PSIB','PSIO','PCCA', 'PDCA',      OUT 5140
3 'SYR ','C165','C166','C167','C168','C169','C170','C171', 'C172 ',      OUT 5150
4'C173','C174','C175','S176','S177','S178','S179', 'S180', 20*'  '/

C
*   INTEGER TYPE (42) /      OUT 5170
*   1'I - ','COMP','ONEN','TS ',3*'  ',      OUT 5180
*   2 'II -',' COM', 'PLEX', 'ES ',3*'  '      OUT 5190
*   3'III ','- FI','XED ','SOLI','DS ',2*'  '      OUT 5200
*   4'IV -',' PRE', 'CIPI', 'TATE', 'D SO', 'LIDS',      OUT 5210
*   5 'V -', 'DISS ', 'OLVE', 'D SO', 'LIDS',2*'  ',      OUT 5220
*   6'VI -',' SPE','CIES',' NOT',' CON',' SIDE','RED '/      OUT 5230

C
    DIMENSION AT(6),IDT(6),NTITL (20)      OUT 5240

C
    DOUBLE PRECISION FM
    COMMON/FM_DAT/FM
    COMMON /DATDAT/DAT_DAT      ! BY TP

C
    CHARACTER * 80 OSYS_DAT (10000)      ! BY TP
    COMMON /OSYSDAT/OSYS_DAT, IROW      ! BY TP

C
    CHARACTER * 80 BUFFER      ! BY TP
    CHARACTER * 9 A_C_STRING      ! BY TP
    CHARACTER * 9 DAT_DAT(512)      ! BY TP

C
    INTEGER DAT_ROW      ! BY TP
    COMMON/DATROW/DAT_ROW

C
    DATA DAT_ROW/0/      ! BY TP

* *****      OUT 5250

C   INPUT DATA COMPONENTS      OUT 5260
    ENTRY OINCOMP      OUT 5270

C
*   WRITE (6,390)      OUT 5280
*   WRITE(6,400)      OUT 5300

C
    IF (ITITL.EQ.0) GO TO 20      OUT 5290

C
    DO 10 1=1, ITITL      OUT 5310

C
C   READ(5,410) (NTITL(J),J=1,20)      OUT 5320

C
    IROW = IROW + 1      ! BY TP
    READ (OSYS_DAT (IROW),FMT = '(A80)') BUFFER      ! BY TP
    DO J = 1, 20      ! BY TP
        JLOOP = (J*4)-4 + 1      ! BY TP
        JP3 = JLOOP + 3      ! BY TP
        READ (BUFFER (JLOOP:JP3) , FMT='(A4)') NTITL (J)      ! BY TP
    END DO      ! BY TP

C
    10 WRITE(6,420) (NTITL(J),J=1,20)      OUT 5330
20 CONTINUE

*
*   20 WRITE(6,405) IADS,IONIT,IONPH,IPHFX,IPHA,IPHB,ITITL,IPCP,ICND
20 continue

```

```

*
* WRITE (6,400) OUT 5340
* WRITE (6, 260) TEMP OUT 5350
* IF(IADS.NE.0) WRITE(6,250) AREA OUT 5360
* WRITE(6,270) EPS OUT 5370
* WRITE (6,280) OUT 5380
*
* DO 30 J=1,NNN OUT 5390
*
* 30 WRITE(6,290) IDX (J) , X (J) , GX (J) , T (J) , NAME ( IDX (J) ) OUT 5400
* 30 continue
*
* RETURN OUT 5410
* ***** OUT 5420
C INPUT DATA SPECIES OUT 5430
  ENTRY OINSPC OUT 5440
  L=0 OUT 5450
  M=1 OUT 5460
  DO 70 I=1,NSP - OUT 5470
  IF(M.NE.I) GO TO 50 OUT 5480
40 L=L+1 OUT 5490
  IF (NN(L) EQ.0) GO TO 40 OUT 5500
  M=M+NN(L) OUT 5510
  L2=L*7 OUT 5520
  L1=L2-6 OUT 5530
*
* WRITE (6,300) (TYPE(N) ,N=L1,L2) OUT 5540
*
* 50 K=0 OUT 5550
*
* DO 60 J=1,NNN OUT 5560
* IF (A(I, J).EQ.0) GO TO 60 OUT 5570
* K=K+1 OUT 5580
* IDT(K) =IDX(J) OUT 5590
* AT(K)=A (I, J) OUT 5600
* 60 CONTINUE OUT 5610
*
* 70 WRITE (6, 310) IDY(T) ,GK(I) ,DELH(T),(NAME(IDT (J)),AT(J),J=1,K) OUT 5620
* 70 continue
* RETURN OUT 5630
* ***** OUT 5640
C COMPONENT OUTPUT OUT 5650
  ENTRY OUTCMP OUT 5660
  IF(ICYCLE(I).EQ.0.OR.ITRPR.NE. ITMAX) WRITE (6, 340) OUT 5670
*
* WRITE(6,320) ITER OUT 5680
* IF (IADS. EQ.0) GO TO 80 OUT 5690
* PSIO=-GX(IADX(161))*ETSF QUT 5700
* PSIB=-GX(IADX(160))*ETSF OUT 5710
* SIGO= (PSIO-PSIB)*9.65E+6*C1/AREA OUT 5720
* SIGD=-11.74*DSINH(ETFSC*PSID*ZEL)*XIS OUT 5730
* SIGB=-SIGO-SIGD OUT 5740
*
* WRITE (6, 330) PSIO, PSIB, PSID, SIGO , SIGB, SIGD OUT 5750
* 80 WRITE (6,350) OUT 5760
* 80 continue
*
* DO 90 J=1,NNN OUT 5770
*

```

```

*      90 WRITE(6,360) IDX (J) ,X{J} ,GX(J) ,T(J),Y(J) ,NAME(IDX(J) )           OUT 5780
*      90 continue
*
*      RETURN                                                                    OUT 5790
* ***** OUT 5800
*      ENTRY OUTSPC                                                                OUT 5810
*      CTSP=0.0D0 + TSP
C      CHARGE OF SOLUTION (HOPEFULLY = ZERO)                                     OUT 5820
*      IF (IADS.EQ.0) GO TO 100                                                    OUT 5830
*      IPO = IADX(161)                                                            OUT 5840
*      IPB = IADX(160)                                                            OUT 5850
100  CHRGSF =0.0                                                                  OUT 5860
*      CHRG = 0.0                                                                OUT 5870
*      DO 110 1=1, NNN                                                            OUT 5880
110  CHRG = CHRG+X(I)*IONZ (IDX(I) )                                             OUT 5890
*      I1 = NN(1)+1                                                              OUT 5900
*      I2 = NN(1) +NN(2)                                                         OUT 5910
*      DO 120 1=I1,I2                                                            OUT 5920
*      CION=C(I)*SPION(I,1)                                                      OUT 5930
*      IF (IADS.EQ.0) GO TO 120                                                  OUT 5940
*      IP(A(I, IPO).NE.0.0. OR. A(I,IPB) .NE.0.0) CHRGSF = CHRGSF+CION        OUT 5950
120  CHRG = CHRG+CION                                                            OUT 5960
*      CHRG = CHRG-CHRGSF                                                        OUT 5970
*      GCHRG = 1000000001                                                         OUT 5980
*      IF(CHRG.NE.O .0) GCHRG = ALOGIO (ABS (CHRG) )                            OUT 5990
*
*      WRITE (6, 450) CHRG, GCHRG                                               OUT 6000
*
*      IF(IADS.EQ.0) GO TO 130                                                    OUT 6010
*      GCHRG _ 1000000001                                                         OUT 6020
*      IF (CHRGSF. NE.0.0) GCHRG = ALOGIO (ABS(CHRGSF))                         OUT 6030
*
*      WRITE(6, 460) CHRGSF, GCHRG                                             OUT 6040
*
C      SPECIES OUTPUT                                                            OUT 6050
*      130 L=0                                                                    OUT 6060
*      M=1                                                                        OUT 6070
C
*      DO 170 I=1,NSP                                                            OUT {,000
*      IF (M.NE.I) GO TO 150                                                    OUT 6090
140  L=L+1                                                                        OUT 6100
*      IF (NN(L) .EQ.0) GO TO 140                                               OUT 6110
*      M=M+NN(L)                                                                OUT 6120
*      L2=L*7                                                                    OUT 6130
*      L1=L2-6                                                                    OUT 6140
*
*      WRITE (6,370) (TYPE (N) , N=L1 , L2)                                     OUT 6150
*
150  IF(DABS (C (I) ).LT.CTSP) GO TO 170
*      K = 0                                                                      OUT 6160
*      DO 160 J=1,NNN                                                            OUT 6170
*      IF(ABS(A(I, J) ) .LT. 0.0001) GO TO 160                                  OUT 6180
*      K=K+1                                                                      OUT 6190
*      IDT(K)=IDX(J)                                                            OUT 6200
*      AT(K)=A(I,J)                                                            OUT 6210
160  CONTINUE                                                                    OUT 6220
*
*      WRITE(6,380) IDY(I),C(I),GC(I),GK(I),(NAME(IDT(J)),AT(J),J=1,K)        OUT 6230

```



```

                RETURN
C
250 FORMAT('0',' SURFACE AREA FOR ADSORPTION IN SQUARE METERS = ',
           1PE9.2)
260 FORMAT('0',10X,' TEMPERATURE = ',F5.1,' CELSIUS')
270 FORMAT ('0' , 22X, 'EPS = 1PE8.1)
280 FORMAT(2X,' ID',10X,'X',4X,'LOGX',11X,"T",5X,'COMPONENTS')
290 FORMAT(2X,I5,2X,1PD9.2,2X,OPF6.2/1PE12.3,5X,A4)
300 FORMAT(2X,' ID' , 4X, ' LOGK' , 5X, ' DELH' , 6X, ' SPECIES: TYPE ',7A4)
310 FORMAT(2X,I5,2X,OPF6.2,3X,OPF7.3,5X,6(A4,F5.1,3X))
320 FORMAT(2X,' OUTPUT DATA: ITERATIONS = ',I3)
330 FORMAT('0,' PSIO =',1PD11.3,4X,'PSIB =', 1PD11.3,4X,'PSID =',
           11PD11.3,' VOLT'/0,' SIGO =',1PD11.3,4X,'SIGB =',1PD11.3,4X,
           2'SIGD =',1PD11.3,' MICROCOUL/CM.SQ')
340 FORMAT('1')
350 FORMAT(2X,' ID',11X,'X',5X,'LOGX',11X,"T",11X,'Y',5X,'SPECIES')
360 FORMAT(2X,I5,1PD12.3,OPF9.3,1PD12.3,1PE12.3,5X,A4)
370 FORMAT(2X,' ID' ,11X,'C',5X, 'LOGC',4X, 'LOGK',5X,
           1'SPECIES: TYPE ',7A4)
380 FORMAT(2X,I5,1PD12.3,OPF9.3,OPF8.2,5X,6(A4,1X,F5.1,4X))
390 FORMAT('1',18X,' $$$ INPUT DATA $$$')
400 FORMAT('0' '*****',
           '*****')
405 FORMAT('0','OPTIONS: IADS=',I2,' IONIT'=',I2,' IONPH'=',I2,
           [' IPHF'=',I2,' IPHA'=',I3,' IPHB'=',I2,' ITTTL'=',I2,' IPCP'=',I1,
           [' ICND'=',I1)
410 FORMAT(20A4)
420 FORMAT('0',20A4)
430 FORMAT(2X,A4,3X,F6.1,' PERCENT BOUND IN SPECIES',I7,3X,6(A4,1X,
           1F5.1,3X))
440 FORMAT (2X,' PERCENTAGE DISTRIBUTION OF COMPONENTS')
450 FORMAT ('0',5X,"TOTAL CHARGE IN SOLUTION =",1PE11.3,
           1' MOLES/L; LOGCHARGE =",OPF8.3)
460 FORMAT ('0',5X,"TOTAL SURFACE CHARGE =",1PE11.3,
           1' MOLES/L; LOGCHARGE =",OPF8.3)
C
                END
                *****
                SUBROUTINE SIMQ(Z,Y,N)
                ***** SIMQ(Z,Y,N) *****
                *****
                DIMENSION Z(25,25) , Y (25 )
                DOUBLE PRECISION Z,Y,ZMAX,V
C   PROVISION FOR N=1
                IF (N.NE. 1) GO TO 10
                Y(1)=Y(1)/Z(1,1)
                RETURN
C   ELEMENT OF ELIMINATION
10  N1=N-1
                DO 60  M=1,N1
                ZMAX=0
                IMAX=0
C   FIND MAX OF COLUMN
                DO 20  I=M,N
                IF(DABS (Z(I,M)).LE.ZMAX) GO TO 20
                IMAX=I
                ZMAX=DABS(Z(I,M))
20  CONTINUE

```

C	ERROR RETURN	SMQ 7160
	IF(IMAX.EQ.0) CALL ERROR (8)	SMQ 7170
C	ROW INTERCHANGE	SMQ 7180
	IF(IMAX.EQ.M) GO TO 40	SMQ 7190
	V=Y(M)	SMQ 7200
	Y(M)=Y(IMAX)	SMQ 7210
	Y(IMAX) =V	SMQ 7220
	DO 30 J=M,N	SMQ 7230
	V=Z(M, J)	SMQ 7240
	Z(M, J) =Z(IMAX, J)	SMQ 7250
	30 Z(IMAX,J)=V	SMQ 7260
C	DIAGONALIZE	SMQ 7270
	40 M1=M+1	SMQ 7280
	DO 50 I=M1,N	SMQ 7290
	V=Z (I,M)/Z (M,M)	SMQ 7300
	Y(I)=Y(I)-V*Y (M)	SMQ 7310
	DO 50 J=M,N	SMQ 7320
	50 Z(I,J)=Z(I,J)-V*Z(M,J)	SMQ 7330
	60 CONTINUE	SMQ 7340
C	BACK SUBSTITUTE	SMQ 7350
	Y(N) =Y(N)/Z (N,N)	SMQ 7360
	N1=N-1	SMQ 7370
	DO 80 K=I,NI	SMQ 7380
	I=N-K	SMQ 7390
	I1=I+1	SMQ 7400
	DO 70 J=I1,N	SMQ 7410
	70 Y(I)=Y(I)-Y(I)*Z{I,J}	SMQ 7420
	80 Y(I)=Y(I)/Z(I, I)	SMQ 7430
C	RETURN	SMQ 7440
	END	SMQ 7450

	SUBROUTINE SOLID	SLD 7460
***** SOLID *****		

	COMMON/FARM/IADS,EPS,TEMP,ET,ETSF,ETFSC,NNN,NSP,NN(6) ,ITER,ITRPR	SLD 7480
	COMMON/VAR/GX(25),X(25),C(250),GC(250),Y(25),Z(25,25),	SLD 7490
	1T(25),GK(250),A(250,25),IDX(25),IDY(250)	SLD 7500
	COMMON/COND/IONZ(200),SPION(250,2),CAPPA0(200),SIZE(200),DELH(250)	SLD 7510
	DOUBLE PRECISION GX,X,Y,Z,C,GC	SLD 7520
	DOUBLE PRECISION FM	
	COMMON/FM_DAT/FM	
	COMMON /DATDAT/DAT_DAT	! BY TP
	IF(NN(3)+NN(4).EQ.0) RETURN	SLD 7530
	LL=NN(3)+NN(4)	SLD 7540
	IO=NN(1)+NN(2)+NN(3)+NN(4)+1	SLD 7550
	JO=NNN+1	SLD 7560
	DO 60 L=1,LL	SLD 7580
	I0=I0-1	SLD 7590
	JO=JO-1	SLD 7600
C	FIND JEXC FOR 10	SLD 7610
	DO 10 J=1,JO	SLD 7620
	IF (ABS(A(IO,JO-(J-1))).GT.0.001) GO TO 20	SLD 7630
	10 CONTINUE	SLD 7640
	CALL ERROR(6)	SLD 7650
	20 JEXC=JO-(J-1)	SLD 7660
	CALL EXCOL(JEXC,JO)	SLD 7670

```

NXS=JO-1 SLD 7680
NCS=IO-1 SLD 7690
C MODIFY A,B,T SLD 7700
DO 30 I=1,NCS SLD 7710
DO 30 J=1,NXS SLD 7720
30 A(I,J)=A(I,J)-A(IO,J)*A(I,JO)/A(IO,JO) SLD 7730
DO 40 J=1,NXS SLD 7740
40 T(J)=T(J)-A(IO,J)*T(JO)/A(IO,JO) SLD 7750
DO 50 I=1,NCS SLD 7760
DELH(I) = DELH(I)-A(I,JO)*DELH(IO)/A(10,JO) 50 GK(I)=GK(I)- SLD 7770
A(I,JO)*GK(IO)/A(10,JO) SLD 7780
60 CONTINUE SLD 7730
C SLD 7800
RETURN SLD 7810
END SLD 7820
*****
SUBROUTINE SOLIDX (KK) SDX 7830
***** SOLIDX (KK) ***** SDX 7840
*****
COMMON/PARM/IADS,EPS,TEMP,ET,ETSF,ETFSC,NNN,NSP,NN(6),ITER,ITRPR SDX 7850
COMMON/VAR/GX(25),X(25),C(250),GC(250),Y(25),Z(25,25), SDX 7860
1T(25),GK(250),A(250,25),IDX(25),IDY(250) SDX 7870
COMMON/COND/IONZ(200),SPION(250,2),CAPPAO(200),SIZE(200),DELH(250) SDX 7880
DOUBLE PRECISION GX,X,Y,Z,C,GC,V,VMIN,VMAX SDX 7890
DOUBLE PRECISION FM
COMMON/FM_DAT/FM
COMMON /DATDAT/DAT_DAT ! BY TP
C SDX 7900
KK=0 SDX 7910
C SDX 7920
IF(NN(3)+NN(4).EQ.0) GO TO 80 SDX 7930
LL=NN(3)+NN(4) SDX 7940
II=NN(1)+NN(2) SDX 7950
IO=NN(1)+NN(2)+1 SDX 7960
JO=NNN-NN(3)-NN(4)+1 SDX 7970
C MOLE BALANCE MINUS SOLIDS SDX 7980
DO 10 J=JO,NNN SDX 7990
Y(J)=-T(J) SDX 8000
DO 10 I=1,II SDX 8010
10 Y(J)=Y(J)+A(I,J)*C(I) SDX 8020
C AMOUNT OF SOLIDS SDX 8030
DO 70 L=1,LL SDX 8040
C(IO)=-Y(JO)/A(IO,JO) SDX 8050
GC(IO) = DLOG10(DABS(C(IO))) SDX 8060
DO 20 K=JO,NNN SDX 8070
20 Y(K)=Y(K)+A(IO,K)*C(10) SDX 8080
C UNMODIFY A,B,T,GX,X SDX 8090
NXS=JO-1 SDX 8100
NCS=IO-1 SDX 8110
V=GK(IO) SDX 8120
DO 30 J=1,NXS SDX 8130
30 V=V+A(IO,J)*GX(J) SDX 8140
GX(JO)=-V/A(IO,JO) SDX 8150
X(JO)=10.**GX(JO) SDX 8160
DO 40 I=1,NCS SDX 9170
DO 40 J=1,NXS SDX 8180
40 A(I,J)=A(I,J)+A(IO,J)*A(I,JO)/A(10,JO) SDX 8190
DO 50 J=1,NXS SDX 8200

```

50	(I(J))=T(J)+A(IO,J)*T(JO)/A(10,JO)	SDX 8210
	DO 60 I=1,NCS	SDX 8220
	DELH(I) = DELH(I)+A (I,JO)*DELH(IO)/A(IO,JO)	SDX 8230
60	GK(I)=GK(I)+A(I,JO)*GK(10)/A(10,JO)	SDX 8240
	I0=I0+1	SDX 8250
70	JO=JO+1	SDX 8260
C	SOLUBILITY PRODUCTS	SDX 8270
80	IF(NN(5)+NN(6).EQ.0) GO TO 110	SDX 8280
	IO=NN(1)+NN(2)+NN(3)+NN(4)+1	SDX 8290
	DO 100 I=IO,NSP	SDX 8300
	V=GK(I)	SDX 8310
	DO 90 J=1,NNN	SDX 8320
90	V=V+A(I,J)*GX(J)	SDX 8330
	GC(I)=V	SDX 8340
	IF(V.GT.7.501) V = 7.5D1	
	IF((-V).GT.7.EDI) V = 7.5D1	
	100 C (I)=10.**V	SDX 8350
C		SDX 8360
C	CHECK FOR DISSOLUTION	SDX 8370
110	IF(NN(4).EQ.0) GO TO 140	SDX 8380
	IMIN=0	SDX 8390
	VMIM=0	SDX 8400
	IO=NN(1)+NN(2)+NN(3)+1	SDX 8410
	II=NN(1) + NN(2) +NN(3) +NN(4)	SDX 8420
	DO 120 I=IO,II	SDX 8430
	IF(C(I).GT.VMIN) GO TO 120	SDX 8440
	VMIN=C(I)	SDX 8450
	IMIN-I	SDX 8460
120	CONTINUE	SDX 8470
	IF(IMIN.EQ.0) GO TO 140	SDX 8480
	WRITE(6,130) ITER,IDY(IMIN)	SDX 8490
130	FORMAT('0,' ITERATIONS= ',I3,' SOLID ',15,' DISSOLVES')	SDX 8500
	CALL EXROW(IMIN, II)	SDX 8510
	NN(5)=NN(5)+1	SDX 8520
	NN(4)=NN(4)-1	SDX 8530
	KK = -1	SDX 8540
	RETURN	SDX 8550
C		SDX 8560
C	CHECK FOR PRECIPITATION	SDX 8570
140	IF (NN(B).EQ.0) RETURN	SDX 8580
	VMAX=0	SDX 8590
	IMAX=0	SDX 8600
	IO=NN(1) +NN(2)+NN(3) +NN(4)+1	SDX 8610
	II=NSP - NN(6)	SDX 8620
	DO 150 I=IO,II	SDX 8630
	IF(GC(I).LT.VMAX) GO TO 150	SDX 8640
	VMAX=GC(I)	SDX 8650
	IMAX=I	SDX 8660
150	CONTINUE	SDX 8670
	IF (IMAX.EQ.0) RETURN	SDX 8680
*	WRITE(6,160) ITER, IDY(IMAX)	SDX 8690
160	FORMAT('0,' ITERATIONS= ',I3,' SOLID ',15,' PRECIPITATES')	SDX 8700
	CALL EXROW(IMAX, I0)	SDX 8710
	NN(4)=NN(4)+1	SDX 8720
	NN(5)=NN(5)-1	SDX 8730
	KK = 1	SDX 8740
	RETURN	SDX 8750
	END	SDX 8760

```

*****
DOUBLE PRECISION FUNCTION FSIN(X,Y,Z) FSC 8770
***** FSIN(X,Y,Z); FC03(X,Y,Z) ***** FSC 8780
COMMON/PARM/IADS,EPS,TEMP,ET,ETSF/ETFSC,NNN,NSP,NN(6),ITER,ITRPR FSC 8790
DOUBLE PRECISION X FSC 8800
FSIN = -1.214E-6*DSINH(ETFSC*X*Z)*Y FSC 8810
RETURN FSC 8820
*****
ENTRY FCOS(X,Y,Z) FSC 8830
FCOS = -1.214E-6*DCOSH(ETFSC*X*Z)*19.46*Y*Z FSC 8840
RETURN FSC 8850
END FSC 8860
*****
SUBROUTINE SOLVE
***** SOLVE ***** SLV 8870
*****
COMMON/PARM/IADS,EPS,TEMP,ET,ETSF,ETFSC,NNN,NSP,NN(6),ITER,ITRPR SLV 8890
COMMON/VAR/GX(25),X(25),C(250),GC(250),Y(25),2(25,25), SLV 8900
1T(2B),GK(250),A(2SO,25),IDX(25),IDY(250) SLV 8910
COMMON/CYCLE/ICYCLE(2),ITITL,TPCP,ICND,THRSH,NXDIM,NYDIM,ITMAX SLV 8920
COMMON/VPHF/IONIT,XIS,GFO,IONPH,IPHA,IPHB,PHACT,HBA,HB,HA,IPHFX SLV 8930
COMMON/VSURF/PSID,PSIO,PSIB,SIGD,SIGO,SIGB,AREA,C1,C2,ZEL SLV 8940
DOUBLE PRECISION CX,X,Y,Z,C,GC,PSID,PSIO,PSIB,SIGD,SIGO,SIGB,V,DF, SLV 8950
1 F,VMAX,YTM(25),DEPS SLV 8960
DOUBLE PRECISION FM
COMMON/FM_DAT/FM
COMMON /DATDAT/DAT_DAT ! BY TP
C SLV 8970
DEPS=O.ODO+EPS SLV 8980
IF (IADS.EQ.0) GO TO 20 SLV 8990
PSIB=-GX(IADX(160))*ETSF SLV 9000
PSID=PSIB/3.0 SLV 9010
DO 10 J=1,10 SLV 9020
F=PSIB-PSID+FSIN(PSID,AREA,ZEL)/C2*XIS SLV 9030
DF=-1+FCOS(PSID,AREA,ZEL)/C2*XIS SLV 9040
10 PSID=PSID-F/DF SLV 9050
NO=IADX(161) SLV 9060
NB=IADX(160) SLV 9070
20 NC=NN(1)+NN(2) SLV 9080
NX=NNN-NN(3)-NN(4) SLV 9090
30 IF (IADS.EQ.0) GO TO 50 SLV 9100
PSIO=-GX(NO)*ETSF SLV 9110
PSIB=-GX(NB)*ETSF SLV 9120
DO 40 J=1,10 SLV 9130
F=PSIB-PSID+FSIN(PSID,AREA,ZEL)/C2*XIS SLV 9140
DF=-1+FCOS(PSID,AREA,ZEL)/C2*XIS SLV 9150
40 PSID=PSID-F/DF SLV 9160
C COMPLEXES SLV 9170
50 DO 70 I=1,NC SLV 9180
V=GK(I) SLV 9190
DO 60 J=1,NX 60 SLV 9200
V=V+A(I,J)*GX(J) SLV 9210
GC(I)=V SLV 9220
IF(V.GT.7.5D1) V = 7.5D1
IF((-V).GT.7.5D1) V = -7.5D1
70 C(I)=10.**V SLV 9230
C MOLE BALANCE SLV 9240

```

	DO 90 J=1,NX	SLV 9250
	V=-T(J)	SLV 9260
	DO 80 I=1,NC	SLV 9270
	80 V=V+A(I,J)*C(I)	SLV 9280
	90 Y(J)=V	SLV 9290
	IF (IADS.EQ.0) GO TO 100	SLV 9300
	Y(NB)=FSIN(PSID,AREA,ZEL)*XIS+Y(NO)+Y(NB)	SLV 9310
	Y(NO)=C1*(PSIO-PSIB)-Y(NO)	SLV 9320
C	COMPUTE Z	SLV 9330
	100 DO 110 I=1,NX	SLV 9340
	DO 110 J=1,NX	SLV 9350
	110 Z(I,J)=O.OD0	SLV 9360
	DO 120 J=1,NX	SLV 9380
	DO 120 I=1,NC	SLV 9380
	DO 120 K=1,NX	SLV 9390
	120 Z(J,K)=Z(J,K)+A(I,K)*A(I,J)*C(I)/X(K)	SLV 9400
	IF (IADS.EQ.O) GO TO 140	SLV 9410
	DO 130 J=1,NX	SLV 9420
	130 Z(NB,J)=Z(NB,J)+Z(NO,J)	SLV 9430
	D11=FCOS(P2ID,AREA,ZEL)*XIS	SLV 9440
	D12=1-FCOS(PSID,AREA,ZEL)*XIS/C2	SLV 9450
	D13=-ETSF/2.303*10**(PSIB/ETSF)	SLV 9460
	Z(NB,NB)=D11/D12*D13+Z(NB,NB)	SLV 9470
	Z(NO,NO)=-C1*ETSF/2.303*10**(PSIO/ETSF)-Z(NO,NO)	SLV 9480
	Z(NO,NB)=C1*(-D13)-Z(NO,NB)	SLV 9490
C	CONVERGENCE TEST	SLV 9500
	140 DO 190 J=1,NX	SLV 9510
	VMAX=ABS(T(J))	SLV 9520
	IF(IADS.EQ.0) GO TO 150	SLV 9530
	IF(J.EQ.NB) GO TO 170	SLV 9540
	150 DO 160 I=1,NC	SLV 9550
	160 IF(DABS(A(I,J)*C(I)).GT.VMAX) VMAX=DABS(A(I,J)*C(I))	SLV 9560
	GO TO 180	SLV 9570
	170 VMAX FSIN(PSID,AREA,ZEL)*XIS	SLV 9580
	VMAX=DABS(VMAX)	SLV 9590
	IF (VMAX.LE.1.0D-10) VMAX=1.0D-10	SLV 9600
	180 YTM(J)=DABS(Y(J))/VMAX	SLV 9610
	IF(YTM(J).GT.DEPS) GO TO 200	SLV 9620
	190 CONTINUE	SLV 9630
	IF(IADS.EQ.0) RETURN	SLV 9640
	PSIO=-GX(IADX(161))*ETSF	SLV 9650
	PSIB=-GX(IADX(160))*ETSF	SLV 9660
	SIGO=(PSIO-PSIB)*9.65E+6*C1/AREA	SLV 9670
	SIGD=-11.74*DSINH(ETFSC*PSID*ZEL)*XIS	SLV 9680
	SIGB=-SIGO-SIGD	SLV 9690
	RETURN	SLV 9700
	200 ITER=ITER+1	SLV 9710
	IF(ITER.GT.ITMAX) CALL ERROR(7)	SLV 9720
	IF(ITRPR.EQ.ITMAX) GO TO 220	SLV 9730
	IF(ITER.GT.3.AND.ITER.LE.ITRPR) GO TO 220	SLV 9740
*		
*	IF(ICYCLE(I).EQ.O.OR.(ICYCLE(I).NE.0.AND.ITER.NE.0)) WRITE(6,240)	SLV 9750
*		
*	WRITE(6,250) ITER	SLV 9760
	CALL OUTCMP	SLV 9770
	CALL OUTSPC	SLV 9780
*		
*	WRITE(6,260) (YTM(I),I=1,NX)	SLV 9790

```

*      WRITE(6,280)
*
*      DO 210 1=1,NX
*
* 210  WRITE(6,270) ( Z (I,J) ,J=1,NX)
210  continue
*
C ITERATE
220  CALL SIMQ(Z,Y,NX)
DO 230  J=1,NX
X(J)=X(J)-Y(J)
IF(X(J).LE.0.0D0) X(J) = (X(J) +Y(J) ) /10.0D0
IF(X(0) .EQ.O.ODO) X(J) = 1.OD-38
230  GX(J)= DLOG10(X(J))
GO TO 30
240  FORMAT('1')
250  FORMAT(/'0', '*****', 14, '*****',/)
260  FORMAT(/'0', 'Y/VMAX-'/'0', 5(5(1PD15.5,2X)/))
270  FORMAT( '0',5(1PD15.5, 2X))
280  FORMAT [/'O',' Z MATRIX = ')
END
SLV 9800
SLV 9810
SLV 9820
SLV 9830
SLV 9840
SLV 9850
SLV 9860
SLV 9870
SLV 9880
SLV 9890
SLV 9900
SLV 9910
SLV 9920
SLV 9930
SLV 9940
SLV 9950
*****
*****
*****
SUBROUTINE READAT
*****
C Reads data from DAT.DAT (written from CHEM.FOR) and rewrite al
C in a single file (PLOTIN.DAT) for results pertaining to surface
C adsorption work.
C
C      IMPLICIT NONE
C
C      REAL THOUR(60),AMASS(60),PMASS(60),ABMASS(60),PBMASS(60)
C      REAL PRMASS(60),PSMASS(60)
C      REAL XMASS(60),BMASS(60)
C      REAL AREA,VOL
C      INTEGER J,NTIME,N1COMP,N2THR
C      CHARACTER*14 OUTFIL
C
C      REAL PBC165(60),PBC166(60),PBC167(60) ,PBC168(60),PBC175(60)
C      REAL PBS176(60),PBS177(60),PBS178(60)
C      REAL PBPTOT(60),PBSTOT(60)
C      REAL PBX(60) ,PBB (60) ,PBPR(60) ,PBPS(60)
C
C      INTEGER CALLED /1/, K /1/, L /1/
C
C      CHARACTER *80 OSYS_DAT(10000)
C      COMMON/OSYSDAT/OSYS_DAT
C
C      CHARACTER * 9 DAT_DAT(10)
C      COMMON/DATDAT/DAT_DAT
C
C      CHARACTER * 9 DATA_DAT(256)
C      COMMON/DATADAT/DATA_DAT
C
C      INTEGER MCOUNTER
C      COMMON/COUNTER/MCOUNTER
C

```

```

C   Input conversion parameters and names of OUTFIL and INPFIL
C
      OPEN (UNIT=7,NAME='CONVERT1.DAT',TYPE='OLD',FORM='FORMATTED')
      READ (7,*) N'TIME
      READ (7,*) N1COMP
      READ (7,*) N20THR
      READ (7,33) OUTFIL
      READ (7,*) AREA
      READ (7,*) VOL
C
      33 FORMAT (A8)
      CLOSE (UNIT=7)
C
C   Read actual input data from file to be processed.
C
      IF ( CALLED .EQ. 1 ) THEN                                ! BY TP
      OPEN (UNIT=8,NAME=OUTFIL,TYPE='OLD',FORM='FORMATTED')
      ELSE                                                       ! BY TP
      END IF                                                     ! BY TP
C
      DO J=1,N'TIME
      READ (8,50) THOUR(J),AMASS(J),PMASS(J),ABMASS(J),PBMASS(J),
      1PRMASS(J),PSMASS(J)
      50FORMAT (' ,F5,0, 6(, ,G10.4)) XMASS(J)=AMASS(J)+PMASS(J) BMASS(J)=ABMASS(J)+PBMASS(J)
      END DO
C
      CLOSE (UNIT=8)
C
      DO L = 1, N'TIME
      READ ( DATA_DAT (K), FMT = '(E9.3)' ) PBS178(L)
      READ ( DATA_DAT (K + 1), FMT = '(E9.3)' ) PBS17(L)
      READ ( DATA_DAT (K + 2), FMT = '(E9.3)' ) PBS177(L)
      READ ( DATA_DAT (K + 3), FMT = '(E9.3)' ) PBS165(L)
      READ ( DATA_DAT (K + 4), FMT = '(E9.3)' ) PBC166(L)
      READ ( DATA_DAT (K + 5), FMT = '(E9.3)' ) PBC167(L)
      READ ( DATA_DAT (K + 6), FMT = '(E9.3)' ) PBC168(L)
      READ ( DATA_DAT (K + 7), FMT = '(E9.3)' ) PBC175(L)
C
      PBPTOT(L)=PBC165(L)+PBC166(L)+PBC167(L)+PBC168(L)
      PBSTOT(L)=(PBS176(L)+PBS177(L)+PBS178(L))*1E8
C
      PBX(L)=(PBC175(L)*(XMASS(L)/(XMASS(L)+BMASS(L)*(AREA/VOL))))*1E8
      PBB(L) = (PBC175(L) * ( (BMASS (L)*AREA/VOL) / (XMASS (L) +BMASS(L) *AREA/V
      10L)))*1E8
      PBPR(L)=(PBPTOT(L)*(PRMASS(L)/(PRMASS(L)+PSMASS(L)*(AREA/VOL))))
      1*1E8
      PBPS(L)=(PBPTOT(L)*((PSMASS(L)*AREA/VOL)/(PRMASS(L)+P3MA5S(L)*AR
      1EA/VOL)))*1E8
C
      K = K + 8
C
      END DO
C
      WRITE (11,400)
      400 FORMAT(' THOUR',7X,'PB-X',8X,'PB-B',7X,'PB-PR',6X,'PB-PS',6X,
      1'PB-SURF')

```

```
C      DO J=1,NTIME
      WRITE (11,300) THOUR(J),PBX(J),PBB(J),PBPR(J),PRPS(J),PBRTOT(J)
300  FORMAT (' ',F5.0, 5(' ',G10.4))
      END DO
C
      CALLED = CALLED +1                                !TP
C
      RETURN
      END
```

4.7E-04	KACR	g/Liter	DATA for MOD7CTN3.FOR
4.4E-03	KPCR	g/L	
4.7E-04	KABCR	g/L	
4.4E-03	KPBCR	g/L	
0.95	FAP		fraction of A degraded going to P
0.95	FABP		fraction of AB degraded going to PB
0.10	KPRP	gP/gA	
0.10	KPRPB	gP/gA	
1.0E-02	KDACR	g/L	
1.0E-02	KDABCR	g/L	
0.25	MUA	1/hr	
0.25	MUAB	1/hr	
0.24	MUP	1/hr	
0.24	MUPB	1/hr	
4.0E-02	MUPR	1/hr	
4.0E-02	MUPRB	1/hr	
0.031	KDA	1/hr	
0.031	KDAB	1/hr	
0.16	KDPR	1/hr	
3.00E-08	KAMR	mol/L	
3.00E-08	KABMR	mol/L,	
3.6	ALPHA		
1.7	ALPIIF		
3.6	ALPHAS		
1.7	ALPHPB		
0.0072	KM	1/hr	
0.0072	KMB	1/hr	
0.040	KP	L/m2	
4.7	KA	L/g-hr	Attachment constant
0.0035	KD	1/hr	Detachment constant
8.5E-03	BMAX	g/m2	Maximum biofilm density
0.321	AREA	m2	Total surface area-bioreactor
1.42	VOL	L	Total fluid volume-bioreactor
300.0	RE		Reynold's number-bioreactor
60.	TIM	hr	Total time for batch run
12.	TCTNO	hr	Time in batch before continuous
0.03	AO	g/L	Active biomass
0.01	PO	g/L	Polymer associated with A ₀
6.0E-04	ABO	g/m2	Attached biomass
3.0E-04	PBO	g/m2	Polymer associated with AB ₀
1.0E-06	PRO	g/L	Suspended polymer in solution
1.0E-09	PSO	g/m2	Adhered polymer on surface
2.0	CRO	g/L	Carbon source concentration
0.0	MRO	mol/L	Total metal conc.(free=from MINEQL)
2.0	CRF	g/L	Carbon source conc in feed
120.	TIMCTN	hr	Total time for continuous run
1.0E-06	KE1	mol/L	Enzyme molecular dissociation Constant
1.0E-06	KES1	mol/L	Enzyme molecular dissociation Constant
7.9E-09	KE2	mol/L	Enzyme-substrate molecular dissociation Constant
7.9E-09	KES2	mol/L	Enzyme-substrate molecular dissociation Constant
1.0E-09	HPLUS	mol/L	Fixed hydrogen ion concentration
1.0	PRINT	hour	Time interval of output
5	IDTIM	sec	Time interval of calculation
0.04	FO	L/hr	Flow rate of nutrient feed
0.48	FF	L/hr	Final feed in do loop

BIOREACTOR DATA SET

0.02	DELF	L/hr	loop interval of feed
0.0	ISTEP		value allows step change if not 1.0
0.0	ICONT		value allows calc. cont. if not 1.0
0.0	IMETAL		value requires metal analysis if 1.0
0.0	ISURF		value requires surface adsorption. if 1.0

_UNCC2\$FACULTY: [GMURGEL. ANALMOD 1 .PHDEPEND] CONVERT 1 .DAT; 1

23	N1TIME	# in loop (# of data sets in batch data)
14	N1COMP	# components up to the 8 varied cell comp.
32	N20THR	# of all other components in data file
OUT6.DAT	OUTFIL	file of bioreactor continuous data
0.321	AREA	m2 total surface area
1.42	VOL	L total fluid volume

_UNCC2\$FACULTY: [GMURGEL. ANALMOD 1 .PHDEPEND] CONVERT2.DAT; 1

MMSTESTMETAL.DAT	INPFIL	Source of MINEQL conc. and kinetic data
14	N1COMP	# components in mineral medium recipe
24	N20THR	# of all other components in data file

_UNCC2\$FACULTY: [GMURGEL. ANALMOD 1 .PHDEPEND] CONVERT3.DAT; 1

14	N1COMP	components up to the 8 varied cell comp
32	N20THR	# of all other components in data file
0.70E-4	GMAXP	mol Pb/g polymer – conversion for polymer
9.75E-8	GMAXC	mol Pb/g cells - conversion for cells
7.55E-7	GMAXS	mol Pb/m2 surface – conversion for solid surface
MMSTEST.DAT	INPFIL	file of MINEQ conc. and kinetic data
0.704	FPR1	fraction of polymer (1 of 4)
0.250	FPR2	"
0.017	FPR3	"
0.029	FPR4	"
0.881	FS1	fraction of solid surface (1 of 3)
0.098	FS2	"
0.021	FS3	"
0.321	AREA	m2 total surface area
1.42	VOL	L total fluid volume
0.02	CELLSURF	m2 surface covered/g attached cells

_UNCC2\$FACULTY:[GMURGEL.AN ALMOD1.PHDEPEND]JMMSTESTMETAL.DAT;1

1	-4.00	2.041E-04	Ca+2	!MMS Recipe before cells!	
2	-4.00	1.400E-04	Mg+2	!Fix system pH!	
4	-4.00	1.474E-04	K+	!Open system!	
5	-2.00	4.502E-02	Na+		
101	-6.00	1.000E-05	C03-2		
102	-3.00	1.048E-03	S04-2		
103	-4.00	4.082E-04	Cl-		
107	-3.00	1.816E-03	NM3		
109	-7.00	1.000E-06	P04-3		
115	-3.00	2.438E-02	Acetate-		
157	-2.00	2.078E-02	NO3-		
15	-9.00	1.000E-07	Pb+2		
50	-7.00	1.828E-03	H+		
02					
1490	1.25				
1995	6.11	4	1	115	1
2045	4.35	5	1	115	1
8111	1.06	15	1	103	4
8230	2.68				
8240	4.08				
8243	3.29	15	1	115	3
8246	1,85	15	1	115	4
12575	7.00	50	1	107	1 15 1
12750	4.76				
12752	4.15	50	1	115	2
12754	9.30	50	2	115	2
12756	11.16	50	2	115	3
12757	21,95	50	3	115	3
12758	10.55	50	3	115	4
12759	21.43	50	4	115	4
03					
50	9.00				
25000	21.50				

_UNCC2\$FACULTY:[GMURGEL, ANALMOD 1.PHDEPENDJMMSTEST.DAT; 1

1	-4.00	2.041E-04	Ca+2	!MMS Recipe before cells!
2	-4.00	1.400E-04	Mg+2	!Fix system pH!
4	-4.00	1.474E-04	K+	! Open system !
5	-2.00	4.502E-02	Na+	
101	-6.00	1.000E-05	C03-2	
102	-3.00	1.048E-03	S04-2	
103	-4.00	4.082E-04	Cl-	
107	-3.00	1.816E-03	NH3	
109	-7.00	1.000E-06	P04-3	
115	-3.00	2.439E-02	Acetate-	
157	-2.00	2.078E-02	N03-	
15	-9.00	1.000E-07	Pb+2	
50	7.00	1.828E-03	H+	
165	-4.00	1.340E-05	C165	C165 - C168 are for expolymer
166	-5.00	4.750E-06	C166	
167	-6.00	3.230E-07	C167	
168	-6.00	5.510E-07	C168	
175	-8.00	1.130E-08	C175	C175 is for cell surfaces
176	-8.00	8.340E-08	S176	S176-S178 are for solid surface
177	-9.00	9.280E-09	S177	
178	-9.00	1.990E-09	S178	

02				
1490	1.25			
1995	6.11	4	1	115 1
2045	4.35	5	1	115 1
8111	1.06	15	1	103 4
8230	2.68			
8240	4.08			
8243	3.29	15	1	115 3
8246	1.85	15	1	115 4
12575	7.00	50	1	107 1 15 1
12750	4.76			
12752	4.15	50	1	115 2
12754	9.30	50	2	115 2
12756	11.16	50	2	115 3
12757	21.95	50	3	115 3
12758	10.55	50	3	115 4
12759	21.43	50	4	115 4
30050	4.61	15	1	165 1
30052	4.64	15	1	166 1
30054	5.82	15	1	167 1
30056	6.56	15	1	168 1
30060	-5.32	15	1	50 -1 175 1
30070	-6.61	15	1	50 -1 176 1
30072	-6.61	15	1	50 -1 177 1
30074	-6.61	15	1	50 -1 178 1

03				
50	9.00			
25000	21.50			

4.7E-04	KACR	g/Liter	DATA for MOD7CTN.FOR, MOD7CTN2.FOR
4.4E-03	KPCR	g/L	MOD6CTN.FOR, MOD6CTN2.FOR
4.7E-04	KABCR	g/L	MOD6CTN3.FOR
4.4E-03	KPBCR	g/L	
0.95	FAP		Fraction of A degraded going to P
0.95	FABP		Fraction of AB degraded going to PB
0.10	KPRP	gP/gA	
0.10	KPRPB	gP/gA	
1.0E-02	KDACR	g/L	
1.0E-03	KDABCR	g/L	
0.25	MUA	1/hr	
0.25	MUAB	1/hr	
0.24	MUP	1/hr	
0.24	MUPB	1/hr	
4.0E-02	MUPR	1/hr	
4.0E-02	MUPBR	1/hr	
0.031	KDA	1/hr	MULTIGEN DATA SET
0.031	KDAB	1/hr	
0.16	KDPR	1/hr	
3.00E-08	KAMR	mol/L	
3.00E-08	KABMR	mol/L	
3.6	ALPHA		
1.7	ALPHP		
3.6	ALPHAB		
1.7	ALPHPB		
0.0072	KM	1/hr	
0.0072	KMB	1/hr	
0.040	KP		
4.7	KA	L/g-hr	Attachment constant
0.0035	KD	1/hr	Detachment constant
8.5E-03	BMAX	g/m2	Maximum biofilm density
0.321	AREA	m2	Total surface area
1.42	VOL	L	Total fluid volume
300.0	RE		Reynold's number
60.	TIM	hr	Total time for batch run
12.	TCTNO	hr	Time in batch before continuous
0.03	AO	g/L	Active biomass
0.01	PO	g/L	Polymer associated with AO
6.0E-04	ABO	g/m2	Attached biomass
3.0E-04	PBO	g/m2	Polymer associated with ABO
1.0E-06	PRO	g/L	Suspended polymer in solution
1.0E-09	PSO	g/m2	Adhered polymer on surface
2.0	CRO	g/L	Carbon source concentration
1.0E-07	MRO	mol/L	FREE metal concentration
2.0	CRF	g/L	Carbon source cone in feed
120.	TIMCTN	hr	Total time for continuous run
1.0E-06	KE1	mol/L	Enzyme molecular Dissociation Constant
1.0E-06	KES1	mol/L	Enzyme molecular Dissociation Constant
7.9E-09	KE2	mol/L	Enzyme molecular Dissociation. Constant
7.9E-09	KES2	mol/L	Enzyme molecular Dissociation Constant
1.0E-09	HPLUS	mol/L	Fixed hydrogen ion concentration
1.0	PRINT	hour	Time interval of output.
5	IDTIM	seC	Time interval of calculation